AD716510

FTD-HC-23-461-69

FOREIGN TECHNOLOGY DIVISION

LIQUID PROPELLANT ROCKET AS A CONTROLLED OBJECT

By

K. S. Kolesnikov

DDC
RECEIVED
JAN 14 1971
A

Distribution of this document is unlimited. It mat be released to the Clearinghouse, Department of Commerce, for sale to the general public.

Reproduced by
NATIONAL TECHNICAL
INFORMATION SERVICE
Springfield, Va. 22151

FTD-HC-23-461-69

EDITED TRANSLATION

LIQUID PROPELLANT ROCKET AS A CONTROLLED OBJECT

By: K. S. Kolesnikov

English pages: 362

Source: Zhidkostnaya Raketa kak ob"yekt Regulirovaniya 1969, pp. 1-299

Translated under: F33657-70-D-0607

UR/0000-69-000-000

THIS TRANSLATION IS A RENDITION OF THE ORIGINAL FOREIGN TEXT WITHOUT ANY ANALYTICAL OR EDITORIAL COMMENT. STATEMENTS OR THEORIES ADVOCATED OR IMPLIED ARE THOSE OF THE SOURCE AND DO NOT NECESSARILY REFLECT THE POSITION OR OPINION OF THE FOREIGN TECHNOLOGY DIVISION.

PREPARED BY:

TRANSLATION DIVISION
FOREIGN TECHNOLOGY DIVISION
WP-AFB, OHIO.

A

TABLE OF CONTENTS

ABSTRACT

The book discusses the differential equations of the perturbed motion of a rocket for three different dynamic models: 1) an ideally rigid body, 2) an elastic inhomogeneous rod, 3) a rigid body with cavities partially filled with liquid.

In the study of the dynamic characteristics of the rocket, the oscillations of liquid in tanks were replaced by the oscillations of mathematical pendulums, since the differential equations for the two phenomena are completely analogous. Results are given of an experimental investigation of the fuel oscillating in tanks. A presentation is made of the methods of determining the modes and frequencies of the natural vibrations of the fuselage with and without taking the slave force into consideration.

On the basis of an analysis of the dynamic rocket properties, a determination is made of the amplitude-phase frequency characteristics of the rocket, and of those features of the characteristics that are due to the fuel oscillating in tanks and the elastic vibrations of the fuselage. A stability analysis of rocket motion leads to a formulation of additional requirements on the frequency characteristics of the control system and on the location of the gyroscope along the fuselage. Attention is given to certain methods of stabilizing the oscillating motion of fuel in tanks as well as the elastic vibrations of the fuselage.

The book may be used by scientists and engineers working at institutes and bureaus of industrial design. It may also be useful to undergraduate and graduate students as well as teachers at the institutions of higher education.

9 Tables. 126 Illustrations. 108 Names in the References.

PREFACE

In the present book, which is being called to the attention of the reader, an attempt is made to generalize the results of investigations of the stability of motion of a liquid-propellant rocket in a systematic way taking into account the elastic lateral vibrations of the rocket fuselage as well as the oscillations of fuel in tanks.

Characteristic features of the properties of liquid-propellant rockets with an elastic fuselage are of interest to both mechanical engineers dealing with rocket design and their dynamic characteristics and to designers responsible for designing guidance and control systems based on the knowledge of these characteristics.

It is also clear that mechanical engineers should , on the one hand, know which dynamic properties of a rocket are most important for the control system, i.e., which properties have the greatest effect on the functioning of the control system, and on the other hand — to what extent design changes may influence the stability of motion. To the specialists in the area of automatic control it is in turn important to know not only the structure of the equations of motion of a rocket and the variation of the equation coefficients during the time of flight, but also the more general dynamic properties of the rocket as an object of control which influence the structure

and characteristics of the control system. It is also advisable to know the possible changes in the dynamic characteristics of the rocket, since this makes it possible to simplify the requirements imposed on the control system, and to improve the stability of motion of the rocket.

The desire to satisfy the interests of both groups of readers caused certain difficulties as to the depth of coverage and a method of presentation. The author considered it necessary to, above all, devote special attention to the physical meaning of the dynamic problems discussed and only then give their mathematical treatment. In discussing the equations of rocket motion that take into account fuel oscillations and elastic vibrations of the fuselage, the author took care to make the treatment as accessible as possible to specialists in theory of automatic control. In analyzing the control equations and establishing requirements on the control system, the author attempted to make the properties and potentialities of the control system understandable to mechanical engineers.

In the analysis of the dynamic characteristics, the rocket was represented by various dynamic models: an ideally rigid body, an elastic inhomogeneous rod, a rigid body with cavities, partially filled with liquid. Such a representation of a rocket of course does not express all the numerous specific properties that are peculiar to each rocket design, but it has the advantage of revealing basic dynamic characteristics that are common in almost all rocket designs.

In the analysis of the effect of fuel oscillations on the dynamic characteristics of a rocket, a mechanical analog is used, namely a mathematical pendulum or a mass suspended from a spring. The amplitude-phase frequency characteristics of a rocket with account taken of fuel oscillations in narrow frequency bands, including the natural frequencies of liquid oscillations in stationary tanks, differ considerably from the amplitude-phase characteristics of the rocket modeled as a rigid body. An analysis is made of the effect

that the parameters of the system have on these characteristics, and additional requirements are formulated to be imposed on the frequency characteristics of the control system.

Forced elastic vibrations of the fuselage are represented by expansion in series in the natural oscillatory modes, and in a general form (without the expansion into a series in natural modes). The effect is shown of axial slave force and the inertial characteristics of rotating engines on the dynamic characteristics and stability of rocket motion. Since in elastic vibrations the mismatch signal coming from the sensing element into a computer depends on the location of the sensor along the rocket fuselage length, then the choice of sensor locations must be included among the additional requirements that must be imposed on the characteristics of the control system.

The analysis of the dynamic characteristics is made on the basis of linearized equations which, generally speaking, does not exhaust all the peculiarities of certain problems, and gives only first approximations to their solution. In a number of cases this turns out to be sufficient.

The author considers it his pleasant duty to express his sincere thanks to A. I. Pozhalostin, V. N. Sukhov, Yu. A. Tsurikov, and I. M. Rapoport for valuable remarks made upon seeing the manuscript.

The author will be grateful to those readers who send their critical remarks and desires as to the contents of the book to the address: Publishing House: "Mashinostroyeniye", Moscow, K-51, Petrovka 24.

BASIC NOTATION

The Rocket as a Rigid Body (Chapter 1)

c_x	drag coefficient of the rocket;
$c_y^\alpha = (\partial c_y/\partial \alpha)_{\alpha=0}$	derivative of the aerodynamic lift coefficient with respect to the angle of attack;
$c_z^\beta = (\partial c_z/\partial \beta)_{\beta=0}$	derivative of the lateral aerodynamic force coefficient with respect to the angle of sideslip;
c_m^α, c_m^β	derivatives of the aerodynamic moment coefficients with respect to the angle of attack and the angle of sideslip;
$c_m^{\dot\beta}$, $c_m^{\dot\alpha}$	derivatives of the aerodynamic damping moment coefficients;
$I_z = I_y = I$	moment of inertia of the rocket relative to the lateral axes through the center of mass;
l_p	the distance between the point of the application of a lateral control force (of the vanes) and the center of mass of the rocket;
m	mass of the rocket;
M_a	aerodynamic moment;
M_x	damping moment;
P	thrust of one or a group of rocket engines;
$P_e = P - X_p$	effective thrust of an engine;
$q = \frac{\rho v^2}{2}$	pressure head;
K_{yp}^β, K_{zp}^β	gradients of the lateral control force of the vanes;
v_x, v	nominal rocket velocity, variation of rocket velocity;
v_z, v_y	variation of the velocity of the center of mass in the direction of the stationary axes Oz, Oy;
X_p	drag force on vanes;

X drag force on the rocket;

x_m distance between the upper tip of the rocket and its center of mass;

x_p distance between the upper tip of the rocket and the center of pressure of the aerodynamic forces;

Y the drag force; aerodynamic buoyancy

Y_δ lateral control force of the vanes;

α angle of attack;

β angle of sideslip;

δ angle of deflection of the control element or of a rotating engine;

θ_0, θ the nominal angle made by the velocity vector and the horizontal plane, variation of this angle;

ϑ_0, ϑ nominal angle of pitch, variation of the angle of pitch;

γ angle of roll;

ψ angle of yaw.

Oscillations of Liquid (Chapter II and III)

$g^0 = \frac{P_0 - X}{m}$ longitudinal acceleration of the rocket produced by the engine thrust beyond the gravitational field of the Earth;

P_0^j force due to pressure of liquid on the walls of the cylindrical tank;

h, h_j height of liquid column in a tank;

I_0 moment of inertia of "solidified" liquid relative to the lateral axis of rotation;

$J_1\left(\mu_n \frac{r}{r_0}\right)$ Bessel function of first kind and first order;

l_j length of a $j^{\underline{th}}$ pendulum;

l^0 length of a pendulum, identical for all tanks;

l_j^0 distance between the upper tip of the rocket and the unperturbed free surface of a liquid in the $j^{\underline{th}}$ tank.

l_n length of pendulum corresponding to an $n^{\underline{th}}$ oscillatory mode of the liquid;

L_n distance between the lateral axis of rotation of the cylinder and the effective mass of the oscillating liquid for the $n^{\underline{th}}$ mode;

L_j^0 distance between the center of mass of the rocket and the mass of the pendulum in a $j^{\underline{th}}$ tank;

L, L_j distance between the center of mass of the rocket and the free surface of liquid in a tank;

m mass of liquid in a tank;

m_{cj} fuel consumption per second from a $j^{\underline{th}}$ tank;

m_n effective mass of liquid, being in an $n^{\underline{th}}$ oscillatory mode;

m_j^* effective mass of liquid in a $j^{\underline{th}}$ tank in the first oscillatory mode;

M_C^0 moment of the forces of pressure of liquid on the tank walls relative to a lateral axis of rotation through point C;

p pressure of liquid;

r arbitrary radius;

r_0 radius of a cylindrical tank;

s_n distance between the undisturbed free surface of liquid and the pendulum mass for an $n^{\underline{th}}$ oscillatory mode;

x_C displacement of the center of mass (point C) of a rigid rod in the Ox direction;

y_C displacement of point C on the longitudinal axis of a tank with liquid in a perturbed motion in the direction of the Ox coordinate axis;

$\gamma = p/\omega$ dimensionless frequency of forced vibrations;

ε_1 damping coefficient of the first natural mode of liquid;

ζ_n, ζ_m eigenvalues of Bessel's functions;

$\lambda_n(t)$ generalized coordinate of the oscillations of the free surface of liquid, displacement of the pendulum from the axis of the rod;

μ_1, μ_2, μ_3 dimensionless parameters of pendulums;

ρ density of liquid;

φ velocity potential of liquid;

$\Phi(x, r, \chi, t)$ absolute velocity potential of liquid;

χ displacement of the free surface of liquid in oscillations;

ψ part of the absolute velocity potential of liquid;

ω_n frequency of the $n^{\underline{th}}$ oscillatory mode of liquid;

ω_j frequency of the natural oscillations of a $j^{\underline{th}}$ pendulum;

ω_1 frequency of the first oscillatory mode of liquid oscillations.

Elastic Vibrations of a Rod (Rocket Fuselage) (Chapter IV)

$f_n(x)$ $n^{\underline{th}}$ bending, natural oscillatory mode of a rod;

$f_n(x_p)$ value of a natural oscillatory mode at a point where the control elements (vanes) are placed;

$f_n(l)$ value of a natural oscillatory mode at the end of a rod;

$f_n'(l)$ angle made by the tangent to a natural oscillatory mode at the end of a rod and the horizontal;

h_n effective viscous friction coefficient of a rod in the state of bending vibrations of an $n^{\underline{th}}$ mode;

k_n effective rigidity coefficient of a rod executing bending vibrations of an $n^{\underline{th}}$ mode;

k_j stiffness of the spring belonging to a j^{th} pendulum;

m mass of the rod;

m_n effective mass of a rod executing vibrations of $n^{\underline{th}}$ mode;

$Q_y, Q_\theta, Q_{\varphi n}$ generalized forces;

$q(x, t)$ external distributed force acting on a rod;

$q_n(t)$ generalized coordinate of $n^{\underline{th}}$ mode of the lateral vibrations of a rod;

x_m distance between the upper tip of a rod and its center of mass;

x_s distance between the upper tip of a rocket and the main frame that is subject to the engine thrust;

x_p distance between the upper tip of a rocket and the point of application of a lateral control force;

x_j distance between the upper tip of a rocket and the pendulum in a $j^{\underline{th}}$ tank;

x_j^0 distance between the unperturbed free surface of liquid and the pendulum mass for the first oscillatory mode;

$y(x, t)$ lateral displacement of a rod in a stationary coordinate system Oxy;

y_m displacement of the center of mass of a rod in the direction of the Oy coordinate axis;

z_m displacement of the center of mass of a rod in the direction of the Oz coordinate axis;

$\beta = \frac{Pl^2}{EJ}$ parameter characterizing the value of an axial slave force;

$\gamma = p/\omega$ dimensionless frequency of forced oscillations;

ε_n damping coefficient of $n^{\underline{th}}$ oscillatory mode;

$\xi_n = \frac{\varepsilon_n}{\omega_n}$ relative coefficient of the damping of elastic vibrations;

$\varphi_n(x)$ natural oscillatory mode of a rod subject to a slave force;

$\phi(x, p)$ forced bending oscillatory mode of a rod;

ω_n $n^{\underline{th}}$ natural frequency of a rod.

Control System (Chapter I, III, and V)

$A(\gamma)$, $A(\omega)$ modulus of a complex transfer number;

$f'_n(x_1)$ the slope angle of the tangent to a natural oscillatory mode of the fuselage at a point where a sensing element (gyroscope) is located;

$W(p)$ transfer function;

$K(j\omega)$ complex transfer number;

$K_{p.o}(j\omega)$ complex transfer number of a controlled object;

$K_{AC}(j\omega)$ complex transfer number of the control system;

k_y, k_{y1} amplification coefficient of the amplifier with respect to the main signal;

$k_{o.c}$, $k_{y.o.c}$ amplification coefficient of the amplifier with respect to the feedback signal;

k, k_1, k_2 amplification coefficient of the control system;

p Laplace operator, characteristic exponent, frequency of forced vibrations;

P_y thrust force of a control rotating engine;

$Q(p)$ denominator of the transfer function;

$R(p)$ numerator of the transfer function;

U real part of the complex transfer number;

V imaginary part of the complex transfer number;

δ angle of rotation of a control element of a rotating engine;

$\varphi(\gamma)$, $\varphi(\omega)$ argument of the complex transfer number — phase frequency characteristic;

$\varphi_{p.o}(\gamma)$, $\varphi_{p.o}(\omega)$ the same for the controlled object;

$\varphi_{AC}(\gamma)$, $\varphi_{AC}(\omega)$ the same for the control system;

ω_0 frequency for which the phase lag of the control system vanishes;

ω_π, $\omega_{2\pi}$, ... frequencies at which the phase lags of the control system are $\pi, 2\pi, \ldots$.

INTRODUCTION

Contemporary liquid-propellant rockets are guided by varying the direction and magnitude of the engine thrust vector in such a way as to make the rocket follow the prescribed trajectory. In the case of an autonomous guidance and control system, the direction and magnitude of the thrust vector are varied according to a program calculated earlier.

Motion of a rocket subject to given forces has come to be called unperturbed motion. In addition to these forces, a rocket in flight may be subject to random forces such as, for example, wind gusts, small variations of engine thrust, etc. A rocket subject to these perturbing forces will be in a state called perturbed motion.

Stability of rocket motion is achieved using a system that stabilizes the center of mass, and three systems stabilizing the rocket relative to the angles of pitch, yaw, and roll. Each control system consists of sensing elements (pickups), a computer, and the actuators. Usually a gyroscopic mechanism serves as a sensor, a differentiating circuit and an amplifier serve in the simplest case as a computer, and electro-hydraulic control actuators are used as a final control element. In the control process, as soon as the longitudinal rocket axis deviates, for example, from the pitch plane by some angle ψ (angle of yaw), a potentiometric sensor will emit a signal into the computer whose magnitude will be proportional to

the value of that angle. The computer, in accordanc ith a given algorithm, works out a control signal which passes to the control actuators. The actuators deflect the control elements of the rocket in such a way as to reduce the deviation to zero. The rocket as an object of control, together with the stabilization system, forms a closed system of automatic control. Therefore, the algorithm used by the computer to work out a control signal depends on the dynamic characteristics of the rocket.

In the analysis of the equations of motion of a rocket, one usually makes use of its various dynamic models, for instance, to a first approximation a rocket can be represented as an absolutely rigid body.

With an increase in the diameter and length of the fuselage, such a model becomes very inaccurate, and when it comes to certain questions it is even an inadmissible simplification. In the analysis of motion of very long rockets, the elastic vibrations of the fuselage may be of great significance, and for rockets with large tank diameters the oscillations of liquid fuel may be very important. However, the equations of motion of a rocket with account taken of these factors become very complicated, and their analysis is difficult. Therefore, it is necessary to introduce substantiated assumptions to make the equations simpler.

We know from theory of oscillations that if the partial frequencies (for example, such as the frequencies of the fuselage elastic vibrations and the oscillations of liquid in the tanks of the rocket) are far away from one another, then the coupling between separate partial systems will be weak. The frequencies and modes of the natural oscillations of the complete oscillatory system will then differ little from the frequencies and forms of the natural oscillatory modes of the partial systems. On the basis of this assumption, the dynamic characteristics of the rocket may be analyzed separately: (1) taking account of the elastic lateral vibrations of the fuselage, and (2) taking account of the oscillations of liquid in the tanks. In the first case, an inhomogeneous elastic rod may

serve as a model of the rocket. In the second case, the fuselage may be assumed to be rigid, and its internal cavities partially filled with an ideal liquid. For specific ratios of the parameters, either the oscillations of the liquid or the elastic vibrations of the fuselage will have a predominate effect on the motion of the rocket.

In engineering practice, one question always arises: for what relative values of partial frequencies is it possible to consider separately the elastic vibrations of the fuselage and the oscillations of liquid in the tanks? This question can be answered only by analyzing the equations that make allowances for both the oscillations of liquid and the elastic vibrations of the rocket fuselage. This type of analysis can, unfortunately, be done only for certain special cases.

An analysis of the equations of perturbed motion by separately taking into account the liquid oscillations and the elastic vibrations of the fuselage shows that, for small damping coefficients, there is a considerable variation in the amplitude-phase frequency characteristic of the rocket within a small range of its natural frequencies. Outside of these ranges, the effect of the liquid oscillations and the elastic vibrations of the fuselage on the dynamic characteristics of the rocket is weak, and can be neglected in calculations. For this reason, the above mentioned effects sometimes are discussed separately, even when the differences among the partial frequencies of the oscillatory systems are not very large. It is, however, impossible to give a quantitative estimate of the error made in such a separate analysis.

CHAPTER I

DYNAMIC CHARACTERISTICS OF A ROCKET AS A SOLID BODY

1. Forces Acting on a Rocket During Flight

In the calculation of the external forces, we shall assume that the unsteady character of the motion of the rocket will not be taken into consideration, and the forces will be determined as if the motion were steady, parameter values being constant and equal to their instantaneous values.

The forces acting on a rocket during flight can be divided into the aerodynamic forces, forces of gravity, and the forces of the engine thrust.

Let us first define the coordinate systems that will be used henceforth. All these systems will be rectangular and right-handed (Figure 1.1). The system of coordinates $Ax_0y_0z_0$ whose axes are stationary relative to the Earth will be called the Earth system or the starting system. The origin of the coordinates coincides with the starting point. The Ay_0 axis is directed vertically upward; the Ax_0 axis points along the tangent line to the arc of the great circle that connects the starting point with the target. This coordinate system is used to calculate the trajectory of the rocket.

The moving coordinate system $Ox_1y_1z_1$ whose axes are attached to the body of the rocket is called the body system. Its origin is at

the center of mass of the rocket, point O; the coordinate axes Ox_1, Oy_1, Oz_1 point along the principal axes of the moment of inertia of the rocket. The Ox_1 axis is directed along the axis of the rocket, and is called its longitudinal axis. The lateral axis Oy_1 is oriented in such a way that in the starting position the planes x_1Oy_1 and x_0Ay_0 coincide.

Let us introduce another moving coordinate system and attach it to the flight trajectory of the rocket. The origin of the coordinates will be located at the center of mass of the rocket. The Ox axis will point along the tangent line to the trajectory, and the Oy axis will lie in the vertical plane perpendicularly to Ox. The moving system Oxyz is called the velocity (of flow) coordinate system. Since the Ox axis coincides with the direction of the velocity vector v, the components X, Y, Z of the aerodynamic force acting on the body of the rocket will be computed in the velocity coordinate system.

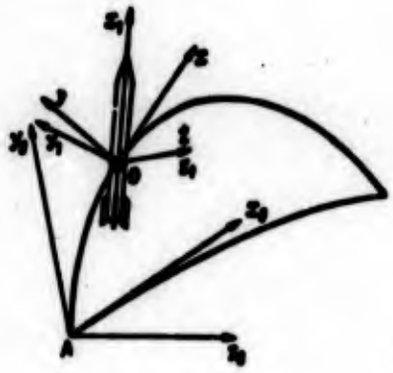

Figure 1.1

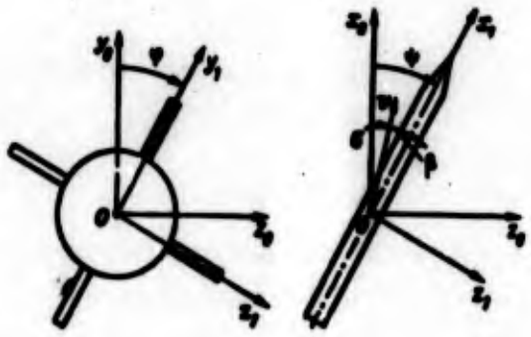

Figure 1.2

Now we introduce some angular coordinates. The ϑ angle between the longitudinal axis Ox_1 of the rocket and the horizontal plane at the point of launch is called the pitch angle. The angle θ between the velocity vector and the horizontal plane at the launch point is usually called the inclination angle of the trajectory to the launching horizon.

The angle ψ which the longitudinal axis Ox_1 makes with the plane x_0Oy_0 is called the yaw angle (Figure 1.2). The angle φ which the lateral axis Oy_1 makes with the plane x_0Oy_0 is referred to as the banking angle. The banking angle determines the rotation of the body relative to the longitudinal axis of the rocket.

We shall always assume below that a rocket has two planes of symmetry that coincide with the planes x_1Oy_1 and x_1Oz_1.

The angle of attack α is defined as the angle between a projection of the velocity vector onto the vertical plane of symmetry x_1Oy_1 and the longitudinal axis Ox_1. The sideslip angle β is defined as the angle between the velocity vector and the vertical plane of symmetry x_1Oy_1.

For a rigid body, the system of the aerodynamic forces distributed over the surface of the body is in the case of a plane motion reduced to a resultant which, for convenience, is represented as consisting of two components: the lifting force Y and the drag force X, applied to the center of thrust.

For small angles of attack α, the lifting force is proportional to the attack angle. The effect of the shape and dimensions of the body on the lifting force is taken into account by means of a certain characteristic parameter S, the area of the center section, and the dimensionless lifting force coefficient c_y. In contrast with the lifting force Y, the force of drag X for small angles of attack hardly depends on the magnitude of this angle. Therefore,

$$Y = qSc_y^{\alpha}\alpha, \quad X = qSc_x, \tag{1.1}$$

where ρ is the density of the air; $q = \rho v^2/2$ is the pressure due to velocity; v is the velocity of flight; $c_y^{\alpha} = (\partial c_y/\partial\alpha)_{\alpha=0}$; c_x is the drag coefficient. The angle of attack α will be expressed in radians.

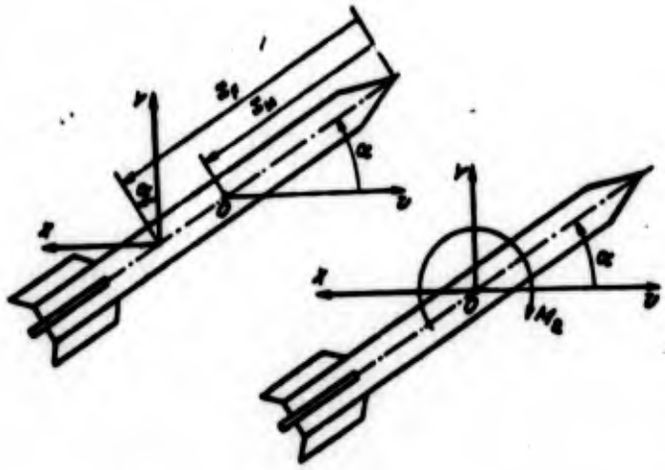

Figure 1.3

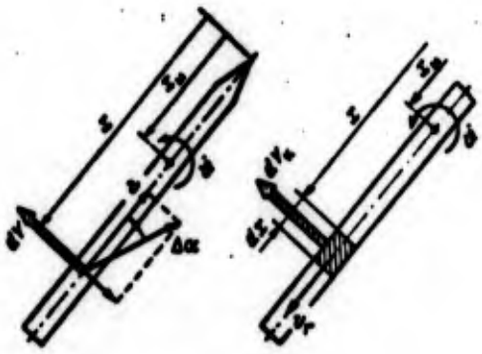

Figure 1.4

The coefficients c_y^a and c_x characterize the external configuration of an object, and depend on a number M and the angle α so that

$$c_y^a = c_y^a(M, a), \quad c_x = c_x(M, a).$$

In a study of rocket motion, one has to determine the moment M_a of the aerodynamic forces Y and X relative to the lateral axis passing through the point 0 — the center of mass of the rocket (Figure 1.3):

$$M_a = Y(x_p - x_a)\cos a + X(x_p - x_a)\sin a.$$

For small attack angles $\cos a \approx 1, \sin a \approx a$, and

$$M_a = qSlc_m^a a, \quad c_m^a = \frac{x_p - x_a}{l}(c_y^a + c_x), \tag{1.2}$$

where l is the length of the rocket body.

The moment M_a depends, consequently, on both the aerodynamic characteristics and on the distribution of mass of the rocket which changes with the burning of the fuel. The relative location of the thrust center and the center of mass is important for the stabilization of the rocket during flight.

We may distinguish between:

a) a statically stable rocket, when $x_p > x_m$, $c_m^\alpha > 0$;

b) a statically unstable rocket for $x_p < x_m$, $c_m^\alpha < 0$;

c) a neutral rocket for $x_p = x_m$, $c_m^\alpha = 0$.

If the center of thrust is located ahead of the center of gravity ($c_m^\alpha < 0$), then if the axis of the rocket is deflected from the direction of flight, the aerodynamic forces exert a moment deflecting the axis of the rocket by an even greater angle. Such a rocket will not fly without a stabilizing mechanism.

To make sure the rocket is statically stable or to lower its static instability, the rocket is equipped with tail fins. A finless rocket is usually statically unstable. A reserve of static stability is determined from

$$\frac{x_p - x_m}{l} 100\%.$$

In addition to the moment M_a which for $c_m^\alpha > 0$ is called the stabilizing moment, during the rotation of the rocket body about the lateral axis Oz_1 with angular velocity $\dot{\vartheta}$ another moment arises, called the damping moment. This moment is composed of the aerodynamic damping moment caused by the appearance of the secondary angles of attack

$$\Delta\alpha = \frac{\dot{\vartheta}(x - x_m)}{v},$$

and the moment of the Coriolis forces (Figure 1.4). The x coordinate for any cross section is measured from the top end of the body.

The aerodynamic damping moment is everywhere directed in the opposite direction from the rotation of the rocket body:

$$M_z' = \int_0^l (x - x_m) \frac{\partial Y}{\partial x} dx = qSl^2 c_m^{\dot{\alpha}} \frac{\dot{\vartheta}}{v}, \qquad (1.3)$$

where $c_m^{\dot{\alpha}}$ is the rotational derivative of the coefficient of the aerodynamic damping moment.

The damping moment due to the Coriolis forces arises as a result of the movement of the stream of liquid in the tanks and the pipelines of the rocket, and of the stream of gases moving in the combustion chamber and the nozzle of the engine. This moment can be calculated if one assumes that the liquid and gas streams rotate with the body of the rocket.

The magnitude and direction of the Coriolis acceleration are given by the vector product

$$\bar{a}_k = 2\bar{\omega} \times \bar{v}_r,$$

where $\bar{v}_r$ is the relative velocity of the stream moving in the rocket. If, for example, the mass of the element of the liquid stream moving in a pipeline is equal to $\rho S_t dx$, where S_t is the flow passage cross sectional area of the pipeline, ρ is the density of the liquid, then with $\sin(\bar{\omega} \wedge \bar{v}_r) = 1$ the Coriolis force will be equal to

$$dY_k = 2\rho S_t \omega v_r dx$$

and directed opposite to the acceleration.

The elementary moment of the Coriolis force relative to the center of mass is

$$dM_k = 2\omega S_t v_r \rho (x - x_m) dx.$$

In view of the fact that, when the engine reaches its steady-state operation, the flow of mass per second m_{cj} across any cross section of the stream from the surface of the liquid in the tank to a section of the nozzle is constant

$$\rho_j S_{tj} v_{rj} = m_{cj} = \text{const},$$

the moment M_c can be determined by summing the elementary moments over all streams in the tanks from which the components disperse:

$$M_x = 2\dot{\vartheta} \sum_{(j)} m_{cj} \int_{x_{0j}}^{l_t} (x - x_u)\, dx, \qquad (1.4)$$

where x_{0j} is the distance from the top of the rocket to the surface of the liquid in the j-th tank; l_t is the distance from the top of the rocket to a section of the engine nozzle.

For $x > x_u$ the direction of the moment is opposite to the rotation of the body; for $x < x_u$ the direction is the same.

When the rocket is flying through the dense layers of the atmosphere, the moment of the Coriolis forces, M_c, is significantly less than the damping moment M_d of the aerodynamic forces. Beyond the atmosphere, the moment of the Coriolis force becomes dominant. Thus,

$$M_z = M_z' + M_x. \qquad (1.5)$$

The lateral force

$$Y_z = -\int_0^l \frac{\partial Y}{\partial x}\, dx + 2\dot{\vartheta} \sum_{(j)} m_{cj} (l_u - x_{0j})$$

is very small and is usually neglected in calculations.

The liquid-fuel rockets utilize rotational engines and jet vanes as their principal guiding devices [13, 17, 21]. Sometimes additional devices are used such as air vanes, but they are effective only at high velocity pressures.

The gasdynamic surface forces acting on the vane are reduced to the following forces: the lift $Y_{g.r}$, the drag $X_{g.r}$, both of which are applied to the rotation axis of the vane, and the hinge moment $M_{g.sh}$. These quantities can be calculated from the usual formulas:

$$Y_{r.p} = q_r S_r c_{yr}^{\delta} \delta_r, \quad X_{r.p} = q_r S_r c_{xr}, \qquad (1.6)$$
$$M_{r.m} = q_r S_r l_r c_{mr}^{\delta} \delta_r,$$

where q_g is the impact pressure of the gas stream flowing past the vane; S_g, l_g are the characteristic area and length of the jet vane; δ_g is the rotation angle of the jet vane.

The rotation angle varies within a considerable range in the powered section of the trajectory. Therefore, the coefficients c_{yg}^{δ}, c_{xg}, c_{mg}^{δ} depend not only on the shape of the vane and the location of the rotation axis, but also on the angle δ_g.

The force of drag $X_{g.r}$ reduces the thrust of the gas vanes. In the case of the air vanes, we have similarly as before:

$$Y_{a.p}=qS_a c_{ya}^{\delta}\delta_a, \quad X_{a.p}=qS_a c_{xa}, \qquad (1.7)$$
$$M_{a.m}=qS_a l_a c_{ma}^{\delta}\delta_a, \quad q=\frac{\rho v^2}{2}.$$

Here δ_B is the rotation angle of the air vane relative to the body.

In addition to the hinge moments, deflections of the gas and air vanes result in damping moments which are proportional to the angular velocity $\dot{\delta}$. The magnitudes of the hinge and damping moments are, however, extremely small compared to the magnitude of the moment of force $Y_{g.r}$ (or $Y_{v.r}$) relative to the center of mass of the rocket. Therefore, they are usually neglected in the equations of motion. The hinge moment of the vane is important only in analyzing the operation of the control actuators (servos) that deflect the vanes.

If the rotational engines serve as the guiding devices, then

$$Y_p=P\sin\delta, \quad X_p=P(1-\cos\delta),$$

and for small rotation angles

$$Y_p\approx P\delta, \quad X_p\approx P\frac{\delta^2}{2}\approx 0. \qquad (1.8)$$

Irrespective of what guiding devices are used, we shall assume below that for small rotation angles δ the vane force of drag X_p does not depend on the angle δ, and the lateral guiding force Y_p is proportional to the angle δ.

We have in general

$$Y_y = R'_{yy}\delta, \tag{1.9}$$

where R'_{yy} is the gradient of the vane guiding force.

The thrust of the rocket engine at a constant fuel consumption per second depends on the flight altitude. This dependence may be represented by the following formula

$$P = P_0 + S_a(p_0 - p_H),$$

where P_0 is the engine thrust at the surface of the Earth; S_a is the cross sectional area of the nozzle; p_0, p_H are the static air pressure at the surface of the Earth and at an altitude H. During the ascent stage the thrust smoothly increases as the atmospheric pressure decreases.

Depending on the character of the engine start-up, the thrust may increase faster or slower, continuously or in steps. In the same way, when the engine is shut off the thrust does not disappear suddenly, and one observes the lag effect. After the engine cut-off, a small thrust is still produced as a result of the after burn. The amount of time that the engine needs to reach a normal mode of operation and in particular the lag period, are, however, a small fraction of the total operating time of the engine.

The thrust is called effective if it is smaller than the engine thrust by the amount of drag of the gas vanes, i.e.

$$P_e = P - X_{r.g}$$

The weight of the rocket during flight changes both as a result of a change in the mass m of the rocket, and a variation in the gravitational acceleration g.

The mass of the rocket at a given time of flight t is equal to the initial mass m_0 minus the mass of the fuel consumed, i.e.

$$m = m_0 - \int_0^t m_c dt.$$

The gravitational acceleration at a height H above the surface of the Earth is

$$g = g_0 \frac{R_0^2}{(R_0 + H)^2}, \tag{1.10}$$

where g_0 is the gravitational acceleration at the surface of the Earth; R_0 is the Earth's radius.

2. Equations of Motion for a Rocket

During the burn of the engine, the mass of the rocket decreases so that the rocket becomes a body with a variable mass. We shall deduce the equations of motion using the principle of solidification. Based on this principle, the equations of motion for an arbitrary moment of time will be written as the equations of motion for a solid body of constant composition (for that moment of time) with the reactive and Coriolis forces included among the external forces.

The equations of motion of the center of mass and of rotation relative to the center of mass are in vector form

$$m\bar{a} = \Sigma F, \quad \frac{d\bar{K}}{dt} = \Sigma \bar{M}, \tag{1.11}$$

where m is the mass of the rigid body (rocket); $\bar{a} = d\bar{v}/dt$ is the acceleration of the center of mass in the inertial coordinate system;

ΣF is the sum of all external forces applied to the body;
$\bar{K}$ is the principal angular momentum of the solid body;
$\Sigma \bar{M}$ is the principal moment of the external forces applied to the body.

We shall project the first equation in (1.11) onto the moving rectangular coordinate axes Oxyz with the origin at the center of inertia of the rigid body. We obtain [3]

$$\begin{aligned} m\left(\frac{dv_x}{dt}+\Omega_y v_z-\Omega_z v_y\right)&=\Sigma F_x,\\ m\left(\frac{dv_y}{dt}+\Omega_z v_x-\Omega_x v_z\right)&=\Sigma F_y,\\ m\left(\frac{dv_z}{dt}+\Omega_x v_y-\Omega_y v_x\right)&=\Sigma F_z. \end{aligned} \tag{1.12}$$

Here v_x, v_y, v_z are the projections of the velocity vector for the center of inertia onto the moving axes;

$\Omega_x, \Omega_y, \Omega_z$ are the projections of the angular velocity vector of the moving axes relative to the stationary axes onto the moving axes;

$\Sigma F_x, \Sigma F_y, \Sigma F_z$ are the sums of the projections of the external forces acting on the solid body, onto the moving axes.

The second equation in (1.11), for the rotational motion, will be put in Euler's form [21] using the principal axes of inertia of the rocket as the moving coordinate axes. We assume that the directions of these axes relative to the body are independent of the fuel consumption and remain constant. We have

$$\begin{aligned} I_1\frac{d\omega_1}{dt}+(I_3-I_2)\omega_2\omega_3&=\Sigma M_1,\\ I_2\frac{d\omega_2}{dt}+(I_1-I_3)\omega_3\omega_1&=\Sigma M_2,\\ I_3\frac{d\omega_3}{dt}+(I_2-I_1)\omega_1\omega_2&=\Sigma M_3. \end{aligned} \tag{1.13}$$

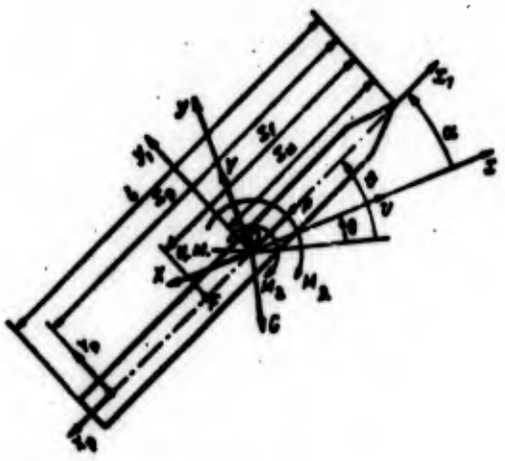

Figure 1.5

Here I_1, I_2, I_3 are the principal moments of inertia of the rigid body (the rocket);

$\omega_1, \omega_2, \omega_3$ are the projections of the angular velocity vector of the moving

axes relative to the stationary axes onto the principal axes of inertia;

$\Sigma M_1, \Sigma M_2, \Sigma M_3$ are the sums of the projection of the moment of external forces onto the principal axes of inertia.

A programmed flight stipulates that the ballistic rocket move in the vertical plane x_0Ay_0 which coincides with the vertical plane of symmetry of the rocket x_1Oy_1. Thus, in the programmed motion we usually have $\psi=\beta=\varphi=0$. The motion of a rocket in the vertical plane will also be called longitudinal motion or a motion in the plane of pitch.

For certain reasons the real motion will always deviate from the programmed one, so that in addition to the longitudinal motion there may at the same time exist a lateral motion with the coordinates ψ and β which is called a motion in the plane of yawing or a yawing motion. A motion measured by the coordinate φ is called a rotation relative to the longitudinal axis of the rocket or a banking motion.

The presence of the planes of symmetry in a rocket makes it possible to divide a general motion, described by Equations (1.12) and (1.13), into the longitudinal motion (in the yawing plane), and a rotation relative to the longitudinal axis.

If the kinematic parameters of motion in the yawing plane and the deflections of the guiding devices due to this motion are assumed small, and if the flight trajectory deviates little from the plane, then the longitudinal motion will be practically independent of the motion in the yawing plane. The analysis of the yawing and banking motion can, however, be done only after the longitudinal motion parameters are calculated.

Let us assume that the stabilization of the rocket is done separately with respect to the pitch, yaw, and banking. Then the equations describing the operation of the guiding system in the planes of pitch, yaw, and banking will be independent of each other. In

this case the equations of motion for a guided rocket in the plane of pitch may be obtained and analyzed independently of the equations of motion in the yawing plane.

Figure 1.5 shows the forces acting on a rocket. Let us find the equations of motion for a rocket moving in a vertical plane in the moving coordinate system. Assuming that in Equations (1.12) and (1.13), we obtain $v_x=v$, $v_y=v_z=0$, $\Omega_y=\omega_1=\omega_2=0$, $\omega_3=\dot{\vartheta}$, $\Omega_z=\dot{\theta}$,

$$\begin{aligned} m\dot{v} &= (P-X_p)\cos\alpha - X - G\sin\vartheta - Y_p\sin\alpha + X_в, \\ mv\dot{\theta} &= (P-X_p)\sin\alpha + Y - G\cos\vartheta + Y_p\cos\alpha + Y_в, \\ I_z\ddot{\vartheta} &= -M_в - M_д - Y_p(x_p - x_м) + M_в. \end{aligned} \tag{1.14}$$

Here $X_в$, $Y_в$, $M_в$ are the perturbing forces and moment; G is the weight of the rocket.

To guarantee control and stability of motion, the rocket stabilization system utilizes sensor signals which are proportional to the accelerations along the longitudinal and lateral axes of the rocket. These signals can be computed directly from the equations of motion in the body coordinate system.

The projections of the velocity onto the Ox_1 and Oy_1 axes of the body coordinate system (cf. Figure 1.5) will be $v_{x1}=v\cos\alpha$, $v_{y1}=-v\sin\alpha$. For this coordinate system in Equations (1.12) and (1.13) one should set $v_{z1}=0$, $\Omega_y=\Omega_z=\omega_2=\omega_1=0$, $\omega_3=\Omega_z=\dot{\vartheta}$. Then we get

$$\begin{aligned} m(\dot{v}_{x1} - \dot{\vartheta}v_{y1}) &= (P-X_p) - X\cos\alpha + Y\sin\alpha - G\sin\vartheta + X'_в, \\ m(\dot{v}_{y1} + \dot{\vartheta}v_{x1}) &= Y\cos\alpha + X\sin\alpha - G\cos\vartheta + Y_p + Y'_в, \\ I_z\ddot{\vartheta} &= -M_в - M_д - Y_p(x_p - x_м) + M'_в, \\ v_x &= v\cos\alpha, \\ \operatorname{tg}\alpha &= -\frac{v_{y1}}{v_{x1}}. \end{aligned} \tag{1.15}$$

Here $X'_в$, $Y'_в$, $M'_в$ are the perturbing forces and moments which we shall regard as given.

In order to find a solution of Equations (1.14) or (1.15) one must know how the control forces $Y_p(t)$ vary with time. This time dependence is given by a system of equations and depends on the type and structure of the system. The equation of the control system can be represented as follows

$$\delta(t)=\delta(\theta, \dot{\theta}, \ldots, v_y). \tag{1.16}$$

Equations (1.14) and (1.15) were obtained under the assumption that the starting system of coordinates is inertial. The rotation of the starting system with Earth makes it necessary, in general, to consider the centrifugal, $\bar{a}_{per}$ and Coriolis accelerations, $\bar{a}_c$, of the rocket as well [4].

3. Calculation of the Rocket Trajectory of Motion

If we regard the time dependence of the rotation angle of the control devices $\delta=\delta(t)$ as given, then from Equations (1.14) one can for any moment of time determine the velocity v and angle θ, and from the equations

$$x_0=\int_0^t v\cos\theta\,dt, \quad y_0=\int_0^t v\sin\theta\,dt$$

one can calculate the coordinates of the center of mass in the system $Ax_0y_0z_0$, i.e., the trajectory of the rocket. However, Equations (1.14) are non-linear with variable coefficients, and are not easy to solve.

In the practical calculation of the flight trajectory and the parameters of the unperturbed motion, Equations (1.14) are considerably simplified. Thus, since the preset motion of a rocket involves only small angular velocities and accelerations, we can assume that $\dot{\theta}_{pr}\approx\ddot{\theta}_{pr}\approx 0$. In this case the third equation in (1.14) will represent an equation of equilibrium between the aerodynamic moment and the moment of the control forces, called the balance equation

$$qSlc_m^{\alpha}\alpha_{ap}=-R_p^1(x_p-x_m)\delta_{ap}.$$

where x_p is the distance between the top of the rocket and a point of application of the control force. From this equation, one can determine the programmed rotation angle of the vanes δ_{pr} which is necessary to maintain the required programmed angle of attack α_{pr}. In the calculations of the trajectory and the parameters of unperturbed motion, the control system is assumed to be ideal. In other words, changes in the rotation angle of the control devices are assumed to follow exactly the programmed changes.

If the form of the trajectory, i.e., the time dependence of the angle θ_{pr} representing the slope of the tangent line, is known beforehand, then the second equation in (1.14) may be used to determine the angle of attack required to obtain a given trajectory

$$\alpha_{np} = \frac{\dot{\theta}_{np} + \frac{g \cos \theta_{np}}{v}}{P - X_p + \frac{\rho v^2}{2} S \left(c_y^\alpha - \frac{l}{x_p - x_u} c_m^\alpha \right)}.$$

Since the angle of attack for ballistic missiles in flight is usually small, we may neglect it as a first approximation, and consider a trajectory with $\alpha = 0$. Thus, the most simplified equations to calculate velocity v, acceleration $\dot{v}$, and the trajectory will have the form

$$\dot{v} = \frac{1}{m} \left(P - X_p - \frac{\rho v^2}{2} S c_x \right) - g \sin \theta_{np}.$$

$$x_0 = \int_0^t v \cos \theta_{np} dt, \quad y_0 = \int_0^t v \sin \theta_{np} dt.$$

In this case the error with which the acceleration $\dot{v}$ is determined is 10 - 20% smaller than the error due to an inexact value of the coefficient c_x.

If the trajectory is calculated for a distance larger than 50 km, then it is necessary to take into account the curvature of the Earth.

The relationship between the coordinates x_0, y_0, the chord L of an arc along Earth's circumference, and a local altitude H may be determined from the following geometric relations (Figure 1.6):

$$(R_0+H)\cos\varphi=R_0+y_0,$$

$$x_0-H\sin\varphi-L\cos\left(\frac{\varphi}{2}\right)=0,$$

$$\sin\left(\frac{\varphi}{2}\right)=\frac{L}{2R_0}.$$

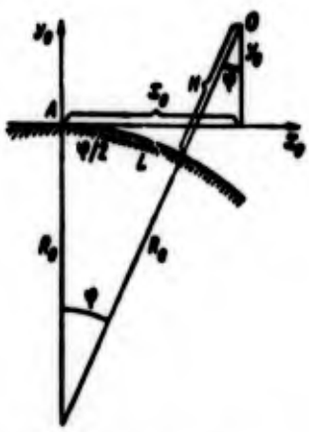

Figure 1.6

In addition, if one wants to determine the full range of the flight more precisely it is necessary to include the Coriolis acceleration.

4. Equations of the Perturbed Motion

As mentioned above the real motion will always differ from the programmed one. The causes of this difference will be called the perturbing factors. These factors may be both constant and random.

A distortion in the external geometry of the body, lack of alignment between the engine and the body, a deviation from the calculated values of the engine thrust and the initial weight, a change in the effectiveness of the guiding devices, and other factors act in a stationary way, and for a given rocket are the systematic perturbing factors. These perturbations may be accounted for in Equations (1.14) by the terms X_B, Y_B and M_B.

Since the perturbing factors X_B, Y_B, M_B may be different for different rockets, the actual trajectories and motion parameters in

the powered stage will be, as it were, enclosed in a tube whose axis is the programmed trajectory.

The motion of a rocket in a tube of trajectories will be called nominal motion. From the characteristics of the perturbations, one can determine the size of the tube of trajectories, which is the starting data in computing a scattering of the trajectories.

Short-time perturbations such as wind gusts, brief changes of the engine thrust, noise and ghost signals in the guiding system, are usually random, and it is impossible to take them into account in the equations of motion although they also influence the motion of a rocket. This is explained by the fact that we do not know the time and the magnitude of these random perturbing factors.

These random disturbances have an effect of changing the parameters of motion. Therefore, the value of any of the parameters may be represented as consisting of the nominal value (without considering the disturbance) and some small deviation, called the perturbation:

$$v_1=v_2+v,\ \theta_1=\theta_2+\theta,\ \vartheta_1=\vartheta_2+\vartheta,\ \alpha_1=\alpha_2+\alpha,\ \delta_1=\delta_2+\delta. \tag{1.17}$$

Equations (1.14) and (1.15) are valid for arbitrary functions $v_2, \theta_2, \vartheta_2, \delta_2$; in particular they are also valid for the functions representing the nominal motion: $v_2, \theta_2, \vartheta_2, \delta_2$.

Usually in linearizing the equations of motion one neglects the effect that an increase in altitude has on the aerodynamic forces and moments, and on the engine thrust since for short time intervals this effect is insignificant.

Let us substitute the values of variables from Equations (1.17) into Equations (1.14). This will bring Equations (1.14) into the form involving the parameters of the nominal motion. Assume that

$\cos\alpha_н \approx 1$, $\sin\alpha_н \approx \alpha_н$, and that the perturbations v, θ, ϑ, α and δ are small. Retaining only first order terms, we shall obtain the following equations in the moving coordinate system in terms of the perturbations:

$$\begin{aligned}
m\dot{v} &= -P_{н}x_{а}z - \rho v_{н}Sc_{x}v - G\cos\theta_{н}\theta - R^{1}_{yp}(x_{а}\delta + \delta_{н}z),\\
mv_{н}\dot{\theta} &= P_{н}x + G\sin\theta_{н}\theta + \frac{\rho v_{н}^{2}}{2}Sc^{\alpha}_{y}z + \rho v_{н}Sc^{\alpha}_{y}x_{а}v + R^{1}_{yp}(\delta - \delta_{н}x_{а}z),\\
I_{z}\ddot{\vartheta} &= -\frac{\rho v_{н}^{2}}{2}Slc^{\alpha}_{m}z - \rho v_{н}Slc^{\alpha}_{m}x_{а}v - \frac{\rho v_{н}}{2}Sl^{2}c^{\dot{\vartheta}}_{m}\dot{\vartheta} - \\
&- R^{1}_{yp}(x_{p} - x_{т})\delta - \frac{\rho}{2}Sl^{2}c^{\dot{\delta}}_{m}\dot{\delta}_{н}v - 2\sum_{(n)} m_{cj}\int_{x_{cj}}^{x_{k}}(x - x_{т})\,dx\,\dot{\vartheta}.
\end{aligned} \tag{1.18}$$

The unknowns here are the perturbations of the parameters of motion v, θ, ϑ, α, δ. The functions $v_{н}$, $\theta_{н}$, $\vartheta_{н}$, $\alpha_{н}$, and $\delta_{н}$ that characterize the nominal motion are considered as known. They can be obtained by solving Equations (1.14) and Equation (1.16). Since the nominal motion differs only slightly from the preset motion, in Equations (1.18) one can use instead of the nominal values the programmed values v_{pr}, G_{pr}, $\dot{\vartheta}_{pr}$, and α_{pr} which have already been computed for the programmed motion. Then Equations (1.18) will be written as

$$\begin{aligned}
\dot{v} + c_{vv}v + c_{v\theta}\theta + c_{v\dot{\vartheta}}\dot{\vartheta} + c_{v\delta}\delta &= 0,\\
\dot{\theta} + c_{\theta v}\theta + c_{\theta\dot{\vartheta}}\dot{\vartheta} + c_{\theta v}v + c_{\theta\delta}\delta &= 0,\\
\ddot{\vartheta} + c_{\dot{\vartheta}\dot{\vartheta}}\dot{\vartheta} + c_{\dot{\vartheta}\theta}\theta + c_{\dot{\vartheta}\dot{\theta}}\dot{\theta} + c_{\dot{\vartheta}v}v + c_{\dot{\vartheta}\delta}\delta &= 0.
\end{aligned} \tag{1.19}$$

Here we introduced the following notation for the coefficients: in the first equation

$$\begin{aligned}
c_{vv} &= \frac{1}{m}\rho v_{н}Sc_{x},\\
c_{v\theta} &= \frac{1}{m}(G\cos\theta_{н} - P_{н}x_{а} - R^{1}_{yp}\delta_{н}),\\
c_{v\dot{\vartheta}} &= \frac{1}{m}(P_{н}x_{а} + R^{1}_{yp}\delta_{н}),\\
c_{v\delta} &= -\frac{1}{m}R^{1}_{yp}x_{а};
\end{aligned} \tag{1.20}$$

and in the second and third equation

$$
\begin{aligned}
c_{00} &= \frac{1}{m v_n}\left(P_0 - G\sin\theta_n + \frac{\rho v_n^2}{2} S c_y^\alpha - R_{yy}^\delta \delta_n z_n\right),\\
c_{01} &= \frac{1}{m v_n}\left(-P_0 - \frac{\rho v_n^2}{2} S c_y^\alpha + R_{yy}^\delta \delta_n z_n\right),\\
c_{02} &= -\frac{1}{m v_n}\rho v_n S c_y^\alpha z_n,\\
c_{04} &= -\frac{1}{m v_n} R_{yy}^\delta,\\
c_{10} &= \frac{1}{I}\left(\frac{\rho v_n}{2} S l c_m^\delta + 2\sum_{(l)} m_{cj}\int_{x_{aj}}^{l_n}(x - x_n)\,dx\right),\\
c_{11} &= \frac{1}{I}\cdot\frac{\rho v_n^2}{2} S c_m^\alpha = -c_{01},\\
c_{12} &= \frac{1}{I}\left(\rho v_n S c_m^\alpha z_n + \frac{\rho}{2} S l^2 c_m^\delta \delta_n\right),\\
c_{14} &= \frac{1}{I} R_{yy}^\delta (x_p - x_n),\quad I = I_z.
\end{aligned}
\tag{1.21}
$$

As distinguished from Equations (1.14), Equations (1.19) are called equations of the perturbed motion or equations with variations. They are linear differential equations with variable coefficients. The coefficients in the equations can be expressed in terms of the rocket characteristics m, I, P_0, R_{yy}^δ, x_p, x_n, parameters of the undisturbed motion v_n, θ_n, $\dot{\theta}_n$, α_n, δ_n, the air density, and aerodynamic coefficients. Therefore, these coefficients can be calculated.

How we shall find the equations of the perturbed motion of a rocket in the moving coordinate system in the plane of yaw.

An undisturbed motion of a rocket takes place in the pitch plane. Therefore, in the yaw plane all the parameters of the nominal motion and the external forces are identically equal to zero. We shall assume that the perturbations in the plane of yaw are small, and define them in terms of the yaw angle ψ, the sideslip angle β, the angle of rotation of the trajectory with respect to the plane of the unperturbed motion σ, and the angle of rotation of the control elements δ.

In view of the smallness of perturbations and planes of symmetry in a rocket, the perturbed motion in the plane of yaw will not depend on disturbances in the plane of pitch.

With the appearance of the sideslip angle there arises a lateral aerodynamic force Z and aerodynamic moment M_{ya}, equal to

$$Z = qSc_z^\beta \beta, \quad M_{ya} = qSlc_m^\beta \beta.$$

Here as a result of the axial symmetry in the fuselage of a rocket for $\alpha_n = 0$ the derivative $c_z^\beta = c_y^\alpha$ and $c_m^\beta = c_m^\alpha$.

A rotation of the fuselage with angular velocity $\dot{\psi}$ causes a damping moment in the yaw plane. On the basis of Equations (1.3) and (1.4) we have

$$M_{yz} = \frac{\rho v^2}{2} Slc_m^{\dot{\beta}} \frac{\dot{\psi} l}{v} + 2\frac{\dot{\psi}}{v} \sum_{(l)} m_{cj} \int_{x_{0j}}^{l_n} (x - x_m)\, dx.$$

The equations of the perturbed motion in the plane of yaw may be obtained from Equations (1.18) by replacing variations $\theta, \vartheta, \alpha$ with variations σ, ψ, β, respectively, and setting $G = 0$, $\beta_n = \psi_n = \delta_n = 0$. In this case, the second and third equation will not connect with the first one. Thus, equations of the perturbed motion in the moving coordinate system will assume the form

$$\begin{aligned} &\dot{\sigma} + c_{\sigma\sigma}\sigma + c_{\sigma\dot{\psi}}\dot{\psi} + c_{\sigma\psi}\psi = 0, \\ &\ddot{\psi} + c_{\dot{\psi}\dot{\psi}}\dot{\psi} + c_{\dot{\psi}\psi}\psi + c_{\psi\sigma}\sigma + c_{\psi\psi}\psi = 0, \\ &\beta = \psi - \sigma, \end{aligned} \tag{1.22}$$

where

$$\begin{aligned} c_{\sigma\dot{\psi}} &= -c_{zz} = \frac{1}{mv_a}\left(P_0 + \frac{\rho v_a^2}{2} Sc_z^\beta\right), \\ c_{z\psi} &= -\frac{1}{mv_a} R_{xp}^\beta, \\ c_{\dot{\psi}\dot{\psi}} &= \frac{1}{I}\left(\frac{\rho v_a}{2} Sl^2 c_m^{\dot{\beta}} + 2\sum_{(l)} m_{cj} \int_{x_{0j}}^{l_n} (x - x_m)\, dx\right), \\ c_{\psi\psi} &= -c_{\psi\sigma} = \frac{1}{I}\frac{\rho v_a^2}{2} Slc_m^\beta, \\ c_{\psi\psi} &= \frac{1}{I} R_{xp}^\beta (x_p - x_m), \quad I = I_y = I_z. \end{aligned} \tag{1.23}$$

Under the assumptions made earlier a small perturbation φ in the plane of roll will depend only on the perturbations in the angles of rotation of the control elements. The moment of the control forces acting on vanes relative to the longitudinal axis of the rocket is

$$M_{xp} = M^{\delta}_{xp}\delta_x,$$

where δ_x is a generalized angle of rotation of the control elements relative to the longitudinal axis Ox_1; M^{δ}_{xp} is the gradient of the control moment.

The equation for the perturbed motion relative to the longitudinal axis will be

$$\ddot{\varphi} + c_{\varphi\dot{\varphi}}\dot{\varphi} + c_{\varphi\delta}\delta_x = 0, \quad c_{\varphi\delta} = \frac{1}{I_x} M^{\delta}_{xp}. \tag{1.24}$$

Here $I_x c_{\varphi\dot{\varphi}}\dot{\varphi}$ denotes the damping moment relative to the longitudinal axis which may arise, for example, with the presence of fins on the fuselage of a rocket.

Let us find the equations of the perturbed motion of a rocket in the pitch plane relative to the body coordinate system. Equations in this system of coordinates are necessary for the analysis of the accelerations measured by the sensor elements of the stabilizing system, inasmuch as the orientation of the sensor elements is connected with the geometric axes of the rocket airframe.

Letting in (1.15) $v_{x1B} = v_{x1n} + v_{x1}$, and $v_{y1B} = v_{y1n} + v_{y1}$ and taking (1.17) into account, we obtain the following equations of the perturbed motion in the body coordinate system Ox_1y_1:

$$m(\dot{v}_{x1}-\dot{\theta}v_{y1n}-\dot{\theta}_n v_{y1})=\frac{\rho v_n^2}{2}Sc_x\alpha_n\alpha-\rho v_n Sc_x v+$$

$$+\frac{\rho v_n^2}{2}Sc_y^{\alpha}2\alpha_n\alpha+\rho v_n Sc_y^{\alpha}\alpha_n^2 v-G\cos\vartheta_n\vartheta,$$

$$m(\dot{v}_{y1}+\dot{\theta}v_{x1n}+\dot{\theta}_n v_{x1})=-\frac{\rho v_n^2}{2}Sc_y^{\alpha}\alpha_n^2\alpha+\frac{\rho v_n^2}{2}Sc_y^{\alpha}\alpha+\rho v_n Sc_y^{\alpha}\alpha_n v+ \quad (1.25)$$

$$+\frac{\rho v_n}{2}Sc_x\alpha+\rho v_n Sc_x\alpha_n v+G\sin\vartheta_n\vartheta+R_{yp}^{\delta}\delta,$$

$$I_z\ddot{\vartheta}=-\frac{\rho v_n^2}{2}Slc_m^{\alpha}-\rho v_n Slc_m^{\alpha}\alpha_n v-\frac{\rho v_n}{2}Sl^2c_m^{\dot{\vartheta}}\dot{\vartheta}-R_{yp}^{\delta}\times$$

$$\times(x_p-x_n)\delta-\frac{\rho}{2}Sl^2c_m^{\dot{\delta}}\dot{\delta}_n v-2\sum_{(l)}m_{cj}\int_{x_{0j}}^{l_n}(x-x_n)\,dx\dot{\vartheta}.$$

Let us express variations v and α in terms of v_{x1} and v_{y1}. Since $v_{x1}=v\cos\alpha$ and $v_{y1}=-v\sin\alpha$, we have

$$v_{x1n}+v_{x1}=(v_n+v)\cos(\alpha_n+\alpha),$$
$$v_{y1n}+v_{y1}=-(v_n+v)\sin(\alpha_n+\alpha).$$

Up to second order infinitesimals, we have

$$v_{x1}=v-v_n\alpha_n\alpha,\quad v_{y1}=-v\alpha_n-v_n\alpha.$$

Neglecting α_n^2, we find

$$v=v_{x1}-\alpha_n v_{y1},$$
$$\alpha=-\frac{1}{v_n}(\alpha_n v_{x1}+v_{y1}). \quad (1.26)$$

Replacing in (1.25) variations v and α by their expressions from (1.26), we obtain the equations of the perturbed motion in the body coordinate system

$$\dot{v}_{x1}+c_{v_xv_x}^{\dot{}}v_{x1}+c_{v_xv_y}^{\dot{}}v_{y1}+c_{v_x\vartheta}^{\dot{}}\vartheta+c_{v_x\dot{\vartheta}}^{\dot{}}\dot{\vartheta}=0,$$
$$v_{y1}+c_{v_yv_y}^{\dot{}}v_{y1}+c_{v_yv_x}^{\dot{}}v_{x1}+c_{v_y\vartheta}^{\dot{}}\vartheta+c_{v_y\dot{\vartheta}}^{\dot{}}\dot{\vartheta}+c_{v_y\delta}^{\dot{}}\delta=0, \quad (1.27)$$
$$\ddot{\vartheta}+c_{\dot{\vartheta}\dot{\vartheta}}^{\dot{}}\dot{\vartheta}+c_{\vartheta\vartheta}^{\dot{}}\vartheta+c_{\dot{\vartheta}v_x}^{\dot{}}v_{x1}+c_{\dot{\vartheta}v_y}^{\dot{}}v_{y1}+c_{\vartheta\delta}^{\dot{}}\delta=0,$$

where the following notation was introduced for the coefficients in the first equation

$$\begin{aligned} c'_{v_x v_x} &= \frac{1}{m}\rho v_n S c_x, \\ c'_{v_x v_y} &= -\dot{\vartheta}_n + \frac{1}{m}\frac{\rho v_n}{2} S a_n (2c_y^a - c_x), \\ c'_{v_x \vartheta} &= \frac{1}{m} G\cos\vartheta_n, \\ c'_{v_x \dot{\vartheta}} &= v_n a_n; \end{aligned} \tag{1.28}$$

and the second equation

$$\begin{aligned} c'_{v_y v_y} &= \frac{1}{m}\frac{\rho v_n}{2} S (c_y^a + c_x), \\ c'_{v_y v_x} &= \dot{\vartheta}_n - \frac{1}{m}\frac{\rho v_n}{2} S a_n (c_y^a + c_x), \\ c'_{v_y \vartheta} &= -\frac{1}{m} G\sin\vartheta_n, \\ c'_{v_y \dot{\vartheta}} &= v_n, \\ c'_{v_y \delta} &= -\frac{1}{m} R^{\delta}_{zp}. \end{aligned} \tag{1.29}$$

In (1.28) and (1.29) the terms proportional to a_n^2, $\dot{\vartheta}_n a_n$, a_n^3 being negligible were left out. For the third equation the variation of the angle of attack is defined by

$$a = \vartheta - \frac{v_{y1}}{v_n}.$$

Therefore,

$$\begin{aligned} c'_{\dot{\vartheta} v_x} &= \frac{1}{I v_n}\frac{\rho v_n^2}{2} S l \left(c_m^a a_n + \frac{l c_m^{\dot{\vartheta}} \dot{\vartheta}_n}{v_n} \right), \\ c'_{\dot{\vartheta} v_y} &= -\frac{1}{I v_n}\frac{\rho v_n^2}{2} S l c_m^a, \quad I = I_z. \end{aligned} \tag{1.30}$$

The coefficients $c_{m\dot{\vartheta}}$, $c_{m\vartheta}$ and $c_{m\delta}$ were defined in (1.21).

The equations in the body coordinate system in the plane of yaw can be obtained from (1.27) - (1.30) by setting

$$v_{y1} = v_{z1},\ \vartheta = \psi,\ a = \beta,\ a_n = \vartheta_n = \dot{\vartheta} = 0,\ G = 0.$$

In order to investigate the effect of brief disturbances within a short time interval, we shall assume below that the trajectory of the undisturbed motion of the rocket center of mass is a straight line. We shall set up equations of the perturbed motion in the pitch plane relative to a fixed system of coordinates. Equations of this sort are more convenient in studying the perturbed motion of a rocket where the oscillations of liquids and elastic oscillations of the fuselage are taken into account.

Let the Ox axis of the fixed coordinate system point along the tangent to the trajectory of the unperturbed motion, and the Oy axis be perpendicularly to it (Figure 1.7).

An unperturbed motion in the plane of pitch relative to a fixed coordinate system is characterized by the following equations

$$\begin{gathered} m\dot{v}_{xn} = P_n \cos\alpha_n - X_n - G\sin\theta_n - Y_{p.n}\sin\alpha_n, \quad v_{xn} = v_n, \\ \dot{v}_{yn} = 0, \quad Y_n + P_n \sin\alpha_n - G\cos\theta_n + Y_{p.n}\cos\alpha_n = 0, \\ \dot{\theta}_n = 0, \quad M_{z.n} + Y_{p.n}(x_p - x_n) = 0. \end{gathered} \tag{1.31}$$

Let v_x and v_y denote small perturbations of the projections of the center of mass velocity onto the fixed coordinate axes. Let ϑ be a small perturbation in the pitch angle, and δ a small perturbation in the angle of rotation of a control element. As a result of the perturbations the velocity vector will be deflected by an angle v_y/v_n, and a new value of the angle of attack will be

$$\alpha_n = \alpha_n + \alpha, \quad \alpha = \vartheta - \frac{v_y}{v_n}. \tag{1.32}$$

The plane motion in the fixed coordinate system Oxy is determined by the following equations

$$\begin{gathered} m\dot{v}_x = P_n \cos(\alpha_n + \vartheta) - G\sin\theta_n - X^a \cos\left(\frac{v_y}{v_n}\right) - Y^a \sin\left(\frac{v_y}{v_n}\right) - \\ - Y_p^a \sin(\alpha_n + \vartheta), \\ m\dot{v}_y = P_n \sin(\alpha_n + \vartheta) - G\cos\theta_n - X^a \sin\left(\frac{v_y}{v_n}\right) + Y^a \cos\left(\frac{v_y}{v_n}\right) + \\ + Y_p^a \cos(\alpha_n + \vartheta), \\ I\ddot{\vartheta} = -M_z^a - M_z^a - Y_p^a (x_p - x_n). \end{gathered} \tag{1.33}$$

Expressing the disturbing forces and moments X^*, Y^*, Y_p^*, M_D^*, M_a^* in terms of the quantities in (1.17), and subtracting (1.31) from (1.33), we obtain equations of the rocket motion in the fixed coordinate system in terms of the perturbations v_x, v_y, ϑ and δ;

$$\begin{aligned}
&\dot{v}_x + c_{v_x v_x} v_x + c_{v_x v_y} v_y + c_{v_x \vartheta} \vartheta + c_{v_x \delta} \delta = 0,\\
&\dot{v}_y + c_{v_y v_y} v_y + c_{v_y v_x} v_x + c_{v_y \vartheta} \vartheta + c_{v_y \delta} \delta = 0,\\
&\dot{\delta} + c_{\delta\delta} \delta + c_{\delta\vartheta} \vartheta + c_{\delta v_x} v_x + c_{\delta v_y} v_y + c_{\delta\delta} \delta = 0.
\end{aligned} \tag{1.34}$$

In the first equation the coefficients are defined as follows:

$$\begin{aligned}
c_{v_x v_x} &= \frac{1}{m} \rho v_a S c_x,\\
c_{v_x v_y} &= \frac{1}{m} \frac{\rho v_a}{2} S c_y^a z_a,\\
c_{v_x \vartheta} &= \frac{1}{m} (P_a z_a + R_{yy}^1 \lambda_a),\\
c_{v_x \delta} &= \frac{1}{m} R_{yy}^1 z_a.
\end{aligned} \tag{1.35}$$

Here the variation v is taken as equal to variation v_x. In the second equation

$$\begin{aligned}
c_{v_y v_y} &= \frac{1}{m} \frac{\rho v_a}{2} S (c_y^a + c_x),\\
c_{v_y v_x} &= -\frac{1}{m} \rho v_a S c_y^a z_a,\\
c_{v_y \vartheta} &= -\frac{1}{m} \left(P_a + \frac{\rho v_a^2}{2} S c_y^a - R_{yy}^1 \delta_a z_a \right).
\end{aligned} \tag{1.36}$$

The remaining coefficients $c_{v_y \delta}$, $c_{\delta\delta}$, $c_{\delta\vartheta}$, $c_{\delta v_y}$, $c_{\delta v_x}$ and $c_{\delta\delta}$ are defined in (1.21), (1.29), (1.30).

5. An Analysis of the Equations of the Perturbed Motion

The coefficients in the equations of the perturbed motion (1.19), (1.22), (1.27), and (1.34) are defined in terms of the characteristics of the rocket, air density, and the kinematic parameters of the unperturbed motion, i.e., are known functions of time.

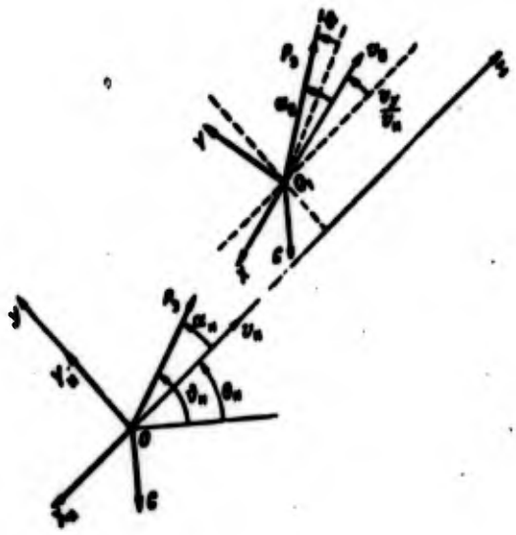

Figure 1.7.

Disregarding the fact that the above mentioned systems of equations are linear with respect to perturbations, their analysis is made more difficult by the presence of variable coefficients. Equations of this type can usually be solved by numerical integration using digital computers or by utilizing analog computers.

In a preliminary analysis done when designing the rocket and its control systems, one commonly uses the so-called method of "freezing" the coefficients of equations [3, 8, 15]. This method allows us to obtain results which, although crude, are nevertheless very general and instructive.

The essence of the method consists in the following. Let, us for example, assume that the coefficients in the system of equations of the perturbed motion (1.19) $c_{11}(t),\ldots,c_{1n}(t)$ were computed for a certain trajectory of unperturbed motion. On this trajectory one selects a number of characteristic points, and instead of the system (1.19) with variable coefficients one considers a set of analogous systems with constant coefficients $c_{11}(t_k),\ldots,c_{1n}(t_k)$, which represent the values of the coefficients in Equations (1.19) at fixed points in time t_k. In other words, the flight time is divided into small segments that include points t_k, and in these segments the equation coefficients are considered constant. This assumption in many cases gives satisfactory results.

The method of "freezing" the coefficients allows us to utilize methods that are widely known in engineering practice such as methods

of solving linear differential equations with constant coefficients, methods of estimating the stability of solutions, frequency methods of the theory of automatic control. At the same time investigations using the technique of "freezing" the coefficients ought to be considered as preliminary and essentially of qualitative nature. They should be supplemented with investigations utilizing other methods, in particular, those making use of analog and digital computers. In these studies it is customary to take into account the specific properties of systems of equations, for instance, their non-linearities. As a result it is possible to increase the precision of results obtained on the basis of linear equations.

Let us consider a perturbed motion of a rocket in the plane of pitch which is described by Equations (1.19). For simplicity we shall assume that the undisturbed motion is rectilinear and steady, and that equation coefficients are constant. We shall use the symbolic notation $\dot{\vartheta}=p\vartheta, \ddot{\vartheta}=p^2\vartheta, \ldots$.

The characteristic polynomial for the system in (1.19) with $\delta=0$ will be

$$L(p)=p^4+a_1p^3+a_2p^2+a_3p+a_4. \qquad (1.37)$$

The coefficients a_1, a_2, a_3, and a_4 are real. Therefore, the roots of the polynomial may be either real or complex conjugate.

As numerous calculations for a statically stable rocket indicate, the characteristic polynomial has two pairs of complex conjugate roots, where the real and imaginary parts of one pair of roots are considerably larger in absolute magnitude than the real and imaginary parts of the second pair of roots. This means that a free perturbed motion can be represented as a sum of two motions: short-period motion, corresponding to the pair of complex roots with large absolute value, and long-period motion, corresponding to the pair of complex roots with small absolute value.

For example, for a hypothetical statically stable rocket the roots of the polynomial (1.37) have at some point in time t_k the following values:

$$p_{1,2} = -0{,}684 \pm i1{,}387; \quad p_{3,4} = -0{,}0066 \pm i0{,}0623;$$

The periods of oscillation are equal to, respectively, $\tau_1 = 4{,}54$ sec; $\tau_2 = 100{,}83$ sec.

Let the disturbed motion of the rocket be caused by an instantaneous deflection of the vanes, where at the moment of deflection we have $v = \theta = \vartheta = \dot{\vartheta} = 0$. If we take the roots of the characteristic equation as p_1, p_2, p_3, and p_4, then we shall obtain the following expressions for the variations $v, \theta, \vartheta, \alpha$.

$$x = A_0 + A_1 e^{-0{,}684t} \cos(1{,}387t + z_1) + A_2 e^{-0{,}0066t} \cos(0{,}0623t + z_2),$$
$$x = v, \theta, \vartheta, \alpha,$$

where for the variation v we always have $|A_1| \ll |A_2|$. Consequently, a change in v is determined mostly by a slowly damped term and has a long period.

A change in the angle of attack α is essentially determined by a rapidly damped term, and thus has a short period of motion. In the expressions for the angles ϑ and θ both the slowly damped and ped rapidly damped terms have real values.

This type of time dependence of the parameters in a perturbed motion does not depend on the type of the rocket. A rocket may change its angle of attack very rapidly by rotating relative to the center of mass. At the same time the velocity of the rocket will change in value relatively slowly, since the longitudinal accelerations $\dot{v}$, related to a change of forces caused by a change of the angle of attack, are very small.

From this we can reach a conclusion that will be used in Chapter III and V: if φ and θ are variations of the first order in smallness, then the variation of the acceleration $\dot{v}(\dot{v}_x)$ caused by deviations in φ and θ, will be second order in smallness. In other words, in the linear setup of the problem the longitudinal acceleration of the rocket does not depend on small deviations φ and θ.

Thus, a perturbed motion of the rocket may be taken to consist of two stages. The first stage has a short period and consists essentially of a rotation of the rocket relative to the center of mass and a rapid change of the angle of attack. Toward the end of this stage the moment of the aerodynamic forces relative to the lateral axis is practically balanced by the moment of the control forces, and the angular velocity $\dot{\varphi}$ is close to zero. However, in the presence of deflections φ and θ the conditions of the equilbrium of forces in the direction of the normal and the tangent to the trajectory will not be satisfied. The second stage of motion has a long period and is slowly damping.. This stage lasts as long as there is no equilibrium of forces. This is a stage of a slow variation in velocity v.

The process of guidance basically consists of changing the direction of the engine thrust vector P_{ef}. This force is directed along the longitudinal axis of the rocket, and thus, its direction is determined by the pitch angle. Since both the angle of attack and the pitch angle practically only change in the short-period stage of the perturbed motion, then just this stage is important in designing the stabilization system for the angular motion. At the same time in the analysis of the velocity control system v, the long period stage will be the most significant one.

We can easily convince ourselves of the negligible effect that velocity v has on variations φ and θ by comparing the connecting coefficients in the second and third equation of (1.19). Thus in the second equation

$$\left|\frac{a_{2v}}{a_{22}}\right| \ll \left|\frac{a_{2\alpha}}{a_{22}}\right|.$$

and in the third one

$$\left|\frac{c_{\alpha_n}}{c_{\omega_n}}\right| \approx \left|\frac{2v_n}{g_n}\right|.$$

Only at the beginning of the flight when the speed v_n is small, and the angle of attack large, is the connection between the equations of importance.

Thus, for the short period stage of the disturbed motion does one assume v = 0 in Equations (1.19). Then

$$\begin{aligned} \dot{\theta} + c_{\omega\omega}\theta + c_{\omega\theta}\theta + c_{\omega\delta}\delta = 0, \\ \ddot{\theta} + c_{\theta\omega}\dot{\theta} + c_{\theta\theta}\theta + c_{\theta\theta}\theta + c_{\theta\delta}\delta = 0. \end{aligned} \tag{1.38}$$

Equations (1.38) are usually referred to as equations of the perturbed motion in the plane of pitch. An analysis of (1.21) implies that the values of the coefficients practically do not change if the small quantities δ_n and α_n are set equal to zero, i.e., if one assumes that an unperturbed motion occurs with the angle of attack c_n=0. Under this assumption Equations (1.38) will differ from the equations of the perturbed motion in the plane of pitch (1.22) by only a value of one coefficient. The formula for $c_{\omega\theta}$ contains a variations of the projections of the weight forces onto the normal to the trajectory($G \sin\theta_n$), whereas the forces of weight have no effect on the pitch motion, and therefore the coefficient $c_{\omega\theta}$ does not depend on them.

In the body and fixed coordinate systems the projection of the forces of the longitudinal axis also changes very little with perturbations. Therefore, just as in the case of the moving coordinate system, by virtue of the smallness of the acceleration $\dot{v}_x$ in the first stage of the perturbed motion, the variation v_x turns out to be small compared to the variations v_y and θ. On that basis in the second and third equation in (1.27) and (1.34) in the short-period stage we may set v_x = 0 and consider these equations as independent of the first one.

Thus, in addition to Equations (1.38), the equations of the short-period disturbed motion in the pitch plane may be written:
in the body coordinate system as

$$\begin{gathered}\dot{v}_{yn}+c_{v_y v_y}^{\cdot}v_{yn}+c_{v_y\vartheta}^{\cdot}\vartheta+c_{v_y\dot{\vartheta}}^{\cdot}\dot{\vartheta}+c_{v_y\delta}^{\cdot}\delta=0,\\ \ddot{\vartheta}+c_{\dot{\vartheta}\dot{\vartheta}}\dot{\vartheta}+c_{\vartheta\vartheta}\vartheta+c_{\dot{v}_y}^{\cdot}v_{yn}+c_{\vartheta\delta}\delta=0;\end{gathered} \tag{1.39}$$

in the fixed coordinate system as

$$\begin{gathered}\dot{v}_y+c_{v_y v_y}^{\cdot}v_y+c_{v_y\vartheta}^{\cdot}\vartheta+c_{v_y\dot{\vartheta}}^{\cdot}\dot{\vartheta}=0,\\ \ddot{\vartheta}+c_{\dot{\vartheta}\dot{\vartheta}}\dot{\vartheta}+c_{\vartheta\vartheta}\vartheta+c_{\dot{v}_y}^{\cdot}v_y+c_{\vartheta\delta}\delta=0.\end{gathered} \tag{1.40}$$

The equations of the short-period perturbed motion in the yaw plane relative to the moving coordinate system assume the following form on the basis of (1.22).

$$\begin{gathered}\dot{\beta}+c_{\beta\beta}^{\cdot}\beta+c_{\beta\dot{\psi}}^{\cdot}\dot{\psi}+c_{\beta\delta}^{\cdot}\delta=0,\\ \ddot{\psi}+c_{\dot{\psi}\dot{\psi}}\dot{\psi}+c_{\psi\dot{\psi}}^{\cdot}\dot{\psi}+c_{\psi\beta}^{\cdot}\beta+c_{\psi\delta}\delta=0.\end{gathered} \tag{1.41}$$

We shall show that Equations (1.40) are identical with Equations (1.38). In fact, since in the initial stage of the perturbed motions v_{xn} = const then from the first equation in (1.31) we have the equality of forces

$$P_0-G\sin\theta_0-\frac{\rho v_0^2}{2}Sc_x-R_{yy}^{\cdot}\lambda_{y_0}v_{y_0}=0. \tag{1.42}$$

In addition, in the fixed coordinate system we have the kinematic relation

$$v_y=\vartheta v_x. \tag{1.43}$$

Comparing the coefficient c_{yy} from (1.21) with the coefficient $c_{v_y v_y}$ from (1.36), we obtain $c_{yy}=c_{v_y v_y}$. Taking (1.23) into consideration, we also obtain

$$v_0c_{y\vartheta}=c_{v_y\vartheta},\quad v_0c_{\dot{v}_y}=c_{y\dot{\vartheta}},\quad v_0c_{y_\delta}=c_{v_y\delta}.$$

We shall assume that the equation of the control system (1.16) admits of linearization. Upon linearizing, we obtain an equation of the control system in terms of the variations

$$\delta = F(\theta, \delta, \ldots, v_p, \ldots). \tag{1.44}$$

Equations (1.38) - (1.40) together with (1.44) form a homogeneous linear system of differential equations describing a perturbed motion of a closed-loop system of automatic control.

6. Transfer Functions and Properties of Characteristic Polynomials

The equations of the perturbed motion of a rocket with "frozen" coefficients can be symbolically written in an operator form as

$$Q(p)x_1 = R(p)x_2,$$

where Q(p), R(p) are operator polynomials; x_1 may be any of the quantities we are interested in such as $\theta, \dot{\theta}, \vartheta, v_y, v_x$ etc; $x_2 = \delta$. In what follows x_2 will be referred to as input, and x_1 as output.

The transfer function of the system $K_{x1}(p)$ will be defined as

$$K_{x1}(p) = \frac{R(p)}{Q(p)}.$$

The equations of motion in the symbolic operator form imply that

$$\frac{x_1}{x_2} = K_{x1}(p),$$

in which we have a ratio, as it were, of the result x_1 (output) to the action x_2 (input), expressed in a symbolic operator form [16].

Assuming the coefficients have been "frozen", we shall first discuss the equations of the perturbed motion in the plane of pitch (1.38) and (1.40), and analogous equations in the plane of yaw (1.41).

We shall write Equations (1.38) in the symbolic operator form

$$\begin{aligned}(p+c_{11})\theta+c_{12}\theta+c_{13}\delta=0,\\ (p^2+pc_{22}+c_{23})\theta+c_{24}\theta+c_{24}\delta=0.\end{aligned} \tag{1.45}$$

Eliminating θ, we shall find the transfer fuction

$$K_\delta(p)=\frac{\theta}{\delta}=\frac{-c_{24}(p+c_{22})+c_{24}c_{23}}{p^3+a_1p^2+a_2p+a_3}, \tag{1.46}$$

in which

$$\begin{aligned}a_1&=c_{11}+c_{22},\\ a_2&=c_{11}c_{22}+c_{23},\\ a_3&=c_{11}(c_{22}+c_{23})=-\frac{c_{24}}{mv_0}G\sin\theta_0.\end{aligned} \tag{1.47}$$

Eliminating θ from (1.45), we find the transfer function

$$K_\delta(p)=\frac{\theta}{\delta}=\frac{-c_{24}(p^2+pc_{22}+c_{23})+c_{24}c_{23}}{p^3+a_1p^2+a_2p+a_3}. \tag{1.48}$$

The denominator of the transfer function is a characteristic polynomial of the systems (1.38) and (1.40)

$$L(p)=p^3+a_1p+a_2p+a_3. \tag{1.49}$$

For the system (1.41), describing a perturbed motion in the plane of yaw, the coefficient $a_3 = 0$, so that

$$L(p)=p(p^2+a_1p+a_2). \tag{1.50}$$

The roots of this polynomial are

$$p_{1,2}=-\frac{1}{2}(c_{11}+c_{22})\pm\frac{1}{2}\sqrt{(c_{11}-c_{22})^2-4c_{12}};\quad p_3=0.$$

The zero root corresponds to the long period motion. Upon simplifying Equations (1.19), the degree of the characteristic polynomial is lowered by one. Due to the zero root, th. deflections σ and ψ in the perturbed motion described by Equations (1.41) for $\delta=0$, do not disappear.

Depending on the sign of the coefficient $c_{\psi\psi}$, the roots p_1 and p_2 may be either real or complex conjugate with negative real parts.

If the rocket is statically stable $(c_{\psi\psi}>0)$, and in addition $(c_{zz}-c_{\psi\dot{\psi}})^2<4c_{\psi\psi}$, then

$$p_{1,2}=s\pm i\omega,\quad s=-\frac{1}{2}(c_{zz}+c_{\psi\dot{\psi}}),\quad \omega=\sqrt{c_{\psi\psi}-s^2}, \tag{1.51}$$

where ω is the natural frequency of the angular oscillations of a statically stable rocket in an air stream.

If a rocket is statically unstable $(c_{\psi\psi}<0)$, then the roots p_1, p_2 will be real, and

$$p_1>0,\quad p_2<0,\quad |p_2|>|p_1|. \tag{1.52}$$

The quantities p_1, p_2 are in addition the roots of the denominator of the transfer functions, found from Equations (1.41):

$$K_{\dot{\sigma}}(p)=\frac{\dot{\sigma}}{\delta},\quad K_{\dot{\psi}}(p)=\frac{\dot{\psi}}{\delta}.$$

Therefore for a statically stable rocket the transfer process relative to the rates $\dot{\sigma}$ and $\dot{\psi}$ is oscillatory and damped, and for a statically unstable rocket the transfer process is characterized by an instability of an aperiodic type.

When $c_{\psi\psi}=0$, then $p_1=-c_{zz}$, $p_2=-c_{\psi\dot{\psi}}$, and the motion is stable relative to the rates $\dot{\sigma}$ and $\dot{\psi}$. When $(c_{zz}-c_{\psi\dot{\psi}})^2-4c_{\psi\psi}=0$ the roots p_1, p_2 will be real, negative and equal. The free motion of a rocket relative to the rates $\dot{\sigma}$ and $\dot{\psi}$ is also stable.

Now let us analyze the properties of the characteristic polynomial (1.49). If $c_{\theta\theta}=0$, then

$$p_1=-c_{\theta\dot{\theta}},\quad p_2=-c_{\dot{\theta}\dot{\theta}},\quad p_3=0. \tag{1.53}$$

With the stated initial conditions free motion relative to the coordinates θ and ϑ is not damped, and relative to the rates $\dot{\theta}$ and $\dot{\vartheta}$ it is attenuated aperiodically.

When the center of pressure of the aerodynamic forces does not coincide with the center of mass of the rocket ($c_{\theta\theta}\neq 0$), then in the analysis of the polynomial coefficients in (1.49) there arise two basic cases:

a) if $c_m^{\alpha}>0$ ($c_{\theta\theta}>0$), then $a_1>0$, $a_2>0$, $a_3<0$, and the polynomial (1.49) will have one real positive root and a pair of complex conjugate roots with a negative real part

$$p_{1,2}=\sigma\pm i\omega,\ (\sigma<0),\ p_3>0; \tag{1.54}$$

b) if $c_m^{\alpha}<0$ ($c_{\theta\theta}<0$), then $a_1>0$, $a_2<0$, $a_3>0$ and all three roots of the polynomial (1.49) are real, two being positive and one negative:

$$p_1>0,\ p_2>0,\ p_3<0. \tag{1.55}$$

Thus, free motion in the pitch plane is unstable for $c_{\theta\theta}\neq 0$.

One of the more important parameters of a perturbed motion is the acceleration in the direction of the lateral axis of the rocket $Oy_1(Oz_1)$, in terms of which one determines the lateral loads acting on the fuselage. This acceleration may be an input coordinate to the automatic stabilizer. The transfer function with respect to the lateral acceleration $\dot{v}_{y1}$ may be found from Equations (1.39). We obtain

$$K_{\dot{v}_{y1}}(p)=\frac{\dot{v}_{y1}}{\vartheta}=\frac{p\left(b_2'p^2+b_1'p+b_0'\right)}{p^3+a_2'p^2+a_1'p+a_0'}. \tag{1.56}$$

The coefficients in the denominator of the transfer function (1.56) may be expressed in terms of the coefficients (1.47) as follows:

$$a_1'=a_1,\quad a_2'=a_2+c_{00},$$
$$a_3'=\frac{c_{00}}{mv_0}\left[\frac{\rho v_0^2}{2}S(c_y^0+c_x)-G\sin\theta_0\right]. \tag{1.57}$$

The coefficients in the numerator of (1.56) are determined from the formulas

$$b_0'=-c_{v_y\beta},$$
$$b_1'=-c_{v_y\dot{\beta}}c_{00}+c_{01}c_{v_y\beta}, \tag{1.58}$$
$$b_2'=-c_{v_y\dot{\beta}}c_{00}+c_{02}c_{v_y\beta}.$$

They differ a little from the coefficients for similar powers of the operator p in the numerator of (1.48). The coefficients in the denominator of the transfer functions in Equations (1.48) and (1.56) are also different. Therefore, Equations (1.39) are generally speaking not identical with Equations (1.38), and the transfer function

$$K_{\dot{\vartheta}_{y1}}(p)\neq K_{\dot{\vartheta}}(p)v_0.$$

7. Structure of the Automatic Stabilizer

The control system of a rocket consists of: 1) prevention of an accidental deflection of a rocket from the desired trajectory, 2) guiding the rocket to a target by generating and applying control signals. Therefore the entire system consists of two parts — the control system proper and the guidance system.

An ideal calculated trajectory of a ballistic rocket is a plane curve located in the vertical plane, the pitch plane. The forces acting on a rocket in the powered portion of the trajectory are the engine thrust, the force of gravity, and the aerodynamic forces. The time dependence of the force of gravity is known. The aerodynamic forces change depending on the dynamic pressure and the angle of attack which is defined as the angle between the longitudinal axis of the rocket and the tangent to the trajectory. The direction of thrust

is determined by the inclination of the fuselage. Thus, in order to make sure that the rocket follows a desired trajectory, one has to control the deflections of a rocket in the plane of pitch, or in other words, one must control the deflections of the engine thrust vector.

The starting equations in the solution of the control problem are Equations (1.14).

The control system is designed to protect a stable angular motion of the rocket fuselage, and minimize the deflections of the center of mass of a rocket from the calculated trajectory. This problem is solved by placing on the fuselage automatic angular stabilizers that stabilize motion relative to the center of mass, and automatic stabilizers of the center of mass itself. The linear stabilizers may be set up either in the plane of pitch or the plane of yaw. The angular stabilization is usually accomplished separately in each of the three planes — the planes of pitch, yaw, and roll [3, 9, 24].

The starting equations in the solution of the stabilization problem are the equations of the perturbed motion obtained in Section 4 (see pages 29, 31, 33, 36).

The control system of a rocket is analogous to the autopilot systems [3, 13, 17]. The system consists of sensors measuring the mismatch signals (free gyroscopes, rate-of-turn pickups, acceleration pickups, etc), computers (or a correcting circuit and an amplifier), and the actuating mechanisms (control actuators, servos). The part of the control system consisting of the amplifier, control actuator, and a feedback going from the output shaft of the actuator to the amplifier, is usually called a servo. One and the same servo may serve the actuators simultaneously for two control channels, for instance, a channel of the angular stabilization, and a channel of the lateral stabilization of the center of mass in the yaw or pitch planes.

There are several types of control systems in existence [3,9]: control systems without an internal feedback; continuous control systems and relay control systems; self-adjusting systems or systems incorporating a digital computer.

It is not the objective of this book to discuss the properties and advantages of various control systems. A control system is just a part of a closed system without which it is impossible o analyze methodically the dynamic properties of rockets. Therefore, below in the analysis of dynamic properties we shall base our discussion on the control system used by V-2 rocktes [3, 9].

In Figure 1.8, we see a typical block diagram of one of the channels — the channel of the angular stabilization in the yaw plane. We shall give the equations for separate links of the control system, which are usually used in the analysis of the dynamic properties of rockets within a linear framework.

A gyroscopic pickup (GP) experiences a voltage u_ψ proportional to the yaw angle ψ:

$$u_\psi = k_{\text{гп}}\psi. \tag{1.59}$$

As a correcting circuit (CC) one may use differentiating circuits of first or second order with inductive and ohm loads (amplifier windings).

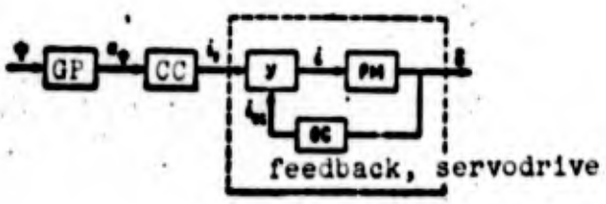

Figure 1.8
PM = activating mechanism
OC = feedback

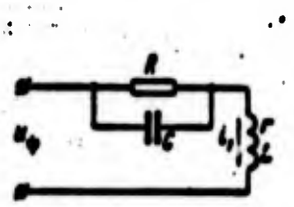

Figure 1.9

Figure 1.9 shows a differentiating circuit of first order. The relationship between the input voltage u_ψ and the output current i_1 is expressed by the following differential equation

$$(a_2p^2+a_1p+1)i_1=k_a(T_dp+1)u_\psi, \tag{1.60}$$

where

$$a_2=LT_dk_a,$$
$$a_1=k_a[T_d(R+r)+L],$$
$$T_d=RC,$$

R, r is the ohmic resistance, C is the capacitance, and L is the inductance.

Since the feedback (OC) is negative, then the equation of the amplifier (Y) may be put in the form

$$(T_1p+1)i=k_{y.o.c}\left(\frac{k_{a_\psi}}{k_{y.o.c}}u_\psi-i_1-i_{o.c}\right), \tag{1.61}$$

where k_{a_ψ} is the amplification coefficient relative to the main signal;

$k_{a.f.s.}$ is the amplification coefficient relative to the feedback signal;

T_1 is the time constant of the amplifier.

The linearized equation of the actuating mechanism (PM) may be written as

$$p(m_2p^2+m_1p+m_0)\delta=i, \tag{1.62}$$

where m_0, m_1, m_2 are coefficients accounting for the parameters of the actuator and the reduced mass of the control elements.

A rigid negative feedback may be expressed by the equation

$$i_{o.c}=k_{o.c}\delta. \tag{1.63}$$

If the amplifier, the actuator, and the rigid feedback are put together into one actuating link, then the linearized equation for this servomechanism will be

$$[(1+T_1 p)(m_2 p^2 + m_1 p + m_0)p + k_{y.o} c k_{o.c}]\delta = k_{y\phi} i_1. \tag{1.64}$$

The coefficients on the left-hand side of Equation (1.64) are usually selected so that the characteristic polynomial of this equation does not contain roots with a positive real part. In other words, it is necessary that the servomechanism as a closed system be stable.

The equation for the entire channel of the angular stabilization may be written in general form as

$$Q_{AC}(p)\delta = R_{AC}(p)\psi, \tag{1.65}$$

where the operator polynomials $Q_{AC}(p)$ and $R_{AC}(p)$ are determined in an elementary way on the basis of Equations (1.59), (1.60), and (1.64).

The transfer function of the angular stabilizer is

$$K_{AC}(p) = K_{\psi\delta}(p) = \frac{\delta}{\psi} = \frac{R_{AC}(p)}{Q_{AC}(p)}. \tag{1.66}$$

The stability of the separate parts [(1.59), (1.60), and (1.64)] guarantees the stability of the entire channel of angular stabilization. In other words, the characteristic polynomial of the angular stabilizer $Q_{AC}(p)$ does not have roots with a positive real part. The complex transfer number of the control system relative to any channel may be written as

$$K_{AC}(i\omega) = \frac{R_{AC}(i\omega)}{Q_{AC}(i\omega)} = U_{AC}(\omega) + iV_{AC}(\omega) = A_{AC}(\omega)e^{i\varphi_{AC}(\omega)}, \tag{1.67}$$

where $A_{\lambda c}(i\omega)$ is the absolute value of a complex number; $\varphi_{\lambda c}(\omega)$ is the argument of a complex number. Or, in other words, $A_{\lambda c}(\omega)$ is the amplitude-frequency characteristic; $\varphi_{\lambda c}(\omega)$ is the phase-frequency characteristic of the control system.

8. The Effectiveness of the Control Organs

The effectiveness of the control organs is characterized by the amplification coefficients $c_{\vartheta\delta}$, $c_{\psi\delta}$, $c_{\gamma\delta}$, and by maximum moments. Thus, in the pitch or yaw plane the coefficients are, respectively, equal to

$$|c_{\vartheta\delta}| = \frac{R^{\delta}_{zp}(x_p - x_m)}{I_z},$$

$$|c_{\psi\delta}| = \frac{R^{\delta}_{zp}(x_p - x_m)}{I_y};$$

and in the plane of roll

$$|c_{\gamma\delta}| = \frac{M^{\delta}_{xp}}{I_x}.$$

The maximum moment that the control organs are capable of in the plane of pitch and yaw is, respectively

$$(M_z)_{max} = R^{\delta}_{zp}(x_p - x_m)\delta_{max},$$

$$(M_y)_{max} = R^{\delta}_{zp}(x_p - x_m)\delta_{max};$$

and in the plane of roll

$$(M_x)_{max} = M^{\delta}_{xp}\delta_{max}.$$

The values of the coefficients $c_{\vartheta\delta}$, $c_{\psi\delta}$ have an effect on the amplification coefficient of the control system, since the total amplification coefficient of a disconnected circuit is equal to the product of the amplification coefficient of the control system and the controlled object.

The moment produced by the control units may be arbitrarily divided into three parts

$$M_{упр} = M_{пр} + M_{пер} + M_{стаб}.$$

Here M_{pr} is the programmed control moment necessary to guide the rocket along the desired trajectory. If $\dot{\vartheta}_{pr}$ ($\dot{\vartheta}_n$) and $\ddot{\vartheta}_{pr}$ ($\ddot{\vartheta}_n$) are small, then M_{pr} is also small; M_{per} is the moment needed to parry disturbances caused by wind, misalignments of the thrust chamber, aerodynamic asymmetry, etc. This moment may be considerable M_{st} is the moment produced by the control organs in the process of stabiliziation which is determined by the requirements of the speed of response, accuracy, and the oscillational nature of the transition processes.

At an arbitrary moment of flight the maximum moment that may be produced by the control system should be larger than the needed control moment

$$(M_{упр})_{max} > (|M_{пр}| + |M_{пер}| + |M_{стаб}|)_{max}.$$

For example, in the plane of pitch

$$R^{\delta}_{yp}(x_p - x_m)\delta_{max} > (|M_{пр}| + |M_{пер}| + |M_{стаб}|)_{max}.$$

Since the right-hand side of the inequality may be known from the analysis of the possible trajectories, conditions of flight, the values of perturbations, etc., and the angle δ_{max} is determined by the construction of the organs limiting the rotation of the control organs, then from the last inequality one may determine the minimum gradient of the control force

$$R^{\delta}_{yp} > \frac{(|M_{пр}| + |M_{пер}| + |M_{стаб}|)_{max}}{\delta_{max}(x_p - x_m)}.$$

This inequality should be satisfied at any time of the flight.

Inasmuch as the control signal is usually "obstructed" by noise, a useful deflection of the control organs is superimposed with accidental deflections. The left-hand side of the inequality should be larger than the right-hand side by an amount that would guarantee that the rotation of the control units does not reach the maximum angle δ_{max}.

Thus, the effectiveness of the control units should be such that the control system be able to parry all the disturbances and guide the rocket along the programmed (nominal) trajectory. The effectiveness should also be high enough to secure stability of the motion relative to the center of mass, and a stability of the center of mass relative to the required trajectory.

9. The Concept of Stability of Motion and of Natural Oscillations

One of the most important definitions of stability is that given by Lyapunov [14].

Any system of linear differential equations, including the linearized equations of perturbed motion (1.19) - (1.24), may be brought to a normal form

$$\frac{dy_s}{dt} = Y_s(t, y_1, \ldots, y_n) \quad (s = 1, 2, \ldots, n),$$

where y_s are the coordinate perturbations.

A determination of stability is formulated as follows according to Lyapunov.

An unperturbed motion is stable if for any positive number ε no matter how small, one can find another positive number $\eta(\varepsilon)$ such that for all perturbed motions $y_s = y_s(t)$ which satisfy at the initial point in time $t = t_0$ the inequalities $|y_s(t_0)| \leq \eta$, also the inequalities $t > t_0$ will be satisfied for all $|y_s(t)| < \varepsilon$.

If an unperturbed motion is stable, and if η can be selected so small that for all perturbed motions, satisfying the inequalities $|y_s(t_0)| \leqslant \eta$, the following conditions will be satisfied

$$\lim_{t \to \infty} y_s(t) = 0,$$

then the unperturbed motion is called asymptotically stable.

Is it possible to judge the stability of a real system on the basis of the linearized equations? An answer is provided by the following three theorems given by Lyapunov [16].

1. If the characteristic equation of the linearized system has all roots with negative real parts, then the actual system will be stable just as the linearized system, i.e., no additions of terms involving second and higher powers of variables and their derivatives will in this case disturb the stability of the system.

2. If the characteristic equation of the linearized system has even one root with a positive real part, then the actual system will be unstable, i.e., no additions of terms involving second and higher powers of variables and their derivatives will impart stability to the system.

3. When zero or purely imaginary roots are present after the linearization, then it is impossible to determine whether the actual system is stable or not. The rejected terms involving second and higher degree powers of variables and their derivatives may in some cases radically change the dynamics of the system.

In Section 4 we obtained a system of linearized differential equations with variable coefficients for the perturbed motion of a rocket. Using the technique of "freezing" the coefficients, this system can be reduced to a system of ordinary differential equations with constant coefficients. A motion, described by a system of ordinary differential equations with constant coefficients, will be asymptotically stable if all the

roots of the corresponding characteristic equation are located in the left half-plane. That this condition is satisfied can be deduced from the criteria established by Routh-Hurwitz, Nyquist, and Mikhaylov [14, 16]. In the following exposition we shall mainly use the Nyquist frequency criterion which makes it possible to estimate the stability of a closed system from its hodograph, i.e., the amplitude-phase characteristic of the corresponding open circuit.

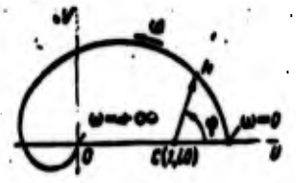

Figure 1.10

In the process of setting up the equations of the perturbed motion (see Section 4) we took as positive that direction of the control force which causes a decrease in the angles ϑ, ψ, φ. In this case in the formulations of the Nyquist criterion one uses the positive real half-axis (Figure 1.10), and point C is located on this half-axis, with coordinates (1,i0). Let us formulate the Nyquist criterion for the case when the degrees of the characteristic polynomial of the closed system and the open circuit are identical.

The first formulation. For a closed linear system to be stable it is necessary and sufficient that the vector CN, obtained by moving point N along the hodograph of an open circuit for $0 \leqslant \omega \leqslant +\infty$, rotates by an angle $\varphi = m\pi$ (counterclockwise). Here m is equal to the number of roots with positive real parts in the characteristic equation of the open circuit. For example, a hodograph (see Figure 1.10) attests to the stability of a closed system if the characteristic equation of the open circuit has one root with a positive real part, i.e., m = 1. Conversely, the system is unstable if $m \neq 1$.

Second formulation. For a closed linear automatic system to be stable it is necessary and sufficient that for $0 \leqslant \omega \leqslant +\infty$ the difference between the positive and negative passages of the hodograph through the segment $(1, +\infty)$ of the real axis be equal to m/2. By a positive passage we consider a passage of the hodograph from the lower half-plane to the upper one. The origin of the hodograph on the

indicated segment is considered as half-passage.

We should remember, however, that a system of equations of the perturbed motion with frozen coefficients only approximately describes the behavior of a system with variable coefficients. Therefore, the solutions obtained on the basis of an analysis of the former have only a qualitative character. The determination of an asymptotic stability formulated at the beginning of the section was done for systems with an unbounded time of motion, i.e., $0<t<\infty$. Since the duration of the motion of a rocket is bounded, one should speak of the so-called stability within a finite time interval $(t_0<t\leqslant t_1)$ in which the motion takes place.

In for any positive number ε, no matter how small, one can find another positive number $\eta(\varepsilon)$ such that for all perturbed motions which initially satisfy the conditions $|y_s(t_0)|\leqslant\eta$, the conditions $t_0<t\leqslant t_1$ will be satisified for all $|y_s(t)|<\varepsilon$, then the motion will be stable within a finite time interval. Stability within a finite time interval is also called a technical stability.

In some cases the requirements of the technical stability will be weaker than the requirements of the asymptotic stability. This circumstance is of great importance, and one is advised to use it in certain cases, since the time interval corresponding to the powered section of the trajectory is not large [5]. If a system is unstable, then the linearized equation of motion may be used to describe the motion of the system only if its deviations from equilibrium are small. To describe the motion involving large deviations, it is necessary to use nonlinear equations.

In the real closed system consisting of a rocket and the control system there may arise increasing oscillations which usually develop into a stationary auto-oscillating process. In this connection we shall discuss some notions relating to that process.

The self-oscillating systems mainly differ from the remaining oscillating systems in that stationary oscillations may take place in them with the absence of an external periodic action. In each self-oscillating system, one can distinguish three principal parts: the oscillating system, the source of energy, and the feedback through which the oscillating system acts on the source of energy.

Self-oscillation is a self-exciting oscillation. Self-oscillations are characteristic of the nonlinear systems. At the same time, one can determine a possiblitiy of self-exciting in some cases even from the linearized equations.

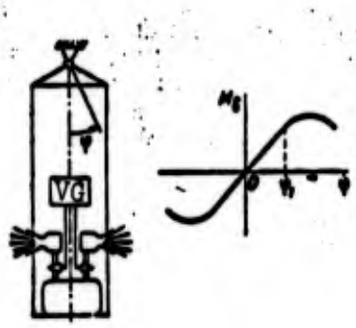

Figure 1.11

Figure 1.12

Excitation of oscillations and a transition of growing oscillations into self-oscillations may be quite clearly seen from the example of a system shown in Figure 1.11. A physical pendulum serves as a oscillating system, air compressed in a balloon is a source of energy, and a velocity gyroscope (VG) forms the feedback. The velocity gyroscope measures the angular velocity $\dot{\varphi}$ of pendulum oscillations, and depending on the velocity, it gives the air access to the nozzle. There arises a moment $M_{\text{в}}$ of the reaction force relative to the axis of rotation of the pendulum.

In this example, the feedback contributes to growing oscillations of the pendulum. As will be shown later (Chapters III, V), this type

of feedback occurs in an elastic liquid-fuel rocket equipped with a control system.

The equation of small oscillations of the pendulum is of the form

$$I\ddot{\varphi}+(h-b)\dot{\varphi}+gma\varphi=0, \tag{1.68}$$

where h is the coefficient of external friction; m, I are the mass and moment of inertia of the pendulum; a is the distance from the center of mass of the pendulum along the axis of roation; $b=(\partial M_t/\partial\dot{\varphi})_{\dot{\varphi}=0}$.

If $b>h$, then small motions of the pendulum will be unstable and the oscillations will be on the increase.

As soon as the amplitudes of oscillations reach valuesalues such that the angular velocity is greater than $\dot{\varphi}_n$, the oscillations will be determined by a nonlinear equation; the intensity of the energy influx into the system will decrease. For some value of the amplitude the influx of the energy into the oscillating system $E_{(+)}$ and the dissipation of the energy $E_{(-)}$ will be equal, the growth of oscillations will stop, and in the system there will be set up stable periodic oscillations with an amplitude a_p, i.e., self-oscillations.

In the phase plane self-oscillations are represented by a stable limiting cycle (Figure 1.12). If in the system containing self-oscillations one creates small disturbances, then the trajectory in the phase-time diagram will again approach the limiting cycle.

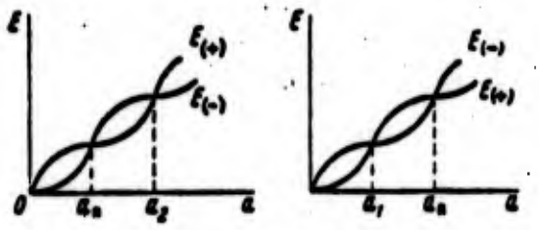

Figure 1.13

One can gain an intuitive notion of how self-oscillations are set up and about the stability of limiting cycles by considering the relations between energies. Figure 1.13 shows, for example, graphs representing the dependence of $E_{(+)}$ and $E_{(-)}$ on the amplitudes of oscillations for two different systems. As evident, with amplitudes equal to a_1 and a_2, the influx of energy into the systems is equal to the dissipation of energy by the systems, but these oscillations are unstable, i.e., the limit cycle is unstable. The difference between the systems is that for the system on the left infinitesimal disturbances are enough to set up self-oscillations, whereas in the system on the right self-oscillations will be induced only if the amplitude of the disturbance exceeds a_1. The first system is called a "soft" excitation system, and the second — a "hard" excitation system.

One can get acquainted with the peculiarities of self-oscillations and methods of calculating them by consulting [19, 20, 22].

In a closed system consisting of the rocket and the control system, the principal nonlinear components are the servomechanism for which the saturation with respect to velocity is characteristic, and the amplifier (saturation with respect to current). In addition, oscillations of the liquid in tanks, friction forces in the structure, etc., may be nonlinear. The self-oscillations in the system rocket control loop are detrimental since they increase the dynamic loads on the fuselage and the structural elements, and "clog up" the control channels with parasite currents. However, in some cases (when using complex dynamic structures, when there is a considerable dispersion of parameters, etc.) it is hard to prevent self-oscillations

from being set up, and they have to be tolerated if they are not dangerous to the stability of the design, and do not cause an inadmissible distortion of the properties of the guidance and control system.

10. Frequency Characteristics of a Rocket Considered as a Rigid Body in Relation to the Requirements of the Control System

The rocket, together with the control system, forms a closed system of automatic control (Figure 1.14). The dynamic properties of this system depend on the properties of both the rocket and the control system. The main part of the closed system is the rocket which is the object of control (OC). The control system (CS) is supposed to guarantee the stability of the motion of the rocket. Therefore, its properties depend on the dynamic properties of the object of control. We shall discuss in this connection the frequency characteristics of a perfectly rigid rocket, and the requirements imposed on the control system to make sure that the closed system is stable.

We shall analyze the equations of perturbed motion in the plane of yaw. Instead of Equations (1.41) we shall consider the equations of motion obtained in the fixed coordinate system. By symmetry they will be the same as Equations (1.40) for the plane of pitch,

$$\begin{aligned} \dot{v}_z + c_{v_z v_z} v_z + c_{v_z \psi} \psi + c_{v_z \delta} \delta = 0, \\ \ddot{\psi} + c_{\psi\psi} \dot{\psi} + c_{\psi\psi} \psi + c_{\psi v_z} v_z + c_{\psi\delta} \delta = 0, \end{aligned} \tag{1.69}$$

where

$$c_{v_z v_z} = \frac{1}{m_a} \frac{\rho v_a^2}{2} S (c_x' + c_a),$$

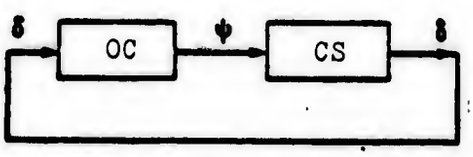

Figure 1.14

$$
\begin{aligned}
c_{v^2\psi} &= -\frac{1}{m}\left(P_0 + \frac{\rho v_0^2}{2} S c_x^\delta\right),\\
c_{v_z\beta} &= -\frac{1}{m} R_{zy}^\beta,\\
c_{\psi\psi} &= \frac{1}{I}\left(\frac{\rho v_0^2}{2} S l c_m^{\dot\psi} + 2\sum_{(l)} m_{el}\int_{x_{el}}^{l_k} (x - x_m)\,dx\right).\\
c_{\psi\psi} &= \frac{1}{I}\frac{\rho v_0^2}{2} S l c_m^\delta,\\
c_{\psi v_z} &= -\frac{c_{\psi\psi}}{v_0},\\
c_{\psi\delta} &= \frac{1}{I} R_{zy}^\delta (x_p - x_m).
\end{aligned}
\tag{1.70}
$$

The lateral motion of the center of mass relative to the nominal trajectory is slower than the angular motion relative to the center of mass. Therefore, in the analysis of the angular motion one can neglect to a first approximation the displacements of the center of mass. Similarly, in the analysis of the lateral motion of the center of mass one can neglect the angular acceleration $\ddot{\psi}$ and the angular velocity $\dot{\psi}$. Then instead of (1.69), we shall obtain two simplified independent systems of equations:
the equation of the angular motion relative to the center of mass

$$
\ddot{\psi} + c_{\psi\dot\psi}\dot\psi + c_{\psi\psi}\psi + c_{\psi\delta}\delta = 0 \tag{1.71}
$$

and the equations of the lateral motion of the center of mass

$$
\begin{aligned}
\dot v_z + c_{v_z v_z} v_z + c_{v_z\psi}\psi + c_{v_z\delta}\delta &= 0,\\
c_{\psi\psi}\psi + c_{\psi v_z} v_z + c_{\psi\delta}\delta &= 0.
\end{aligned}
\tag{1.72}
$$

The transfer function relative to the yaw angle on the basis of the simplified equation (1.71) will be

$$
K_\psi(p) = \frac{\psi}{\delta} = \frac{-c_{\psi\delta}}{p^2 + pc_{\psi\dot\psi} + c_{\psi\psi}}. \tag{1.73}
$$

Letting $p = i\omega$, we shall get the complex transfer number

$$
K_\psi(i\omega) = \frac{-c_{\psi\delta}}{c_{\psi\psi} + i\omega c_{\psi\dot\psi} - \omega^2} = U(\omega) + iV(\omega). \tag{1.74}
$$

The sign of the coefficient $c_{\varphi\varphi}$ is determined by the sign of the coefficient c_m^1. For a statically stable rocket $c_m^1>0$, for a statically unstable one $c_m^1<0$, for a neutral one $c_m^1=0$.

What properties should the control system have to make sure that the angular motion relative to the center of mass of the closed system is stable? To answer this question, we shall analyze the properties of the complex transfer number $K_\varphi(i\omega)$ for the object of control, the number being determined from Equation (1.74). For simplicity, we shall neglect the damping, i e., set $c_{\varphi\dot\varphi}=0$. Three various cases will be considered.

1. A statically unstable rocket, $c_{\varphi\varphi}<0$.

The hodograph of the complex transfer number $K_\varphi(i\omega)$ in the plane $Z=U(\omega)+iV(\omega)$ is shown in Figure 1.15. It is a segment of the positive real half-axis $\left[0, \left|\frac{c_{z\delta}}{c_{\varphi\varphi}}\right|\right]$, where as can be seen from equating the coefficients $c_{z\delta}$ and $c_{\varphi\varphi}$, on certain segments of the trajectory we can have $c_{z\delta}/c_{\varphi\varphi}<1$, and on others $c_{z\delta}/c_{\varphi\varphi}>1$.

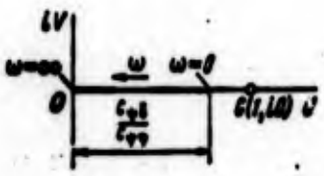

Figure 1.15

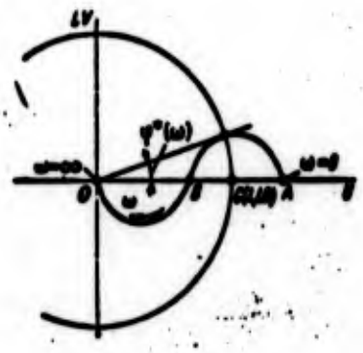

Figure 1.16

The denominator of the complex transfer number $K_\varphi(p)$ has one positive root $p=\sqrt{c_{\varphi\varphi}}$. Therefore, by the Nyquist criterion, for a closed system to be stable it is necessary and sufficient that the hodograph of the complex transfer number for the entire open circuit

$$K(i\omega)=K_\varphi(i\omega)K_{AC}(i\omega)=A_\varphi(\omega)A_{AC}(\omega)e^{i[\psi_\varphi(\omega)+\psi_{AC}(\omega)]}=A(\omega)e^{i\psi(\omega)}$$

make one positive half-passage through the OU axis to the right of C(1, i0). With a retardation of the control system at high frequencies taken into account, such a hodograph is shown in Figure 1.16.

To insure the stability of motion, the amplitude-phase characteristics of the control system should possess the following properties.

First of all, for small frequencies, including of course $\omega=0$, the control system should amplify the signal, i.e., the amplification coefficient $k>1$. This is necessary to make sure that point A on the U axis be located on the right of point C(1, i0).

Secondly, the control system should for small frequencies produce a phase lead to ensure that the phase of the open circuit

$$\varphi(\omega)=\varphi_0(\omega)+\varphi_{\Lambda C}(\omega)$$

be positive for small frequencies. This phase lead is achieved using a differentiating circuit.

Thirdly, to ensure that the hodograph $K(i\omega)$ makes one positive half-passage through the U axis to the right of C(1, i0), it is necessary to have a phase lead in the frequency interval $[0, \omega_0]$. Here, ω_0 is the frequency for which the phase lead of the control system develops into a retardation $\varphi_{\Lambda C}(\omega_0)=0$. The larger the amplification coefficient k, the higher the frequency should be for which the phase lead is still produced. This is to make sure that point B on the U axis is always located left of point C.

Consequently, the amplification coefficient k should be no smaller than some number, say k_{min}, to ensure that point $A(\omega=0)$ on the U axis lies to the right of point C, and at the same time should be no larger than k_{max} to ensure that point $B(\omega=\omega_0)$ lies to the left of point C. In other words, the amplification coefficient should be bounded from above and from below

$$k_{min}<k<k_{max}. \qquad (1.75)$$

If point B coincides with C, then the closed system will be on the border of stability, small disturbances will cause sustained oscillations in the system. Since $\varphi_{AC}(\omega_0)=0$, we have $\delta=k(\omega_0)\psi$, and for this case

$$K(i\omega)=-\frac{k(\omega_0)c_{\psi\delta}}{c_{\psi\psi}-\omega^2}. \tag{1.76}$$

From this expression, one can find the frequency of the natural oscillations of the closed system

$$\omega=\sqrt{k(\omega_0)c_{\psi\delta}+c_{\psi\psi}}.$$

For the closed system to be stable, point B should lie to the left of point C. Therefore, the control system should produce a phase lead up to frequencies

$$\omega_0>\sqrt{k(\omega_0)c_{\psi\delta}+c_{\psi\psi}}. \tag{1.77}$$

In the analysis of the stability of closed systems, one uses conventional notions such as stability margin relative to the phase, the stability margin relative to the amplitude or, which is the same thing, the stability margin relative to the amplification coefficient. The stability margin with respect to the phase is characterized by the lead angle $\varphi^*(\omega)$ for $A(\omega)=1$. The stability margin relative to the amplitude can be described by the ratio of the length of segment BC (in the same way as the length of segment AC) to the length of segment OC, equal to 1. The larger the segment BC (AC), the higher the stability margin relative to the amplitude. The stability margin makes it possible to determine the admissible limits within which the parameters of the system may change without disturbing its stability.

In order for a closed system to have a stability margin relative to the amplitude, on the basis of (1.75) and (1.76) for a statically unstable rocket ($c_{\psi\psi}<0$) it is necessary that the following inequalities be satisfied:

$$k_{min} > \left| \frac{c_{\psi\dot{\psi}}}{c_{\psi\delta}} \right|,$$
$$k(\omega_0)_{max} < \left| \frac{\omega_0^2 - c_{\psi\psi}}{c_{\psi\delta}} \right|. \qquad (1.78)$$

In order for a closed system to have a stability margin relative to the phase it is necessary that the control system regulating the ψ channel have a phase lead in the frequency range $[0, \omega_0]$.

2. A statically stable rocket, $c_{\psi\psi} > 0$.

The hodograph of the complex transfer number for the object under control is shown in Figure 1.17. The hodograph lies on the real axis of the complex plane Z. The dashed line indicates the hodograph with the damping coefficient $c_{\psi\dot{\psi}}$ taken into account. For $c_{\psi\dot{\psi}} = 0$ the denominator the complex transfer number in (1.73) has two purely imaginary roots, the controlled object is on the border of stability; for $c_{\psi\dot{\psi}} > 0$ the object is stable, and has a small stability margin with respect to the phase. An addition to the controlled object of a control system which has a property of retardation at high frequencies causes an appearance of point B (in Figure 1.17 part of the hodograph for the open circuit is represented by curve a).

In order for a closed system to have a stability margin relative to the phase it is necessary that the control system possess a phase lead up to frequencies ω_0 determined by the inequality (1.77). The magnitude of ω_0 is an important characteristic of the control system. As will be shown later it is used in estimating the stability of a rocket with the movement of liquids in tanks taken into account.

A closed system will have a stability margin with respect to amplitude if the amplification coefficient of the control system is bounded from above, i.e.,

$$k_{max}(\omega_0) < \frac{\omega_0^2 - c_{\psi\psi}}{c_{\psi\delta}}.$$

The amplification coefficient is not bounded from below in the case under consideration.

3. A neutral rocket, $c_{\psi\psi}=0$.

The hodograph of the complex transfer number for $c_{\psi\dot{\psi}}=0$ coincides with the real half-axis (Figure 1.18); the denominator of the complex transfer number in (1.73) has two zero roots.

If at low frequencies we neglect dynamic properties of the control system and set

$$\delta=k\psi,$$

then the equation of the closed system will be

$$p^2\psi+kc_{\psi\dot{\psi}}\psi=0.$$

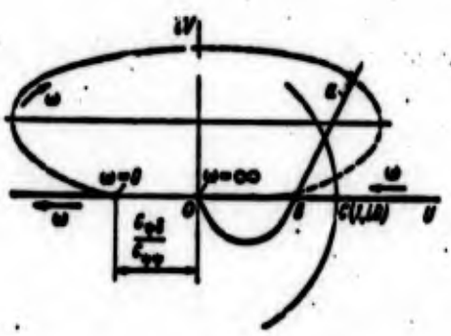

Figure 1.17

Figure 1.18

In the presence of disturbances the closed system will execute sustained oscillations with the natural frequency

$$\omega=\sqrt{kc_{\psi\dot{\psi}}}.$$

These oscillations indicate that the closed system is on the boundary of stability

$$k(i\omega)=\frac{kc_{y\delta}}{\omega^2}=1.$$

A hodograph of an open system in Figure 1.18 is represented by curve a. As a result of retardation caused by the control system at high frequencies, there appears a negative passage through the real axis — point B. In order for the closed system to have a stability margin relative to amplitude it is necessary that the control system produce a phase lead in the frequency interval $[0, \omega_0]$, where

$$\omega_0 > \sqrt{k(\omega_0)c_{y\delta}}.$$

Consequently, the amplification coefficient here should be bounded only from above, i.e.,

$$k_{max}(\omega_0) < \frac{\omega_0^2}{c_{y\delta}}.$$

An addition to the neutral rocket of a control system possessing the indicated properties causes the closed system to become a damped oscillating circuit.

The magnitude of the coefficient $c_{y\delta}$ depends on the velocity head q, the moment of inertia of the rocket, the relative location of the center of mass and of the center of pressure, which change during the flight. Therefore, even for one and the same rocket at various moments of time there may be situations when $c_{y\delta}>0$, $c_{y\delta}<0$, $c_{y\delta}=0$. In all these cases the control system should guarantee the stability of motion.

Summing up, we can formulate the following two basic requirements on the angular control system: 1) the control system should ensure a phase lead within the frequency range $[0, \omega_0]$; 2) the amplification coefficient of the control system should be bounded both from above and from below.

The amplitude-frequency and phase-frequency characteristics of the control system, corresponding to calculated requirements and the structure described in Section 7, are shown in Figure 1.19.

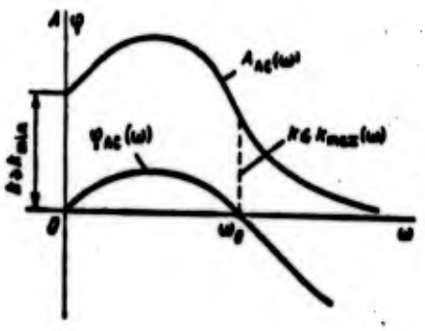

Figure 1.19

An increase in the coefficient $k(\omega) = A_{AC}(\omega)$ as compared to the static value in some frequency range is caused by the presence in the control loop of a differentiating circuit.

In order to decide what the frequency range $[0, \omega_0]$ should be and what limits should be imposed on the amplification coefficient $k_{max}(\omega_0)$, k_{min}, one has to analyze the complex transfer numbers of the controlled object and the entire open circuit for all possible instants of flight time.

As an example, in Figure 1.20 we have shown the typical amplitude frequency characteristics of a statically stable rocket for three characteristic instants of flight — immediately following the launch, for small and large velocity head q. In constructing the characteristics, we have used the following complex transfer number

$$K_\phi(i\omega) = \frac{-c_{\phi\delta}(i\omega + \omega_\xi)}{i\omega[c_{\phi\phi} + i\omega(c_{\vartheta_2\vartheta_2} + c_{\dot{\phi}\dot{\phi}}) - \omega^2]} = A_0(\omega)e^{i\varphi_0(\omega)}, \tag{1.79}$$

$$\omega_\xi = c_{\vartheta_2\vartheta_2} - c_{\dot{\phi}\vartheta_2}\frac{c_{\vartheta_2\delta}}{c_{\phi\delta}},$$

corresponding to the complete system of Equations (1.69), and considering that $c_{\vartheta_2\vartheta_2}c_{\dot{\phi}\dot{\phi}} \ll c_{\phi\phi}$.

The characteristics were plotted using a logarithmic scale which is very convenient in practical calculations of control systems. Such characteristics are called the logarithmic amplitude-frequency characteristics (LAC). On the ordinate axis, we plot

$$L_\phi(\omega) = 20 \lg A_0(\omega),$$

which is measured in decibels (db). An increase in $L_\varphi(\omega)$ by every 20 db corresponds to an increase of amplitude by a factor of 10. The zero point on the ordinate axis corresponds to an amplitude amplification $A_0(\omega)=1$. A decrease in amplitude $A_0(\omega)<1$ is associated with negative values of the orinate $L_\varphi(\omega)$.

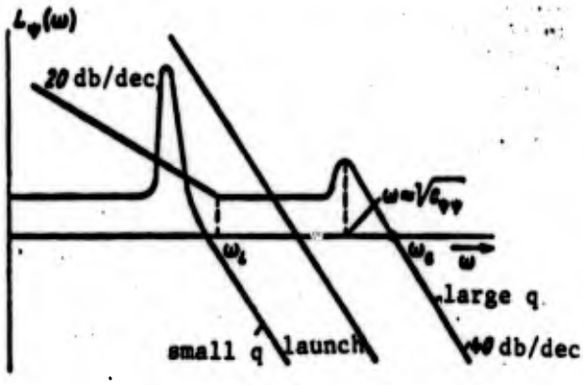

Figure 1.20

On the axis of abscissas we plot the values of ω in the logarithmic scale. The scale units used on the horizontal axis are the octave and the decade. Each octave is associated with an increase of frequency by a factor of 2, and each decade with an increase by a factor of 10. The frequency for which the logarithmic characteristic crosses the horizontal axis is called the <u>crossover frequency</u> ω_c.

For a large q and low frequencies the logarithmic characteristic has a form identical with that of the integrating circuit; the slope of the characteristic is -20 db/decade; the slope decreases to 0 db/decade for the frequency ω_L. At $\omega\approx\sqrt{c_{\varphi\varphi}}$ a resonance peak occurs, and its magnitude depends on the total damping $(c_{v_s v_s}+c_{\varphi\dot{\varphi}})$. The damping $c_{\varphi\dot{\varphi}}$ is achieved through an angular motion of the rocket, and the damping $c_{z_s v_s}$ through a lateral motion of the center of mass. For $\omega>\sqrt{c_{\varphi\varphi}}$ the logarithmic characteristic has a form identical with that for an oscillating circuit; the slope of the characteristic is equal to -40 db/decade.

On the initial portion of the trajectory and at high altitudes the velocity head decreases and the amplitude-frequency characteristic (Bode diagram) will be similar to that for low q. The values of ω_c, $\omega\approx\sqrt{c_{\varphi\varphi}}$, ω_L are in this case considerably smaller, and the resonance

amplitude is slightly larger compared to the corresponding values for large q. During the time of flight, under usual conditions, the resonance frequency $\omega \approx \sqrt{c_{\psi\psi}}$ may, as an example, change from 0.2 to 10 1/sec. The resonance amplitude may change by a factor of 3 to 4 for large q, and, say, by a factor of 100 for small q [17].

Immediately following the launch the aerodynamic forces are practically nonexistent. Therefore, it is impossible to show in a Bode diagram where the resonance frequency or the frequency ω_L are located. The only lateral force is in this case the force of the control elements, and the cross-over frequency depends on the moment of this force. On the basis of (1.79) the cross-over frequency is

$$\omega_c = \sqrt{c_{\psi\delta}}.$$

The slope of the amplitude-frequency characteristic immediately following the launch is equal to -40db/decade. This is easy to see since

$$20 \lg A_0(\omega_1) - 20 \lg A_0(10\omega_1) = 20 \lg \frac{A_0(\omega_1)}{A_0(10\omega_1)} =$$

$$= 20 \lg \frac{\frac{c_{\psi\delta}}{\omega_1^2}}{\frac{c_{\psi\delta}}{(10\omega_1)^2}} = 20 \lg 100 = 40 \; \partial\delta/\partial\kappa.$$

More complete information needed to select the amplification coefficients for the control system can be obtained by constructing regions of stability. In this connection we shall analyze the equations of the closed system, consisting of equations for the controlled member (1.69) and the equations of the control system. The equations of the controlled member will be written without considering the damping forces

$$\begin{aligned} \dot{v}_z + c_{v_z\psi}\psi + c_{v_z\delta}\delta = 0, \\ \ddot{\psi} + c_{\psi\psi}\psi + c_{\psi\delta}\delta = 0. \end{aligned} \tag{1.80}$$

The equation of the control system (1.65) may be put in the form

$$T_2^2\ddot{\delta} + T_1\dot{\delta} + \delta = k_\psi\psi + k_{\dot{\psi}}\dot{\psi}. \tag{1.81}$$

The characteristic equation of the system (1.80) and (1.81) will be

$$(a_0p^4+a_1p^3+a_2p^2+a_3p+a_4)=0, \tag{1.82}$$

where

$$a_0=T_2^2,$$

$$\begin{aligned} a_1&=T_1,\\ a_2&=1+T_2^2c_{\psi\psi},\\ a_3&=k_{\dot\psi}c_{\psi\beta}+T_1c_{\psi\psi},\\ a_4&=k_\psi c_{\psi\beta}+c_{\psi\psi}. \end{aligned} \tag{1.83}$$

We shall use the Hurwitz criterion [16]. The closed system (1.80) and (1.81) will be stable if all the coefficients of Equations (1.82) and the discriminant Δ_3 are positive, i.e.,

$$a_0>0,\ a_1>0,\ a_2>0,\ a_3>0,\ a_4>0,$$
$$\Delta_3=a_3(a_1a_2-a_0a_3)-a_4a_1^2>0.$$

The coefficient $c_{\psi\beta}>0$. Therefore, it is not difficult to find values of k_ψ and $k_{\dot\psi}$ such that for an aerodynamically unstable rocket ($c_{\psi\psi}<0$) the coefficients in (1.83) will all be positive. The conditions $\Delta_3=0$ and $a_4=0$ are decisive. The latter condition is the limit of an aperiodic stability.

Let us find an equation for the stability boundary from the condition $\Delta_3=0$. Substituting in this equality values of the coefficients in (1.83), we get

$$c_1k_{\dot\psi}^2+c_2k_{\dot\psi}k_\psi+c_3k_\psi^2+c_4k_{\dot\psi}+c_5k_\psi=0. \tag{1.84}$$

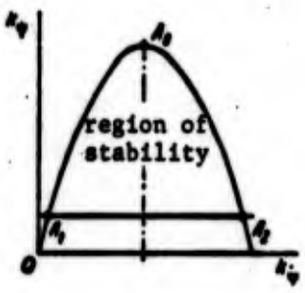

Figure 1.21

Equation (1.84) is an equation of a parabola in the coordinates $Ok_{\dot\psi}k_\psi$. The parabola passes through the origin; the axis of the parabola is parallel to the coordinate axis Ok_ψ (Figure 1.21). The set of values of $k_{\dot\psi}$, k_ψ, lying in the region bounded by a parabola and the horizontal axis satisfies condition $\Delta_3>0$.

The inequality $a_4<0$ determines a region of a non-periodic unstable system. The boundary of a non-periodic instability can be found from

$$a_4=k_\psi c_{\psi\delta}+c_{\psi\psi}=0,$$

Or

$$k_\psi=-\frac{c_{\psi\psi}}{c_{\psi\delta}}. \tag{1.85}$$

Consequently, the region of stability lies between the parabola in (1.84) and the straight line (1.85). For a statically unstable rocket ($c_{\psi\psi}<0$) this region is shown in Figure 1.21. In order for a rocket to be stable it is necessary that

$$k_\psi>\left|\frac{c_{\psi\psi}}{c_{\psi\delta}}\right|.$$

This condition is identical with the first condition in (1.78) which was obtained by analyzing the system by frequency response methods.

The apex of the parabola A_0 is located at the point with coordinates

$$A_0\left(\frac{T_1(1-T_3^2c_{\psi\psi})}{2T_3^2c_{\psi\delta}};\ \frac{(1-T_3^2c_{\psi\psi})^2}{4T_3^2c_{\psi\delta}}\right).$$

Ordinarily $1\gg T_3^2c_{\psi\psi}$. Therefore, the ordinate of the apex is practically independent of the degree of aerodynamic instability, and is determined by the effectiveness of the control elements ($c_{\psi\delta}$) and by the parameter of the control system T_3^2.

We may make an arbitrary convention and say that the abscissa of the apex of the parabola determines the width of the stability region. It is proportional to T_1 and inversely proportional to the product $T_3^2c_{\psi\delta}$.

By considering a family of characteristics (see Figure 1.20) and a region of stability (see Figure 1.21), we can arrive at a more

concrete frequency range $[0, \omega_0]$ and an upper and lower bound for the amplification coefficient of the control system. However, we cannot make a final choice of values for these quantities just as we cannot determine the stability margins relative to the amplification coefficient (with respect to the amplitude) and relative to the phase on the basis of such characteristics. A selection of the stability margin is a very complex task. There one has to take into account all the possible deviations in rocket parameters, the deviations of the parameters and characteristics of the control system, the temperature-dependence of the characteristics, vibrations, and other factors. The values of these parameters may be determined empirically from the actual performance of rockets and control systems.

Now let us discuss the dynamic properties of the autonomous system controlling the lateral motion of the center of mass relative to a desired trajectory. The equations of the lateral motion of the center of mass (1.72) will be written with the right-hand sides equal to

$$\begin{aligned} \dot{v}_z + c_{v_z v_z} v_z + c_{v_z \psi} \psi + c_{v_z \delta} \delta &= \frac{Z_w}{m}, \\ c_{\psi v_z} v_z + c_{\psi\psi} \dot{\psi} + c_{\psi\delta} \delta &= \frac{M_{yw}}{I}. \end{aligned} \tag{1.86}$$

Here Z_w and M_{yw} are disturbing factors, acting lengthwise caused by winds, lack of parallel alignment between the thrust vector and the longitudinal axis of the fuselage, etc.

The system controlling the center of mass should be able to compensate for the action of the disturbing factors. Let, for example, force Z_w and moment M_{yw} arise as a result of wind acting on the rocket. Then the angular control system will turn the vanes by some angle δ in order to balance the disturbing moment and keep the fuselage parallel to the Z_w plane ($\psi=0$). In addition to the lateral force the fuselage will be acted on by a lateral control force Z_c. In the case of a statically stable rocket ($c_{\psi\psi}>0$) the forces Z_w and Z_c will have different directions (Figure 1.22 on the left), and for the case of

a statically unstable rocket these forces will have a single direction (Figure 1.22, on the right). Under the action of forces Z_w and Z_c, the center of mass of the rocket will be displaced in a lateral direction.

In order to compensate for the action of Z_w and Z_c the system controlling the center of mass has to rotate the fuselage of the rocket (the thrust vector) so that the sum of the projections of forces Z_w, Z_c, and P_E on the z axis is equal to zero, or more exactly, the rotation has to have an effect of bringing the velocity component v_z of the center of mass to zero. For a statically unstable rocket the angle of rotation should be greater than for a statically stable rocket.

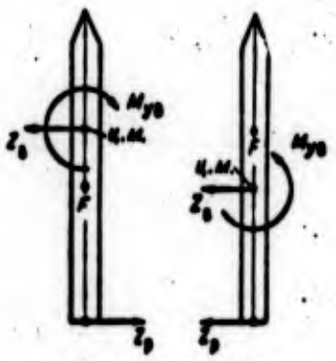

Figure 1.22

Thus, the angular control system strives to keep the axis of the rocket in the pitching plane, and the linear control system should displace this axis from the firing plane.

One of the possible laws of signal formation in the linear control channel [3], is

$$\delta = k_1\vartheta - k_1 v_z - k_2 z, \qquad (1.87)$$

where z is the coordinate giving the displacement of the center of mass. Since the linear and angular stabilization is achieved by the same auxiliary elements, a block diagram of the system exercising control in the plane of pitch will be as shown in Figure 1.23.

Let us determine some requirements that will be imposed on the choice of the amplification coefficients k_1 and k_2, and for this purpose let us establish a correlation from Equations (1.66) and (1.87) between the coordinate z giving the displacement of the center of mass and the perturbing force Z_w. Letting $v_z = pz$, $M_{yw} = 0$, we get

$$[p^2(c_{\psi\psi}+kc_{\psi\dot{z}})+p[c_{v_z v_z}(c_{\psi\psi}+kc_{\psi\dot{z}})-c_{\psi v_z}(c_{v_z\psi}+kc_{v_z\dot{z}})+$$
$$+k_1(c_{v_z\psi}c_{\psi\dot{z}}-c_{\psi\psi}c_{v_z\dot{z}})]+k_2(c_{v_z\psi}c_{\psi\dot{z}}-c_{\psi\psi}c_{v_z\dot{z}})]z=$$
$$=-\frac{Z_w}{m}(c_{\psi\psi}+kc_{\psi\dot{z}}).$$

With a corresponding choice of the coefficients k_1 and k_2 we can secure a high quality of the transfer process. The higher the coefficient k_2, the smaller the static displacement of the center of mass, i.e.,

$$z=\frac{Z_w}{m}\frac{c_{\psi\psi}+kc_{\psi\dot{z}}}{k_2(c_{v_z\psi}c_{\psi\dot{z}}-c_{\psi\psi}c_{v_z\dot{z}})},$$

and the higher the natural frequency of center of mass oscillations

$$\omega=\sqrt{\frac{k_2(c_{v_z\psi}c_{\psi\dot{z}}-c_{\psi\psi}c_{v_z\dot{z}})}{c_{\psi\psi}+kc_{\psi\dot{z}}}}.$$

However, as k_2 increases there may occur a slight decrease in the stability margin relative to the ψ channel.

As we see from the equation for the displacement of the center of mass, k_1 determines the damping in the system. The larger k_1 is, the faster the center of mass oscillations are attenuated.

A selection of values for the amplification coefficients k_1 and k_2 of the linear control system may be achieved as follows: given disturbances Z_w and M_{yw}, we solve Equations (1.79) and (1.87) for various fixed instants of flight time, and find the functional relationships between v_z and z and coefficients k_1 and k_2. Furthermore if the values of k_1 and k_2 are large, then in the momentum equation we shall have to take $\ddot{\psi}$ into account. Making use of the requirements on the accuracy of flight, on the basis of the obtained relationships, one can select acceptable values of the coefficients k_1 and k_2.

An analysis of equations with constant coefficients gives only a qualitative notion of how the stabilization of the center of mass is achieved. Under the actual conditions the coefficients of equations and the disturbing forces change during the time of flight. This means that we can only get an idea of what the maximum speed v_z and the maximum accumulated error in the deviation of the z coordinate are, by solving equations with variable coefficients on a digital or analog computer. Only if this is done, can one make the final choice of values for k_1 and k_2.

The structure of equations of the perturbed motion in the pitch plane (1.40) is identical with that for the yaw plane (1.69). Therefore, the requirements on the linear and angular control systems are practically the same as those applying to the system controlling motion in the yaw plane.

Equation (1.24) representing perturbed motion relative to the longitudinal axis is simpler:

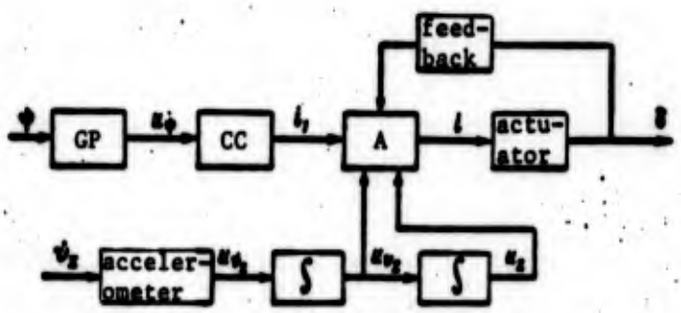

Figure 1.23

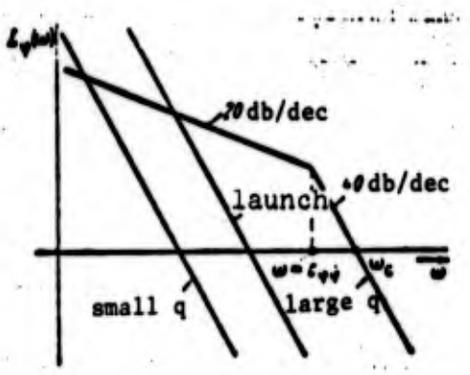

Figure 1.24

$$\ddot{\varphi}+c_{\varphi\dot{\varphi}}\dot{\varphi}+c_{\varphi\delta}\delta=0. \qquad (1.88)$$

The coefficient $c_{\varphi\dot{\varphi}}$ is determined by the aerodynamic forces, and the coefficient $c_{\varphi\delta}$ — by the control forces, which when air vanes are used, will depend also on the velocity head.

The complex transfer number with respect to the angle of roll is

$$K_\varphi(i\omega)=\frac{-c_{\varphi\delta}}{i\omega c_{\varphi\dot{\varphi}}-\omega^2}.$$

Examples of Bode diagrams in the logarithmic scale are shown in Figure 1.24. For large q and low altitudes, the slope of the Bode plot is equal to -20db/decade, and changes to -40db/decade for frequency $\omega = c_{\varphi\dot{\varphi}}$. The point of intersection of this plot with the frequency axis determines the cross-over frequency ω_c. As q gets smaller at high altitudes, the Bode diagram changes in accordance with the diagrams for small q. The launch Bode diagram corresponds to conditions existing immediately after the launch when $c_{\varphi\dot{\varphi}} = 0$, and $c_{\varphi\delta}$ does not depend on the velocity head q, and is completely determined by the effectiveness of jet vanes or revolving chambers.

The structure of Equation (1.88) is analogous to the structure of the equation of moments in the plane of yaw for $c_{\psi\dot{\psi}} = 0$. Therefore, the requirements on the system controlling the roll channel are analogous to the requirements on the angular control channel for $c_{\psi\dot{\psi}} = 0$. The frequency of the natural oscillations of a rocket with a control system relative to the longitudinal axis is

$$\omega = \sqrt{k(\omega_0) c_{\varphi\delta}} \tag{1.89}$$

where $k(\omega_0)$ is the amplification coefficient of the control system; $c_{\varphi\delta} = M^{\delta}_{xp}/I_x$.

The dynamic model of a liquid-fueled rocket as an absolutely rigid body is true only to a first approximation. On the basis of that model we can calculate the trajectory of flight and formulate the basic requirements which will be imposed on the guidance and control system. In some cases this model is sufficient. However, as the length of the rocket increases the assumption of the rigidity of the fuselage becomes rather arbitrary. Under lateral disturbances a long fuselage moves not as a rigid body, but as an elastic piston. If the elasticity of the fuselage is taken into account, additional dynamic properties are revealed which are important, for example, for the angular control of a rocket. In addition, there are in the tanks of a rocket considerable masses of liquid fuel which may move relative to the walls and create additional forces.

Before we study the dynamics of a rocket with the oscillations of liquids taken into account, we shall first analyze the dynamic properties of a tank with a liquid as a component part of a rocket.

REFERENCES

1. Appazov, R. F., S. S. Lavrov and V. P. Mishin. Ballistika upravlyayemykh raket dal'nego deystviya (Ballistics of Long-Range Guided Missiles) Izdatel-stvo Nauka, 1966.

2. Gantmakher, F. R. and L. M. Levin. Teoriya poleta neupravlyayemykh raket (Flight Theory of Unguided Rockets), Fizmatgiz, 1959.

3. Dobrolenskiy, Yu, P., V. I. Ivanova, and G. S. Pospelov Avtomatika upravlyayemykh snaryadov (Automatization in Guided Missiles). Oborongiz, 1963.

4. Dmitriyevskiy, A. A. and V. N. Koshevoy. Osnovy teorii poleta raket (Fundamentals of the Theory of Rocket Flight) Voyenizdat, 1964.

5. Karacharov, K. A. and A. G. Pilyutik. Vvedeniye v tekhnicheskuyu teoriyu ustoychivosti dvizheniya (Introduction to the Technical Theory of the Stability of Motion), Fizmatgiz, 1962.

6. Krasnov, N. F. Aerodinamika tel vrashcheniya (The Aerodynamics of Bodies of Revolution), Oborongiz, 1958.

7. Litvin-Sedoy, M. Z. Vvedeniye v mekhaniku upravlyayemogo poleta (Introduction to the Mechanics of a Guided Flight). Izdatel'stvo "Vysshaya Shkola", 1962.

8. Lebedev, A. A. and L. S. Chernobrovkin. Dinamika poleta bespilotnykh letatel'nykh apparatov (Flight dynamics of Unmanned Aircraft). Oborongiz, 1962.

9. Lebedev, A. A. and V. A. Karabanov. Dinamika sistem upravleniya bespilotnymi letatel'nymi apparatami (Dynamics of the Control Systems in Unmanned Aircraft). Mashgiz, 1965.

10. Lokk, A. S. Upravleniye snaryadami (Missile Guidance) GITTL (Gosudarstvennoye izdatel'stvo tekhnicheskoy i teoreticheskoy literatury), 1957.

11. Loytsyanskiy, L. G. and A. I. Lur'ye. Kurs teoreticheskoy mekhanika (Course on theoretical Mechanics), Gostekhizdat, Vol. 1, 1954.

12. Loytsyanskiy, L. G. and A. I. Lur'ye. Kurs teoreticheskoy mekhanika (Course on Theoretical Mechanics). Gostekhizdat, Vol. 2, 1955.

13. Makkormak, Optimal'naya sistema upravleniye uglovym polozheniyem rakety (Optimum angular Control System for a Rocket), "Voprosy raketnoy tekhniki", No. 6, 1964.

14. Malkin, I. G. Teoriya Ustoychivosti dvizheniya (Theory of the Stability of Motion), Gostekhizdat, 1952.

15. Ostoslavskiy, I. V. and I. V. Strazheva. Dinamika poleta. Trayektorii letatel'nykh apparatov (Flight dynamics. Aircraft Trajectories). Oborongiz, 1963.

16. Popov, Ye. P. Dinamika sistem avtomaticheskogo regulirovaniya (Dynamics of Automatic Control Systems) Gostekhizdat, 1954.

17. Ril. Trebovaniya k sistemam upravleniya snaryadami. Stabilizatsiya i navedeniye (Requirements imposed on missile Control Systems. Guidance and Control). "Voprosy raketnoy tekhniki", No. 4, 1958.

18. Solodovnikov, V. V. Chastotnyy metod analiza kachestva sistem avtomaticheskogo regulirovaniya (Frequency Response Method in Analyzing Automatic Control System Quality. Mashgiz, 1950.

19. Strelkov, S. P. Vvedeniye v teoriyu kolebaniy (Introduction to Theory of Oscillations) Izdatel'stvo "Nauka", 1964.

20. Teodorchik, K. F. Avtokolebatel'nyye sistemy (Auto-Oscillatory Systems), Gostekhizdat, 1952.

21. Feodos'yev, V. I., and B. G. Sinyarev. Vvedeniye v raketnuyu tekhniku (Introduction to Rocket Technology) Oborongiz, 1960.

22. Kharkevich, A. A. Avtokilebaniya (Auto-Oscillations) Gostekhizdat, 1953.

23. Kheysserman, Oblasti ustoychivosti sistemy regulirovaniya upravlyayemogo snaryada (Stability regions of the Control System in a Guided Missile). "Voprosy raketnoy tekhniki", No. 1, 1958.

24. Khobbs, M. Tekhnika upravleniya raketami (Rocket Guidance and Control Techniques). Voyennoye Izdatel'stvo Ministerstva Oborony SSSR, 1963.

CHAPTER II

OSCILLATIONS OF A FLUID IN A CYLINDRICAL TANK

1. Laplace Equation

The study of oscillations of liquids in tanks is one of the tasks of classic hydrodynamics [8, 12] where to describe motion of a fluid one makes use of either Lagrangian coordinates or Eulerian coordinates.

The Lagrangian coordinates describe the motion of a specific fluid element, and depend on the initial time and position coordinates of this element. The study of motion of a liquid using those coordinates consists in analyzing the changes in various vector and scalar quantities (for example, velocity,pressure, etc.) describing the motion of some fixed fluid element as a function of time.

The Eulerian coordinates characterize the state of fluid elements that are found at a given point with coordinates x, y , z at various instants of time t. In other words, various vector and scalar quantities used to describe fluid motion are expressed as functions of position and time, i.e., as functions of four arguments: x, y, z, t.

We shall use Eulerian coordinates.

In our analysis of oscillations of liquids we shall make the following assumptions:

1) the liquid in a cylindrical tank is ideal and incompressible;

2) the displacements and velocities of all fluid particles and walls of the tank are small in the sense that their products and squares may be neglected compared to the values of the quantities themselves;

3) the motion of liquid in the Oxyz coordinate system is associated with a velocity potential. Assuming that the initial flow is irrotational and that the field of body forces has a potential, on the basis of Lagrange's theorem we come to a conclusion that the flow is potential at any time instant;

4) the total acceleration vector of the field of body forces g at all times coincides with the axis of the tank or makes a small angle with it.

In an undisturbed flow the free surface of the fluid makes a right angle with the vector g.

Figure 2.1 shows an elementary volume as a rectangular parallelepiped with the sides dx, dy, dz, Let the fluid velocity in the direction of the main coordinate axes on the planes x = 0, y = 0, z = 0, be represented by the components v_xm v_y, v_z. Then on the faces located at distance dx, dy, dz, the velocity components will be

$$v_x+\frac{\partial v_x}{\partial x}dx,\quad v_y+\frac{\partial v_y}{\partial y}dy,\quad v_z+\frac{\partial v_z}{\partial z}dz.$$

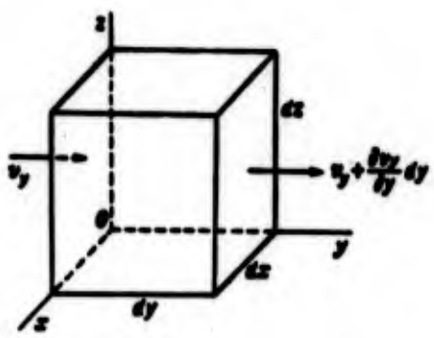

Figure 2.1

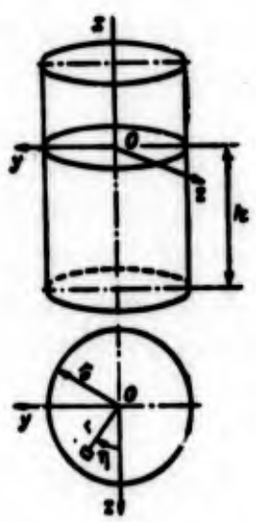

Figure 2.2

In case the fluid is incompressible the volumes of liquid flowing into the parallelepiped and flowing out must be equal. Then

$$\frac{\partial v_x}{\partial x}dxdydz+\frac{\partial v_y}{\partial y}dydxdz+\frac{\partial v_z}{\partial z}dzdxdy=0.$$

This relation gives the continuity equation

$$\frac{\partial v_x}{\partial x}+\frac{\partial v_y}{\partial y}+\frac{\partial v_z}{\partial z}=0, \tag{2.1}$$

which should be satisfied at any point in the volume of liquid.

The fact that the flow is irrotational is in vector form expressed as

$$v=\operatorname{grad}\phi.$$

Projecting grad ϕ on the coordinate axes, we get

$$v_x=\frac{\partial\phi}{\partial x},\quad v_y=\frac{\partial\phi}{\partial y},\quad v_z=\frac{\partial\phi}{\partial z}. \tag{2.2}$$

Substituting (2.2) into (2.1), we obtain Laplace's equation for the function ϕ

$$\Delta\phi=\frac{\partial^2\phi}{\partial x^2}+\frac{\partial^2\phi}{\partial y^2}+\frac{\partial^2\phi}{\partial z^2}=0. \tag{2.3}$$

A function $\phi(x, y, z)$ is called harmonic in a finite region if it has in this region continuous first and second derivatives and satisfies Laplace's equation at all points of the region. A potential ϕ, consequently, will be a harmonic function at any point of the volume occupied by a liquid.

It is convenient to solve the problem of liquid oscillations in a cylindrical tank using cylindrical coordinates instead of Cartesian coordinates. Letting the Ox axis point along the axis of a tank and introducing variables r and η instead of y and z (Figure 2.2), where

$$y=r\sin\eta,\quad z=r\cos\eta, \tag{2.4}$$

we obtain Laplace's equation in cylindrical coordinates

$$\frac{\partial^2\varphi}{\partial r^2}+\frac{1}{r}\frac{\partial\varphi}{\partial r}+\frac{1}{r^2}\frac{\partial^2\varphi}{\partial\gamma^2}+\frac{\partial^2\varphi}{\partial x^2}=0. \tag{2.5}$$

A solution of Laplace's equation should satisfy boundary and initial conditions.

2. Boundary and Initial Conditions

Let us place the origin of the coordinates at the center of the free surface. Let the Oy and Oz axes lie in the horizontal plane, and the Ox axis point upward. The value r_0 will denote the radius of the circular cylindrical tank, and h will be the height of the column of liquid. The velocity of liquid at the walls and bottom along the normal to the surface is zero if the tank is stationary. If the tank is in motion, the velocity of liquid at the walls and bottom along the normal to the immersed surface is equal to the velocity of motion of the walls and bottom in the same direction.

Thus,

$$\frac{\partial\varphi}{\partial r}=v_r^* \text{ for } r=r_0, \tag{2.6}$$

$$\frac{\partial\varphi}{\partial x}=v_x^* \text{ for } x=-h, \tag{2.7}$$

where v_r^*, v_x^* are velocities of points in the boundary surface in the direction of the normal to this surface.

Now let us discuss the boundary conditions at the free surface where the pressure p has a constant value p_0, equal to the pressure of gas located above the liquid.

We know that in case of a stationary flow the pressure of a liquid can be calculated from Bernoulli's integral [8, 12]

$$p+\frac{1}{2}v^2+V=\Gamma,$$

where Γ is a quantity which remains constant along a given streamline; V is the potential of body forces.

If the Ox axis is directed vertically upward, and the acceleration of gravity is equal to g, then the potential of body forces is expressed as

$$V = gx.$$

In the case of unsteady flow there arises an additional dynamic pressure, equal to $\rho\partial\phi/\partial t$ [8, 12]. Therefore, pressure p at any point of the volume occupied by liquid can be determined from

$$\frac{p-p_0}{\rho} = -\frac{\partial\phi}{\partial t} - \frac{1}{2}v^2 - gx, \tag{2.8}$$

which is referred to as the Cauchy integral [8, 12].

We shall assume that the flow is sufficiently slow so that in (2.8) we may neglect the term $v^2/2$, and write

$$\frac{p-p_0}{\rho} = -\frac{\partial\phi}{\partial t} - gx. \tag{2.9}$$

Let the equation of free surface at a time t be of the form

$$\chi = \chi(y, z, t).$$

From Equation (2.9) and the condition that the free surface $p = p_0$ we conclude that

$$\left(\frac{\partial\phi}{\partial t}\right)_{x=\chi(y,z,t)} + g\chi = 0.$$

Since the oscillations of the liquid were assumed to be n infinitesimal, in Equation (2.9) we can use the value of $\partial\phi/\partial t$ for $x = 0$ (instead of $x = \chi$). Then we obtain

$$\chi = -\frac{1}{g}\left(\frac{\partial\phi}{\partial t}\right)_{x=0}. \tag{2.10}$$

Upon differentiating this expression with respect to t, we get

$$\frac{\partial \chi}{\partial t} = -\frac{1}{g}\left(\frac{\partial^2 \phi}{\partial t^2}\right)_{x=0}.$$

But $\partial\chi/\partial t$ is only slightly different from v_x. In fact, consider an arbitrary particle on the free surface, with coordinates y, z, x = χ. The velocity projection of this particle on the coordinate axis will be

$$v_y = \frac{dy}{dt}, \quad v_z = \frac{dz}{dt}, \quad v_x = \frac{dx}{dt} = \frac{\partial \chi}{\partial t} + \frac{\partial \chi}{\partial y}\frac{dy}{dt} + \frac{\partial \chi}{\partial z}\frac{dz}{dt}$$

or

$$v_x = \frac{\partial \chi}{\partial t} + \frac{\partial \chi}{\partial y} v_y + \frac{\partial \chi}{\partial z} v_z.$$

The last two terms may be neglected if one considers that $\partial\chi/\partial y$ and $\partial\chi/\partial z$ are small, i.e., that the plane tangent to the free surface is almost horizontal. Thus, on the free surface we have an approximate equality

$$v_x = \frac{\partial \phi}{\partial x} = \frac{\partial \chi}{\partial t},$$

which, also as before, may be considered to hold for x = 0 (instead of for x = χ).

Consequently, instead of (2.10) one may write

$$\int_0^t \left(\frac{\partial \phi}{\partial x}\right)_{x=0} dt = -\frac{1}{g}\left(\frac{\partial \phi}{\partial t}\right)_{x=0}. \qquad (2.11)$$

The function Φ must also satisfy the initial conditions. These conditions may be expressed, in particular, as initial perturbations of the free surface.

The initial conditions give us the values of the arbitrary constants in a general solution of the homogeneous differential Equation (2.5).

In what follows we shall analyze the question of the stability of motion of the system using frequency response methods based on an analysis of the dynamic properties of the system with steady harmonic perturbations. In this case the flows caused by the initial conditions are of no interest to us, and will not be calculated.

Thus, the problem of a perturbed flow in a tank reduces to a calculation of the potential function $\Phi(x, r, \eta, t)$, that satisfies Laplace's equation and the boundary conditions. If the function Φ is found, then the pressure at any point of the liquid volume will be calculated from Formula (2.9). Now we shall proceed to determine Φ.

3. A Calculation of the Potential of the Absolute Velocity of a Liquid.

Let us introduce two rectangular coordinate systems — an absolute Oxyz and a moving system $O_1x_1y_1z_1$ attached to a cylinder (Figure 2.3). The motion of the moving coordinate system relative to the absolute frame will determine the motion of the tank.

The origin of the moving frame will be located at the center of the free surface, and the O_1x_1 axis will point upward along the tank axis, whereas the O_1y_1 and O_1z_1 axes will lie in the plane of the circular cross section of the tank. The orientation of the absolute frame Oxyz will be selected in such a way that the $O_1x_1y_1z_1$ and Oxyz frames will coincide if the tank is stationary.

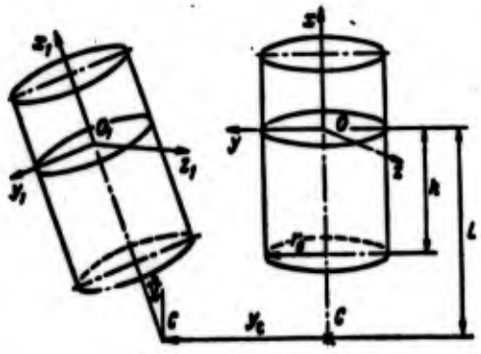

Figure 2.3

The problem of finding the potential function Φ will be analyzed as applied to the case of a planar motion of the tank. Let us focus our attention on some point C located on the longitudinal axis of the tank at a distance L beneath an undisturbed free surface. Then the position of the tank in

the Oxy plane will be determined by the coordinates of point $C(-L, y_c)$ and an angle ϑ. The tank pivots about point C relative to an axis passing through C and parallel to Oz. Displacements given by $y_c(t)$ and $\vartheta(t)$ will determine the perturbed motion of the tank.

The absolute velocity potential Φ must satisfy Laplace's equation

$$\Delta\phi = \frac{\partial^2\phi}{\partial r^2} + \frac{1}{r}\frac{\partial\phi}{\partial r} + \frac{1}{r^2}\frac{\partial^2\phi}{\partial\eta^2} + \frac{\partial^2\phi}{\partial x^2} = 0, \tag{2.12}$$

the boundary conditions at the walls of the tank

$$\frac{\partial\phi}{\partial r} = v_r^* \quad \text{for } r = r_0, \tag{2.13}$$

$$\frac{\partial\phi}{\partial x} = v_x^* \quad \text{for } x = -h \tag{2.14}$$

and the condition requiring the pressure to be constant at the free surface

$$\int_0^t \frac{\partial\phi}{\partial x}\,dt = -\frac{1}{g}\frac{\partial\phi}{\partial t} \quad \text{for } x = 0. \tag{2.15}$$

Since the motion of the tank is determined by a displacement $y_c(t)$ and rotation $\vartheta(t)$, the radial velocity of the tank walls is given by

$$v_r^* = [\dot{y}_c + \dot{\vartheta}(L + x)]\sin\eta. \tag{2.16}$$

The velocity component of the tank bottom in the Ox direction is equal to

$$v_x^* = -\dot{\vartheta} r \sin\eta. \tag{2.17}$$

In order to make it easier for us to find the potential Φ, we shall represent it, following D. Ye. Okhotsimskiy [23], as a sum of two functions

$$\phi(x, r, \eta, t) = \psi(x, r, \eta, t) + \varphi(x, r, \eta, t). \tag{2.18}$$

A method to determine a function ψ was proposed by N. Ye. Joukowski [6]. Let us select an expression for ψ that would correspond to the boundary conditions (2.13) and (2.14). To make it simpler for ψ to satisfy (2.13), it is advisable to include the expression in (2.16) in the function ψ. Then

$$\psi(x, r, \eta, t)=F(x, r, \eta)\dot{\theta}+r\sin\eta[\dot{y}_C+\dot{\theta}(L+x)]. \tag{2.19}$$

Function $\psi(x, r, \eta, t)$ will correspond to conditions (2.13) and (2.14) if

$$\frac{\partial F}{\partial r}=0 \quad \text{for} \quad r=r_0, \tag{2.20}$$

$$\frac{\partial F}{\partial x}=-2r\sin\eta \quad \text{for} \quad x=-h. \tag{2.21}$$

Since $\psi(x, r, \eta, t)$ satsifies conditions at the walls (2.13) and (2.14), the boundary conditions for $\varphi(x, r, \eta, t)$ will be

$$\frac{\partial\varphi}{\partial r}=0 \quad \text{for} \quad r=r_0, \tag{2.22}$$

$$\frac{\partial\varphi}{\partial x}=0 \quad \text{for} \quad x=-h. \tag{2.23}$$

The sum of the function $\psi+\varphi$ must satisfy the boundary condition (2.15)

$$\int_0^t \frac{\partial(\psi+\varphi)}{\partial x}\,dt=-\frac{1}{g}\frac{\partial(\psi+\varphi)}{\partial t} \quad \text{for} \quad x=0. \tag{2.24}$$

Let us first find function $F(x, r, \eta)$ that must satisfy Laplace's equation

$$\frac{\partial^2 F}{\partial r^2}+\frac{1}{r}\frac{\partial F}{\partial r}+\frac{1}{r^2}\frac{\partial^2 F}{\partial\eta^2}+\frac{\partial^2 F}{\partial x^2}=0 \tag{2.25}$$

and the boundary conditions (2.20) and (2.21).

We shall solve Equation (2.25) by using Fourier's method (the method of separation of variables). Let $F(x, r, \eta)$ be represented as a product of three functions

$$F(x, r, \eta) = X(x)H(\eta)R(r). \tag{2.26}$$

Substituting the expression for $F(x, r, \eta)$ into Laplace's equation and separating the variables, we obtain the following equations for the functions X(x), H(η),and R(r):

$$\frac{d^2X_n}{dx^2} - k_n^2 X_n = 0, \tag{2.27}$$

$$\frac{d^2H}{d\eta^2} + m^2 H = 0, \tag{2.28}$$

$$\frac{d^2R}{dr^2} + \frac{1}{r}\frac{dR}{dr} + \left(k_n^2 - \frac{m^2}{r^2}\right)R = 0, \tag{2.29}$$

where k_n, m are some undetermined parameters.

The problem of finding nontrivial solutions of equations of type (2.27) - (2.29), satisfying homogeneous boundary conditions, is called the Sturm-Liouville problem or the eigenvalue problem. It has nontrivial solutions only for certain values of k_n and m. The values of k_n and m for which a nontrivial solution does exist are called the eigenvalues of this problem, and the nontrivial solution itself is called an eigenfunction corresponding to a given eigenvalue. The set of all eigenvalues is called the spectrum of a given problem.

A general solution of Equation (2.27) is expressed in terms of hyperbolic functions

$$X_n(x) = C_1 \operatorname{ch} k_n x + C_2 \operatorname{sh} k_n x, \tag{2.30}$$

where the arbitrary constants C_1 and C_2 should be selected so that the boundary conditions at the free surface and the bottom of the cylindrical tank will be satisfied.

A solution of Equation (2.28) will have the form

$$H(\eta) = \sin(m\eta + \eta_0).$$

Since H(η) is periodic, the number m must be an integer (m = 1, 2, 3, ...), and to determine $F(x, r, \eta)$ it is sufficient to consider the simplest form when m = 1, and $\eta_0 = 0$. Consequently, below we shall assume that

$$H(\eta) = \sin \eta. \tag{2.31}$$

Equation (2.29) to determine function R(r) is a linear differential equation with variable coefficients, namely Bessel's equation. A solution of Equation (2.29) for m = 1 may be represented as

$$R_n(r) = A_1 J_1(k_n r) + A_2 Y_1(k_n r),$$

where A_1, A_2 are arbitrary constants; $J_1(k_n r)$; $Y_1(k_n r)$ are Bessel's functions of first and second kind of order one (m = 1). The function $Y_1(k_n r)$ for r = 0 goes to infinity. Therefore, we must set $A_2 = 0$, since otherwise the displacement of liquid for r = 0 will be infinitely large.

By virtue of (2.26) the boundary condition in (2.20) will be equivalent to

$$\frac{dR(r)}{dr} = 0 \quad \text{for} \quad r = r_0.$$

which gives

$$\frac{dJ_1(k_n r)}{d(k_n r)} = 0 \quad \text{for} \quad r = r_0.$$

The roots of this equation are

$$\zeta_1 = k_1 r_0 = 1{,}8412; \quad \zeta_2 = k_2 r_0 = 5{,}3315;$$
$$\zeta_3 = k_3 r_0 = 8{,}5363; \quad \zeta_4 = k_4 r_0 = 11{,}7060; \ldots$$

The functions $R_n(r) = J_1\left(\zeta_n \frac{r}{r_0}\right)$ $(n = 1, 2, 3, \ldots)$, which are a solution of Equation (2.29) can be conveniently normalized by, for example, making them equal to one for r = r_0. We shall obtain

$$R_n(r)=\frac{J_1\left(\zeta_n\frac{r}{r_0}\right)}{J_1(\zeta_n)}. \qquad (2.32)$$

Inasmuch as the function $R_n(r)$ satisfies condition (2.20), the arbitrary constants of the solution in (2.30) should be selected so that (2.21) is satisfied.

For that purpose we shall expand the variable r into a generalized Fourier series in Bessel's functions. We let

$$r=\sum_{n=1}^{\infty} B_n R_n(r),$$

where B_n are the expansion coefficients. In order to calculate them we shall multiply both sides of the equality by the product $R_n(r)$ and integrate over the radius.

The orthogonality condition gives

$$\int_0^{r_0} R_n(r)R_m(r)r\,dr=0 \quad (n\neq m).$$

Integrating and making use of the properties of Bessel's functions, we get

$$N_n=\int_0^{r_0} R_n^2(r)r\,dr=\frac{r_0^2(\zeta_n^2-1)}{2\zeta_n^2},$$

$$D_n=\int_0^{r_0} R_n(r)r^2\,dr=\frac{r_0^3}{\zeta_n^2}.$$

Thus,

$$B_n=\frac{D_n}{N_n}=\frac{2r_0}{\zeta_n^2-1}$$

and

$$r=2r_0\sum_{n=1}^{\infty}\frac{1}{\zeta_n^2-1}\frac{J_1\left(\zeta_n\frac{r}{r_0}\right)}{J_1(\zeta_n)}. \qquad (2.33)$$

Considering (2.33) and the expressions (2.26) and (2.31) the boundary condition (2.21) is identical with

$$\frac{dX_0}{dx} = -\frac{4r_0}{\zeta_n^2 - 1} \quad \text{for} \quad x = -h. \tag{2.34}$$

Thus, to determine two arbitrary constants C_1 and C_2 we only have one condition (2.34) referring to the bottom of the tank. The second condition should relate to the free surface. But, the condition at the free surface is given for the sum of two functions $\phi = \psi + \varphi$ [(see (2.24)] of which one, function φ, has not yet been found. Therefore, in determining the boundary condition for ψ at x = 0 we may allow some degree of arbitrariness which should then be removed on the basis of (2.24) in the process of determining function φ.

Let, for example, for function ψ at x = 0 the boundary condition be identical with one at x = -h, i.e.,

$$\left(\frac{\partial \psi}{\partial x}\right)_{x=0} = -2r \sin \eta. \tag{2.35}$$

Then

$$\left(\frac{\partial P}{\partial x}\right)_{x=0} = -2r \sin \eta, \quad \left(\frac{\partial X_0}{dx}\right)_{x=0} = -\frac{4r_0}{\zeta_n^2 - 1}. \tag{2.36}$$

The physical meaning of the boundary condition (2.35) as well as other possible versions of the boundary conditions for ψ at x = 0 will be discussed in Section 7.

With the boundary conditions (2.34) and (2.36) taken into account, the solution (2.30) will be

$$X_0 = -\frac{4r_0^2}{\zeta(\zeta^2 - 1)} \frac{\operatorname{ch}\left[\frac{\zeta_n}{r_0}\left(\frac{h}{2} + x\right)\right]}{\operatorname{ch}\left(\zeta_n \frac{h}{2r_0}\right)}. \tag{2.37}$$

The functions

$$H(\eta)=\sin\eta,\ R_n(r)=\frac{J_1\left(\zeta_n\frac{r}{r_0}\right)}{J_1(\zeta_n)},$$

$$X_n(x)=-\frac{4r_0^2}{\zeta_n(\zeta_n^2-1)}\frac{\operatorname{sh}\left[\frac{\zeta_n}{r_0}\left(\frac{h}{2}+x\right)\right]}{\operatorname{sh}\left(\zeta_n\frac{h}{2r_0}\right)}$$

are the eigenfunctions of the problem in question. A solution of the problem (2.19), (2.20), and (2.21) is composed of these functions according to Expression (2.26).

Combining the results of the solutions, we shall obtain the following expression for function $\psi(x, r, \eta, t)$:

$$\psi=2r_0\sin\eta\sum_{n=1}^{\infty}\frac{J_1\left(\zeta_n\frac{r}{r_0}\right)}{(\zeta_n^2-1)J_1(\zeta_n)}\times$$
$$\times\left\{\left[-\frac{2r_0}{\zeta_n}\frac{\operatorname{sh}\left[\frac{\zeta_n}{r_0}\left(\frac{h}{2}+x\right)\right]}{\operatorname{ch}\left(\zeta_n\frac{h}{2r_0}\right)}+(L+x)\right]\dot{\theta}+\dot{y}_C\right\}. \tag{2.38}$$

The function $\psi(x, r, \eta, t)$ is a solution of Laplace's equation and satisfies boundary conditions at the walls of the tank.

Since the free surface of a liquid, whose motion is determined by a potential function ψ, will be by condition (2.35) a plane in the absolute coordinate system

$$\chi_0(r, \eta, t)=\int_0^t\left(\frac{\partial\psi}{\partial x}\right)_{x=0}dt=-r\theta\sin\eta, \tag{2.39}$$

which is perpendicular to the longitudinal axis of the tank (O_1x_1), Consequently we may consider that function $\psi(r, x, \eta, t)$ describes a potential flow for which the free surface of a liquid is covered with a "roof" fastened to the wall of the tank, and therefore is not disturbed.

The pressure of the liquid on the "roof", as it is easy to convince oneself, does not remain constant, and since in reality there does not exist any "roof", the nonuniformity in pressure leads to a distortion of the free surface, i.e., to oscillations. Hence, the oscillations should be determined by the function $\varphi(x, r, \eta, t)$.

We shall now proceed to determine the function $\varphi(x, r, \eta, t)$. This function should be a solution of Laplace's equation. Its derivatives should vanish at the walls and the bottom of the tank in accordance with (2.22) and (2.23), and together with $\psi(x, r, \eta, t)$ should satsify the condition that pressure be constant at the free surface (2.24).

Let the function φ be represented as

$$\varphi(x, r, \eta, t) = H(\eta) \sum_{n=1}^{\infty} C_n X_n(x) R_n(r) \lambda_n(t),$$

where C_n is a constant coefficient; $\lambda_n(t)$ is a time-dependent parameter which is as yet undetermined.

A separation of variables leads to Equations (2.27) - (2.29). The conditions determining the selection of functions $H(\eta)$ and $R_n(r)$ are the same as those for ψ. Therefore,

$$H(\eta) = \sin \eta, \quad R_n(r) = \frac{J_1\left(\zeta_n \frac{r}{r_0}\right)}{J_1(\zeta_n)}.$$

Function X_n should be a solution of Equation (2.27) and therefore may be formed of a linear combination of hyperbolic functions of argument $\zeta_n x/r_0$. By (2.23) this function should satisfy the condition at the bottom of the tank

$$\frac{dX_n}{dx} = 0 \text{ for } x = -h. \tag{2.40}$$

Equation (2.27) and condition (2.40) are satisfied by a function

$$X_n(x) = r_0 \frac{\operatorname{ch}\left(\zeta_n \frac{h + x}{r_0}\right)}{\operatorname{ch}\left(\zeta_n \frac{h}{r_0}\right)}.$$

In order to assign the simplest physical sense to the parameter $\lambda_n(t)$, we shall select the coefficient C_n such that the functions ψ and Φ will have a common multiplier. We set

$$C_n=\frac{2}{\zeta_n^2-1}.$$

Then we obtain

$$\varphi=2r_0\sin\eta\sum_{n=1}^{\infty}\frac{J_1\left(\zeta_n\frac{r}{r_0}\right)}{(\zeta_n^2-1)J_1(\zeta_n)}\frac{\operatorname{ch}\left(\zeta_n\frac{h+z}{r_0}\right)}{\operatorname{ch}\left(\zeta_n\frac{h}{r_0}\right)}\dot{\lambda}_n(t). \tag{2.41}$$

Now let us make use of the fact that the pressure is assumed constant at the free surface and find the parameter $\lambda_n(t)$ which is thus far unknown. After substituting (2.38) and (2.41) into (2.24) we obtain the following equation for $\lambda_n(t)$:

$$\ddot{\lambda}_n+g\frac{\zeta_n\operatorname{th}\left(\zeta_n\frac{h}{r_0}\right)}{r_0}\lambda_n=$$

$$=-\left[L-\frac{2r_0}{\zeta_n}\frac{\operatorname{ch}\left(\zeta_n\frac{h}{r_0}\right)-1}{\operatorname{sh}\left(\zeta_n\frac{h}{r_0}\right)}\right]\ddot{\delta}-\ddot{y}_C+g\delta$$

or

$$\ddot{\lambda}_n+\omega_n^2\lambda_n=-L_n\ddot{\delta}-\ddot{y}_C+g\delta. \tag{2.42}$$

Here we assumed the following nomenclature

$$\omega_n=\sqrt{\frac{g\zeta_n}{r_0}\operatorname{th}\left(\zeta_n\frac{h}{r_0}\right)},$$

$$L_n=L\left[1-\frac{2r_0}{\zeta_nL}\frac{\operatorname{ch}\left(\zeta_n\frac{h}{r_0}\right)-1}{\operatorname{sh}\left(\zeta_n\frac{h}{r_0}\right)}\right]- \tag{2.43}$$

$$-L\left[1-\frac{2r_0}{\zeta_n L}\operatorname{th}\left(\zeta_n\frac{h}{2r_0}\right)\right]. \qquad (2.44)$$

In order to find the physical meaning of $\lambda_n(t)$ we shall solve the equation

$$\chi(r,\eta,t)=\int_0^t\left(\frac{\partial\varphi}{\partial x}\right)_{x=0}dt=2r_0\sin\eta\sum_{n=1}^{\infty}\frac{J_1\left(\zeta_n\frac{r}{r_0}\right)}{(\zeta_n^2-1)J_1(\zeta_n)}\times$$
$$\times\left[\frac{\zeta_n}{r_0}\operatorname{th}\left(\zeta_n\frac{h}{r_0}\right)\lambda_n(t)-0\right].$$

This is an equation of the free surface in the absolute coordinate system. Considering (2.33) it may be represented as

$$\chi(r,\eta,t)=-r\theta\sin\eta+\chi_1(r,\eta,t), \qquad (2.45)$$

where

$$\chi_1(r,\eta,t)=2r_0\sin\eta\sum_{n=1}^{\infty}\frac{J_1\left(\zeta_n\frac{r}{r_0}\right)}{(\zeta_n^2-1)J_1(\zeta_n)}\times$$
$$\times\frac{\zeta_n}{r_0}\operatorname{th}\left(\zeta_n\frac{h}{r_0}\right)\lambda_n(t). \qquad (2.46)$$

Up to infinitesimals of second order we have

$$x=x_1-r\theta\sin\eta.$$

Therefore, in Equation (2.45) with the same accuracy a displacement $\chi_1(r,\eta,t)$ represents a displacement of the free surface in the moving (attached) coordinate system (Figure 2.4).

The form of the free surface is represented as a Fourier series in Bessel functions $J_1(\zeta_n r/r_0)$, and along the circumference it changes sinusoidally. For the first three tones of the oscillations the form of the free surface with $\eta=\pi/2$ is shown in Figure 2.5. Each term of the series is associated with its own parameter $\lambda_n(t)$ which is thus a generalized coordinate for the wave motion of the free surface.

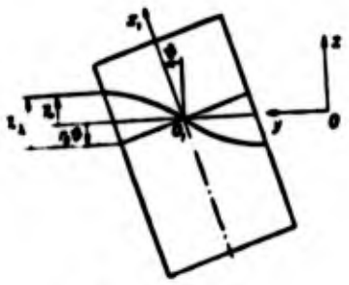

Figure 2.4

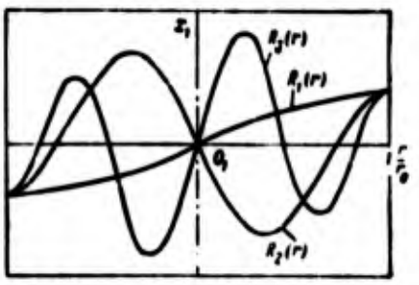

Figure 2.5

Equation (2.46) makes it possible to determine the scale for $\lambda_n(t)$ which will depend on the number n or, in other words, on which oscillation tone number we are dealing with. The maximum displacement of the free surface corresponds to the coordinates $\eta=\pi/2, r=r_0$. If we read it off from the plane O_1y_1,z_1, perpendicular to the axis of the cylinder O_1x_1, the displacement is

$$\chi_{1n}(r_0, \pi/2, t)=\frac{\chi_n}{\zeta_n^2-1}\,\mathrm{th}\left(\zeta_n\frac{h}{r_0}\right)\lambda_n(t).$$

If $h/r_0 \geqslant 1$, then $\mathrm{th}\left(\zeta_n\frac{h}{r_0}\right)\approx 1$. In this case we have for the first tone of oscillations

$$\chi_{1_1}(r_0, \pi/2, t)=1{,}54\lambda_1(t),$$

and for the second tone

$$\chi_{1_2}(r_0, \pi/2, t)=0{,}39\lambda_2(t).$$

All fluid particles participate in the motion whose potential is represented by (2.41). However, the velocity of particles decreases rapidly as we move away from the free surface downwards into the tank.

Equation (2.42) shows that the eigen oscillations of the free surface of the liquid are harmonic at all points. The square of the frequency of these oscillations is proportional to the acceleration g, the root of the derivative of the Bessel function of the corresponding order, and inversely proportional to the radius of the tank. If the depth of the submerged portion of the tank is greater than the radius, the frequency of the eigen oscillations of the liquid is practically independent of this depth. If $h/r_0<1$, the frequency of the oscillations decreases with a decrease in depth. As we increase the tone numbers of the oscillations, the frequency also increases.

4. Pressure of the Liquid on the Walls of the Tank

If the potential ϕ is known, then making use of (2.9) one can find the pressure p at any point of the liquid volume, and thus make a transition to integral quantities, namely the transverse force and the moment relative to the transverse axis passing through point C (see Figure 2.3). These integral quantities are needed to set up the equations of motion of a rocket.

In view of (2.9) and (2.18) we have

$$\frac{p-p_0}{\rho}=-\frac{\partial\psi}{\partial t}-\frac{\partial\varphi}{\partial t}-gx, \tag{2.47}$$

where p_0 is the gas pressure over the free surface; ρ is the density of the liquid; g is the acceleration of gravity.

The velocity potential was determined in Equations (2.38) and and (2.41)

$$\varphi=2r_0\cdot\sin\eta\sum_{n=1}^{\infty}\frac{J_1\left(\zeta_n\frac{r}{r_0}\right)}{(\zeta_n^2-1)J_1(\zeta_n)}\times$$

$$\times\left\{\left[-\frac{2r_0}{\zeta_n}\frac{\operatorname{ch}\left[\frac{\zeta_n}{r_0}\left(\frac{h}{2}+x\right)\right]}{\operatorname{ch}\left(\zeta_n\frac{h}{2r_0}\right)}+(L+x)\right]\dot{\theta}+\dot{y}_C\right\},$$

$$\varphi = 2r_0 \sin\eta \sum_{n=1}^{\infty} \frac{J_1\left(\zeta_n \frac{r}{r_0}\right)}{(\zeta_n^2 - 1) J_1(\zeta_n)} \frac{\operatorname{ch}\left(\zeta_n \frac{h+x}{r_0}\right)}{\operatorname{ch}\left(\zeta_n \frac{h}{r_0}\right)} \lambda_n.$$

The elementary forces and moments should be summed over the entire immersed surface. Up to infinitesimals of first order of smallness the x-coordinate (Figure 2.6) changes from $x = \chi(r, \eta, t)$ to $x = x_0^\circ = -h - r_0 \theta \sin\eta$ at the side walls, and at the bottom of the tank

$$x^\circ = -h - r\theta \sin\eta.$$

The elementary area on the side surface is $r_0 d\eta dx$, and at the bottom the elementary area is $r d\eta dr$. The Oy-component of the elementary force acting on the side surface of the tank is

$$(p)_{r=r_0} r_0 \sin\eta d\eta dx.$$

The same component of the elementary force acting on the bottom of the tank is (see Figure 2.6)

$$(p)_{x=x^\circ} \theta r d\eta dr.$$

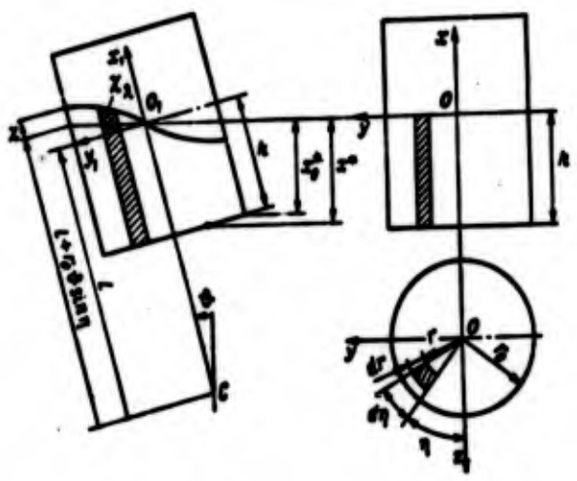

Figure 2.6

They Oy component of the total force of the liquid pressure on the walls of the tank is

$$F_y^\circ = \int_0^{2\pi} \int_{x_0}^{\chi} (p)_{r=r_0} r_0 \sin\eta d\eta dx + \int_0^{2\pi} \int_0^{r_0} (p)_{x=x^\circ} \theta r dr d\eta. \tag{2.48}$$

In accordance with the structure of the formula in (2.47) the total force F_y will be represented as a sum of three forces

$$F_y^\circ = F_\phi + F_\varphi + F_g.$$

An analysis of the expressions on the right hand side of (2.47) shows that the pressures $\rho\partial\dot{\psi}/\partial t$, $\rho\partial\dot{\varphi}/\partial t$ are proportional to the accelerations $\ddot{\theta}$, $\ddot{y}_c$, $\ddot{\lambda}_n$, these being small quantities. The force F_y^0 and the moment of the total force will be calculated retaining only infinitesimals of first order. Since the limiting values of χ, x_0^* and x^* contain infinitesimals of first order, then in the expression (2.48) to calculate the function $\partial\psi/\partial t$ and $\partial\varphi/\partial t$ we shall let $\chi=0$, $x_0^* = x^* = -h$. The force and moment of the hydrostatic pressure ρgx may be determined from (2.48) if the upper x limit is taken to be zero, and the lower one is $x = x_0^*$ and $x = x^*$.

Keeping in mind that the Oy component of the pressure forces $\partial\varphi/\partial t$ and $\rho\partial\psi/\partial t$, acting on the bottom of the tank, are infinitesimals of the second order, we get,

$$F_\psi = -\rho\int_0^{2\pi}\int_{-h}^{0}\left(\frac{\partial\psi}{\partial t}\right)_{r=r_0} r_0\sin\eta\,d\eta\,dx,$$

$$F_\varphi = -\rho\int_0^{2\pi}\int_{-h}^{0}\left(\frac{\partial\varphi}{\partial t}\right)_{r=r_0} r_0\sin\eta\,d\eta\,dx,$$

$$F_g = -\rho\int_0^{2\pi}\int_{x_0}^{0} gxr_0\sin\eta\,d\eta\,dx + \rho\int_0^{2\pi}\int_0^{r_0}(gx)_{x=x^*}\theta r\,d\eta\,dx.$$

Let us introduce the following notation

$$m = \pi r_0^2 h\rho,$$

$$m_n = \pi r_0^3\rho\frac{2\,\mathrm{th}\left(\zeta_n\frac{h}{r_0}\right)}{\zeta_n(\zeta_n^2-1)}, \tag{2.49}$$

where m is the total mass of the liquid; m_n is the reduced mass of the oscillating liquid, corresponding to the generalized coordinate λ_n.

Integrating and using the fact that [6]

$$\sum_{n=1}^{\infty}\frac{1}{\zeta_n^2-1} = \frac{1}{2},$$

we find

$$F_\psi = -\pi r_0^2 h\rho\left[\left(L-\frac{h}{2}\right)\ddot{\vartheta}+\ddot{y}_C\right] = -m\left[\left(L-\frac{h}{2}\right)\ddot{\vartheta}+\ddot{y}_C\right],$$

$$F_\varphi = -\pi r_0^2\rho\sum_{n=1}^{\infty}\frac{2\operatorname{th}\left(\zeta_n\frac{h}{r_0}\right)}{\zeta_n(\zeta_n^2-1)}\ddot{\lambda}_n = -\sum_{n=1}^{\infty}m_n\ddot{\lambda}_n, \qquad (2.50)$$

$$F_g = \pi r_0^2 h\rho g\vartheta - \pi r_0^2 h\rho g\vartheta = 0,$$

$$F_y^0 = -m\left[\left(L-\frac{h}{2}\right)\ddot{\vartheta}+\ddot{y}_C\right]-\sum_{n=1}^{\infty}m_n\ddot{\lambda}_n.$$

Now let us calculate the moment of pressure forces rela ive to the transverse axis passing through point C and parallel to Oz:

$$M_C^0 = \int_0^{2\pi}\int_{x_0}^{0}(p)_{r=r_0}(L+r_0\vartheta\sin\eta+x)\,r_0\sin\eta\,d\eta\,dx + \qquad (2.51)$$

$$+\int_0^{2\pi}\int_0^{r_0}(p)_{x=x^*}r^2\sin\eta\,d\eta\,dr,$$

where $(L+r_0\vartheta\sin\eta+x)$ is the distance from the elementary area on the side surface of the tank to the axis of revolution (cf. Figure 2.6).

For convenience we let

$$M_C^0 = M_\psi + M_\varphi + M_g,$$

$$M_\psi = M_{1\psi}+M_{2\psi},\quad M_\varphi = M_{1\varphi}+M_{2\varphi},\quad M_g = M_{1g}+M_{2g},$$

where index 1 will correspond to the moment of the forces acting on the side surface, and index 2 — to the moment of the forces applied to the bottom of the tank.

Similarly as in the calculation of the force F_y^0, in computing the moments M_ψ and M_φ we shall assume in (2.51) that $\chi = 0$, $x_0^* - x^* = -h$, and that the distance between the axis of revolution and the elementary area on the side surface is equal to (L + x). The moment M_g of the hydrostatic forces will be determined using (2.51) and letting $\chi = 0$. We shall get

$$M_{1\psi} = -\rho\int_0^{2\pi}\int_{-h}^{0}\left(\frac{\partial\psi}{\partial t}\right)_{r=r_0}(L+x)\,r_0\sin\eta\,d\eta\,dx,$$

$$M_{2\psi} = -\rho\int_0^{2\pi}\int_0^{r_0}\left(\frac{\partial\psi}{\partial t}\right)_{x=-h}r^2\sin\eta\,d\eta\,dr,$$

$$M_{2y} = -\rho \int_0^{2\pi} \int_{-h}^{0} \left(\frac{\partial \varphi}{\partial t}\right)_{r=r_0} (L+x) r_0 \sin\eta \, d\eta \, dx,$$

$$M_{2y} = -\rho \int_0^{2\pi} \int_0^{r_0} \left(\frac{\partial \varphi}{\partial t}\right)_{x=-h} r^2 \sin\eta \, d\eta \, dr,$$

$$M_{1g} = -\rho \int_0^{2\pi} \int_{x_0}^{0} gx (L + r_0 \vartheta \sin\eta + x) r_0 \sin\eta \, d\eta \, dx,$$

$$M_{2g} = -\rho \int_0^{2\pi} \int_0^{r_0} (gx)_{x=-h} r^2 \sin\eta \, d\eta \, dr.$$

Let us use the following notation

$$I_0 = \pi r_0^2 \rho \left(L^2 - Lh + \frac{h^2}{3} + \frac{r_0^2}{4}\right),$$

$$I_n' = \pi r_0^4 \rho \left[-\frac{8h - 2L}{\zeta_n^2 (\zeta_n^2 - 1)} + \frac{12 r_0}{\zeta_n^3 (\zeta_n^2 - 1)} \operatorname{th}\left(\zeta_n \frac{h}{2r_0}\right)\right],$$

$$l_n = \frac{r_0}{\zeta_n \operatorname{th}\left(\zeta_n \frac{h}{r_0}\right)}, \qquad (2.52)$$

$$L_n' = L - \frac{r_0}{\zeta_n} \frac{\operatorname{ch}\left(\zeta_n \frac{h}{r_0}\right) - 2}{\operatorname{sh}\left(\zeta_n \frac{h}{r_0}\right)},$$

where I_0 is the moment of inertia of the total mass of liquid relative to the axis passing through point C and parallel to Oz. The liquid is considered "fixed" and the free surface is assumed to coincide with the plane $O_1 y_1 z_1$

Integrating and making use of the fact that [6]

$$\sum_{n=1}^{\infty} \frac{1}{\zeta_n^2 (\zeta_n^2 - 1)} = \frac{1}{8},$$

we get

$$M_\psi = -\left(I_0 + \sum_{n=1}^{\infty} I_n'\right)\ddot{\theta} - \left[m\left(L - \frac{h}{2}\right) + \sum_{n=1}^{\infty} m_n l_n\right]\ddot{y}_C,$$

$$M_\varphi = -\sum_{n=1}^{\infty} m_n L \ddot{\lambda}_n, \qquad (2.53)$$

$$M_g = mg\left(L - \frac{h}{2}\right)\theta + g\theta\sum_{n=1}^{\infty} m_n l_n,$$

$$M_C^0 = M_\psi + M_\varphi + M_g.$$

5. The Equations of Motion

The equations of motion for the tank with liquid can be obtained using Newton's second law if we combine the external forces acting on the tank with forces due to the liquid. However, we shall proceed in a different way. Knowing the velocity at any point of the volume occupied by liquid, we shall compute the kinetic and potential energy of the total mass of the liquid, and using Lagrange's equations of the second kind, we shall obtain the equations of motion for the tank with liquid in terms of the generalized coordinates y_C, θ, λ_n.

Since the velocity components of any liquid particle in the direction of the Ox, Oy, Oz coordinate axes are

$$v_x = \frac{\partial\varphi}{\partial x}, \quad v_y = \frac{\partial\varphi}{\partial y}, \quad v_z = \frac{\partial\varphi}{\partial z},$$

the kinetic energy of the total mass of the liquid is

$$T = \frac{1}{2}\rho\iiint_V\left[\left(\frac{\partial\varphi}{\partial x}\right)^2 + \left(\frac{\partial\varphi}{\partial y}\right)^2 + \left(\frac{\partial\varphi}{\partial z}\right)^2\right]dV,$$

where V is the volume occupied by the liquid.

Let us transform the integrand so that it will be easier to use the Gauss-Ostrogradskiy formula. We get

$$T=\frac{1}{2}\rho\iiint_V\left[\left(\frac{\partial\phi}{\partial x}\right)^2+\left(\frac{\partial\phi}{\partial y}\right)^2+\left(\frac{\partial\phi}{\partial z}\right)^2\right]dV=$$
$$=\frac{1}{2}\rho\iiint_V\left[\frac{\partial}{\partial x}\left(\phi\frac{\partial\phi}{\partial x}\right)+\frac{\partial}{\partial y}\left(\phi\frac{\partial\phi}{\partial y}\right)+\frac{\partial}{\partial z}\left(\phi\frac{\partial\phi}{\partial z}\right)\right]^2dV.$$

By the Gauss-Ostrogradskiy formula the volume integral is replaced by a surface integral [9]. We obtain

$$T=\frac{1}{2}\rho\iint_S\left[\phi\frac{\partial\phi}{\partial x}\cos(n,x)+\phi\frac{\partial\phi}{\partial y}\cos(n,y)+\right.$$
$$\left.+\phi\frac{\partial\phi}{\partial z}\cos(n,z)\right]dS.$$

Here S is the surface of the liquid containing volume V; n is the outer normal to the surface of the liquid.

The surface of the liquid may be divided into three parts: the (see Figure 2.6) side surface, the bottom, and the free surface. For the side surface we have

$$\cos(n,y)=\sin\eta,\ \cos(n,z)=\cos\eta,$$
$$dS=r_0d\eta\,dx,\ \cos(n,x)=0.$$

For the bottom surface

$$\cos(n,x)=-1,\ \cos(n,y)=\cos(n,z)=0,$$
$$dS=rdr\,d\eta.$$

For the free surface

$$\cos(n,x)=1,\ \cos(n,y)=\cos(n,z)=0,$$
$$dS=rd\,rd\eta.$$

Inasmuch as

$$\frac{\partial\phi}{\partial z}=\frac{\partial\phi}{\partial r}\cos\eta-\frac{\partial\phi}{r\partial\eta}\sin\eta,$$
$$\frac{\partial\phi}{\partial y}=\frac{\partial\phi}{\partial r}\sin\eta+\frac{\partial\phi}{r\partial\eta}\cos\eta,$$

then, making transformations, we obtain

$$T=\frac{1}{2}\rho\int_0^{2\pi}\left[\int_0^{r_0}\left(\phi\frac{\partial\phi}{\partial x}\right)_{x=0}r\,dr\,d\eta-\int_0^{r_0}\left(\phi\frac{\partial\phi}{\partial x}\right)_{x=-h}r\,dr\,d\eta+\right.$$
$$\left.+\int_{-h}^{0}\left(\phi\frac{\partial\phi}{\partial r}\right)_{r=r_0}r_0\,d\eta\,dx\right]. \tag{2.54}$$

Using (2.18), (2.38), and (2.41) the expression for the potential function Φ will be

$$\phi=2r_0\sin\eta\sum_{n=1}^{\infty}\frac{J_1\left(\zeta_n\frac{r}{r_0}\right)}{(\zeta_n^2-1)J_1(\zeta_n)}\times$$
$$\times\left\{\left[-\frac{2r_0}{\zeta_n}\frac{\mathrm{sh}\left[\frac{\zeta_n}{r_0}\left(\frac{h}{2}+x\right)\right]}{\mathrm{ch}\left(\zeta_n\frac{h}{2r_0}\right)}+(L+x)\right]\dot{\theta}+\dot{v}_C+\right.$$
$$\left.+\frac{\mathrm{ch}\left(\zeta_n\frac{h+x}{r_0}\right)}{\mathrm{ch}\left(\zeta_n\frac{h}{r_0}\right)}\dot{\lambda}_n\right\}. \tag{2.55}$$

The potential in this form will be used to calculate the first two integrals. To evaluate the third integral from (2.54) the function Φ in view of (2.33) will be represented as

$$\phi=2r_0\sin\eta\sum_{n=1}^{\infty}\frac{J_1\left(\zeta_n\frac{r}{r_0}\right)}{(\zeta_n^2-1)J_1(\zeta_n)}\times$$
$$\times\left\{-\frac{2r_0}{\zeta_n}\frac{\mathrm{sh}\left[\frac{\zeta_n}{r_0}\left(\frac{h}{2}+x\right)\right]}{\mathrm{ch}\left(\zeta_n\frac{h}{2r_0}\right)}\dot{\theta}+\frac{\mathrm{ch}\left(\zeta_n\frac{h+x}{r_0}\right)}{\mathrm{ch}\left(\zeta_n\frac{h}{r_0}\right)}\dot{\lambda}_n\right\}+ \tag{2.56}$$
$$+r\sin\eta[(L+x)\dot{\theta}+\dot{v}_C].$$

Due to the properties of the Bessel functions we have

$$\int_0^{r_0}\left[\frac{J_1\left(\zeta_n\frac{r}{r_0}\right)}{(\zeta_n^2-1)J_1(\zeta_n)}\right]^2 r\,dr=\frac{r_0^2}{2\zeta_n^2(\zeta_n^2-1)},$$
$$\int_0^{r_0}\left\{\frac{d}{dr}\left[\frac{J_1\left(\zeta_n\frac{r}{r_0}\right)}{(\zeta_n^2-1)J_1(\zeta_n)}\right]\right\}^2 r\,dr=\frac{1}{2(\zeta_n^2-1)}. \tag{2.57}$$

Integrating with respect to x (the values of the definite integrals will be stated for reference at the end of the chapter) and grouping all coefficients with variables of the same kind, in view of (2.44), (2.49), and (2.52) we obtain

$$T=\frac{1}{2}\left[\left(I_0+\sum_{n=1}^{\infty}I_n\right)\dot{\vartheta}^2+m\dot{y}_C^2+\sum_{n=1}^{\infty}m_n\dot{\lambda}_n^2+2m\left(L-\frac{h}{2}\right)\dot{y}_C\dot{\vartheta}+\right.$$
$$\left.+2\dot{\vartheta}\sum_{n=1}^{\infty}m_nL_n\dot{\lambda}_n+2\dot{y}_C\sum_{n=1}^{\infty}m_n\dot{\lambda}_n\right], \tag{2.58}$$

$$I_n=\pi r_0^5\rho\left[-\frac{h}{r_0}\frac{8}{\zeta_n^3(\zeta_n^2-1)}+\frac{16}{\zeta_n^3(\zeta_n^2-1)}\operatorname{th}\left(\zeta_n\frac{h}{2r_0}\right)\right]. \tag{2.59}$$

Now let us construct the expression for the potential energy of the liquid mass. The value of the potential energy, corresponding to an undisturbed state of the liquid when $y_C=\vartheta=0$, and all the coordinates $\lambda_n=0$, will be taken as equal to zero.

The potential energy increases if the liquid particles move in the direction of the Ox-axis, and decreases if they move in the opposite direction.

Let us consider a column of liquid with the cross section $rd\eta dr$. The distance between the column and the plane Oxz is equal to r sinη- (see Figure 2.6).

In an undisturbed state of the liquid the height of the column is equal to h, and the distance between the center of the column and the plane Oyz is equal to h/2. In an unsteady state of the liquid the height of the column is equal to $h+\chi_1$, and the distance from the plane $O_1y_1z_1$ to the center of the column is $h/2-\chi_1/2$.

The displacement of the center of gravity of the column of liquid in the absolute frame of reference in the direction of the Ox-axis is composed of a displacement caused by a rotation of the cylinder by an angle ϑ:

$$-\left(L-\frac{h}{2}\right)(1-\cos\vartheta)-r\sin\eta\sin\vartheta$$

and an additional displacement, due to an increase in the height of the column, equal to $\chi_1/2$. The total displacement is

$$\Delta = \frac{\chi_1}{2} - \left(L - \frac{h}{2}\right)(1 - \cos\theta) - r\sin\eta\sin\theta.$$

The potential energy of an elementary column of liquid in an unsteady state is

$$dU = (h + \chi_1)\Delta g\rho r\, d\eta\, dr.$$

Summing over the total volume, we find

$$U = g\rho\int_0^{2\pi}\int_0^{r_0}(h + \chi_1)\left[\frac{\chi_1}{2} - \left(L - \frac{h}{2}\right)(1 - \cos\theta) - r\sin\eta\sin\theta\right] r\, d\eta\, dr.$$

Taking into consideration the following relations

$$(1 - \cos\theta) \approx \frac{\theta^2}{2},\quad \sin\theta \approx \theta,$$

$$\int_0^{r_0} R_n(r)\, r^2\, dr = \frac{r_0^2}{\zeta_n^2},$$

$$\int_0^{r_0} R_n(r)\, r\, dr = \frac{r_0^2}{\zeta_n^2},$$

and using the properties of the Bessel functions (2.57), we obtain an expression for the potential energy of the entire liquid

$$U = -\left(L - \frac{h}{2}\right)mg\frac{\theta^2}{2} - g\theta\sum_{n=1}^{\infty} m_n\lambda_n + \frac{1}{2}\sum_{n=1}^{\infty}\omega_n^2 m_n\lambda_n^2. \qquad (2.60)$$

Here ω_n^2, m, m_n correspond to the nomenclature in (2.43) and (2.49).

The kinetic and potential energy of the liquid are thus expressed in terms of the generalized coordinates of the system y_c, θ, λ_n and their velocities. The expressions (2.58) and (2.60) do not include the kinetic and potential energies of the tank. In solving dynamics problems, in addition to mass m and the moment of inertia I_0 of the liquid one should also consider the mass and moment of inertia of the walls of the tank.

If the tank is acted upon by external forces that can be reduced to a transverse force F_y attached to point C and a force couple M_c, then they will be the generalized forces of the system, corresponding to the coordinates y_c and ϑ.

Applying the Lagrangee equations

$$\frac{d}{dt}\left(\frac{\partial T}{\partial \dot{q}}\right)-\frac{\partial T}{\partial q}+\frac{\partial \Pi}{\partial q}=Q_q \quad (q=y_C, \vartheta, \lambda_n),$$

in which the generalized force Q_q does not include the force of gravity, we shall set up the equations of a perturbed motion of the liquid

$$\begin{gathered}
m\ddot{y}_C+m\left(L-\frac{h}{2}\right)\ddot{\vartheta}+\sum_{n=1}^{\infty} m_n\ddot{\lambda}_n=F_y, \\
\left(I_0+\sum_{n=1}^{\infty} I_n\right)\ddot{\vartheta}-mg\left(L-\frac{h}{2}\right)\vartheta+m\left(L-\frac{h}{2}\right)\ddot{y}_C+ \\
+\sum_{n=1}^{\infty} m_n L_n\ddot{\lambda}_n-g\sum_{n=1}^{\infty} m_n\lambda_n=M_C, \\
\ddot{\lambda}_n+\omega_n^2\lambda_n+L_n\ddot{\vartheta}+\ddot{y}_C-g\vartheta=0 \quad (n=1, 2, \ldots), \\
m=\pi r_0^2 h\rho,
\end{gathered} \tag{2.61}$$

where

$$\begin{gathered}
I_0=\pi r_0^2 h\rho\left(L^2-Lh+\frac{h^2}{3}+\frac{r_0^2}{4}\right), \\
I_n=\pi r_0^4\rho\left[-\frac{h}{r_0}\frac{8}{\zeta_n^2(\zeta_n^2-1)}+\frac{16}{\zeta_n^3(\zeta_n^2-1)}\operatorname{th}\left(\zeta_n\frac{h}{2r_0}\right)\right], \\
m_n=\pi r_0^3\rho\frac{2\operatorname{th}\left(\zeta_n\frac{h}{r_0}\right)}{\zeta_n(\zeta_n^2-1)}, \\
L_n=L\left[1-\frac{2r_0}{L\zeta_n}\operatorname{th}\left(\zeta_n\frac{h}{2r_0}\right)\right].
\end{gathered} \tag{2.62}$$

The last equation, describing a relation between the coordinates ϑ and y_c, is completely analogous to Equation (2.42) obtained from condition (2.24) which asserts that pressure is constant on the free surface.

We shall show that Equations (2.61) can be obtained using the expressions for the transverse force F_y^0 (2.50) and the moment of forces M_C^0 (2.53), acting on the walls of the tank due to the presence of the liquid. Let us first make some transformations. Consider the third equation in (2.61), in which we set $\omega_n^2=g/l_n$:

$$\lambda_n + \frac{g}{l_n}\lambda_n + L_n\ddot{\delta} = -\ddot{y}_C + g\theta.$$

Let us multiply both sides of this equation by the product $m_n l_n$ and sum. We get

$$g\theta\sum_{n=1}^{\infty} m_n l_n - \ddot{y}_C\sum_{n=1}^{\infty} m_n l_n - \sum_{n=1}^{\infty} m_n l_n\left(\ddot{\lambda}_n + \frac{g}{l_n}\lambda_n + L_n\ddot{\delta}\right). \tag{2.63}$$

The term on the left-hand side of the equality appears in the expression for M_ψ and M_g (2.53). Let us replace them in (2.53) by the right hand side of (2.63). After some transformations we obtain

$$\begin{aligned} M_\psi &= -m\left(L - \frac{h}{2}\right)\ddot{y}_C - \left(I_0 + \sum_{n=1}^{\infty} I_n\right)\ddot{\delta}, \\ M_\delta &= -\sum_{n=1}^{\infty} m_n L_n\ddot{\lambda}_n + g\sum_{n=1}^{\infty} m_n\lambda_n, \\ M_g &= mg\left(L - \frac{h}{2}\right)\delta, \end{aligned} \tag{2.64}$$

where I_n, L_n are defined in (2.62). Combining all three expressions, we obtain

$$\begin{aligned} M_C^0 = &-\left(I_0 + \sum_{n=1}^{\infty} I_n\right)\ddot{\delta} - m\left(L - \frac{h}{2}\right)\ddot{y}_C - \sum_{n=1}^{\infty} m_n L_n\ddot{\lambda}_n + \\ &+ g\sum_{n=1}^{\infty} m_n\lambda_n + mg\left(L - \frac{h}{2}\right)\delta. \end{aligned} \tag{2.65}$$

Now we shall set up the equations of motion of the tank. In addition to the external force F_y and moment M_c which are given, the walls of the tank are acted upon by the force F_y^0, and the moment M_c^0 due to the liquid that are also outside the walls of the tank. The directions of $F_y^0 k$ and M_c^0 are the same as the directions of F_y and M_c.

Assuming as before that the mass of the walls of the tank is equal to zero, we get

$$F_y + F_y^0 = 0, \quad M_C + M_C^0 = 0.$$

Substituting here the expressions for F_y^0 from (2.50) and for * from (2.65), and adding Equation (2.42) for the coordinate λ_n of the oscillations of the liquid, we obtain a system of equations

$$m\ddot{y}_C + m\left(L - \frac{h}{2}\right)\ddot{\theta} + \sum_{n=1}^{\infty} m_n \ddot{\lambda}_n = F_y,$$

$$\left(I_0 + \sum_{n=1}^{\infty} I_n\right)\ddot{\theta} - mg\left(L - \frac{h}{2}\right)\theta + m\left(L - \frac{h}{2}\right)\ddot{y}_C +$$

$$+ \sum_{n=1}^{\infty} m_n L_n \ddot{\lambda}_n - g\sum_{n=1}^{\infty} m_n \lambda_n = M_C,$$

$$\ddot{\lambda}_n + \omega_n^2 \lambda_n = -L_n\ddot{\theta} - \ddot{y}_C + g\theta,$$

which is the same as the equations in (2.61)

It will be noted that if the expression for the moment is not transformed to the form in (2.65), and (2.53) is used to obtain the equations of motion, then the structure of the momentum equation will differ slightly from the structure of Equations (2.61). However, this discrepancy is only illusory, and appears as a result of a linear exchange of variables.

Let us analyze the results obtained so far. If the tank is filled completely with liquid, then all the coordinates $\lambda_n = 0$ and Equations (2.61) will become the ordinary equations of a plane motion of a rigid body with mass m and the equivalent moment of inertia

$$I = I_0 + \sum_{n=1}^{\infty} I_n \quad (I_n < 0). \tag{2.66}$$

which differs from the moment of inertia I_0 of a "frozen" liquid. The difference is due to the fact that liquid particles may move relative to the walls of the tank, and thus their trajectories in the absolute frame of reference are not the same as the paths of particles in the "frozen" liquid.

Motion of a solid with cavities completely filled with liquid was first investigated in detail by N. Ye. Joukowski [6]. N. Ye. Joukowski showed that the rectilinear motion of such a body does not differ

*Translators note: Illegible in foreign text.

at all from the rectilinear motion of an absolutely rigid body whose mass is equal to the sum of the masses of the body and the liquid.

The rotational motion of a rigid body with cavities completely filled with a liquid is equivalent to the rotational motion of an absolutely rigid body with some reduced or equivalent moment of inertia. The equivalent moment of inertia is everywhere smaller than the moment of inertia of a body with "frozen" liquid [see (2.66)]. The difference depends on the form of cavities and on the location of these cavities with liquid relative to the axis of rotation. For example, if the tank is in the form of a sphere, and the axis of rotation passes through the center of the sphere, then in the absence of friction, the liquid will not take part in rotation. The moment of inertia will be equal to the moment of inertia of the spherical shell. If the container has the form of a cube, and the axis of rotation passes through its center, then it is not hard to imagine that a considerable portion of the liquid, located in the center will not be dragged along by the walls. The equivalent moment of inertia will equal the moment of inertia of the cube walls and a small portion of the moment of inertia of the "frozen" liquid.

If the liquid has a free surface, then the surface is distorted waves will appear on it. The oscillations of the liquid are described by a series in Bessel functions (2.46). To each term in the series there corresponds its own generalized coordinate $\lambda_n(t)$ and its own frequency of the natural oscillations ω_n.

The cause of the oscillations is the motion of the walls of the tank. The generalized coordinate of the oscillations λ_n can be determined from the third equation in (2.61).

As can be seen from (2.50), due to the oscillations of the liquid, there appears an additional transverse force

$$F_{y\lambda} = -\sum_{n=1}^{\infty} m_n \ddot{\lambda}_n$$

In the case of eigen oscillations each term of the series varies harmonically in the frequency ω_n. The force $F_{y\lambda}$ may be understood as a sum of the products of the masses of the liquid m_n and the generalized accelerations $\ddot{\lambda}_n$. The reduced mass of the liquid participating in the oscillations with a generalized acceleration $\ddot{\lambda}_n$ decreases as the number n of the tone of oscillations (2.62) increases. For the first tone the mass is numerically equal to the mass of the cylinder volume whose height is $\sim 0{,}45 r_0$; for the second tone the mass is 30 times smaller.

In view of (2.65) we may conclude that the moment of the oscillations of the liquid consists of the dynamic moment, proportional to the generalized acceleration $\ddot{\lambda}_n$ and the static moment, proportional to the generalized coordinate λ_n:

$$M_{\alpha} = -\sum_{n=1}^{\infty} m_n L_n \ddot{\lambda}_n + g \sum_{n=1}^{\infty} m_n \lambda_n.$$

From the physical point of view, the static moment arises as a result of a displacement of the free surface and it can be considered to arise due to the transverse motion of the center of mass of the liquid relative to the axis of the tank. The dynamic moment is equal to the transverse force $F_{y\lambda_n}$ multipled by the distance L_n between the center of rotation and the force. As we have already noted on the basis of (2.41), the liquid located in the upper layers has the greatest velocity. As we move downward from the surface the velocity rapidly decreases. Therefore, the reduced mass m_n of the oscillating liquid places itself close to the undisturbed free surface

$$x_n = L_n - L = -\frac{2r_0}{\zeta_n} \operatorname{th}\left(\zeta_n \frac{h}{2r_0}\right). \qquad (2.67)$$

If $h/r_0 \geqslant 1$, for the first tone of oscillations the reduced mass is located at a depth of about one radius; as the tone number n increases the mass comes closer to the free surface.

Just as the force F_{μ} , so the moment M_{cn} strongly decreases with an increase in the oscillation tone number n.

6. A Mechanical Analog of the Oscillations of a Liquid

In view of the fact that the equations of the oscillations of the free surface are analogous to the equations of the oscillations of mathematical pendulums, in the analysis of a rocket motion there arises a natural question of whether the oscillating liquid can be replaced by a system of mathematical pendulums. A possibility of such a model was shown by N. N. Moiseyev [17].

Let us find a mechanical system whichwould possess the dynamic properties in motion that would be identical with the properties of a liquid partially filling a cavity of a circular cylindrical tank. To solve this problem we shall set the given and unknown plane motion of the system equal to each other.

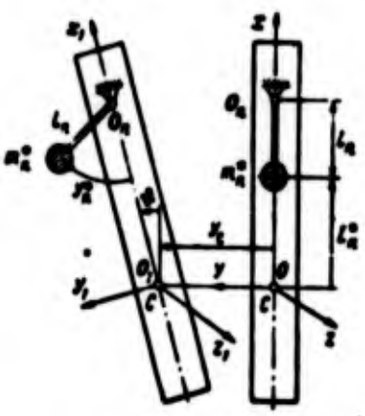

Figure 2.7

The given system is a rigid cavity in the form of a tank partially filled with an ideal liquid. The tank will be assumed weightless.

The\expressions for the kinetic and potential energy as well as the equations of motion for the total mass of the liquid were obtained in the previous section [see (2.58), (2.60), (2.61)].

The unknown mechanical system will be represented in the form of a rigid body (a rod) with n mathematical pendulums. The suspension points of the mathematical pendulums will be located on one straight line which is one of the principal central axes of inertia of the rigid body with pendulum masses attached to this axis

(Figure 2.7). The straight line in question will be considered the longitudinal axis of the rod, and the location of the masses of the pendulums on this axis is undisturbed.

Let m^* denote the mass of the rigid body with n pendulums, m^*_n — the mass of the n^{th} pendulum, I^* — the moment of inertia of the rigid body with masses of the pendulums attached rigidly relative to the transverse axis O_1z_1 passing through the center of mass of the system (point C), L^*_n — the distance between point C and the mass of the n^{th} pendulum, l_n — the length of the n^{th} pendulum.

The given and unknown system is acted upon by external forces that lead to identical moments M_c^0 and identical transverse forces F_y^0 attached to the centers of mass of the systems.

Let us find the parameters of the unknown system with which its motion will be identical with the motion of the given system.

We shall set up the expressions for the kinetic and potential energies of the unknown system. As the generalized coordinates we shall take: $y_c(t)$ — the linear displacement in the direction of the Oy-axis of a point C in the rod, θ — the angle of rotation of the axis of the rod, $y_n^*(t)$ — the linear displacement of the mass of the n^{th} pendulum from the axis of the rod.

The location of any point on the logitudinal axis of the rod in the absolute frame of reference Oxy is given by the coordinates

$$x = x_1 \cos\theta, \quad y = y_c + x_1 \sin\theta,$$

where x_1 is the abscissa of a point on the axis of the rod in the coordinate system attached to the rod $O_1x_1y_1$. The coordinates of the pendulums of the Oxy frame will be

$$x_n = (L_n^* + l_n)\cos\theta - l_n \cos\left(\frac{y_n^*}{l_n} - \theta\right),$$

$$y_n = y_c + (L_n^* - l_n)\sin\theta + l_n \sin\left(\frac{y_n^*}{l_n} - \theta\right).$$

Using the following relations

$$\sin\theta\approx\theta,\ \sin\frac{y_n^\circ}{l_n}\approx\frac{y_n^\circ}{l_n},\ \cos\theta\approx1-\frac{\theta^2}{2},$$
$$\cos\frac{y_n^\circ}{l_n}\approx1-\frac{1}{2}\left(\frac{y_n^\circ}{l_n}\right)^2$$

and retaining infinitesimals of the second order, we get

$$\begin{gathered}x=x_1\left(1-\frac{\theta^2}{2}\right),\\ y=y_C+x_1\theta,\\ x_n=L_n^\circ\left(1-\frac{\theta^2}{2}\right)+\frac{y_n^{\circ2}}{2l_n}-y_n^\circ\theta,\\ y_n=y_C+L_n^\circ\theta+y_n^\circ.\end{gathered}\tag{2.68}$$

Differentiating these expressions with respect to time, we find, up to the infinitesimals of the second order, that

$$\begin{gathered}\ddot{x}=0,\ \dot{x}_n=0,\\ \dot{y}=\dot{y}_C+x_1\dot{\theta},\ \dot{y}_n=\dot{y}_C+L_n^\circ\dot{\theta}+\dot{y}_n^\circ.\end{gathered}\tag{2.69}$$

The kinetic and potential energies of the system consist of the energy of the rod and the energies of the pendulums. Assuming the mass of a unit length of the rod to be $m(x_1)$, and letting x_1 change in the interval $-b\leqslant x_1\leqslant a$, we can write

$$\begin{gathered}T=\frac{1}{2}\left[\int_{-b}^{+a}m(x_1)(\dot{x}^2+\dot{y}^2)\,dx_1+\sum_{n=1}^{n}m_n^\circ(\dot{x}_n^2+\dot{y}_n^{\circ2})\right],\\ U=g\int_{-b}^{+a}m(x_1)x\,dx_1+g\sum_{n=1}^{n}m_n^\circ x_n.\end{gathered}\tag{2.70}$$

In accordance with our nomenclature

$$\begin{gathered}r=\int_{-b}^{+a}m(x_1)x_1^2dx_1+\sum_{n=1}^{n}m_n^\circ L_n^{\circ2},\\ m^\circ=\int_{-b}^{+a}m(x_1)\,dx_1+\sum_{n=1}^{n}m_n^\circ,\\ \int_{-b}^{+a}m(x_1)x_1\,dx_1+\sum_{n=1}^{n}m_n^\circ L_n^\circ=0.\end{gathered}\tag{2.71}$$

The last equality indicates that the static moment of the mass of the system relative to the center of mass is equal to zero.

Substituting (2.68), (2.69) into (2.70), and making use of (2.71) we have

$$T=\frac{1}{2}\left[m\dot{y}_C^2+I^*\dot{\theta}^2+\sum_{n=1}^{\infty}m_n^*(2\dot{y}_C\dot{y}_n^*+2L_n^*\dot{\theta}\dot{y}_n^*+\dot{y}_n^{*2})\right],$$

$$U=g\sum_{n=1}^{\infty}m_n^*\left(\frac{y_n^{*2}}{2L_n}-y_n^*\theta\right). \tag{2.72}$$

Now let us set equal the expressions for the energies of the unknown pendulum system (2.72) and the expressions for the energies of the given system (2.58) and (2.60), setting in them L - h/2 = 0. This equality means that point C (see Figure 2.3) coincides with the center of mass of the liquid when its free surface is perpendicular to the longitudinal axis of the cylindrical tank.

The structure of the expressions for the kinetic and potential energy of the given and unknown systems is the same. This means that the given system can be replaced by the mechanical system, consisting of a rigid body with pendulums. In order for the expressions (2.58), (2.60), and (2.72) to be identical, and, consequently, in order for the coordinates y_c and to have the same values under the influence of the same external forces F_y and M_c, it is necessary that these expressions have the same coefficients with the same variables. By comparing (2.58), (2.60), and (2.72) we conclude that the parameters of the pendulum system should have the following form

$$L_n=\frac{r_0}{\zeta_n\operatorname{th}\left(\zeta_n\frac{h}{r_0}\right)},$$

$$L_n^*=L_n-L\left[1-\frac{2r_0}{\zeta_n L}\operatorname{th}\left(\zeta_n\frac{h}{2r_0}\right)\right], \tag{2.73}$$

$$m_n^*=m_n=\pi r_0^2\rho\frac{2}{\zeta_n(\zeta_n^2-1)}\operatorname{th}\left(\zeta_n\frac{h}{r_0}\right);$$

$$y_n^*=\lambda_n,$$

$$m^*=m=\pi r_0^2 h\rho, \tag{2.74}$$

$$I^*=I=I_0+\sum_{n=1}^{\infty}I_n.$$

Thus, the mechanical pendulum system (rigid body with attached pendulums) in plane motion is dynamically equivalent to a liquid partially filling the cavity of the circular cylindrical tank if the mass of the pendulum system is equal to the mass of the liquid, and the moment of inertia of the rigid body with rigidly attached pendulums is equal to the equivalent moment of inertia of the liquid.

The length of the pendulums, their mass, and position relative to the center of rotation C are determined from (2.73).

Each tone of the oscillations of the liquid is modeled by a mathematical pendulum of a specified length. The mass of the pendulum is equal to the reduced mass of the oscillating liquid. Moreover, the mass of the pendulum decreases with an increase in the number n of the tone of the oscillations. The distance L_n^* from the center of rotation C of the rod to the mass of the pendulum corresponds to the distance L_n between the center of rotation of the cylinder and the center of the reduced mass of the oscillating liquid.

For $h/r_0 \leq 1$ the difference between the distances L and L_n decreases with an increases in number n, and the masses of the pendulums are as if located closer to the free surface (2.67)

With an increase in the number n the frequency of the natural oscillations of the liquid also increases. Hence, the length of the pendulum should be decreased.

A linear displacement of the pendulum from the axis of the suspension is equal to the generalized coordinate of the oscillations of the liquid $\mu_n^* = \lambda_n$. The generalized coordinate λ_n is a relative coordinate which characterizes the oscillations of the liquid in the body frame of reference $O_1x_1y_1z_1$.

Instead of mathematical pendulums the mechanical analog of the oscillations of a liquid may take the form of the oscillations of a weight suspended from weightless springs. In this case to each

tone of the oscillations there correspond oscillations of the weight with mass m_n which is attached to the walls of the tank at a distance x_n (2.67) from the free surface (Figure 2.8) with two springs of stiffness $k_n/2$.

Viscous friction, used to account for the damping properties of the oscillations of a real liquid, is introduced in the mechanical model by setting up two dampers with the coefficient of viscous friction $h_n/2$ between the mass m_n and the wall of the tank.

The stiffness of the springs is determined by the condition of equality between the frequencies of the natural oscillations

$$\omega_n^2 = \frac{g\zeta_n}{r_0}\operatorname{th}\left(\zeta_n\frac{h}{r_0}\right) = \frac{k_n}{m_n}.$$

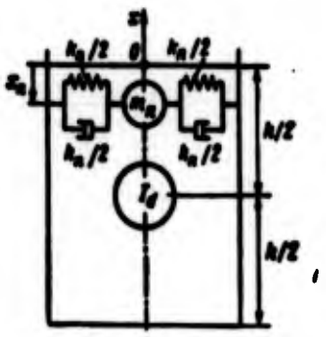

Figure 2.8

Since rotational motion involves only a fraction of the liquid, and the remaining portion is at rest, we have to introduce into the mechanical model without friction some mass with a moment of inertia I_d, that does not participate in rotation, and locate it at the center of mass of the liquid. On the basis of (2.66)

$$I_d = -\sum_{n=1}^{\infty} I_n.$$

Let us consider some examples.

1. A cylindrical tank, partially filled with heavy ideal liquid, is in free back-and-forth motion without friction along straight horizontal guides (Figure 2.9a). Let us determine the frequency of the natural oscillations of the system: the tank plus the liquid, taking into consideration only the first tone of the oscillations of the free surface of the liquid.

Let us apply Equations (2.61). In accordance with the condition we set $\theta=0,\ F_y=0,\ M_C=0$, and obtain the first partial subsystem (2.61):

$$m\ddot{y}_C+m_1\ddot{\lambda}_1=0,$$
$$\ddot{\lambda}_1+\omega_1^2\lambda_1=-\ddot{y}_C.$$

where m is the mass of the cylinder with liquid. The frequency of the oscillations ω_1 and the mass m_1 can be determined from (2.43) and (2.49) for n = 1.

Eliminating y_C, we find

$$\ddot{\lambda}_1\left(1-\frac{m_1}{m}\right)+\omega_1^2\lambda_1=0. \qquad (a)$$

The desired frequency of the natural oscillations of the system

$$\omega_1^*=\frac{\omega_1}{\sqrt{1-\frac{m_1}{m}}} \qquad (b)$$

is everywhere larger than the natural frequency of the oscillations of a liquid in a tank it rest. If $m\gg m_1$, then $\omega_1^*\approx\omega_1$ and the liquid is oscillating as if it were in a stationary tank.

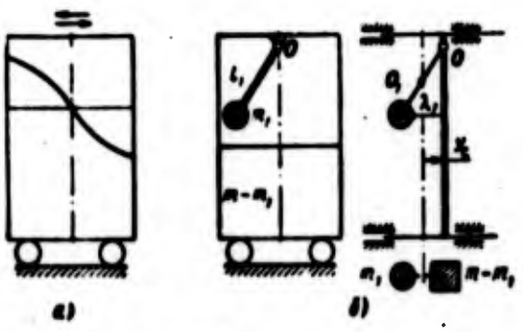

Figure 2.9

The formula obtained above is conveniently interpreted with an aid of pendulum models (see Figure 2.9b). In the case of natural oscillations the center of mass of the system remains stationary and is located on the vertical line passing through point O_1. Therefore,

$$m_1(\lambda_1-y_C)=(m-m_1)y_C.$$

whence

$$y_C = \frac{m_1}{m} \lambda_1.$$

From the similarity of triangles (see Figure 2.9b) we find

$$\frac{\lambda_1}{\lambda_1 - y_C} = \frac{l_1}{l_1'},$$

where l_1' is the distance from the mass of a pendulum to point O_1. Substituting the value of y_c form the previous expression, we get

$$l_1' = l_1\left(1 - \frac{m_1}{m}\right).$$

Now the frequency of the oscillations of the system can be described as the frequency of the natural oscillations of a pendulum of length l_1', since the point O_1 remains stationary. Inasmuch as $\omega_1^2 = g/l_1$, we then have

$$\omega_1' = \sqrt{\frac{g}{l_1'}} = \frac{\omega_1}{\sqrt{1 - \frac{m_1}{m}}}.$$

The reason for an increase in the frequency of the oscillations of the pendulum is the fact that its length has been shortened (l_1').

2. Let a tank, partially filled with liquid, be placed on rectilinear guides and have the freedom of moving only in the horizontal plane by an external force $F_y = F_0 \sin pt$. Considering only the first tone of the oscillations of the liquid, let us find the amplitude of the external force F_0 if the tank moves with an acceleration $\ddot{y}_C = a^0 \sin pt$.

Based on (2.61) the equations of motion of the tank with liquid will have the following form for n = 1

$$\begin{aligned} m\ddot{y}_C + m_1\ddot{\lambda}_1 &= F_0 \sin pt, \\ \ddot{\lambda}_1 + \omega_1^2\lambda_1 &= -\ddot{y}_C. \end{aligned} \qquad (c)$$

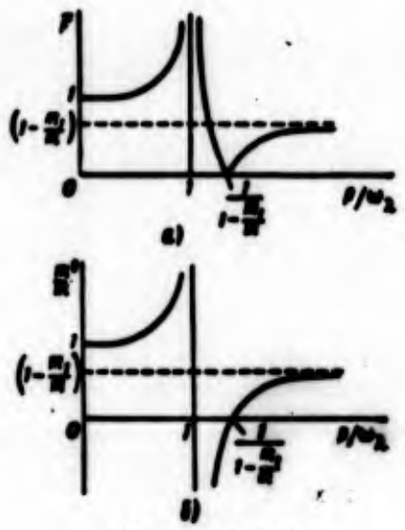

Figure 2.10

Using the notation (b) of the previous problem we shall find the particular solution of Equations (c) with respect to β_c as

$$\beta_c = \frac{F_0}{m\left(1-\frac{m_1}{m}\right)} \frac{\omega_1^2-p^2}{\omega_1^2-p^2} \sin pt. \qquad (d)$$

In view of the condition that $\beta_c = a^0 \sin pt$, we shall get

$$F_0 = a^0 m \left(1-\frac{m_1}{m}\right) \left| \frac{\omega_1^2-p^2}{\omega_1^2-p^2} \right|. \qquad (e)$$

The graph of the dimensionless force $\bar{F} = F_0/a^0 m$ as a function of the ratio of frequencies p/ω_1 is shown in Figure 2.10a. If the frequency of the forced oscillations is equal to the frequency of the natural oscillations of the liquid in a stationary tank, then the force would have to be infinitely large. When the frequency of the external force is the same as the frequency of the natural oscillations of the system $p = \omega_1^0$, then this force is equal to zero. This conclusion was made on the basis of equations for small oscillations without considering the forces of friction. In a real system the force will everywhere have a finite value.

We can ask the following question: if the tank, partially filled with liquid, is replaced with an equivalent rigid body, what should be the mass m^0 of this body?

The equation of motion of the rigid body is

$$m^0 \ddot{y}_c = F_0 \sin pt.$$

From this equation, in view of (d) and (e), we find

$$m^0 = m\left(1-\frac{m_1}{m}\right)\frac{\zeta_1^2-\rho^2}{\zeta_1^2-\rho^2}.$$

The equivalent mass m^0 depends on the frequency of oscillations. A plot of the ratio m^0/m is shown in Figure 2.10b.

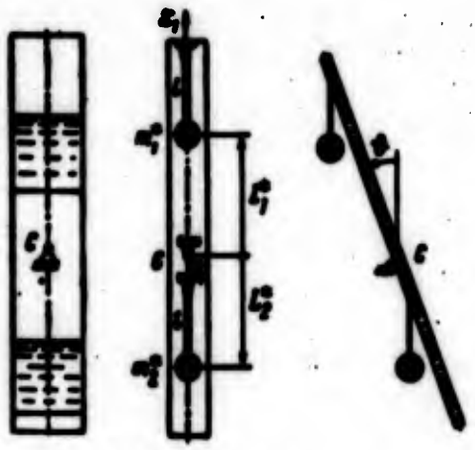

Figure 2.11

3. We shall represent the fuselage of the rocket as a rigid body with two identical circular cylindrical cavities (partially filled with a heavy ideal liquid) whose longitudinal axes lie in one straight line. Let this body, hinged at point C (Figure 2.11), execute planar oscillations. Point C lies on the longitudinal axis of a rocket and coincides with the center of mass of the rigid body with liquid when the free surfaces of the liquid in both cylindrical cavities are perpendicular to the longitudinal axis. We are to determine the frequency of natural oscillations of the system, considering only the first tone of the oscillations of the liquid.

The problem will be solved using the pendulums as a model. The liquid oscillating in the cavities will be replaced with mathematical pendulums of length l with masses m_1^* and m_2^*. The suspension points of the mathematical pendulums must be chosen in such a way that the coordinates of the masses m_1^* and m_2^* will be, respectively,

$$x_1^* = L_1^* = L_1 - \frac{2r_0}{\zeta_1}\,\mathrm{th}\left(\zeta_1\frac{h}{2r_0}\right),$$
$$x_2^* = L_2^* = -\left(L_2 + \frac{2r_0}{\zeta_1}\,\mathrm{th}\left(\zeta_1\frac{h}{2r_0}\right)\right).$$

where h, r_0 are the height to which the tanks are filled and the radius of the tanks, $\zeta_1 = 1{,}8412$. The masses of the pendulums m_1^*, m_2^* are determined from (2.73) with $\zeta_n = \zeta_1, \rho = \rho_1, \rho_2$.

The expressions for the kinetic and potential energies of the system will be obtained using (2.72) with $y_c=0$. We find

$$T=\frac{1}{2}\left[I\dot{\theta}^2+\sum_{j=1}^{s}m_j^*(2L_j^*\dot{\theta}\dot{\lambda}_j+\dot{\lambda}_j^2)\right].$$

$$U=g\sum_{j=1}^{s}m_j^*\left(\frac{\lambda_j^2}{2l}-\lambda_j\theta\right).$$

Here I is the moment of inertia (relative to point C) of the rod with pendulums suspended from its longitudinal axis, θ is the angle of deflection of the rod, λ_j is the linear displacement of the pendulum mass m_j^* from the longitudinal axis of the rod.

Substituting the expressions for the kinetic and potential energies of the system into Lagrange's equations of second kind, we obtain

$$\left.\begin{aligned}I\ddot{\theta}+\sum_{j=1}^{s}m_j^*L_j^*\ddot{\lambda}_j-g\sum_{j=1}^{s}m_j^*\lambda_j=0,\\ \ddot{\lambda}_j+\frac{g}{l}\lambda_j=-L_j^*\ddot{\theta}+g\theta.\end{aligned}\right\}\qquad(f)$$

Letting

$$\theta=\theta_0\cos\omega t,\quad \lambda_j=\lambda_{j0}\cos\omega t$$

and substituting these expressions in Equations (f), we get the following equation for the frequencies of the system:

$$\omega^4\left(I-\sum_{j=1}^{s}m_j^*L_j^{*2}\right)-\omega^2\left(I\frac{g}{l}+2g\sum_{j=1}^{s}m_j^*L_j^*\right)-g^2\sum_{j=1}^{s}m_j^*=0.\qquad(g)$$

Introducing the notation

$$a_0=I-\sum_{j=1}^{s}m_j^*L_j^{*2},\quad a_2=I\frac{g}{l}+2g\sum_{j=1}^{s}m_j^*L_j^*,\quad a_4=g^2\sum_{j=1}^{s}m_j^*,$$

we rewrite Equation (g) as

$$a_0\omega^4-a_2\omega^2-a_4=0.$$

Referring to the frequencies of the system as ω_2 and ω_3, we obtain

$$\omega_{2,3}^2=\frac{a_2}{2a_0}\left(1\pm\sqrt{1+\frac{4a_0a_4}{a_2^2}}\right). \qquad (h)$$

The product $a_0a_4>0$; therefore, for $a_2>0$ the frequency $\omega_2^2>0$, and $\omega_3^2<0$. The system has only one frequency of natural oscillations, namely ω_2. Setting $\omega_3=iu$, we find

$$\cos\omega_3 t=\cos iut=\operatorname{ch} ut.$$

The motion obeying the law ch ut will be non-oscillatory, the deflections of the system increasing continuously. The equilibrium position of the system is unstable in the vertical plane.

Let us make a comparison between the frequency ω_2 and the frequency of natural oscillations of the pendulum $\omega_n=\sqrt{g/l}$ for the case when $\sum_{j=1}^{s} m_j^0 L_j^0=0$. From (h) we have

$$\frac{\omega_2^2}{\omega_n^2}>\frac{1}{1-\frac{1}{I}\sum_{j=1}^{s} m_j^0 L_j^{02}}. \qquad (i)$$

The frequency of the natural oscillations of the system in angular motion is greater than the natural frequency, and the difference is larger, the greater the portion comprised by the moments of inertia of the pendulums in the total moment of inertia I.

The pendulum model was defined for the oscillations of a liquid in the cylindrical tank with a circular cross section. However, the analogy with pendulums is also useful in the general case for any cavity shaped as a solid of revolution. The equations of perturbed motion (2.61) are also valid for any cavity in the shape of a solid of revolution relative to the Ox-axis, and will differ only in the values of coefficients that in turn depend on the shape of the cavity.

In fact, the expression for the kinetic energy of the liquid

$$T=\frac{1}{2}\rho\iint_{S}\left[\phi\frac{\partial\phi}{\partial n}\cos(n,x)+\phi\frac{\partial\phi}{\partial n}\cos(n,y)+\right.$$
$$\left.+\phi\frac{\partial\phi}{\partial n}\cos(n,z)\right]dS$$

is valid for a tank of any shape. If the generalized coordinates are correspondingly selected, then the structure of the expressions for the kinetic and potential energies of the liquid (2.58) and (2.60) will be identical for cavities in the shape of a cylinder, torus, sphere, cone, etc. The shape of the cavity will only affect the values of the coefficients appearing in the expressions for T and U.

7. Determination of Other Expressions for the Absolute Velocity Potential of a Liquid

The representation of the potential function ϕ by expression (2.55) is not unique. In the literature [21, 23, 27] there occur formulas, differing from one another slightly, for the absolute velocity potential of a liquid that apply to the same type of motion of a tank (see Figure 2.3). The discrepancies among the formulas for ϕ are due to the fact that the generalized coordinate $\lambda_m(t)$ has a different meaning in each of them. We shall consider this question in more detail.

In the expression (2.30) which contains two arbitrary constants C_1 and C_2 only one boundary condition at $x = -h$ (2.34) has been determined. The second boundary condition for the function ψ remains undetermined since the condition stating that the pressure is constant on the free surface (2.24) should be satisfied for the sum of function $\phi=\psi+\varphi$. For example, in Section 3 the boundary condition for the function ψ on the free surface was taken in the form (2.35).

The free surface in the direction of the Ox-axis exhibits the same displacement as the bottom of the tank. This means that the potential function $\varphi(x, r, \eta, t)$ describes motion of the liquid in a completely filled tank. The displacement of the free surface of the liquid, defined by the potential $\varphi(r, \eta, t)$, is proportional to the parameters $\lambda_n(t)$ (2.46). It is measured from the plane $O_1y_1z_1$ perpendicularly to the longitudinal axis of the tank (see Figure 2.4).

Instead of (2.37) we can use the expressions

$$X_n = -\frac{2\zeta_n^2}{\zeta_n^2-1}\frac{2\operatorname{ch}\left(\zeta_n\frac{x}{r_0}\right)-\operatorname{ch}\left(\zeta_n\frac{h+x}{r_0}\right)}{\zeta_n\operatorname{ch}\left(\zeta_n\frac{h}{r_0}\right)}, \tag{2.75}$$

or

$$X_n = -\frac{\zeta_n^2}{\zeta_n^2-1}\frac{\operatorname{ch}\left(\zeta_n\frac{x}{r_0}\right)}{\zeta_n\operatorname{ch}\left(\zeta_n\frac{h}{r_0}\right)}, \tag{2.76}$$

which also are solutions of Equation (2.30) and satisfy the boundary condition (2.34) at the bottom of the tank.

At the free surface we shall have:
in case of (2.75)

$$\frac{dX_n}{dx} = -\frac{2\zeta_n}{\zeta_n^2-1} \quad \text{for } x=0,$$

and in case of (2.76)

$$\frac{dX_n}{dx} = -\frac{4\zeta_n}{(\zeta_n^2-1)\operatorname{ch}\left(\zeta_n\frac{h}{r_0}\right)} \quad \text{for } x=0.$$

If instead of (2.37) the function X_n assumes the form in (2.75) or (2.76), we shall then obtain, respectively, the following formulas for the absolute velocity potential

$$\varphi_0 = -2r_0 \sin\eta \sum_{n=1}^{\infty} \frac{J_1\left(\zeta_n \frac{r}{r_0}\right)}{(\zeta_n^2 - 1) J_1(\zeta_n)} \times$$

$$\times \left\{ \left[r_0 \frac{2\sin\left(\zeta_n \frac{x}{r_0}\right) - \sin\left(\zeta_n \frac{b+x}{r_0}\right)}{\zeta_n \sin\left(\zeta_n \frac{b}{r_0}\right)} + (L+x) \right] \dot{\vartheta} + \right. \tag{2.77}$$

$$\left. + \dot{\beta}_c + \frac{\sin\left(\zeta_n \frac{b+x}{r_0}\right)}{\sin\left(\zeta_n \frac{b}{r_0}\right)} \dot{\lambda}_{0n} \right\}.$$

$$\varphi_0 = -2r_0 \sin\eta \sum_{n=1}^{\infty} \frac{J_1\left(\zeta_n \frac{r}{r_0}\right)}{(\zeta_n^2 - 1) J_1(\zeta_n)} \times$$

$$\times \left\{ \left[-2r_0 \frac{\sin\left(\zeta_n \frac{x}{r_0}\right)}{\zeta_n \sin\left(\zeta_n \frac{b}{r_0}\right)} + (L+x) \right] \dot{\vartheta} + \right.$$

$$\left. + \dot{\beta}_c + \frac{\sin\left(\zeta_n \frac{b+x}{r_0}\right)}{\sin\left(\zeta_n \frac{b}{r_0}\right)} \dot{\lambda}_{0n} \right\}. \tag{2.78}$$

From the condition on the free surface (2.24) we shall find the equations for the generalized coordinate λ_n. In case of (2.77) we get

$$\ddot{\lambda}_{0n} + \omega_n^2 \lambda_{0n} = -L_{0n} \ddot{\vartheta} - \ddot{\beta}_c \tag{2.79}$$

where

$$L_{0n} = L - \frac{r_0}{\zeta_n} \frac{\sin\left(\zeta_n \frac{b}{r_0}\right) - 2}{\sin\left(\zeta_n \frac{b}{r_0}\right)}. \tag{2.80}$$

In the case of (2.78) we obtain

$$\ddot{\lambda}_{0n} + \omega_n^2 \lambda_{0n} = -L\ddot{\vartheta} - \ddot{\beta}_c - g\vartheta \left[1 - \frac{2}{\sin\left(\zeta_n \frac{b}{r_0}\right)} \right]. \tag{2.81}$$

Upon comparing Equations (2.42), (2.79) and (2.81) it is evident that the generalized coordinates $\lambda_n, \lambda_{qn}, \lambda_{qn}$ have a different meaning in all three cases. In view of the fact that the boundary condition for X_n on the free surface remains undetermined, we may select an infinite set of combinations involving hyperbolic functions which will be solutions of Equation (2.30) and satisfy condition((2.34). The formulas (2.75) and (2.76) are preferable because the right-hand side of Equation (2.79) does not contain terms proportional to the angle θ, and in (2.81) the coefficient of $\ddot{\theta}$ has the simplest possible form.

Let us investigate quantitatively the differences among the generalized coordinates $\lambda_n, \lambda_{qn}, \lambda_{qn}$ and compare the structures of the equations of motion. For this purpose by exchanging the variables we shall obtain Equations (2.79) and (2.81) from Equations (2.42). Since in all three equations the coefficients of δc are identical, $\lambda_n, \lambda_{qn}, \lambda_{qn}$ are related to one another only through an angle θ. We set

$$\lambda_n = \lambda_{qn} + a_n \theta$$

and

$$\lambda_n = \lambda_{qn} + a_n \theta.$$

Substituting consecutively these relations into Equation (2.42) and comparing the coefficients obtained with the coefficients of the corresponding variables in Equation (2.79) and (2.81), we conclude that the coefficients should be:

$$a_n = -\frac{\eta_n}{\zeta_n \operatorname{sh}\left(\zeta_n \frac{h}{\eta_n}\right)} = l_n$$

$$a_n = -\frac{\eta_n}{\zeta_n \operatorname{sh}\left(\zeta_n \frac{h}{\eta_n}\right)}\left[1 - \frac{1}{\operatorname{ch}\left(\zeta_n \frac{h}{\eta_n}\right)}\right] = 2l_n\left[1 - \frac{1}{\operatorname{ch}\left(\zeta_n \frac{h}{\eta_n}\right)}\right].$$

Consequently

$$\lambda_n = \lambda_{qn} + l_n \theta. \qquad (2.82)$$

$$\lambda_n = \lambda_{nm} + 2\theta_n \left[1 - \frac{1}{\operatorname{ch}\left(\zeta_n \frac{h}{r_0}\right)}\right] \theta_n \qquad (2.83)$$

As applied to the analogy with pendulums, the meaning of the coordinates λ_{nm} and λ_{nm} is clear from Figure 2.12. In (2.82) the generalized coordinate λ_{nm} is measured from the vertical plane passing through point O_n, and in (2.83) the coordinate λ_{nm} is measured from the plane inclined to the vertical by an angle

$$\left[1 - \frac{2}{\operatorname{ch}\left(\zeta_n \frac{h}{r_0}\right)}\right] \theta_n$$

whereas the generalized coordinate λ_n is measured from the axis of the rod.

In a similar way we also measure the deflections of the free surface of the liquid which are proportional to λ_{nm} and λ_{nm}. This is easy to see if one determines the total displacement of the free surface in the absolute frame of reference. We shall have

$$z_{nm}(r, \eta, t) = \int_0^t \left(\frac{\partial z_n}{\partial t}\right)_{r=r_0} dt = 2r_0 \sin \eta \times$$

$$\times \sum_{n=1}^{\infty} \frac{J_1\left(\zeta_n \frac{r}{r_0}\right)}{(\zeta_n^2 - 1) J_1(\zeta_n)} \frac{\zeta_n}{r_0} \operatorname{sh}\left(\zeta_n \frac{h}{r_0}\right) \lambda_{nm}.$$

The total deflection z_m measured from the horizontal plane OYZ is only proportional to λ_{nm}, i.e., $z_{nm} = z_{nm}^{\lambda}$ (Figure 2.13a):

$$z_m(r, \eta, t) = \int_0^t \left(\frac{\partial z_n}{\partial t}\right)_{r=r_0} dt = 2r_0 \sin \eta \sum_{n=1}^{\infty} \frac{J_1\left(\zeta_n \frac{r}{r_0}\right)}{(\zeta_n - 1) J_1(\zeta_n)} \times$$

$$\times \left\{\left[1 - \frac{2}{\operatorname{ch}\left(\zeta_n \frac{h}{r_0}\right)}\right] \theta_n + \frac{\zeta_n}{r_0} \operatorname{sh}\left(\zeta_n \frac{h}{r_0}\right) \lambda_{nm}\right\}.$$

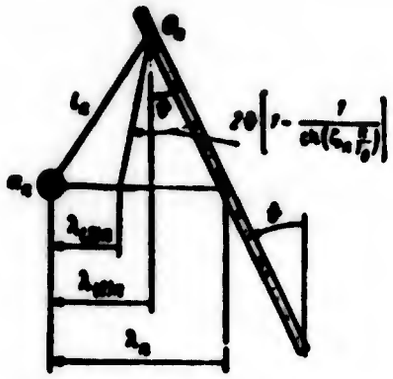

Figure 2.12

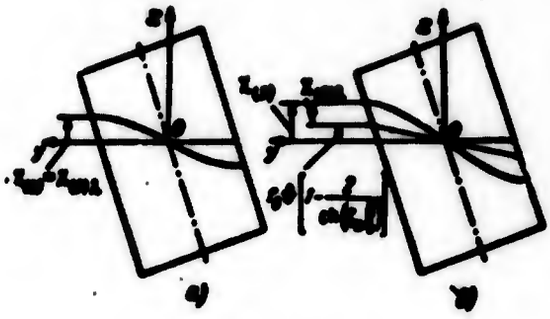

Figure 2.13

Here the total displacement z_m also depends on the angle θ, and the part of the displacement $z_{m\theta}$ that is proportional to $\lambda_{m\theta}$ is measured from the plane inclined at the angle (see Figure 2.13b)

$$\left[1-\frac{z}{\cos\left(l_0\frac{h}{r_0}\right)}\right]\theta.$$

The equations of motion, corresponding to the representation of the absolute velocity potential as (2.77), will be found from Equations (2.61), replacing in them λ_n according to (2.82).

Letting $(L-h/2)=0$, we obtain

$$\begin{aligned}
&m\ddot{y}_C+\sum_{n=1}^{s}m_n\ddot{\lambda}_{(y)n}+\ddot{\theta}\sum_{n=1}^{s}m_nl_n=F_y,\\
&\left[I_0+\sum_{n=1}^{s}I_n+\sum_{n=1}^{s}m_nl_nl_{cn}\right]\ddot{\theta}+\sum_{n=1}^{s}m_nl_n\ddot{\lambda}_{(y)n}-\\
&-g\sum_{n=1}^{s}m_n\lambda_{(y)n}-g\theta\sum_{n=1}^{s}m_nl_n=M_C,\\
&\ddot{\lambda}_{(y)n}+\omega_n^2\lambda_{(y)n}=-(L_n+l_n)\ddot{\theta}-\ddot{y}_C.
\end{aligned}\tag{2.84}$$

If one determines the kinetic and potential energies of a system and substitutes them into Lagrange's equations of the second kind, the equations of motion of the system will have a somewhat different structure: in the second equation the term proportional to $\lambda_{(y)n}$ will be missing, and a new term will appear that depends on θ_C. These

equations may be obtained from (2.84) if in the second equation $\lambda_{(2)n}$ will be replaced by its value as found from the third equation. Then we shall get

$$m\ddot{y}_C+\sum_{n=1}^{\bar{n}} m_n\ddot{\lambda}_{(2)n}+\ddot{\theta}\sum_{n=1}^{\bar{n}} m_n l_n=F_y,$$

$$(I_0+\sum_{n=1}^{\bar{n}} I_{(2)n})\ddot{\theta}+\sum_{n=1}^{\bar{n}} m_n L_{(2)n}\ddot{\lambda}_{(2)n}+\ddot{y}_C\sum_{n=1}^{\bar{n}} m_n l_n-g\sum_{n=1}^{\bar{n}} m_n l_n=M_C, \qquad (2.85)$$

$$\ddot{\lambda}_{(2)n}+\omega_n^2\lambda_{(2)n}=-L_{(2)n}\ddot{\theta}-\ddot{y}_C,$$

where

$$L_{(2)n}=L_n+l_n=L\left(1-\frac{r_0}{LC_n}\frac{\operatorname{ch}\left(C_n\frac{h}{r_0}\right)-2}{\operatorname{sh}\left(C_n\frac{h}{r_0}\right)}\right),$$

$$I_{(2)n}=I_n+m_n l_n(2L_n+l_n)=$$

$$=\pi r_0^3\left[-\frac{1}{r_0}\frac{8h-4L}{(C_n^2-1)C_n^2}+\frac{2}{C_n^2(C_n^2-1)}\frac{8\operatorname{ch}\left(C_n\frac{h}{r_0}\right)-4}{\operatorname{sh}\left(C_n\frac{h}{r_0}\right)}\right]$$

To the same potential there correspond differential equations that have a different structure, for example (2.84) and (2.85), which sometimes leads to misunderstandings.

These discrepancies are, however, purely extraneous, and arise as a result of a linear transformation of equations. Equations (2.85) are still preferable to Equations (2.84) since the matrix of their coefficients is symmetric.

Equations (2.84) and (2.85) were obtained from (2.61) with the condition $(L-h/2)=0$, i.e, with point C being at the same time the center of mass of an undisturbed liquid.

If the location of point C* (center of the reduced mass) is determined from the second condition, namely if

$$m(L-h/2)+\sum_{n=1}^{\bar{n}} m_n l_n=0, \qquad (2.87)$$

then from Equations (2.61) and (2.85) we obtain equations in the form proposed by B. I. Rabinovich [27, 28].

In fact, if in Equation (2.61) on the basis of (2.87) we substitute

$$m(L-h/2)=-\sum_{n=1}^{s} m_n l_n$$

then instead of (2.85) we obtain equations of an identical structure as those in [27, 28]:

$$\begin{gathered} m\ddot{y}_{C^*}+\sum_{n=1}^{s} m_n\ddot{\lambda}_{(3)n}=F_y, \\ (I_0+\sum_{n=1}^{s} I'_{(3)n})\ddot{\theta}+\sum_{n=1}^{s} m_n L^*_{(3)n}\ddot{\lambda}_{(3)n}=M_{C^*}, \\ \ddot{\lambda}_{(3)n}+\omega_n^2\lambda_{(3)n}=-L^*_{(3)n}\ddot{\theta}-\ddot{y}_{C^*}. \end{gathered} \tag{2.88}$$

Here $L^*_{(3)n}=L_{nC^*}+l_n$, L_{nC^*} is the distance from point C* to the mass of the pendulum.

Compared to (2.84) and (2.85) Equations (2.88) are more compact which is due to the fact that the center of reduced mass C* has been selected in a special way. The center of reduced mass as determined by Equation (2.87) is called the <u>metacenter</u> of a system. Let us determine the relative positions of points C and C* using the example of a liquid filling a cylindrical tank (see Figure 2.3). From (2.87) we find

$$L=h/2-\frac{1}{m}\sum_{n=1}^{s} m_n l_n.$$

Substituting the values of m_n from (2.49) and l_n from (2.73), we obtain

$$L=h/2-\frac{\pi r_0^4\rho}{4m}=h/2-\frac{r_0^2}{4h}.$$

The metacenter C* is located above the center of mass C. The quantity $\pi r_0^4\rho/4$ is numerically equal to the equatorial moment of inertia of the free surface of a liquid with density ρ relative to the axis O_1z_1. Let us denote this moment by Ω. Then

$$L=h/2-\frac{\Omega}{m}.$$

If the positions of points C and C* are defined by coordinates x_c and x_{c^*}, then keeping in mind the direction of the O_1x_1 axis we shall have

$$x_C = -h/2,\ x_{C'} = -h/2 + \frac{Q}{m}.$$

The formula for $x_{C'}$ can be written in a more general form [28]

$$x_{C'} = x_C + \frac{Q}{m}. \tag{2.89}$$

Now we shall obtain the equations of motion corresponding to the potential Φ_3. As was the case with the potentials Φ and Φ_2, the equations of motion can be deduced using several methods of which the simplest consists in substituting (2.83) into Equation (2.61). But here we shall use the analogy with pendulums. By virtue of (2.74) and (2.83) let us substitute into the system of equations for the kinetic and potential energies (2.72) the following expression

$$\ldots$$

Noting that

$$\ldots$$

we obtain

$$\ldots$$

Combining the coefficients of $\dot{\theta}^2$ we find

$$I_0+\sum_{n=1}^{\infty}I_n+\sum_{n=1}^{\infty}m_nM_n\left[L_n+l_n\left(1-\frac{1}{\operatorname{ch}\left(\zeta_n\frac{h}{r_0}\right)}\right)\right]\times$$

$$\times\left(1-\frac{1}{\operatorname{ch}\left(\zeta_n\frac{h}{r_0}\right)}\right)=I_0+\sum_{n=1}^{\infty}I_{qn}, \tag{2.90}$$

$$I_{qn}=\pi r_0^4\left\{-\frac{h-L}{r_0}\sum_{n=1}^{\infty}\frac{8}{\zeta_n^4(\zeta_n^2-1)}-\right.$$

$$-\frac{L}{r_0}\sum_{n=1}^{\infty}\frac{8}{\zeta_n^4(\zeta_n^2-1)\operatorname{ch}\left(\zeta_n\frac{h}{r_0}\right)}+\sum_{n=1}^{\infty}\frac{8}{\zeta_n^4(\zeta_n^2-1)}\times$$

$$\left.\times\frac{\operatorname{ch}\left(\zeta_n\frac{h}{r_0}\right)-1}{\operatorname{ch}\left(\zeta_n\frac{h}{r_0}\right)\operatorname{ch}\left(\zeta_n\frac{h}{r_0}\right)}\right\}.$$

By substituting the expressions for T and U into Lagrange's equations of second kind we obtain

$$m\ddot{y}_c+\sum_{n=1}^{\infty}m_n\ddot{\lambda}_{qn}+b\sum_{n=1}^{\infty}2m_n\dot{l}_n\left(1-\frac{1}{\operatorname{ch}\left(\zeta_n\frac{h}{r_0}\right)}\right)=F_{qn}$$

$$(I_0+\sum_{n=1}^{\infty}I_{qn})\ddot{\theta}+\sum_{n=1}^{\infty}m_nL\ddot{\lambda}_{qn}+g\sum_{n=1}^{\infty}m_n\lambda_{qn}\times$$

$$\times\left(1-\frac{2}{\operatorname{ch}\left(\zeta_n\frac{h}{r_0}\right)}\right)+\ddot{y}_c\sum_{n=1}^{\infty}2m_nl_n\left(1-\frac{1}{\operatorname{ch}\left(\zeta_n\frac{h}{r_0}\right)}\right)+ \tag{2.91}$$

$$+\theta g\sum_{n=1}^{\infty}2m_nl_n\left[\frac{1}{\operatorname{ch}^2\left(\zeta_n\frac{h}{r_0}\right)}-\frac{1}{\operatorname{ch}\left(\zeta_n\frac{h}{r_0}\right)}\right]=M_c, \quad (2.91)$$

$$\ddot{\lambda}_{qn}+\omega_n^2\lambda_{qn}=-L\ddot{\theta}-\ddot{y}_c+\theta g\left(1-\frac{2}{\operatorname{ch}\left(\zeta_n\frac{h}{r_0}\right)}\right).$$

The coefficient matrix for these equations is also symmetric. The equations for the coordinates λ_{qn} in (2.91) are identical with the equations obtained by D. Ye. Okhotsimskiy [23].

Thus, a deflection of the free surface of a liquid may be represented in the form of different combinations of functions Φ and λ_n. Each combination has its own expression for potential Φ, and consequently, its own system of the differential equations of motion.

Below in order to set up the equations of motion we shall apply the potential function Φ to which there corresponds the system of equations (2.61)

8. The Absolute Velocity Potential of a Liquid in a Tank Formed by Two Coaxial Circular Cylinders

The problem of determining the absolute velocity potential of a liquid contained in such a tank was solved by D. Ye. Okhotsimskiy [23]. To determine the potential Φ, in addition to the boundary conditions applied in Section 3, we have an additional boundary condition on the external wall of the tank (Figure 2.14)

$$\left(\frac{\partial \Phi}{\partial r}\right)_{r=r_0} = v_n^0$$

where r_0 is the radius of the internal cylinder.

The basic assumptions and the order in which the problem is going to be solved were presented in Section 3. Here we shall only discuss some of the peculiarities that appear in the solving procedure and are due to having introduced the internal boundary.

The solution of Equation (2.29) can be expressed in terms of Bessel's functions of first and second kind and order one

$$R_0(r) = A_1 J_1(kr) + A_2 Y_1(kr).$$

Making use of the two boundary conditions

$$\frac{dR}{dr} = 0 \quad \text{for } r = r_0,\ r = b_0$$

we shall obtain a system of equations for determining the arbitrary constants A_1 and A_2:

$$A_1 J_1(\xi_1) + A_2 Y_1(\xi_1) = 0,$$
$$A_1 J_1(\beta\xi_1) + A_2 Y_1(\beta\xi_1) = 0.$$

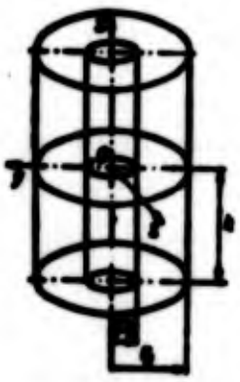

Figure 2.14

Here, just as in Section 3, $\xi_n = k_n r_0$. The coefficients A_1 and A_2 are different from zero if

$$J_1(\xi_1) Y_1(\beta\xi_1) - J_1(\beta\xi_1) Y_1(\xi_1) = 0.$$

This equation gives an infinite spectrum of eigenvalues ξ_n. We denote

$$\frac{A_2}{A_1} = -\frac{J_1(\xi_1)}{Y_1(\xi_1)} = -\frac{J_1(\beta\xi_1)}{Y_1(\beta\xi_1)} = \gamma_n$$

then

$$R_n(r) = \left[J_1\left(\xi_n \frac{r}{r_0}\right) + \gamma_n Y_1\left(\xi_n \frac{r}{r_0}\right)\right] A_1.$$

Choosing A_1 in such a way that on the external wall of the cavity the value of Bessel's function will be $R_n(r_0) = 1$ we get

$$R_n\left(\xi_n \frac{r}{r_0}\right) = a_n\left[J_1\left(\xi_n \frac{r}{r_0}\right) + \gamma_n Y_1\left(\xi_n \frac{r}{r_0}\right)\right]. \qquad (2.92)$$

where

$$a_n = \frac{1}{J_1(\xi_n) + \gamma_n Y_1(\xi_n)}.$$

Setting $\beta = 0$ from (2.92), one can obtain an expression for $R_n(r)$ in the form (2.32).

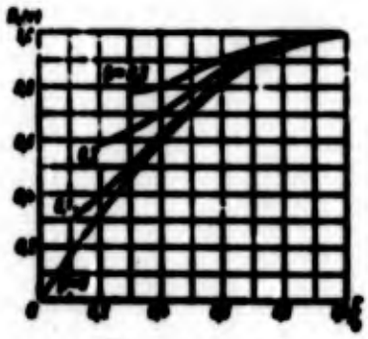

Figure 2.15

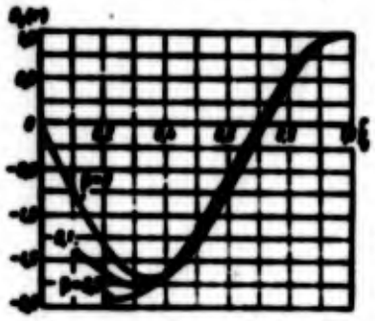

Figure 2.16

The values of the eigenvalues ξ_n and coefficients a_n and γ_n for the first three tones n, adopted from [23], have been shown in Table 2.1.

The form of functions R_n for n = 1.2 and β = 0; 0.1; 0.2; 0.3 is shown in Figures 2.15 and 2.16. Differences among the functions R_n, the latter constituting oscillation modes of the free surface in the radial direction, for the same tone n are relatively small and occur mostly near the internal boundary.

An expansion of the variable radius r into a Fourier series [23] in terms of the functions (2.92) instead of (2.33) gives

$$r = r_0 \sum_{n=1}^{\infty} d_n R_n\left(\zeta_n \frac{r}{r_0}\right)$$

$$d_n = \frac{1 - \beta^2}{\zeta_n^2 - \nu - \beta^2 - \nu \zeta_n^2 \beta^2} \qquad (2.93)$$

On the basis of (2.16) - (2.19), (2.26), (2.31), (2.37), and (2.41), as well as in view of (2.92) and (2.93) we get

$$\psi = 2r_0 \sin\eta \sum_{n=1}^{\infty} d_n R_n\left(\zeta_n \frac{r}{r_0}\right) \times$$

$$\times \left\{ \left[-\frac{2r_0}{\zeta_n} \frac{\sin\left[\frac{\zeta_n}{r_0}\left(\frac{b}{2} + a\right)\right]}{\sin\left(\zeta_n \frac{b}{2r_0}\right)} + (\mu + \lambda) \right] \theta + \dot{\theta}_n \right\}, \qquad (2.94)$$

$$\varphi = 2r_0 \sin\eta \sum_{n=1}^{\infty} d_n R_n\left(\zeta_n \frac{r}{r_0}\right) \frac{\sin\left(\zeta_n \frac{b+a}{r_0}\right)}{\sin\left(\zeta_n \frac{b}{r_0}\right)} \dot{\theta}_n(t),$$

$$\Phi = \psi + \varphi.$$

where R_n and d_n can be determined using (2.92) and (2.93).

Values of d_n are also given in Table 2.1.

TABLE 2.1

β	n	ξ_n	a_n	γ_n	d_n
0	1	1,9412	1,710	—	0,4184
	2	5,3315	−2,000	—	0,0825
	3	8,5073	3,000	0	0,0139
0,1	1	1,9000	1,700	−0,0000	0,4126
	2	5,107	−2,700	−0,1002	0,0000
	3	8,100	3,200	−0,3000	0,0112
0,2	1	1,7000	1,007	−0,0004	0,3000
	2	4,002	−2,011	−0,0720	0,0004
	3	8,000	3,017	−0,1000	0,0002
0,3	1	1,002	1,000	−0,1005	0,2000
	2	5,100	−2,700	−0,1000	0,0707
	3	9,207	2,705	0,0044	0,0072

The equation for determining the generalized coordinate $\lambda_n(t)$ can be obtained from (2.24); it will then assume a form identical with (2.42):

$$\ddot{\lambda}_n+\omega_n^2\lambda_n=-L_n\ddot{\beta}-\ddot{y}_c+g\theta.$$

The formulas for the frequency ω_n of natural oscillations and coefficient L_n also remain the same as (2.43) and (2.44). The values of the eigenvalues ξ_n should be substituted into these formulas from Table 2.1.

The structure of the expressions for the potentials ψ and Φ is identical with the expressions (2.38) and (2.41). Therefore, the equations of motions of the tank with liquid will be analogous with

Equations (2.61). By comparing the values of ξ_n for $\beta = 0$ and $\beta \neq 0$ (see Table 2.1) we may conclude that the frequencies of the natural oscillations of the first few tones for a liquid in a circular cylindrical tank and a tank between two circular coaxial cylinders differ only slightly for small values of β.

9. Oscillations of a Liquid in a Cylindrical Tank with Radial Partitions

In order to reduce oscillations of a liquid, cylindrical tanks are often subdivided by means of radial and cylindrical partitions. Let us consider a tank formed by two circular coaxial cylinders and subdivided by means of radial partitions (Figure 2.17). The angular distance between the radial partitions will be denoted by $2\alpha a$, where α will vary in the interval $0<\alpha<1/2$. For example if the tank is subdivided into six equal sectors, then $\alpha = 1/6$. The position of the sector relative to the Oxz-plane will be defined by an angle $2\alpha\alpha_0$. The radius of the internal cylinder will be denoted by $\beta r_0 (0<\beta<1)$. We assume that the bottom of the tank is a plane, and that the liquid does not leak from one sector to another.

As in Section 3, it will be assumed that the container, partially filled with liquid, executes planar motion in the direction of the cooridnate axis Oy (2.16). The generalized coordinates, defining the motion of the tank, are shown in Figure 2.3. Following the assumptions and the procedure given in Section 3, we shall obtain the absolute velocity potential for the sectored tank shown in Figure 2.17.

The boundary conditions for determining potential Φ are the following:
on the internal and external cylindrical walls

$$\frac{\partial \Phi}{\partial r} = c_i^* \text{ for } r = r_0,\ r = \beta r_0. \tag{2.95}$$

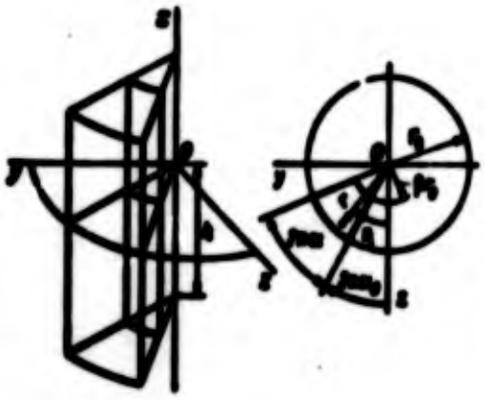

Figure 2.17

on the radial partitions

$$\frac{\partial \Phi}{\partial \eta} = v_\eta^* \text{ for } \eta = 2\pi\alpha_0,\ \eta = 2\pi(\alpha_0 + \alpha), \quad (2.96)$$

where v_r^* and v_η^* are the radial and normal velocity components of any point of the tank wall, the normal component being taken in the direction normal to a partition.

On the bottom of the tank and on the free surface the boundary conditions are expressed by (2.14) and (2.15)

From Figure 2.3 we have

$$\begin{aligned} v_r^* &= -[\dot{\beta}_c + (L + x)\dot{\theta}]\sin\eta, \\ v_\eta^* &= -[\dot{\beta}_c + (L + x)\dot{\theta}]\cos\eta. \end{aligned} \quad (2.97)$$

Let us make use of the method of solution applied earlier in Section 3. Then we shall find additional boundary conditions for the function $F(x, r, \eta)$

$$\frac{\partial \Phi}{\partial \eta} = 0 \text{ for } \eta = 2\pi\alpha_0,\ \eta = 2\pi(\alpha_0 + \alpha),\ r \neq 0. \quad (2.98)$$

In the case of the sectored tank, the potential function Φ is not periodic in the angle η, and thus in the solution

$$H(\eta) = \sin(m\eta + \eta_0)$$

the number m cannot be considered an integer. Using (2.26), and in view of the boundary condition (2.98) for the function H(η) we obtain

$$m\cos(m2\pi\alpha_0 + \eta_0) = 0,\quad m\cos[m2\pi(\alpha_0 + \alpha) + \eta_0] = 0.$$

Hence

$$m \neq 0, \quad m2\alpha_0 + \eta_0 = \frac{\pi}{2}, \quad \sin(m2\alpha) = 0,$$

$$m2\alpha = \nu\pi, \quad m = \frac{\nu}{2\alpha}, \quad \nu = 0, 1, 2, \ldots$$

Thus the function H(η) will be

$$H(\eta) = \sin\left[\frac{\nu}{2\alpha}(\eta - 2\alpha_0) + \frac{\pi}{2}\right] = \cos\frac{\nu}{2\alpha}(\eta - 2\alpha_0). \tag{2.99}$$

Since $m = \nu/2\alpha \neq 1$, the solution of Equation (2.29) will be

$$R_{\nu\alpha}(r) = J_{\nu\alpha}\left(\zeta_{\nu\alpha}\frac{r}{r_0}\right) + \gamma_{\nu\alpha}Y_{\nu\alpha}\left(\zeta_{\nu\alpha}\frac{r}{r_0}\right),$$

$$\gamma_{\nu\alpha} = -\frac{J'_{\nu\alpha}(\zeta_{\nu\alpha}\beta)}{Y'_{\nu\alpha}(\zeta_{\nu\alpha}\beta)} = -\frac{J'_{\nu\alpha}(\zeta_{\nu\alpha})}{Y'_{\nu\alpha}(\zeta_{\nu\alpha})}, \tag{2.100}$$

where $J_{\nu\alpha}$ and $Y_{\nu\alpha}$ are Bessel functions of first and second kind of a fractional $(\nu/2\alpha)$ order.

The values of $\zeta_{\nu\alpha}$ will be given as before by the roots of the equation

$$J'_{\nu\alpha}(\zeta_{\nu\alpha})Y'_{\nu\alpha}(\zeta_{\nu\alpha}\beta) - J'_{\nu\alpha}(\zeta_{\nu\alpha}\beta)Y'_{\nu\alpha}(\zeta_{\nu\alpha}) = 0. \tag{2.101}$$

The function F may now be written as

$$F = \sum_{\nu=0,1,2}^{\infty}\sum_{\alpha=1}^{\infty}\cos\left[\frac{\nu}{2\alpha}(\eta - 2\alpha_0)\right] \times$$

$$\times\left[C_{\nu\alpha}\operatorname{ch}\left(\zeta_{\nu\alpha}\frac{z}{r_0}\right) + B_{\nu\alpha}\operatorname{sh}\left(\zeta_{\nu\alpha}\frac{z}{r_0}\right)\right]R_{\nu\alpha}(r). \tag{2.102}$$

To be able to make use of the boundary conditions (2.21) and (2.36) we shall preliminarily expand r and sin η into the following series [29]:

$$\sin\eta = \sum_{\nu=0,1,2}^{\infty} a_\nu \cos\left[\frac{\nu}{2\alpha}(\eta - 2\alpha_0)\right],$$

$$r = r_0\sum_{\alpha=1}^{\infty} b_{\nu\alpha}R_{\nu\alpha}(r), \quad \nu = 0, 1, 2, \ldots \tag{2.103}$$

Using well-known rules of calculating the coefficients of expansion (used, for example, in Section 3), and taking into consideration the fact that the functions $R_{\nu s}(r)$ are orthogonal on the interval $[r_0, r_1]$, and the functions $\cos\left[\frac{\nu}{2\alpha}(\eta-2\alpha_0)\right]$ are orthogonal on $2\alpha(\alpha_0+\alpha)]$, we obtain

$$a_\nu=\frac{A_\nu^2}{B_\nu^2},\quad b_{\nu s}=\frac{D_{\nu s}^2}{N_{\nu s}^2}\ (\nu=0,1,2,\ldots;\ s=1,2,3,\ldots),$$

$$A_\nu^2=\int_{2\alpha_0}^{2(\alpha_0+\alpha)}\cos\left[\frac{\nu}{2\alpha}(\eta-2\alpha_0)\right]\sin\eta\,d\eta,$$

$$B_\nu^2=\int_{2\alpha_0}^{2(\alpha_0+\alpha)}\cos^2\left[\frac{\nu}{2\alpha}(\eta-2\alpha_0)\right]d\eta, \qquad (2.104)$$

$$D_{\nu s}^2=\int_{r_0}^{r_1}R_{\nu s}(r)r^2\,dr,$$

$$N_{\nu s}^2=\int_{r_0}^{r_1}R_{\nu s}^2(r)r\,dr\ (\nu=0,1,2,\ldots;\ s=1,2,3,\ldots)$$

In view of (2.103) we get

$$\left(\frac{\partial\Phi}{\partial z}\right)_{\substack{z=0\\ z=-h}}=-2r\sin\eta=-2r_0\sum_{\nu=0,1,2}\sum_{s=1}^{\infty}a_\nu b_{\nu s}R_{\nu s}(r)\times$$
$$\times\cos\left[\frac{\nu}{2\alpha}(\eta-2\alpha_0)\right].$$

From the equality obtained and (2.102) it follows that

$$\left(\frac{\partial K_{\nu s}}{\partial z}\right)_{\substack{z=0\\ z=-h}}=2r_0a_\nu b_{\nu s}.$$

Then

$$X_{\nu s}=-\frac{2r_0^2}{\zeta_{\nu s}}\frac{\operatorname{sh}\left[\frac{\zeta_{\nu s}}{r_0}\left(\frac{h}{2}+z\right)\right]}{\operatorname{ch}\left(\zeta_{\nu s}\frac{h}{2r_0}\right)}. \qquad (2.105)$$

Combining these results, we obtain the potential ψ in the form

$$\psi=r_0\sum_{\nu=0,1}\sum_{s=1}^{\infty}a_\nu b_{\nu s}R_{\nu s}\cos\left[\frac{\nu}{2\alpha}(\eta-2\alpha_0)\right]\times$$
$$\times\left\{\left[-\frac{2r_0}{\zeta_{\nu s}}\frac{\operatorname{sh}\left[\frac{\nu}{2\alpha}\left(\frac{h}{2}+z\right)\right]}{\operatorname{ch}\left(\zeta_{\nu s}\frac{h}{2r_0}\right)}+(L+x)\right]\delta+\dot{y}_C\right\}. \qquad (2.106)$$

Now let us find the function φ_* which should be a solution of Laplace's equation, and should satisfy the zero boundary conditions on all walls of the tank. Let

$$\varphi_* = \sum_{\nu=0,1}^{\infty} \sum_{n=1}^{\infty} c_{\nu n} X_{\nu n}(x) R_{\nu n}(r) H(\eta).$$

Using the previously obtained formulas (2.99) and (2.100), keeping in mind the boundary conditions (2.40), and setting $c_{\nu n} = a_{\nu} b_{\nu n}$, we obtain

$$\varphi_* = r_0 \sum_{\nu=0,1}^{\infty} \sum_{n=1}^{\infty} a_{\nu} b_{\nu n} R_{\nu n}(r) \cos\left[\frac{\nu}{2\pi}(\eta - 2\pi\alpha_0)\right] \times \times \frac{\operatorname{ch}\left(\zeta_{\nu n}\frac{z+h}{r_0}\right)}{\operatorname{ch}\left(\zeta_{\nu n}\frac{h}{r_0}\right)} \lambda_{\nu n}(t). \tag{2.107}$$

With such a choice of the coefficient $c_{\nu n}$, the equations for $\lambda_{\nu n}$ will assume the simplest possible form.

Now let us use the condition (2.24). Substituting (2.106) and (2.107) into (2.24), and comparing terms with the same indices we obtain the following equations for the generalized coordinates $\lambda_{\nu n}$:

$$\ddot{\lambda}_{\nu n} + \omega_{\nu n}^2 \lambda_{\nu n} = -L_{\nu n}\ddot{\theta} - \ddot{y}_C + g\theta \quad (\nu = 0, 1, 2, \ldots;\ n = 1, 2, \ldots), \tag{2.108}$$

where

$$\omega_{\nu n} = \sqrt{\frac{\zeta_{\nu n} g}{r_0} \operatorname{th}\left(\zeta_{\nu n}\frac{h}{r_0}\right)},$$
$$L_{\nu n} = L\left[1 - \frac{2r_0}{\zeta_{\nu n} L} \operatorname{th}\left(\zeta_{\nu n}\frac{h}{2r_0}\right)\right]. \tag{2.109}$$

The structure of these equations is the same as that of Equations (2.42) which apply to the usual circular tank. The formulas for the frequency $\omega_{\nu n}$ of the natural oscillations of a liquid, and the distance $L_{\nu n}$ between the axis of rotation and the center of reduced mass are also analogous to the formulas in (2.43) and (2.44). However, for the same value of the external radius r_0 of the tank the frequency of

the natural oscillations of the liquid here may be higher than for a tank without partitions.

The oscillations of a liquid in a sectored tank are represented by a double series. The index n characterizes the wave number in the radial direction, the index ν corresponds to the wave number in the direction along the circumference. The values of the root $\zeta_{n\nu}$ are associated with waves in strictly radial direction, since for $\nu = 0$ the function $H(\eta)=1$. The values of roots for $\nu \neq 0$ are associated with waves both in the circumerential and radial directions. As implied by (2.99), even ν are associated with waves that are symmetric relative to the plane of symmetry of a sector, and odd ν — with antisymmetric waves.

TABLE 2.2

$a=1/4$

n	β	ν=0			ν=1			ν=2		
		$\zeta_{n\nu}$	$\gamma_{n\nu}$	$\Delta_{n\nu}$	$\zeta_{n\nu}$	$\gamma_{n\nu}$	$\Delta_{n\nu}$	$\zeta_{n\nu}$	$\gamma_{n\nu}$	$\Delta_{n\nu}$
1	0	3.0000	0	0.4996	3.054	0	2.000	5.317	0	4.017
	0.1	3.041	0.1071	0.4142	3.055	−0.0020	2.005	5.317	−10⁻⁴	4.011
	0.2	4.300	0.4178	0.3333	3.065	−0.0136	2.020	5.317	−10⁻³	4.008
	0.3	4.700	1.155	0.2632	3.088	−0.0645	2.042	5.318	−0.0026	4.005
	0.4	5.301	26.38	0.2026	3.043	−0.1509	1.943	5.322	−0.0084	4.003
	0.5	6.000	−0.7000	0.2679	2.681	−0.2214	1.842	5.175	−0.0068	4.040
2	0	7.016	0	−0.0000	6.706	0	−0.4000	9.000	0	−1.000
	0.1	7.021	0.0004	−0.0004	6.007	−0.0183	−0.4020	9.000	−10⁻⁴	−1.000
	0.2	8.000	1.0707	−0.0010	6.405	−0.7015	−0.4074	9.270	−0.0000	−1.000
	0.3	9.104	−1.005	−0.0021	6.274	−0.4301	−0.2943	9.152	−0.1178	−1.007
	0.4	10.55	0.4078	−0.0004	8.418	−0.2799	−0.1562	8.002	−0.4014	−1.000
	0.5	12.02	−0.8379	−0.0002	7.0020	0.3509	−0.0002	8.856	−0.4180	−0.0000
3	0	10.17	0	0.0001	9.000	0	0.2542	12.00	0	0.0000
	0.1	10.75	0.6451	0.0004	9.007	−0.0001	0.2531	12.00	−10⁻⁴	0.0002
	0.2	11.00	−5.502	0.0070	9.540	−0.4337	0.1812	12.01	−0.0070	0.0010
	0.3	13.55	0.2251	0.0200	9.910	−0.0502	0.0000	12.24	−0.4412	0.0010
	0.4	15.77	−0.0477	0.0241	11.05	1.705	0.0000	12.00	−0.1720	0.0000
	0.5	18.00	−0.0001	0.0200	12.05	−0.2214	0.0183	13.00	2.307	0.1074

The forms of waves and the frequencies of oscillations associated with them depend on the location of a sector with respect to the plane of oscillations. Thus, for example, if the tank moves in the Oxy-plane in Sectors 3 and 7 (Figure 2.18) the oscillations will be in the radial direction, and their frequency will depend on the linear dimension $r_0(\beta-\beta)$. In sectors 1 and 5 oscillations will occur in the direction along the circumference, and their natural frequency will depend on the linear distance between the radial partitions. With β and α small, the linear distance in sectors 3 and 7 is larger than in sectors 1 and 5. Therefore, the lowest natural frequency in sectors 3 and 7 will be smaller than in sectors 1 and 5.

If the sectored tank is arbitrarily oriented with respect to the plane of oscillations, the oscillations will occur in both the radial direction and around the circumference. This phenomenon will be observed in sectors 2, 4, 6, and 8.

The effect that the dimensions of a sector have on the frequency of the natural oscillations has been accounted for in (2.108) by means of an eigenvalue ξ_m.

For sectors in the form of circular quadrants ($\alpha=1/4$) the eigenvalues ξ_m, calculated from Equation (2.101), have been given in Table 2.2 for several values of β; the coefficients θ_m and ν_m are also shown here.

If the tank has a circular or annular cross section ($\alpha=1$), and also if the tank is subdivided by means of a partition lying in the Oxy-plane (i.e., $\alpha=1/2$), then the expansion of sin η into the series (2.103) becomes an identity. The double sums in (2.106) and (2.107) become single sums over n, and for m = 1, these expressions will assume the forms (2.38) and (2.41).

Now let us calculate the pressure of the liquid on the walls of the tank. The method of doing that was discussed in Section 4. Here we shall, however, consider the additional peculiarities due to the radial partitions.

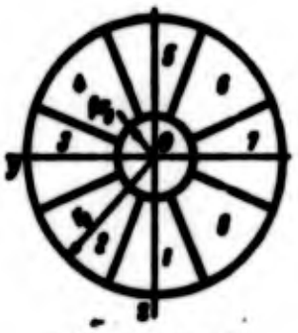

Figure 2.18

For one i^{th} sector, shown in Figure 2.19, the Oy-component of the pressure forces on the immersed walls will be

$$F_{yi}=\int_{x_0}^{x_0}\int_{-a}^{0}[(p)_{\eta=\eta_0}-(p)_{\eta=\eta_0+\alpha}]r_0\sin\eta\,d\eta\,dx+$$

$$+\cos\eta_0\int_{x_0}^{x_0}\int_{-a}^{0}(p)_{\eta=\eta_0}\,dr\,dx-\cos\eta_1\int_{x_0}^{x_0}\int_{-a}^{0}(p)_{\eta=\eta_0}\,dr\,dx. \quad (2.110)$$

$$[\eta_1=2\pi-\eta_0;\ \eta_0=2\pi-(\eta_0+\alpha)].$$

The pressure of liquid p can be calculated using (2.47), and the functions ψ and φ can be determined from (2.106) and (2.107).

The Oy-component of the forces acting on all sectors of the tank is

$$F_y=\sum_{i=1}^{k}F_{yi} \quad (2.111)$$

where k is the number of sectors in the tank.

The moment of force, produced by oscillations of liquid in any sector relative to the transverse axis passing through point C is

$$M_{zi}=\int_{x_0}^{x_0}\int_{-a}^{0}(p)_{\eta=\eta_0}(L+r_0\sin\eta+x)r_0\sin\eta\,d\eta\,dx-$$

$$-\int_{x_0}^{x_0}\int_{-a}^{0}(p)_{\eta=\eta_0+\alpha}(L+r_0\cos\eta+x)r_0\sin\eta\,d\eta\,dx+$$

$$+\cos\eta_0\int_{x_0}^{x_0}\int_{-a}^{0}(p)_{\eta=\eta_0}(L+r\sin\eta+x)\,dr\,dx-$$

$$-\cos\eta_1\int_{x_0}^{x_0}\int_{-a}^{0}(p)_{\eta=\eta_0}(L+r\sin\eta+x)\,dr\,dx+$$

$$+\int_{x_0}^{x_0}\int_{\eta_0}^{\eta_1}(p)_{x=x^0}r^2\sin\eta\,dr\ [\eta_1=2\pi-\eta_0;\ \eta_0=2\pi-(\eta_0+\alpha)].$$

Here the lower limit of the variable x is the same as in Section 3, namely

$$x_0^0=-h-r_0\sin\eta_0,\ x_{00}^0=-h-r_0\sin\eta_0,$$

$$x^0=-h-r\sin\eta.$$

The moment produced by the oscillations of liquid in all sectors is

$$M_C = \sum_{i=1}^{N} M_{Ci} \tag{2.113}$$

In view of (2.110) and (2.112), and also taking into consideration (2.9), (2.18), (2.104), (2.106), and (2.107), the force $F_{y\Sigma}$ and the moment $M_{C\Sigma}$ acting on the sectored tank and determined by the oscillations of the free surface may be written as

$$\begin{gathered} F_{y\Sigma} = -\sin^2\varphi_{1i}\sum_{n=1}^{\infty}\sum_{i=1}^{N} m_n\ddot{\lambda}_n - \cos^2\varphi_{1i}\sum_{n=1}^{\infty}\sum_{i=1}^{N} m_n\ddot{\lambda}_n \\ M_{C\Sigma} = -\sin^2\varphi_{1i}\sum_{n=1}^{\infty}\sum_{i=1}^{N}(m_n l_n\ddot{\lambda}_n - g m_n\lambda_n) - \\ -\cos^2\varphi_{1i}\sum_{n=1}^{\infty}\sum_{i=1}^{N}(m_n l_n\ddot{\lambda}_n - g m_n\lambda_n) \end{gathered} \tag{2.114}$$

Here

$$\varphi_{1i} = 2\pi(\alpha_{1i} + \alpha/2)$$

is the angle between the Oz-axis and the plane of symmetry of the i^{th} sector (Figure 2.19).

Each term of the sum in the formula for $F_{y\Sigma}$ forms a product of the reduced mass m_n of the oscillating liquid and the generalized acceleration $\ddot{\lambda}_n$. Each tone number is associated with its own mass m_n, and own acceleration $\ddot{\lambda}_n$. The moment of force relative to the transverse axis passing through point C is composed of the moment of the hydrodynamic forces, proportional to $\ddot{\lambda}_n$, and the moment of the hydrostatic forces due to the deflections of the free surface and proportional to λ_n.

From the point of view of the analogy with pendulums, the formulas (2.114) can be given a physical interpretation. If these formulas are compared with the formulas for F_y^0 and M_c^0 from Section 5, we can make the conclusion that the mechanical model of the oscillations of liquid in a sectored tank involves two groups of mathematical pendulums.

The plane of oscillations of one group of pendulums coincides with the plane of symmetry of the sectored tank (see Figure 2.19). These pendulums correspond to symmetric oscillations in the direction around the circumference ($\nu = 0, 2, 4, \ldots$). In this the projection of the hydrodynamic forces applied to the immersed surface coincides with the plane of symmetry of the sectored tank.

The plane of oscillations of the second group of pendulums is perpendicular to the plane of symmetry of the tank (see Figure 2.19). These pendulums are a mechanical analog of antisymmetric oscillations in the direction around the circumference ($\nu = 1, 3, 5, \ldots$), in which the projections of the hydrodynamic forces are perpendicular to the plane of symmetry of the tank.

The forces arising in the plane of symmetry $q = q_{\omega} = \Omega \times (a_{\omega} + \dot{a}/\Omega)$ and in the plane perpendicular to it, have projections on the Oy-axis that are proportional to $\sin \varphi_{\omega}$ and $\cos \varphi_{\omega}$, respectively. The additional factors $\sin \varphi_{\omega}$ and $\cos \varphi_{\omega}$ appeared as a result of coefficients involved in the decomposition of q (see Formulas 9 - 14 at the end of the chapter). These factors are hence not included in the expression for the reduced masses m_{ω}, and as a result the reduced masses do not depend on the location of a sector relative to the plane of forced oscillations of the tank.

The total force F_{Φ}^{0} and the total moment M_{Φ}^{0} may be obtained on the basis of (2.111) and (2.113). Using (2.114) the summation is done only with respect to $\sin \varphi_{\omega}$, and $\cos^2 \varphi_{\omega}$.

We set

$$A = \sum_{i=1}^{k} \sin^2 \varphi_{0i}, \quad B = \sum_{i=1}^{k} \cos^2 \varphi_{0i}.$$

For example, if we take $k = 4$ and $\alpha_{01} = 0$, we obtain:

$$\alpha = 1/4, \ \varphi_{02} = 1/4, \ \varphi_{03} = 1/2, \ \varphi_{04} = 3/4,$$
$$\varphi_{05} = \pi/4, \ \varphi_{06} = 3\pi/4, \ \varphi_{07} = 5\pi/4, \ \varphi_{08} = 7\pi/4$$

and the coefficients A = B = k/2 = 2.

Applying the techniques discussed in Section 5 we shall set up the equations of motion for a tank subdivided by means of radial partitions.

Let the mass of the entire liquid be m. We obtain

$$\begin{gathered}
m\ddot{y}_C - m\left(l - \frac{h}{2}\right)\ddot{\theta} - A\sum_{\nu=0}^{\infty}\sum_{s=1}^{\infty} m_{\nu s}\dot{\lambda}_{\nu s} - B\sum_{\nu=1}^{\infty}\sum_{s=1}^{\infty} m_{\nu s}\dot{\lambda}_{\nu s} = F_0, \\
I\ddot{\theta} - m\left(l - \frac{h}{2}\right)\ddot{y}_C - A\sum_{\nu=0}^{\infty}\sum_{s=1}^{\infty}(m_{\nu s}l_{\nu s}\dot{\lambda}_{\nu s} - g m_{\nu s}\lambda_{\nu s}) - \\
- B\sum_{\nu=1}^{\infty}\sum_{s=1}^{\infty}(m_{\nu s}l_{\nu s}\dot{\lambda}_{\nu s} - g m_{\nu s}\lambda_{\nu s}) = M_C, \\
\ddot{\lambda}_{\nu s} + \omega_{\nu s}^2\lambda_{\nu s} = -l_{\nu s}\ddot{\theta} - \ddot{y}_C + g\theta \quad (\nu = 0, 1, 2, \ldots;\ s = 1, 2, \ldots).
\end{gathered} \tag{2.115}$$

Here

$$I = I_0 - A\sum_{\nu=0}^{\infty}\sum_{s=1}^{\infty} l_{\nu s} - B\sum_{\nu=1}^{\infty}\sum_{s=1}^{\infty} l_{\nu s}$$

and I_0 — is the moment of inertia of the "frozen" liquid relative to the transverse axis passing through point C.

In the case of a tank subdivided into sectors, the frequencies of the natural oscillations $\omega_{\nu s}$ (and the reduced masses $m_{\nu s}$) for low tones may be close. Therefore, here one should not limit himself to considering only the first tone of oscillations. Usually in the equations of motion one takes into account the lower two or three tones.

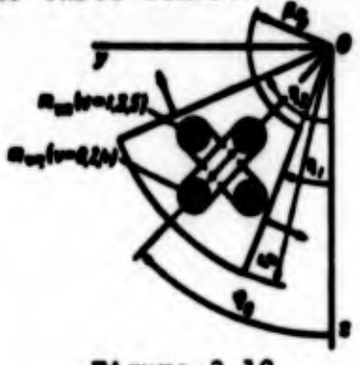

Figure 2.19

Oscillations of a liquid in a circular cylindrical tank with radial partitions are discussed also in [11, 28, 29].

10. Use of Variational Methods in Solving the Problem of the Oscillations of a Liquid

In Section 6 we noted that the equations of the perturbed motion and the equations of a pendulum as a model for the oscillations of a liquid do not depend on the form of the tank.

If the problem of the oscillations of a liquid in a tank can be solved using Fourier methods, then the pendulum parameters and the coefficients in the equations of perturbed motion will become known. However, this method allows us to solve the problem of the oscillations of a liquid only for very few forms of tanks. For example, for spherical, toroidal, and conical tanks it is impossible to obtain a solution using Fourier methods.

In order to solve the problem of the oscillations of a liquid in a tank of arbitrary shape the variational methods are widely used [19, 28]. Digital computers are needed, however, to be able to apply these methods.

A tank, partially filled with an ideal liquid, represents a conservative system to which we shall apply the Hamilton-Ostrogradskiy principle. The action integral according to Hamilton is

$$J=\int_{t_0}^{t_1} \mathcal{L}\,dt, \qquad (2.116)$$

where $\mathcal{L}$ is the Lagrangian

$$\mathcal{L}=T-U.$$

Here T, U, are the kinetic and potential energies of the liquid. According to Hamilton's principle for real motion, the action integral (2.116) assumes a stationary value, i.e., the variation $\delta J = 0$.

In [19] it is shown that the action integral as introduced by Hamilton differs by a constant factor $\rho/2\omega$ from the functional

$$F(\varphi)=g\int_V(\nabla\varphi)^2dV-\omega^2\int_S\varphi^2dS, \tag{2.117}$$

where ω is the natural frequency of oscillations; V, S, are the volume and the area of the free surface of the liquid in an unperturbed state; ∇ is the gradient operator

$$\nabla=\frac{\partial}{\partial x}\mathbf{I}+\frac{\partial}{\partial y}\mathbf{J}+\frac{\partial}{\partial z}\mathbf{K},$$

where $\mathbf{I}$, $\mathbf{J}$, $\mathbf{K}$ are unit vectors.

Thus, the problem of the natural oscillations of a liquid in volume V reduces to a variational problem for the functional (2.117). To solve this problem it is convenient to use Ritz's method. The idea of the method consists in the following.

Let us choose a system of coordinate functions φ_n, complete in volume V, where completeness is defined with respect to energy convergence [20]. The solution of the problem will be sought in the form of a finite sum

$$\varphi=\sum_{n=1}^{k}a_n\varphi_n.$$

If this sum is substituted in the functional (2.117), the latter is converted into a function of k variables

$$F(a_1,\ldots,a_k)=g\sum_{n,m=1}^{k}b_{nm}a_na_m-\omega^2\sum_{n,m=1}^{k}c_{nm}a_na_m.$$

From the conditions for an extremum of $F(a_1, \ldots, a_k)$ we obtain k homogeneous equations from which we can determine the unknowns a_1, $\ldots$, a_k

$$g\sum_{m=1}^{k}b_{sm}a_m-\omega^2\sum_{m=1}^{k}c_{sm}a_m=0\quad(s=1,2,\ldots,k). \tag{2.118}$$

In order for the homogenous system to have a nonzero solution, it is necessary and sufficient that the determinant of the system be equal to zero.

$$|\varepsilon p_{mn} - \sigma^2 q_{mn}|_{n,m=1}^{k} = 0.$$

By solving this equation, one can determine the first k natural frequencies of the oscillations of a liquid. To each natural frequency there corresponds a solution of the system (2.118) which gives us the n^{th} mode of the natural oscillations. Both the natural frequency and the natural mode can be determined from this approximation. For $k \to \infty$ the solution will become exact.

We use the results obtained with the aid of the variational method by B. I. Rabonovich, L. V. Dokuchayev, Z. M. Polyakova [28]. The coefficients in the equations of perturbed motion are in that work expressed in terms of some parameters $\tilde{\omega}_n, \nu_n, \nu_{0n}$ and p_n. These parameters are for each tank dimensionless and are related to the coefficients of Equations (2.88) by the following formulas:

$$\omega_n^2 = \tilde{\omega}_n^2 \frac{g}{r_0},$$
$$m_n = \rho r_0^3 \frac{\nu_n^2}{p_n}, \qquad (2.119)$$
$$l_{(2)n}^{*} = r_0 \sqrt{\frac{\nu_{0n}^2}{p_n} \frac{p_n}{\nu_n^2}} = r_0 \frac{\nu_{0n}}{\nu_n}.$$

Here ρ is the density of the liquid, r_0 is the characteristic dimension of a cavity, $l_{(2)n}^{*}$ is the distance between the suspension point of the pendulum and a certain characteristic point 0 of the cavity, namely, the center of the reduced mass (see Figure 2.20).

Figures 2.20 and 2.21 show plots of the natural frequencies, and the reduced masses of the liquid versus the submerged height h for a cavity between two coaxial circular tanks with toroidal bottoms. In the calculation it is assumed that the radius of the external tank $r_0 = 1$, the radius of the internal tank $r_0\beta = 0.4$, the radius of curvature of the bottom in the diametral plane $R = 0.3$. The dotted line in Figure 2.21 corresponds to the coefficients calculated for

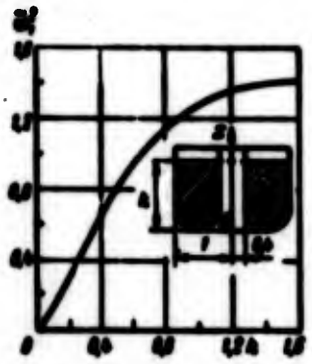

Figure 2.20

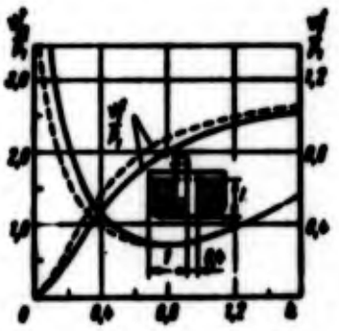

Figure 2.21

the coaxial tanks with a flat bottom. The plots show clearly how fast the effect of the toroidal bottom diminishes as the depth of the liquid increases.

Figures 2.22 - 2.24 present values of the natural frequencies $\bar{\omega}_i$ and the reduced masses of the oscillating liquid m_n [expressed according to (2.119) in terms of the quantity v_n^2/β_n] for toroidal cavities with various values of β (here β is the ratio of the internal radius of a torus to the external one). The maximum depth of the liquid for each value of β is $h_{max} = 1 - \beta$

Figure 2.25 shows the results of calculations for a spherical cavity. The solid line corresponds to the values obtained using the variational method involving the spherical Legendre functions. The dot-dash line corresponds to values obtained by the variational method and involving Bessel's functions. The dotted line gives values obtained for a tank with a flat bottom; the radius of the tank is equal to the radius of the liquid surface.

Figure 2.26 gives results of the calculation of coefficients for a conical tank with a large submerged height. The dotted lines correspond to the circular cylindrical tank whose radius is equal to the radius of the free surface, and the submerged height is considerably larger than the radius.

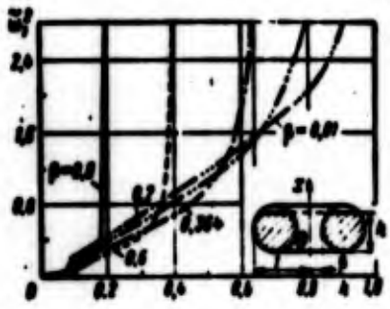

Figure 2.22

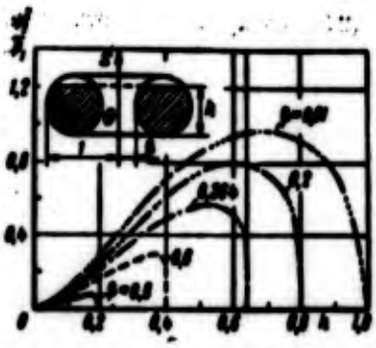

Figure 2.23

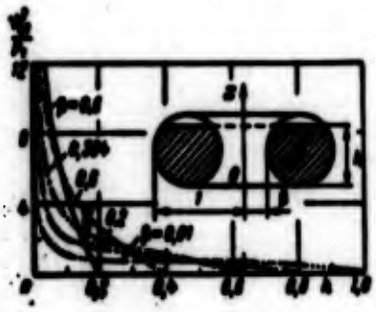

Figure 2.24

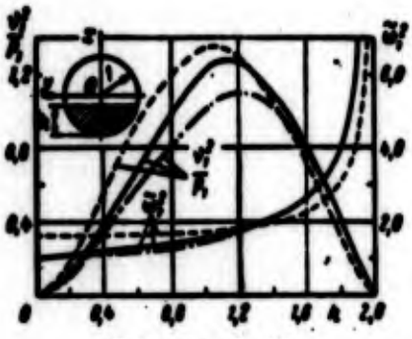

Figure 2.25

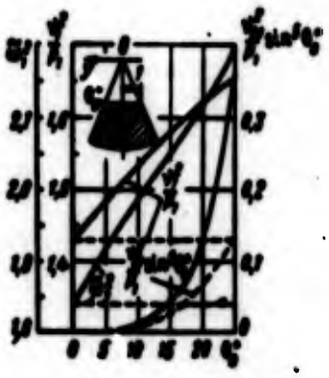

Figure 2.26

11. Some Results of an Experimental Study of the Oscillations of a Liquid

The experimental investigation of the oscillations of a liquid is desirable both to verify the initial assumptions used in analytical solutions, and to determine the values of the coefficients appearing in the differential equations of perturbed motion, which are impossible to determine theoretically because of the complexity of the tank form or for any other reason.

In Equations (2.88) we have four unknown coefficients: ω_n — which is the natural frequency of the oscillations of the liquid in a tank, $L^*_{(2)n}$ — which denotes the distance between the axis of the suspension of a pendulum and a certain characteristic point, namely the center of reduction, m_n — which stands for the reduced mass of the oscillating liquid, and $I=I_0+\sum_{n=1}^{\infty} I_{(2)n}$ — which is the moment of inertia of the liquid. To simplify the treatment of the obtained data, it is advisable to conduct the experiment in such a way that in each case one has to consider the oscillations of only one partial system: 1) oscillations of a tank for $\vartheta=0$ and 2λ oscillations of the tank for $y_{C^*} \equiv 0$ relative to the transverse axis passing through the metacenter (point C*) of the system tank-liquid.

Considering only the first tone of the oscillations of the liquid, we have

$$m\ddot{y}_{C^*}+m_1\ddot{\lambda}_{(2)1}=F_p, \tag{2.120}$$

$$\ddot{\lambda}_{(2)1}+\omega_1^2\lambda_{(2)1}+\ddot{y}_{C^*}=0,$$

$$I\ddot{\vartheta}+m_1L^*_{(2)1}\ddot{\lambda}_{(2)1}=M_{C^*}, \tag{2.121}$$

$$\ddot{\lambda}_{(2)1}+\omega_1^2\lambda_{(2)1}+L^*_{(2)1}\ddot{\vartheta}=0.$$

Here m is the mass of the tank including the liquid; I is the moment of inertia of the tank with the added liquid.

The coefficients of the equations can be determined in various ways: by measuring the forces and moments acting on the tank from

the side of the liquid, by analyzing the relationships between the amplitudes of the oscillations of the liquid and the walls of the tank, by measuring the frequencies of the partial system, corresponding to the translational and rotational movement of the cavity. The last technique is described in [15]. Let us explain it briefly.

The translational oscillations of a tank, described by Equations (2.120), can be practically realized by means of an experimental setup sketched in Figure 2.27. A tank in a vertical position is

Figure 2.27

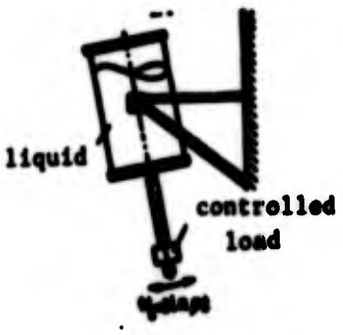

Figure 2.28

mounted on a sufficiently rigid and light frame which in turn is hinged at two points to a fixed base. We may consider that for small angles of rotation of the frame the tank executes a translational movement.

The rotational oscillations of a tank, described by Equations (2.121), can be reproduced by means of a setup shown in Figure 2.28. The axis of rotation of the tank passes through the metacenter (point C*) of the tank-liquid system.

Each of the partial systems (2.120) and (2.121) has one non-trivial natural frequency. Let this frequency be denoted by ω_1^* for the first system, and by ω_2^* for the second one. For the natural frequencies, we can obtain from Equations (2.120) and (2.121) the following relationships:

$$\frac{\omega_1^2}{\omega^2} = 1 - \left(\frac{\omega_1}{\omega}\right)^2. \qquad (2.122)$$

$$\frac{\omega_2^2}{\omega^2} = 1 - \left(\frac{\omega_2}{\omega}\right)^2. \qquad (2.123)$$

The frequencies of the partial systems ω_1^0, ω_2^0, can be determined by recording the free oscillations of the tank with liquid in a translational motion, and in rotation about the metacenter, respectively. The frequency of the natural oscillations of liquid, ω_1, can be determined by recording free damped oscillations of the liquid in a fixed tank or by using the resonance method.

Thus, the right hand sides of the equalities in (2.122) and (2.123) can be found experimentally. If the moment I is known, then from these equalities one can determine the coefficients m_1 and $L^0_{(2)1}$. The moment of inertial I can be determined experimentally if in addition we introduce the angular rigidity into the setup (see Figure 2.28).

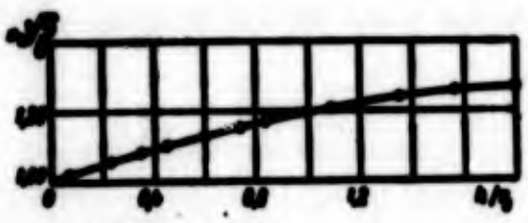

Figure 2.29

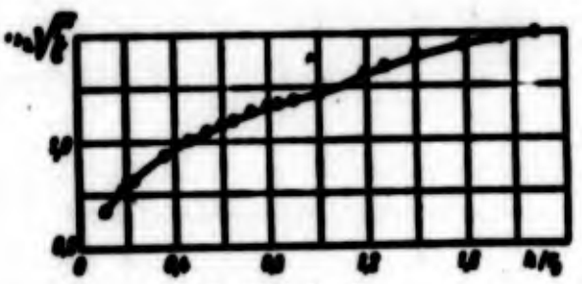

Figure 2.30

In Figure 2.29, we present for a cylindrical tank with a spherical bottom (radius of the sphere being equal to the radius of the cylinder), and in Figure 2.30 for a spherical tank, the relationships obtained experimentally [14] between the natural frequencies of the principal tone, ω_1, and the submerged height h/r_0. In the case of a spherical tank, h is the total depth of the liquid, and in the case of a cylindrical tank, h is the submerged height of the cylindrical portion of the tank. By r_0 we mean the radius of the cylinder and the radius of the sphere; r^0 denotes the radius of the free surface.

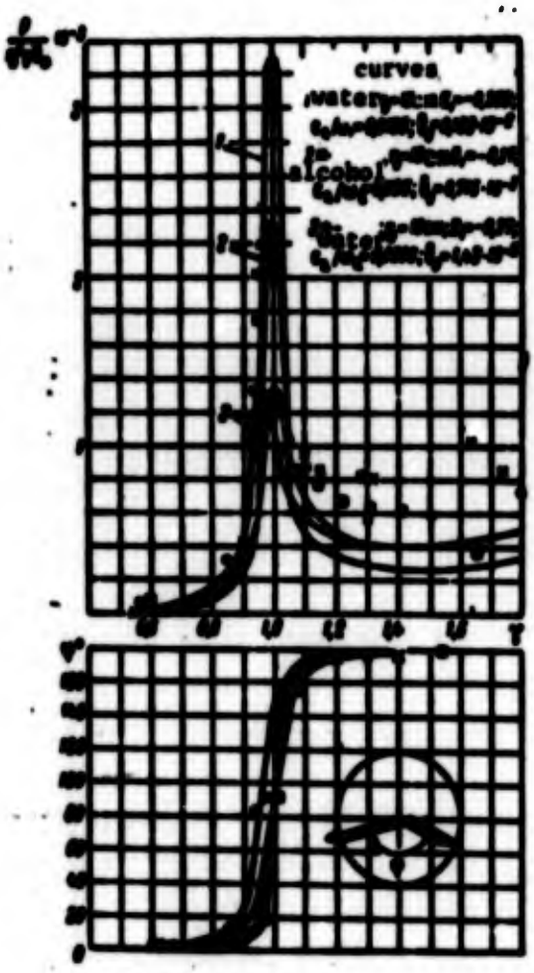

Figure 2.31

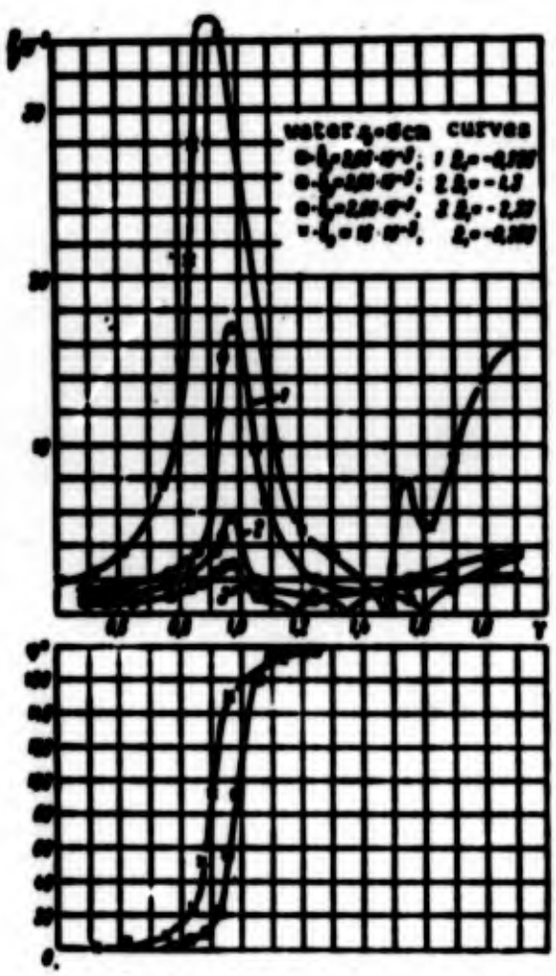

Figure 2.32

Just as any real system, the liquid does not turn out to be ideal, and the forces of friction appear in motion. Therefore, at resonance the amplitude of the oscillations of the liquid remains finite. We can convince ourselves of the presence of frictional forces in the liquid by observing its natural oscillations.

Figures 2.31 and 2.32 show the amplitudes of the hydrodynamic pressure of a liquid (water and alcohol) on the walls of a cylindrical circular tank versus the dimensionless frequency of forced oscillations, $\gamma=\beta/\omega_1$. The variation of the phase φ of this pressure with respect to the motion of the tank is also shown therein. On the ordinate axes we plot the ratio of the pressure p to the density of the liquid, ρ, for $\eta=a/2$. The experiment was done on a kinematic stand, and the motion of the tank was plane-parallel in accordance with the harmonic law $y_c = y_0 \sin pt$. Pressure sensors were located at a distance $\bar{x}_1 = x_1/r_0$. The experiment was repeated with various amplitudes $\bar{\delta}_0=y_0/r_0$ of the motion of the tank.

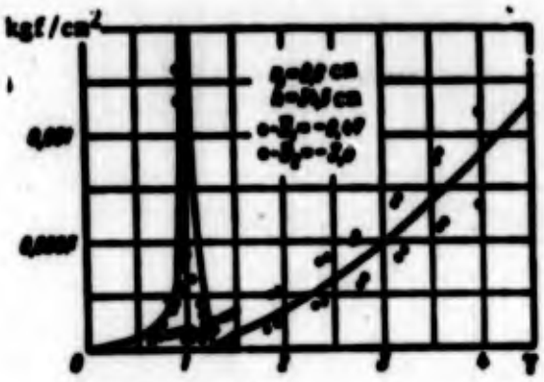

Figure 2.33

Figure 2.31 shows the theoretical resonance curves for various values of the relative damping coefficient $\beta=\varepsilon/\omega_1$. The curve 3 was plotted in two versions — with the frictional forces taken, and not taken, into consideration as far as their effect on the frequencies of the natural oscillations is concerned.

The distribution of the hydrodynamic pressure as a function of the depth of the liquid with $\bar{\delta}_0=2.86\cdot10^{-3}$ is given in Figure 2.32. The hydrodynamic pressure rapidly diminishes as one recedes from the free surface of the liquid.

Figure 2.33 shows a plot of the pressure for a large range of the frequencies of the forced oscillations of a tank, obtained with an amplitude $\bar{\delta}_0=5.8\cdot10^{-3}$.

The experimental study leads us to conclude that the resonance corresponding to the principal tone of the oscillations is one which is most essential. The pressure of liquid on the walls under the conditions of the second resonance differs only slightly from the pressure of the "frozen" liquid.

The pressure of liquid on the walls at second resonance is considerably smaller than at first one. According to (2.62) for the second tone, the reduced mass of the oscillating liquid constitutes only 3% of the mass for the first tone. Therefore, in some practical calculations the oscillations of the higher tones can be neglected.

The maximum displacement of the free surface of the liquid in the direction of the longitudinal axis of the tank, just as the maximum pressure of the liquid on the walls of the resonance of the first tone is bounded, which indicates the presence of the frictional forces, arising in the oscillations of the liquid. The plot of the hydrodynamic pressure as a function of the frequency of oscillations is the same as the plot of the motion of a mass suspended from a spring (or a mathematical pendulum) for small coefficients of the viscous friction.

In practical calculations, the forces of friction in a liquid can be calculated in a comparatively simple fashion . Limiting ourselves to a linear formulation of the problem, and using the analogy with a one-mass oscillating system, we can add to the lefthand side of the equation of the oscillations of the liquid (2.42), a term proportional to the speed $2\varepsilon_n\dot{\lambda}_n$, and determine the proportionality coefficient ε_n experimentally.

Thus, instead of Equation (2.42), for the first tone of the oscillations of liquid in a tank we shall have

$$\ddot{\lambda}_1+2\varepsilon_1\dot{\lambda}_1+\omega_1^2\lambda_1=-L_1\ddot{\theta}-\ddot{r}_c+g\theta. \qquad (2.124)$$

Here α_1 and ω_1 denote values of the damping coefficient and the frequency of the natural oscillations of first tone, respectively.

The damping coefficient α_1 can be determined by analyzing the natural oscillations of liquid in a stationary tank. For this purpose it is necessary to set up oscillations of the first tone in the free surface, and plot a graph of the amplitude of oscillations as a function of time.

A detailed experimental study of the free oscillations of the liquid was made by the authors of [14].

Let the logarithmic decrement of oscillations be denoted by δ. If the damping coefficients are small, the relationship between the logarithmic decrement and the value of the damping coefficient α_1 can be expressed by the formula

$$\frac{\alpha_1}{\omega_1} = \frac{\delta}{2\pi}.$$

The relationships between the logarithmic decrement δ and the relative depth of the liquid h/r_0, obtained experimentally for the first tone of oscillations, are shown in Figure 2.34 for a cylindrical tank with a spherical bottom (radius of the sphere is equal to the radius of the cylinder), and in Figure 2.35 for a spherical tank [14]. We assume that

$$\delta = C_1 \frac{1}{\sqrt{\mathrm{Re}}}, \quad \mathrm{Re} = \frac{\omega r^2}{\nu}, \quad \omega_1 = \sqrt{\frac{1.84g}{r_0}},$$

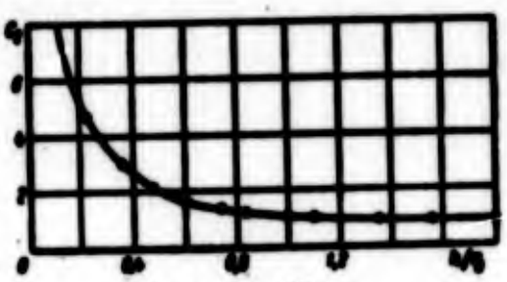

Figure 2.34

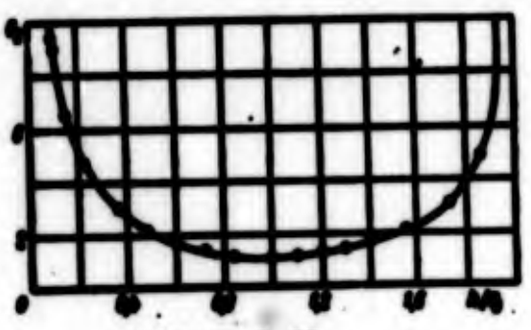

Figure 2.35

Here ν_0 is the coefficient of the kinematic viscosity of the liquid; Re is the Reynolds number.

When the height of the liquid column is less than the radius of the tank, the logarithmic decrement increases as the height of the column is lowered.

In estimating the experimentally obtained logarithmic decrements δ, we have to keep in mind that the damping coefficient depends on the material of the tank and the quality of finish on the submerged surface. This dependence is especially important for tanks with small cross sections. The surface tension increases the damping coefficient for small tank radii, but for larger radii its influence is insignificant.

The damping coefficient for the oscillations of a liquid in a cylindrical tank was determined in [7]. A formula was obtained from which the logarithmic decrement for the oscillations of the first tone with $h/r_0 > 1$ can be determined as follows:

$$\delta = \frac{1.66\alpha}{\sqrt{\mathrm{Re}}}.$$

Here $\mathrm{Re} = \frac{\omega r_0^2}{\nu_0}$. The kinematic viscosity coefficient of various liquids at t = 0°C is, for example, for water $\nu_0 = 1.79 \cdot 10^{-6}$ m^2/sec, for 96% alcohol (C_2H_5OH) $\nu_0 = 2.58 \cdot 10^{-6}$ m^2/sec, for T-1 kerosene the coefficient $\nu_0 = 3.64 \cdot 10^{-6}$ m^2/sec. The formula agrees well with the experimental data.

An example is in order. For a cylindrical tank $r_0 = 0.5$ m, filled with T-1 kerosene up to a height $h/r_0 > 1$ at t = 0°C we are given: $\nu_0 = 3.64 \cdot 10^{-6}$ m^2/sec. It is required to determine the damping coefficient δ. We get

$$\omega = \sqrt{\frac{1.84g}{r_0}} = 1.92\sqrt{g}, \quad \mathrm{Re} = \frac{\omega r_0^2}{\nu_0} = 1.32 \cdot 10^5 \sqrt{g},$$

$$\delta = \frac{1.66\alpha}{\sqrt{\mathrm{Re}}} = \frac{0.00\alpha}{\sqrt{g}}, \quad \frac{h}{r_0} = \frac{1}{2\alpha} = \frac{0.00}{\sqrt{g}}.$$

where $[g^0] = m/sec^2$.

Experimental studies of the oscillations of liquids are usually conducted using small scale physical models. The shapes of the cavities and their locations relative to the center of mass are geometrically similar to the original system. (Some questions related to the modeling of the oscillations of liquids in tanks are discussed in [15, 29]). The experimental results, obtained using these models, can be transferred to the natural systems under the following similarity conditions:

1) By Froude number

2) By Strouhal number

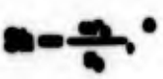

3) By Reynolds number

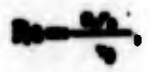

4) By Bond number

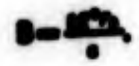

Here v_0, r_0, ω are, respectively, the characteristic velocity, the linear dimension, and the oscillation frequency, ν_0 is the kinematic viscosity coefficient of the liquid, α is the surface tension coefficient.

With sufficiently large models, the influence of the surface tension of the oscillations of the liquid is insignificant; therefore, the Bond number criterion is usually not taken into consideration in modeling. From the Fr, Re, Sh numbers, one can construct new dimensionless combinations by eliminating from them v_0:

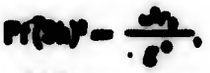

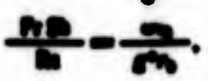

Introducing the scale factors (ratios of the corresponding model parameters to the original parameters) $k_{r_0}, k_g, k_\omega, k_t$ we can obtain the following ratios:

$$k_\omega = \sqrt{\frac{k_g}{k_{r_0}}}, \quad k_\nu = k_g^{1/2} k_{r_0}^{3/2}.$$

The first relation gives a scale factor to convert the oscillation frequencies, obtained using models, the natural conditions. The second relation determines a choice of viscosity of the modeling liquid, necessary for the Re number similarity to be satisfied. In practice, however, in the majority of cases it is impossible to secure a complete similarity relative to the Re number.

The fact that similarity relative to Re and B numbers is not satisfied usually only brings about an increase of the damping coefficient in the equations of the oscillations of the liquid.

The oscillations of the free surface of the liquid can be considered linear only for small amplitudes. The experimental results show that if the amplitude of the oscillations of the free surface is greater than 0.1 r_0, then the oscillations of the liquid cannot be considered linear. For forced oscillations of the liquid, both the pressure on the wall and the amplitude of oscillations increase by a smaller factor as compared to the amplitude of the tank oscillations. This is seen in Figures 2.36 and 2.37.

Figure 2.36 gives $p/\rho g r_0 \bar{\delta}_0$ as a function of $\bar{\delta}_0$, where p is the maximum pressure with resonance oscillations; r_0 is the radius of the cylindrical tank; ρ is the density of the liquid; $\bar{\delta}_0 = \delta_0/r_0$ is the amplitude of the transverse oscillations of the tank as referred to the radius. In the case of very small oscillations $\bar{\delta}_0 \leq 0.0015$ this relationship changes very little; when $\bar{\delta}_0 > 0.0015$ in contrast with a linear system the quantity $p/\rho g r_0 \bar{\delta}_0$ to a considerable degree depends on $\bar{\delta}_0$.

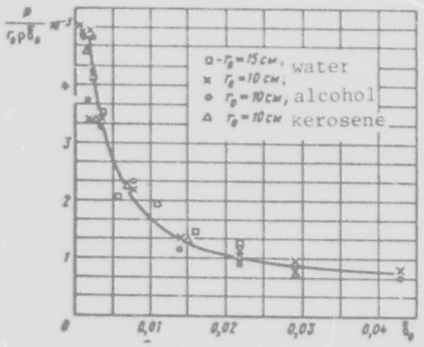

Figure 2.36

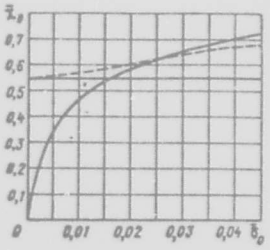

Figure 2.37


Figure 2.38

Figure 2.37 shows the experimental relationship between the amplitude of the wave $\bar{\chi}_0 = \chi_0/r_0$ and the amplitude of the forced oscillations at resonances of the first tone. From the graph it is also evident that the ratio $\bar{\chi}_0/\bar{\delta}_0$ decreases with increasing $\bar{\delta}_0$. When the amplitude of oscillations increases, the damping coefficient of the oscillations of the liquid also grows.

At frequencies close to the natu. l frequency of the first tone, and small amplitudes of the forced oscillations, the form of the liquid free surface is close to a plane, the amplitude of the wave is almost proportional to $\bar{\delta}_0$, and the height of the protuberance and the depth of the depression are approximately equal (Figure 2.38).

As the amplitude $\bar{\delta}_0$ increases, the free surface of the liquid increasingly deviates from a plane, the center of the free surface moves down along the axis of the tank, and the height of the protuberance becomes greater than the depth of the depression. The wave remains well behaved until its double amplitude reaches a value of $\sim(1.2 - 1.3)\, r_0$. If the amplitude of the forced oscillations

increases further, the wave begins to disintegrate. In hydrodynamics this type of a limit wave is called the Stokes wave. For higher tones of oscillations, the waves on the surface of the liquid disintegrate for amplitudes that are considerably smaller than the amplitudes of the first tone.

The experimental results indicate that for certain amplitudes the planar oscillations of the liquid become unstable. The wave may turn into a plane, perpendicular to the motion of the tank, and even begin to turn in the circumferential direction.

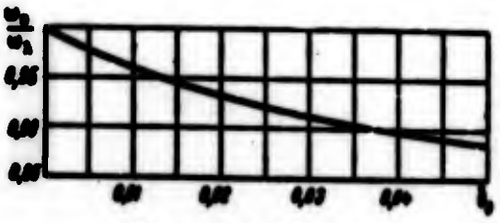

Figure 2.39

Studies of the nonlinear oscillations of liquids show that with an increasing amplitude, the resonance frequency of oscillations decreases. This phenomenon, established by means of calculations in [22], is shown in Figure 2.39.

Thus, if the amplitudes $\chi_{max} < 0{,}1 r_0$, the oscillations of the liquid may be considered linear. With $\chi_{max} > 0{,}1 r_0$ the nonlinear effects have to be considered.

Formulas for Certain Coefficients and Definite Integrals

1. $\int_0^{\ell} \operatorname{sh}\left[\frac{\zeta_n}{r_0}\left(\frac{h}{2}+x\right)\right] dx = 0$

2. $\int_0^{\ell} \operatorname{ch}\left[\frac{\zeta_n}{r_0}(h+x)\right] dx = \frac{r_0}{\zeta_n} \operatorname{sh}\left(\zeta_n \frac{h}{r_0}\right)$

3. $\int_0^{\ell} \operatorname{sh}^2\left[\frac{\zeta_n}{r_0}\left(\frac{h}{2}+x\right)\right] dx = \frac{r_0}{\zeta_n} \operatorname{sh}\left(\zeta_n \frac{h}{2r_0}\right) \operatorname{ch}\left(\zeta_n \frac{h}{2r_0}\right) - \frac{h}{2}$

4. $\int_0^{\ell} \operatorname{ch}^2\left[\frac{\zeta_n}{r_0}\left(h+x\right) dx = \frac{r_0}{2\zeta_n} \operatorname{sh}\left(\zeta_n \frac{h}{r_0}\right) \operatorname{ch}\left(\zeta_n \frac{h}{r_0}\right) + \frac{h}{2}$

5. $$\int_{-h}^{0} \operatorname{sh}\left[\frac{\zeta_n}{r_0}\left(\frac{h}{2}+x\right)\right](L+x)\,dx=$$

$$=\frac{r_0 h}{\zeta_n}\operatorname{ch}\left(\zeta_n\frac{h}{2r_0}\right)-\frac{2r_0^2}{\zeta_n^2}\operatorname{sh}\left(\zeta_n\frac{h}{2r_0}\right)$$

6. $$\int_{-h}^{0} \operatorname{ch}\left[\frac{\zeta_n}{r_0}(h+x)\right](L+x)\,dx=$$

$$=\frac{r_0}{\zeta_n}L\operatorname{sh}\left(\zeta_n\frac{h}{r_0}\right)-\frac{r_0^2}{\zeta_n^2}\left(\operatorname{ch}\zeta_n\frac{h}{r_0}-1\right)$$

7. $$\int_{-h}^{0} \operatorname{ch}\left[\frac{\zeta_n}{r_0}(h+x)\right]\operatorname{sh}\left[\frac{\zeta_n}{r_0}\left(\frac{h}{2}+x\right)\right]dx=$$

$$=\frac{r_0}{2\zeta_n}\operatorname{sh}\left(\zeta_n\frac{h}{r_0}\right)\operatorname{sh}\left(\zeta_n\frac{h}{2r_0}\right)-\frac{h}{2}\operatorname{sh}\left(\zeta_n\frac{h}{2r_0}\right)$$

8. $$\int_0^{r_0}\left[\frac{J_1\left(\zeta_n\frac{r}{r_0}\right)}{J_1(\zeta_n)}\right]^2 r\,dr=\frac{\zeta_n^2-1}{2\zeta_n^2}r_0^2$$

9. $$a_0=\frac{\sin\pi\alpha}{\pi\alpha}\cos\eta_0=d_0\cos\eta_0$$

10. $$a_\nu=-\frac{2\cos\pi\alpha\cos\eta_0}{\pi\alpha\left[\left(\frac{\nu}{2\alpha}\right)^2-1\right]}=c_\nu\cos\eta_0\quad(\nu=1,3,5,\ldots)$$

11. $$a_\nu=-\frac{2\sin\pi\alpha\sin\eta_0}{\pi\alpha\left[\left(\frac{\nu}{2\alpha}\right)^2-1\right]}=a_\nu\sin\eta_0\quad(\nu=2,4,6,\ldots)$$

12. $$d_0=\frac{\sin\pi\alpha}{\pi\alpha}$$

13. $$c_\nu=-\frac{2\cos\pi\alpha}{\pi\alpha\left[\left(\frac{\nu}{2\alpha}\right)^2-1\right]}\quad(\nu=1,3,5,\ldots)$$

14. $$d_\nu=\frac{2\sin\pi\alpha}{\pi\alpha\left[\left(\frac{\nu}{2\alpha}\right)^2-1\right]}\quad(\nu=2,4,6\ldots)$$

15. $$b_{\nu n}=\frac{2\left\{R_{\nu n}(r_0)-\beta R_{\nu n}(\beta r_0)+\frac{2}{\zeta_{\nu n}}\left[\left(\frac{\nu}{2\alpha}\right)^2-1\right]Q_{\nu n}\right\}}{\left[\zeta_{\nu n}^2-\left(\frac{\nu}{2\alpha}\right)^2\right]R_{\nu n}^2(r_0)-\left[\beta^2\zeta_{\nu n}^2-\left(\frac{\nu}{2\alpha}\right)^2\right]R_{\nu n}^2(\beta r_0)}$$

16. $$\int_{\beta r_0}^{r_0} R_{\nu n}\,dr=\frac{2r_0}{\zeta_{\nu n}}Q_{\nu n}$$

17. $$Q_{\nu n}=\sum\left[Z_{\frac{\nu}{2\alpha}+2k+1}(\zeta_{\nu n})-Z_{\frac{\nu}{2\alpha}+2k+1}(\beta\zeta_{\nu n})\right]$$

18. $$Z_{\frac{\nu}{2\alpha}+2k+1}(\zeta_{\nu n})=J_{\frac{\nu}{2\alpha}+2k+1}(\zeta_{\nu n})+\gamma_{\nu n}Y_{\frac{\nu}{2\alpha}+2k+1}(\zeta_{\nu n})$$

19. $$m_{0n}=\rho r_0^3\sin\pi\alpha d_0 b_{0n}\left[R_{0n}(r_0)-\beta R_{0n}(\beta r_0)-\frac{1}{r_0}\int_{\beta r_0}^{r_0}R_{0n}\,dr\right]\times$$
$$\times\frac{2}{\zeta_{0n}}\operatorname{th}\left(\frac{\zeta_{0n}h}{r_0}\right)$$

20. $$m_{\nu n}=\rho r_0^3\begin{cases}d_\nu\sin\pi\alpha\\ \nu=2,4,6\\ \\ c_\nu\cos\pi\alpha\\ \nu=1,3,5\end{cases}b_{\nu n}\left[\frac{R_{\nu n}(r_0)-\beta R_{\nu n}(\beta r_0)}{\left(\frac{\nu}{2\alpha}\right)^2-1}+\right.$$
$$\left.+\frac{1}{r_0}\int_{\beta r_0}^{r_0}R_{\nu n}\,dr\right]\frac{2}{\zeta_{\nu n}}\operatorname{th}\left(\frac{\zeta_{\nu n}h}{r_0}\right)$$

21. $$I_{\nu n}=\rho r_0^5\begin{cases}d_\nu\sin\pi\alpha\\ \nu=0,2,4\\ \\ c_\nu\cos\pi\alpha\\ \nu=1,3,5\end{cases}b_{\nu n}\Delta R_{\nu n}\left(\frac{8h}{\zeta_{\nu n}^2r_0}-\frac{16}{\zeta_{\nu n}^2}\operatorname{th}\zeta_{\nu n}\frac{h}{2r_0}\right)$$

22. $$\Delta R_{\nu n}=\frac{R_{\nu n}(r_0)-\beta R_{\nu n}(\beta r_0)}{\left(\frac{\nu}{2\alpha}\right)^2-1}+\frac{1}{r_0}\int_{\beta r_0}^{r_0}R_{\nu n}\,dr\quad(\nu=1,2,3,\ldots)$$

23. $$\Delta R_{0n}=R_{0n}(r_0)-\beta R_{0n}(\beta r_0)-\frac{1}{r_0}\int_{\beta r_0}^{r_0}R_{0n}\,dr$$

REFERENCES

1. Abramsov, Rensleben. The distribution of pressure on the wall due to the movement of liquid in rigid tanks. Raketnaya tekhnika, No. 4, 1961.

2. Abramson, Rensleben. A comparison of the conditions under which liquid moves in cylindrical tanks with a flat and conical bottom. Raketnaya tekhnika, No. 4, 1961.

3. Abramsov, Chu, Gartsa. Motion of liquid in spherical tanks. Raketnaya tekhnika i kosmonavtika, No. 2, 1963.

4. Bauer. Motion of the liquid (splashing) in a cylindrical tank, subdivided into 45° sectors. Raketnaya tekhnika i kosmonavtika, No. 4, 1964.

5. Dokuchayev, L. F. Solution of a boundary value problem on the oscillations of a liquid in conical cavities. PMM (Prikladnaya matematika i mekhanika), Vol. XXVIII, No. 1, 1964.

6. Zhukovskiy, N. Ye. O dvizhenii tverdogo tela, imeyushchego polosti, napolnennyye odnorodnoy kapel'noy zhidkost'yu (Motion of a rigid body with cavities filled with a homogeneous dripping liquid). Collected papers, Gostekhizdat (Gosudarstvennoye izdatel'stvo tekhno-teoreticheskoy literatury; State Publishing House of Technical and Theoretical Literature). Vol. 1, 1955.

7. Kirillov, V. V. Study of the oscillations of a liquid in a stationary container with the escape of liquid taken into consideration. Trudy Moskovskogo fizikotekhnicheskogo instituta. No. 5, 1960.

8. Kochin, N. Ye, I. A. Kibel' and N. V. Roze. Teoreticheskaya gidromekhanika (Theoretical hydromechanics) Gostekhizdat, Vol. 1, 1955.

9. Kochin, N. Ye. Vektornoye ischisleniye i nachala tenzornogo ischisleniya (Vector calculus and an introduction to tensor calculus) "Nauka" press, 1965.

10. Kolesnikov, K. S. Oscillations of a liquid in a cylindrical container.

11. Kolesnikov, K. S. and V. Ye. Samodayev. Oscillations of a liquid in a cylindrical tank with radial partitions. Izvestiya AN SSSR, Mekhanika zhidkosti i gaza, No. 4, 1967.

12. Lamb. Gidrodinamkia (Hydrodynamics.) Gostekhteoretizdat, 1947.

13. Loytsyanskiy, L. G. and A. I. Lur'ye. Kurs teoreticheskoy mekhaniki (Course on theoretical mechanics) Part II, Gostekhizdat, 1954.

14. Mikishev, G. N. and Ya. N. Dorozhkin. An experimental study of the free oscillations of liquids in containers. Izvestiya AN SSSR, OTN (Otdeleniye tekhnicheskikh nauk; Division of Technical Sciences), Mekhanika i mashinostroyeniye, No. 4, 1961.

15. Mikishev, G. N., A. Ye. Nevskaya, I. M. Mel'nikova, and N. Ya. Dorozhkin. On an experimental study of the perturbed motion of a rigid body with cavities partially filled with liquid. Kosmicheskiye issledovaniya, "Nauka" press, Vol. III., No. 2, 1965.

16. Mikishev, G. N. and Ya. N. Dorozhkin. An experimental determination of the hydrodynamic coefficients for a cylindrical cavity with radial partitions. Izvestiya AN SSSR, Mekhanika zhidkosti i gaza, No. 1 1967.

17. Moiseyev, N. N. Motion of a body with cavities partially filled by drops with an ideal liquid. Doklady AN SSSR (DAN) Vol. 85, No. 4, 1952.

18. Moiseyev, N. N. Two pendulums with liquid. PMM, Izdatel'stvo AN SSSR, No. 6, 1952.

19. Moiseyev, N. N., and A. A. Petrov. Numerical methods of calculating the natural frequencies in the oscillations of a confined volume of liquid. Computation center of AN SSSR, 1966.

20. Mikhlin, S. G. Variatsionnyye metody v matematicheskoy fizike (Variational methods in mathematical physics). Gostekhizdat, 1957.

21. Narimanov, G. S. On the motion of a rigid body whose cavity is partially filled with liquid. PMM, Izd. AN SSSR, No. 1, 1956.

22. Narimanov. G. S. Oscillations of a liquid in moving cavities. Izvestiya AN SSSR, OTN, No. 10, 1957.

23. Okhotsimskiy, D. Ye. Toward a theory of a body with cavities partially filled with liquid; PMM, Izdatel'stvo AN SSSR, No. 1, 1956.

24. Pavlenko, G. Ye. Kauchka sudov (The rocking motion of ships), Gostekhizdat, 1936.

25. Smirnov, V. I. Kurs vysshey matematiki (Course of higher mathematics),Vol. III, part 2; Vol. 4. 1951.

26. Sretenskiy,L. N. Teoriya volnovykh dvizheniy zhidkosti (Theory of the wave motion of a liquid) ONTI, Moscow, 1936.

27. Rabinovich, B. I. On the equations of the perturbed motion of a rigid body with a cylindrical cavity partially filled with liquid. Izdatel'stvo AN SSSR, No. 1, 1956.

28. Rabinovich, B. I., L. V. Dokuchayev and Z. M. Polyakova. On Calculating the coefficients in the equations of the perturbed motion of a rigid body with cavities partially filled with liquid. Kosmicheskiye issledovaniya, "Nauka" Press, Vol. III, No. 2, 1965.

29. Bauer, H. F. Treibstaffschwingungen in Raketenbehältern und ihr Einfluss auf die Gesamtstabilitat,(Fuel oscillations in rocket containers and their influence on total stability.) Zeitschrift fur Flugwissenschaften, Vol. 12, No. 3, 1964.

CHAPTER III

DYNAMIC CHARACTERISTICS OF A RIGID ROCKET WITH THE OSCILLATIONS OF LIQUID IN TANKS TAKEN INTO CONSIDERATION

1. Formulation of the Problem

In Chapter 1 we discussed the dynamic properties of an ideally rigid rocket, and we established the principal requirements imposed on the attitude control system. However, to represent a liquid fuel rocket as a rigid body is of course a gross oversimplification. The presence of liquid fuel in tanks leads, as it was shown in Chapter II, to the appearance of additional forces whose effect on the dynamic properties of the rocket in the frequency range of the natural oscillations may be considerable.

If the control system is designed with the rocket assumed to be a rigid body, then in flight there may arise transverse oscillations of the rocket with a frequency close to the frequency of the natural oscillations of the liquid in tanks. Such oscillations are undesirable since they are capable of producing significant transverse inertial loads on the fuselage of the rocket, and of jamming the control system channels with "parasite" currents.

If the oscillations of liquid are taken into consideration in the equations of the perturbed motion, we are then able to reveal some specific properties of the control system and formulate the additional requirements to be imposed on the control system that would damp

these oscillations.

This hydrodynamic problem was solved in the preceding chapter under the assumption that the axis of the cylindrical tank may be deflected from the vertical by a small angle, and the vector of the terrestrial acceleration $\bar{g}$ that characterizes the intensity of mass forces stays constant. The projection of the $\bar{g}$ vector on the fixed coordinate axis Ox did not change with the motion of the cylinder with liquid in it. This assumption was also adopted when analyzing the dynamic properties of the mechanical analog of the oscillations of liquid.

Are the obtained results applicable to liquid fuel rockets in the case when the longitudinal axis of the rocket is arbitrarily oriented relative to the horizon? Let us consider this question in more detail.

The intensity of the mass forces acting on the liquid in a moving frame of reference attached to the tank (the fuselage of the rocket) will be expressed by the acceleration vector $\bar{a}^*$. The movement of the moving frame will be assumed to be translational. The movement of liquid together with the moving frame will be referred to as the transport movement, and the acceleration vector of the transport movement will be denoted by $\bar{a}_e$.

If the liquid does not move relative to the tank, then

$$\bar{a}^* = \bar{g} - \bar{a}_e$$

where $\bar{g}$ is the terrestrial acceleration vector.

Suppose the tank with liquid is in translational motion toward the center of the Earth beginning at some altitude under only the influence of the force of gravity. Then $\bar{a}_e = \bar{g}$ and $\bar{a}^* = 0$, i.e., in a freely falling tank the mass forces of the liquid are equal to zero. The quasi-static position of the free surface of liquid in a

tank is perpendicular to the vector $\bar{a}^*$. In this case the orientation of the free surface is indeterminate.

If, in addition to the weight, the tank with liquid is acted upon by other external forces, then $\bar{a}^* \neq 0$, and the free surface of liquid will be perpendicular to $\bar{a}^*$.

Let us focus our attention on an unperturbed rectilinear movement of the rocket in the powered phase of the trajectory. The main vector of the external forces will be denoted by $\bar{R}$, where

$$\bar{R} = \bar{R}^* + \bar{G}; \quad \bar{R}^* = \bar{P}_{ef} + \bar{Y} + \bar{X} + \bar{Y}_p. \tag{3.1}$$

Here $\bar{R}^*$ is the main vector of the external forces (without the weight of the rocket), G is the weight of the rocket, P_{ef} is the effective thrust, Y is the aerodynamic lift, X is the drag, and Y_p is the control surface force.

The acceleration vector in the transport motion is

$$\bar{a}_t = \frac{\bar{R}}{m} = \frac{\bar{R}^*}{m} + \bar{g}.$$

where m is the mass of the rocket.
The acceleration vector is

$$\bar{a}^* = \bar{g} - \bar{a}_t = -\frac{\bar{R}^*}{m}.$$

Just as in the free fall of the tank, in the powered stage of the trajectory the terrestrial acceleration does not have any effect on the forces acting on the liquid from the side of the tank. In an unperturbed rectilinear motion of the rocket the free surface of liquid fuel in a tank is perpendicular to $\bar{R}^*$.

Since the direction of $\bar{R}^*$ does not in general coincide with the longitudinal axis of the rocket, the normal to the unperturbed free surface of liquid fuel does not coincide with that axis either. However, the deflection is small, and therefore below the unperturbed free surface of liquid fuel in tanks will be considered perpendicular

to the longitudinal axis of the rocket.

The trajectory of the unperturbed motion of the rocket will be assumed to be rectilinear in a small time interval, and thus it will be identical with the stationary coordinate axis Ox.

Let the projection of $\bar{R}^*/m$ on the Ox axis be denoted by g^*. If the aerodynamic forces are small compared to the effective thrust, then $\bar{R}^* \approx \bar{P}_{ef}$ and

$$g^* \approx \frac{P_{ef}}{m}.$$

Small perturbations of the rocket motion do not, as it was shown in Chapter I, change the acceleration of the rocket in the Ox direction. Therefore, in spite of the fact that the engine thrust follows the rocket axis, the magnitude of g^* is not affected by small deflections of the rocket away from the Ox axis. This conclusion will also be confirmed in the following section for pendulum models.

Thus, the results of solving the hydrodynamic problem, obtained in Chapter II, are indeed applicable also to a tank with liquid, in motion, under the condition that instead of the terrestrial acceleration g one must take the acceleration g^*.

Figure 3.1

To describe the motion of a rocket with account taken of the oscillations of liquid in tanks, we shall use a pendulum model consisting of an absolutely rigid straight rod and k mathematical pendulums. The suspension points of the pendulums will be located on a straight line, namely the longitudinal axis of the rod. It will be agreed that the longitudinal axis from which the pendulums are suspended will be the principal central axis of inertia of the rigid body (the system) consisting of the rod with the attached pendulums.

Let the origin of the attached coordinate system $O_1x_1y_1z_1$ be located at point C of the rod (Figure 3.1). Point C coincides with

the center of mass of the system when the mass m_j^* of all pendulums is located on the longitudinal axis of the rod. Let l_j, m_j^* denote the length and mass of the j^{th} pendulum, and let L_j^* refer to the x_1 coordinate of the mass of the j^{th} pendulum when this mass is located on the longitudinal axis of the rod.

Based on the conclusions make in Chapter II, such a pendulum system may be adopted as a mechanical analog of a physical system containing several tanks with liquid. In each tank usually only the first tone of the oscillations of liquid is considered but in some cases also the higher tones must be dealt with.

In the particular case of a circular cylindrical tank with a flat bottom, the parameters of the pendulum system can be determined from the following formulas

$$
\begin{aligned}
l_j &= \frac{r_j}{\zeta_0 \operatorname{th}\left(\zeta_0 \frac{h_j}{r_j}\right)}, \\
m_j^* &= \pi r_{0j}^2 h_j \frac{2 \operatorname{th}\left(\zeta_0 \frac{h_j}{r_j}\right)}{\zeta_0 \left(\zeta_0^2 - 1\right)}, \\
L_j^* &= L_j \left[1 - \frac{2 r_j}{\zeta_0 L_j} \operatorname{th}\left(\zeta_0 \frac{h_j}{2 r_j}\right)\right], \\
I &= I_0 + \sum_{j=1}^{k} \sum_{n=1}^{\infty} I_{jn}, \\
I_{jn} &= \pi r_{0j}^2 \rho_j \left[-\frac{h_j}{r_j} \frac{8}{\zeta_n^2 \left(\zeta_n^2 - 1\right)} + \frac{16}{\zeta_n^3 \left(\zeta_n^2 - 1\right)} \operatorname{th}\left(\zeta_n \frac{h_j}{2 r_j}\right)\right]
\end{aligned}
\qquad (3.2)
$$

where h_j, r_{0j} and ρ_j are, respectively, the submerged height, the radius, and the density of liquid in the j^{th} cylinder; I_0 is the moment of inertia relative to the transverse axis passing through the center of mass of the physical system with liquid if the latter is assumed to be "frozen" in the position when its free surface is perpendicular to the longitudinal axis of the tank: L_j is the distance from the center of mass of the physical system to the free surface of liquid in the j^{th} tank. In accordance with the convention adopted in Chapter II $L_j > 0$, if the free surface is located above the center of mass, and $L_j < 0$ if the free surface is below the center of mass.

2. Equations of the Perturbed Motion for Pendulum Models

Suppose that the rod of the pendulum system in the Oxy plane is acted upon by the following set of forces (Figure 3.2):

-- the effective engine thrust P_{ef} directed along the longitudinal axis of the rod, O_1x_1; the magnitude of this force P_{ef} is greater than the wieght of the rod with the pendulums;

-- the control surface force Y_p whose direction is always parallel to the transverse axis of the rod, O_1y_1; here $Y_p = R^{\delta}_{y}\delta$, where δ is the angle of rotation of the control element;

-- the aerodynamic lift Y, the drag X, and moment M_a of these forces relative to the center of mass of the system (point C);

-- the force of gravity G = mg;

-- the moment of the damping forces M_d relative to point C.

The aerodynamic forces act only during flight in comparatively dense layers of the atmosphere.

Consider a planar motion of the pendulum system in the fixed frame of reference Oxy (the Ox axis is directed vertically upward). As the generalized coordinates we shall adopt: $x_c(t)$, $y_c(t)$ which are the coordinates of point C, $\varphi(t)$ which refers to the angle between the Ox and O_1x_1 axes, and $\lambda_j(t)$ which denotes the deflection of a mass m_j* in the direction of the O_1y_1 axis of the body coordinate system $O_1x_1y_1$ (see Figure 3.2).

Without loss of generality we shall assume $x_c(t)$ to be finite, and $Yc(t)$, $\varphi(t)$, $\lambda_j(t)$ to be small perturbations.

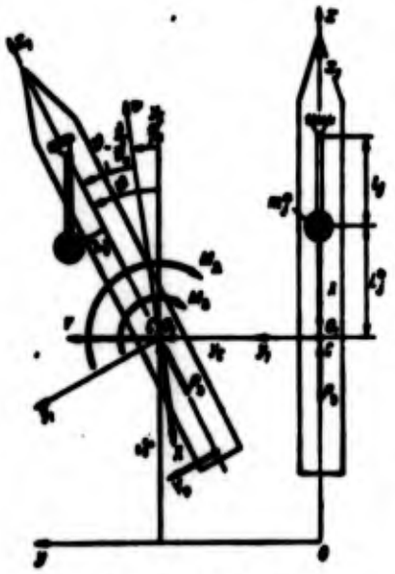

Figure 3.2

If all perturbations are identically equal to zero

$$y_C \equiv 0,\ \vartheta \equiv 0,\ \lambda_j \equiv 0 \quad (j = 1, 2, \ldots, k),$$

then the angle of rotation of the control element $\delta(t) \equiv 0$ and the angle of attack $\alpha_n \equiv 0$. In this case, the rod is acted upon by only three external forces P_{ef}, X, and G, and the rod moves in the Ox direction with an acceleration

$$\ddot{x}_C = \frac{P_0 - X - G}{m} = \frac{P_0 - X}{m} - g,$$

where m is the mass of the rod with the pendulums; $g \approx g_0$ is the terrestrial acceleration.

If within a small time interval the mass m and forces P_{ef} and X are considered constant, then the acceleration $\ddot{x}_c$ will also be constant.

Such a motion will be called unperturbed.

The coordinates x, y of any point of the longitudinal axis of the rod and the coordinates x_j, y_j of the mass of the j^{th} pendulum in the Oxy system in view of (2.68) will be

$$x = x_C + x_1\left(1 - \frac{\vartheta^2}{2}\right),$$
$$y = y_C + x_1\vartheta,$$
$$x_j = x_C + L_j^0\left(1 - \frac{\vartheta^2}{2}\right) + \frac{\lambda_j^2}{2l_j} - \lambda_j\vartheta,$$
$$y_j = y_C + L_j^0\vartheta + \lambda_j.$$

Differentiating with respect to time, we find

$$\dot{x}=\dot{x}_C-x_1\theta\dot{\theta},$$

$$\dot{y}=\dot{y}_C+x_1\dot{\theta},$$

$$\dot{x}_j=\dot{x}_C-L_j^*\theta\dot{\theta}+\frac{\lambda_j\dot{\lambda}_j}{l_j}-\lambda_j\dot{\theta}-\dot{\lambda}_j\theta,$$

$$\dot{y}_j=\dot{y}_C+L_j^*\dot{\theta}+\dot{\lambda}_j.$$

The formulas for the kinetic and potential energies of the system have the following form

$$T=\frac{1}{2}\left[\int_{-b}^{a}m(x_1)(\dot{x}^2+\dot{y}^2)\,dx_1+\sum_{j=1}^{k}m_j^*(\dot{x}_j^2+\dot{y}_j^2)\right],$$

$$U=g\int_{-b}^{a}m(x_1)x\,dx_1+g\sum_{j=1}^{k}m_j^*x_j,$$

where a, (-b) are the x_1 coordinates of the ends of the rod. Substituting here the expressions for the coordinates and velocities of all points of the system, and retaining only infinitesimals of second order we get

$$\begin{aligned}2T&=m\dot{x}_C^2+m\dot{y}_C^2+I\dot{\theta}^2+\sum_{j=1}^{k}m_j^*\times\\&\times\left[\dot{\lambda}_j^2+2\dot{y}_C\dot{\lambda}_j+2L_j^*\dot{\theta}\dot{\lambda}_j+2\dot{x}_C\left(\frac{\lambda_j\dot{\lambda}_j}{l_j}-\lambda_j\dot{\theta}\right)\right],\\U&=mgx_C+g\sum_{j=1}^{k}m_j^*\left(\frac{\lambda_j^2}{2l_j}-\lambda_j\theta\right).\end{aligned}\qquad(3.3)$$

Let the projections of the aerodynamic forces X and Y on the fixed coordinate axes be denoted by F_x and F_y. Then the generalized coordinates x_C, y_C, θ, λ_j will have the following generalized forces associated with them.

$$\begin{aligned}Q_x&=P_a\left(1-\frac{ac}{2}\right)+F_x-R_{yy}^{\lambda}\delta\theta,\\Q_y&=P_a\theta+R_{yy}^{\lambda}\delta+F_y,\\Q_\theta&=-R_{yy}^{\lambda}(x_a-x_m)\delta-M_a-M_x,\\Q_{\lambda_j}&=0.\end{aligned}\qquad(3.4)$$

Let us substitute (3.3) and (3.4) into Lagrange's equations of second kind. The equation corresponding to the generalized coordinate x_c will assume the form

$$m\ddot{x}_c + mg + \frac{\lambda_j \ddot{\lambda}_j}{l_j} + \frac{\dot{\lambda}_j^2}{l_j} - \ddot{\lambda}_j\theta - 2\dot{\lambda}_j\dot{\theta} - \lambda_j\ddot{\theta} =$$

$$= P_0\left(1 - \frac{\theta^2}{2}\right) + F_x - R_{yp}^{*}\delta\theta.$$

Leaving out infinitesimals of second order, we get

$$m\ddot{x}_c + mg = P_0 + F_x.$$

Up to infinitesimals of second order, small perturbations λ_j and θ do not affect the motion of the center of mass in the direction of the Ox axis. With the magnitudes of m, P_{ef}, and F_X remaining constant, this motion continues with constant acceleration and remains unperturbed.

Since for $\alpha_n = 0$ the Ox component of the aerodynamic forces is $F_x = -X$, the Ox component of the main vector of the external forces $\bar{R}^*$ will be

$$\frac{P_0 - X}{m} = g^* = \ddot{x}_c + g. \qquad (3.5)$$

For small θ and λ_j, g^* remains constant.

This conclusion is also valid in a more general case when the longitudinal axis of the rod O_1x_1 in an unperturbed motion makes with the horizon an angle $\theta_0 \neq \pi/2$ (Figure 3.3). Rotating the Ox axis of the fixed coordinate system so that it coincides with the attached axis O_1x_1 in an unperturbed motion, we find

$$g^* = \ddot{x}_c + g\sin\theta_0 = \frac{P_0 - X}{m}. \qquad (3.5a)$$

For small deflections of the θ and λ_j coordinates, the acceleration g^* does not change, just as previously. This result will not change if the main vector of the external forces $\bar{R}^*$ (3.1) makes a small angle with the O_1x_1 axis.

Now let us find Lagrange's equations for the generalized coordinates y_c, ϑ, λ_j. Retaining only infinitesimals of first order and using the notation of (3.5), we get

$$\begin{gathered}
m\ddot{y}_c+\sum_{j=1}^{k}m_j^{\circ}\ddot{\lambda}_j-P_{\circ}\vartheta=R_{yp}^{\delta}\delta+F_y,\\
I\ddot{\vartheta}+\sum_{j=1}^{k}m_j^{\circ}L_j^{\circ}\ddot{\lambda}_j-g^{\circ}\sum_{j=1}^{k}m_j^{\circ}\lambda_j=-R_{yp}^{\delta}l_p\delta-M_{\omega}-M_{\dot{\alpha}},\\
\ddot{\lambda}_j+\frac{g^{\circ}}{l_j}\lambda_j+L_j^{\circ}\ddot{\vartheta}+\ddot{y}_c-g^{\circ}\vartheta=0\quad(j=1,2,\ldots,k),
\end{gathered}\tag{3.6}$$

where

$$\begin{gathered}
l_p=x_p-x_m,\\
m=\int_{-b}^{a}m(x_1)dx_1+\sum_{j=1}^{k}m_j^{\circ},\\
I=\int_{-b}^{a}m(x_1)x_1^2dx_1+\sum_{j=1}^{k}m_jL_j^{\circ 2},\\
\int_{-b}^{a}m(x_1)x_1dx_1+\sum_{j=1}^{k}m_j^{\circ}L_j^{\circ}=0\quad(-b\leqslant x_1\leqslant a)
\end{gathered}$$

If for any reason it is necessary to consider several tones of the oscillations of liquid, then in Equations (3.6) one must use the corresponding number of pendulums, i.e. take

$$\begin{gathered}
\sum_{j=1}^{k}m_j^{\circ}\lambda_j=\sum_{j=1}^{k}\sum_{n=1}^{n_0}m_{jn}^{\circ}\lambda_{jn},\quad\sum_{j=1}^{k}m_j^{\circ}\ddot{\lambda}_j=\sum_{j=1}^{k}\sum_{n=1}^{n_0}m_{jn}^{\circ}\ddot{\lambda}_{jn},\\
\sum_{j=1}^{k}m_j^{\circ}L_j^{\circ}\ddot{\lambda}_j=\sum_{j=1}^{k}\sum_{n=1}^{n_0}m_{jn}^{\circ}L_{jn}^{\circ}\ddot{\lambda}_{jn},
\end{gathered}$$

where n_0 is the number of tones that is to be determined. The equation for λ_{jn} will have the form

$$\begin{gathered}
\ddot{\lambda}_{jn}+\frac{g^{\circ}}{l_{jn}}\lambda_{jn}+L_{jn}^{\circ}\ddot{\vartheta}+\ddot{y}_c-g\vartheta=0\\
(j=1,2,\ldots,k;\quad n=1,2,\ldots,n_0).
\end{gathered}$$

Now let us write out the expressions for the projections of the aerodynamic forces and moments that appear in Equations (3.6). The angle of attack in a perturbed motion of the rocket is

$$\alpha=\vartheta-\frac{\dot{y}_c}{v_m}.$$

In view of (1.1) and (1.2), and also taking into consideration Equations (1.40), we find

$$F_y = Y - X\frac{\dot{y}_C}{v_0} = \frac{\rho v_0^2}{2} Sc_y^a\left(\vartheta - \frac{\dot{y}_C}{v_0}\right) - \frac{\rho v_0^2}{2} Sc_x \frac{\dot{y}_C}{v_0} =$$
$$= \frac{\rho v_0^2}{2} Sc_y^a \vartheta - \frac{\rho v_0^2}{2} S(c_y^a + c_x)\frac{\dot{y}_C}{v_0},$$
$$M_z = \frac{\rho v_0^2}{2} Slc_m^a\left(\vartheta - \frac{\dot{y}_C}{v_0}\right), \qquad (3.7)$$
$$M_z = Ic_{zz}^{\omega}\dot{\vartheta}.$$

According to (1.21) the coefficient c_{zz}^{ω} combines the coefficients of the aerodynamic damping and the damping due to the Coriolis forces.

Let us transform Equations (3.6) by excluding from them all the variables λ_j. We shall use a symbolic operator form of notation and then from the third equation in (3.6) we find

$$\lambda_j = \frac{1}{f_j(p)}\left[(-L_j^* p^2 + g)\vartheta - p^2 y_C\right], \quad f_j(p) = p^2 + 2\varepsilon_j p + \frac{g^*}{l_j} \qquad (3.8)$$

Substituting expressions for λ_j in the first two equations in (3.6), we get

$$p^2 y_C\left[m - p^2\sum_{j=1}^{k}\frac{m_j^*}{f_j(p)}\right] - \vartheta\left[P_0 + p^4\sum_{j=1}^{k}\frac{m_j^* L_j^*}{f_j(p)} - g^* p^2\sum_{j=1}^{k}\frac{m_j^*}{f_j(p)}\right] =$$
$$= R_{yy}^{\omega}\dot{\vartheta} + F_y,$$
$$\vartheta\left[p^2 I - p^4\sum_{j=1}^{k}\frac{m_j^* L_j^{*2}}{f_j(p)} + 2p^2 g^*\sum_{j=1}^{k}\frac{m_j^* L_j^*}{f_j(p)} - g^{*2}\sum_{j=1}^{k}\frac{m_j^*}{f_j(p)}\right] - \qquad (3.9)$$
$$- p^2 y_C\left[p^2\sum_{j=1}^{k}\frac{m_j^* L_j^*}{f_j(p)} - g^*\sum_{j=1}^{k}\frac{m_j^*}{f_j(p)}\right] = -R_{yy}^{\omega} I_p \dot{\vartheta} - M_a - M_z.$$

In what follows, for simplicity an analysis of Equations (3.9) will be done for the particular case when all the pendulums have the same length $l_j = l^*$, and the same damping coefficient $\varepsilon_j = \varepsilon_\lambda$. The fact that the lengths of the pendulums are equal indicates that the shape of the tanks and their submerged heights are such that the frequency of a given tone of the natural oscillations of liquid is the same in all tanks; the density of liquid may differ from tank to tank.

3. The Frequencies of the Natural Oscillations of the System

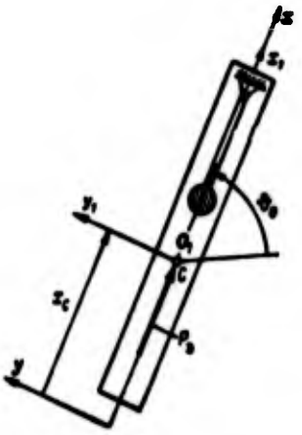

Figure 3.3

Let us first discuss a simplified dynamic system in which the aerodynamic forces may be neglected. This makes it possible to determine the natural frequencies of the rocket vibrations that are due to the oscillations of liquid in tanks. Letting in (3.6) or (3.9) $F_y = M_a = M_d \equiv 0$, we shall obtain the equations of the perturbed motion of a rocket in air-free space.

We set in Equations (3.9) $e_j = e_1$, $l_j = l^*$, $f_j(p) = f(p)$ and introduce dimensionless parameters of the pendulum system

$$\mu_1 = \frac{1}{m}\sum_{j=1}^{k} m_j^*, \quad \mu_2 = \frac{1}{I}\sum_{j=1}^{k} m_j^* L_j^{*2}, \qquad (3.10)$$

$$\mu_3 = \frac{1}{m r_0}\sum_{j=1}^{k} m_j^* L_j^*$$

where

$$r_0 = \sqrt{\frac{I}{m}}.$$

The dimensionless parameters μ_1, μ_2, μ_3 have the following physical meaning: μ_1 represents the ratio of the sum of the masses of all pendulums to the mass of the entire system (the rod and the pendulums); μ_2 is the ratio of the sum of the moments of inertia of the masses of all pendulums relative to the lateral axis of the rod, passing through point C, to the moment of inertia of the rod with the attached pendulums relative to the same axis; μ_3 is the ratio of the sum of the static moments of the pendulums relative to the lateral axis of the rod, passing through point C, to the product of

the mass of the system and its radius of inertia ρ_0 corresponding to the attached pendulums.

In accordance with (3.10), the parameter ranges will be

$$0<\mu_1<1,\ 0<\mu_2<1,\ -1<\mu_3<1,\ \mu_3^2\leqslant\mu_1\mu_2,\ 0<\rho_0<\infty.$$

Eliminating y_c, we transform Equations (3.9) so that they assume the following form

$$Q(p)\theta=R(p)\delta. \tag{3.11}$$

Here

$$Q(p)=p^2(a_0p^4+a_1p^3+a_2p^2+a_3p+a_4)f^{k-2}(p),$$

$$R(p)=-\frac{R_{y\varphi}^0 l_p}{I}f^{k-1}(p)\times$$

$$\times\left\{p^2\left[(1-\mu_1)-\frac{\mu_3}{\bar{l}_p}\right]+2\varepsilon_1 p+\omega_1^2\left(1+\frac{\mu_3\bar{l}^2}{\bar{l}_p}\right)\right\}. \tag{3.12}$$

where the following notation was used:

$$\begin{aligned}
a_0&=(1-\mu_1)(1-\mu_2)-\mu_3^2,\\
a_1&=2\varepsilon_1(2-\mu_1-\mu_2),\\
a_2&=\omega_1^2(2-\mu_1-\mu_2+\mu_3\bar{l}^2)+4\varepsilon_1^2,\\
a_3&=2\varepsilon_1\omega_1^2(2+\mu_3\bar{l}^2),\\
a_4&=\omega_1^4(1-\mu_3\bar{l}^2),\\
\bar{l}&=\frac{l^*}{l_0},\ \bar{l}_p=\frac{l_p}{l_0},\ \omega_1^2=\frac{g^*}{l^*}.
\end{aligned} \tag{3.13}$$

As we know any polynomial of even positive degree with real coefficients may be represented as a product of polynomials of second degree with positive coefficients. Therefore, the operator polynomial Q(p) can be written as

$$Q(p)=a_0p^2(p^2+2p\varepsilon_1+\omega_1^2)(p^2+2p\varepsilon_2+\omega_2^2)f^{k-2}(p). \tag{3.14}$$

Here ω_1, ω_2 are the natural frequencies of the system with no damping, ε_1, ε_2 are the corresponding damping coefficients, f(p) is the operator polynomial defined in (3.8)

Let us calculate ω_1 and ω_2 for the case when $\varepsilon\lambda = 0$.

The equation for the frequencies can be obtained from the equality $Q(p) = 0$ by substituting $p = i\omega$. The operator polynomial $f(p)$ will not be considered since the natural frequencies of liquid in a stationary tank can be computed from $f(i\omega) = 0$. We have

$$\omega^2(a_0\omega^4 - a_2\omega^2 + a_4) = 0. \tag{3.15}$$

With the pendulums of the same length, the highest degree of Equation (3.15) is six and for $k \geqslant 2$ it does not depend on the number of pendulums.

The value of the root $\omega^2 = 0$ in Equation (3.15) corresponds to that motion of the system in which all $\lambda_j = 0$ and

$$m\ddot{y}_C = P\vartheta.$$

A small angle ϑ corresponds to a small lateral acceleration of the center of mass. However, the lateral displacement y_c of the center of mass may be arbitrarily large, and in this sense the motion of a system with zero frequency is unstable.

Now let us consider the second factor in Equation (3.15)

$$a_0\omega^4 - a_2\omega^2 + a_4 = 0. \tag{3.16}$$

For small values $\bar{l}^0 = l^0/\rho_0$ (the length of the large rod compared to the length of the pendulum) the discriminant of Equation (3.16)

$$D = a_2^2 - 4a_0a_4$$

is positive, and the system has two natural frequencies;

$$\omega_1^2 = \frac{a_2 + \sqrt{D}}{2a_0}, \quad \omega_2^2 = \frac{a_2 - \sqrt{D}}{2a_0}. \tag{3.17}$$

The case when the pendulums are situated on the rod in such a way that the sum of their static moments relative to point C is zero ($\mu_3 = 0$) is of particular interest. For a rocket with two tanks this means that

$$m_1^* L_1^* + m_2^* L_2^* = 0 \quad (L_2^* < 0).$$

In this case Equation (3.16) may be put in the form

$$[\omega^2(1-\mu_1) - \omega_\lambda^2][\omega^2(1-\mu_2) - \omega_\lambda^2] = 0,$$

whence the frequencies of the system are

$$\omega_1^* = \frac{\omega_\lambda}{\sqrt{1-\mu_1}}, \quad \omega_2^* = \frac{\omega_\lambda}{\sqrt{1-\mu_2}}. \tag{3.18}$$

Both the first and the second frequency of the system, due to the oscillations of liquid in tanks, are greater than the natural frequency of the liquid in a stationary tank, and the difference becomes larger, the larger the coefficients μ_1 and μ_2. It is interesting to note that the formula for ω_1^* coincides with Formula (b) obtained in Section 6 of Chapter II, when solving the problem of the natural translational oscillations of a cylindrical tank with liquid ($\phi = 0$). The frequency of the system is the same as the partial frequency. The formula for ω_2^* slightly differs from Formula (i) of Chapter II obtained for the case when $y_c \equiv 0$. Instead of the sign "greater" Formula (3.18) contains the equality sign. This discrepancy is a consequence of the fact that in the first equation of (3.6) there is a term $P_{ef}\phi$ which represents a projection of force P_{ef} on the Oy axis. An analogous term is missing from Equations (2.61).

Rockets of short length will have a large length l^* of the pendulum and a small radius of inertia ρ_0 associated with them, this being caused by the fact that in these rockets $\bar{l}^* = l^*/\rho_0$ is considerably larger than in long rockets. An increase in $\bar{l}^*$ for $\mu_3 > 0$ will not change the properties of Equation (3.15). An increase in $\mu_3 \bar{l}^*$ only leads to an increase in the difference between the frequencies ω_1 and ω_2.

For large values of $\bar{\gamma}^*$ and $\mu_3<0$ the discriminant D of Equation (3.16) may become negative and then the system will possess entirely different properties.

Let us consider the characteristic equation obtained by equating the second factor in (3.12) to zero with $\varepsilon\lambda = 0$. We shall have

$$a_0 p^4 + a_2 p^2 + a_4 = 0. \tag{3.19}$$

When the discriminant of Equation (3.19) is zero, the equation has multiple roots.

When $D > 0$ the roots $p^2_{1,2}$ of the biquadratic Equation (3.19) are complex conjugate and have negative real parts. The following values will be obtained for p:

$$p_{1,2} = -\varepsilon \pm i\omega, \quad p_{3,4} = +\varepsilon \pm i\omega, \tag{3.20}$$

where

$$\varepsilon = \sqrt{\frac{b}{2a_0}}, \quad \omega = \sqrt{\frac{c}{2a_0}}, \quad D = -bc, \tag{3.21}$$

$$b = 2\sqrt{a_0 a_4} - a_2, \quad c = 2\sqrt{a_0 a_4} + a_2.$$

The solutions (3.20) are peculiar in the sense that one of the complex conjugate roots has a positive real part which indicates that the natural oscillations increase.

Thus, the case when $D = 0$ (natural frequencies are equal) corresponds to the boundary of the stability region for the system. The case when the natural frequencies are identical will be encountered below when analyzing flexural vibrations of a rod loaded with a slave force.

When the engine thrust force is activated, the dynamic rocket system is no longer conservative, and such systems are characterized

by a loss of stability when the parameters are in a certain relation to one another. This also explains the appearance of the roots of the characteristics Equation (3.19) having positive real parts.

Inasmuch as $\mu_3^2 < \mu_1\mu_2$ it may happen that $D < 0$ if $a_2 > 0$. This means that a solution of (3.20) may exist only if the parameter $\mu_3\bar{f}^0$ lies in the range

$$-1 < \mu_3\bar{f}^0 < 0.$$

The condition $b > 0$ will be satisfied when

$$\mu_3\bar{f}^0 \approx -(\mu_1+\mu_2),\ \mu_1\mu_2 > \mu_3^2.$$

The larger the values of $(\mu_1\mu_2 - \mu_3^2)$ and $(\mu_1+\mu_2)$, the greater the coefficient of the oscillations growth will be.

In what follows we shall consider the case when $D > 0$ unless stated to the contrary.

Consider the case when only one pendulum is attached to the rod ($k = 1$). This means that the physical system has a free surface in only one tank. The equation of the natural oscillations will be obtained from (3.6) by setting $F_y = 0$, $M_a = 0$, $M_d = 0$, $\delta = 0$. Since $P_{ef}/m = g^0$, we get from the first and second equation in (3.6)

$$\ddot{y}_c - g^0\theta = -\mu_1\ddot{\lambda}_j,$$

$$\theta = -\frac{m_j l_j^0}{I}\ddot{\lambda}_j + \frac{g^0 m_j^0}{I}\lambda_j$$

and substituting these in the third equation we obtain

$$\ddot{\lambda}_j(1-\mu_1-\mu_2) + \lambda_j\frac{g^0}{l^0}(1+\mu_3\bar{f}^0) = 0. \tag{3.22}$$

This system has one nonzero natural frequency

$$\omega^2 = \frac{g^0}{l^0}\,\frac{1+\mu_3\bar{f}^0}{1-\mu_1-\mu_2}. \tag{3.23}$$

4. The Transfer Function of the Controlled Object and its Properties

The differential equations in (3.9) written in a symbolic operator form may be conventionally written as

$$\frac{\vartheta}{\delta} = K(p) = \frac{R(p)}{Q(p)}. \tag{3.24}$$

by first eliminating from them the variable y_c. Here the deflection ϑ is the output coordinate and δ is the input coordinate. The degrees of the operator polynomials R(p), Q(p) depend on the number of tanks.

For simplicity let us assume that the natural frequencies and the damping coefficients of the oscillations of liquid are the same in all tanks so that

$$f_j(p) = f(p) = p^2 + 2\varepsilon_1 p + \omega_1^2 \quad (j = 1, 2, \ldots, k).$$

The aerodynamic forces will not be taken into consideration. This simplifies the problem somewhat and makes it possible to reveal more clearly the peculiarities of the dynamic properties of a rocket that are due to the oscillations of liquid in tanks. The operator polynomials Q(p), R(p) are in this case expressed by Formulas (3.12).

Let us write the operator polynomial R(p) of (3.12) in a different form. We introduce the notation

$$\varepsilon_3 = \frac{\varepsilon_1}{1 - \mu_1 - \frac{\mu_2}{\bar{l}_p}}, \quad \omega_3^2 = \omega_1^2 \frac{1 + \frac{\mu_1 \bar{r}_0}{\bar{l}_p}}{1 - \mu_1 - \frac{\mu_2}{\bar{l}_p}}, \tag{3.25}$$

$$N_1 = \frac{R_{yy}^2 l_p}{I} \left(1 - \mu_1 - \frac{\mu_2}{\bar{l}_p}\right).$$

We shall write the operator polynomial R(p), making use of the above notation, as

$$R(p) = -N_1(p^2 + 2\varepsilon_\lambda p + \omega_\lambda^2)^{k-1}(p^2 + 2\varepsilon_3 p + \omega_3^2).$$

The operator polynomial Q(p) will be represented as an equality (3.14)

$$Q(p) = a_0 p^2 (p^2 + 2\varepsilon_1 p + \omega_1^2)(p^2 + 2\varepsilon_2 p + \omega_2^2)(p^2 + 2\varepsilon_\lambda p + \omega_\lambda^2)^{k-2}.$$

Then the transfer function for the system can be expressed as a product of three transfer functions

$$K(p) = \frac{R(p)}{Q(p)} = NK_0(p)K_1(p)K_2(p), \qquad (3.26)$$

where

$$K_0(p) = -\frac{R'_{yp}/_p}{p^2 I},$$

$$K_1(p) = \frac{p^2 + 2\varepsilon_3 p + \omega_3^2}{p^2 + 2\varepsilon_1 p + \omega_1^2},$$

$$K_2(p) = \frac{p^2 + 2\varepsilon_3 p + \omega_\lambda^2}{p^2 + 2\varepsilon_2 p + \omega_2^2},$$

N is a constant.

$$N = \frac{1 - \mu_1 - \frac{\mu_3}{I_p}}{(1-\mu_2)(1-\mu_2) - \mu_3^2}.$$

$K_0(p)$ is a transfer function for an absolutely rigid body, i.e., a rod with attached pendulums; $K_1(p)$ and $K_2(p)$ may be considered to be transfer functions of the "associated" oscillating loops (pendulums).

For $\varepsilon_{1,2,3,\lambda} = 0$ the natural frequencies ω_1, ω_2 are the poles of the transfer function, and $\omega\lambda$, ω_3 are zeros of the transfer function. The frequencies $\omega_1, \omega_2, \omega_3, \omega_\lambda$ will be called below the characteristic frequencies of the system.

If in the expression for the transfer function one sets p = iω, where ω is an arbitrary frequency of forced oscillations, then one

obtains a complex transfer number which can be represented in the complex plane as a vector with a modulus A and the phase angle φ. The hodograph of the vector in the frequency range $0<\omega<+\infty$ is called the amplitude-phase frequency characteristic.

Let us analyze the properties of the amplitude-phase frequency characteristics $K_0(i\omega), K_1(i\omega), K_2(i\omega)$.

The complex transfer number $K_0(i\omega)$ of the rod with pendulums attached to it represents a set of real numbers which are inversely proportional to ω^2.

Let us study the properties of the amplitude-phase frequency characteristic $K_2(i\omega)$. Introducing the notation

$$\gamma=\frac{\omega}{\omega_1},\quad \bar{\omega}_2=\frac{\omega_2}{\omega_1},\quad \bar{\varepsilon}_1=\frac{\varepsilon_1}{\omega_1},\quad \bar{\varepsilon}_2=\frac{\varepsilon_2}{\omega_1},$$

where ω_1, ε_1 are the natural frequency and the damping coefficient of the first tone of the oscillations of liquid in a tank, we get

$$K_2(i\omega)=\frac{1+2\bar{\varepsilon}_1\bar{\gamma}_1-\gamma^2}{\bar{\omega}_2^2+2\bar{\varepsilon}_2\bar{\gamma}_2-\gamma^2}. \tag{3.27}$$

Here γ is the dimensionless frequency of forced oscillations, i.e., the frequency of oscillations divided by the frequency of natural oscillations of liquid in a stationary tank. The complex transfer number can also be represented in an alternative form

$$K_2(i\omega)=U(\gamma)+iV(\gamma)=\frac{A_2^0(\gamma)}{A_{20}(\gamma)}\exp i[\varphi_2^0(\gamma)-\varphi_{20}(\gamma)]=A_2(\gamma)e^{i\varphi_2(\gamma)},$$

where $A_2^0(\gamma), \varphi_2^0(\gamma)$ are the modulus and the argument of the complex transfer number in the numerator of (3.27), and $A_{20}(\gamma), \varphi_{20}(\gamma)$ are the modulus and the argument of the complex transfer number in the denominator of (3.27). They are, respectively, equal to

$$A_2^0(\gamma)=\sqrt{(1-\gamma^2)^2+(2\bar{\varepsilon}_1\gamma)^2},\quad A_{20}(\gamma)=\sqrt{(\bar{\omega}_2^2-\gamma^2)^2+(2\bar{\varepsilon}_2\gamma)^2},$$

$$\varphi_2^0(\gamma)=\operatorname{arctg}\frac{2\bar{\varepsilon}_1\gamma}{1-\gamma^2},\quad \varphi_{20}(\gamma)=\operatorname{arctg}\frac{2\bar{\varepsilon}_2\gamma}{\bar{\omega}_2^2-\gamma^2}, \tag{3.29}$$

$$A_2(\gamma)=\frac{A_2^0(\gamma)}{A_{20}(\gamma)},\quad \varphi_2(\gamma)=\varphi_2^0(\gamma)-\varphi_{20}(\gamma).$$

The real and imaginary parts of the complex transfer number $K_2(i\omega)$ will be

$$U(\gamma) = A_2(\gamma)\cos\varphi_2(\gamma), \quad V(\gamma) = A_2(\gamma)\sin\varphi_2(\gamma).$$

The modulus $A_2(\gamma)$ and the argument $\varphi_2(\gamma)$ of a complex transfer number are the functions of frequency γ. The graphic representation of $A_2(\gamma)$ is called the amplitude frequency characteristics (or the resonance curve), and the graphic plot of $\varphi_2(\gamma)$ is called the phase frequency characteristic.

For future purposes let us define the relations among the characteristic frequencies ω_1, ω_1, ω_2, ω_2. We shall limit ourselves to the case when in Equation (3.16) the discriminant D > 0.

For $\bar{\varepsilon}_1 = 0$ on the basis of (3.17) and (3.18) we have

$$\omega_1 < \omega_2^* < \omega_1^*.$$

For small $\bar{\varepsilon}_1$ this inequality usually allows for a generalization in which, instead of the partial frequencies ω_1^* and ω_2^*, we can take the frequencies of the system to be ω_1 and ω_2. Then we get

$$\omega_1 < \omega_2 < \omega_1.$$

By comparing Formulas (3.18) and (3.25) we can conclude that a case is possible when $\omega_2 > \omega_1$ and $\omega_2 < \omega_1$. Therefore, below we shall consider two relations which in the dimensionless case can be written as

$$1 < \bar{\omega}_1 < \bar{\omega}_2 < \bar{\omega}_1, \tag{3.30}$$

$$1 < \bar{\omega}_2 < \bar{\omega}_1 < \bar{\omega}_2. \tag{3.31}$$

Here

$$\bar{\omega}_2 = \frac{\omega_2}{\omega_1}.$$

The relation (3.30) occurs much more often than (3.31).

The functions $A_2^0(\gamma)$ and $\varphi_2^0(\gamma)$, $A_{20}(\gamma)$ and $\varphi_{20}(\gamma)$ are plotted in Figure 3.4. The frequency characteristics $A_2(\gamma)$ and $\varphi_2(\gamma)$ are also shown there. The dotted lines represent the case when the damping coefficient of the oscillations of liquid is neglected $(\bar{\varepsilon}_1=0)$.

The amplitude frequency characteristic $A_2(\gamma)$ has a maximum and a minimum. The minimum corresponds to a zero, and the maximum — to a pole of the transfer function. Inasmuch as $\bar{\omega}_2>1$, as the frequency γ increases from zero one first encounters a minimum of the characteristic, and then the maximum. The larger the difference between $\bar{\omega}_2$ and a unity, the higher the maximum of the characteristic. In addition, the maxima of the characteristics are inversely proportional to the damping coefficient of the oscillations of liquid $\bar{\varepsilon}_1(\bar{\varepsilon}_2)$.

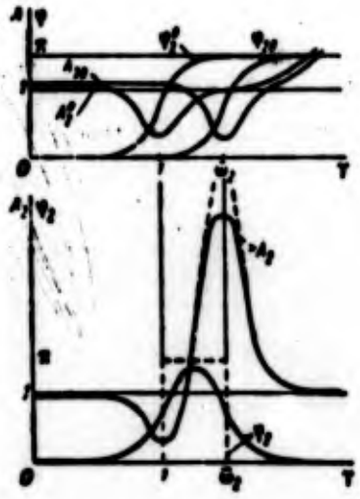

Figure 3.4

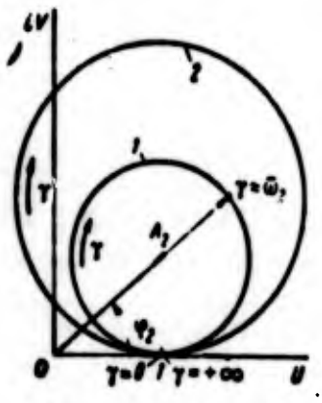

Figure 3.5

The phase frequency characteristic $\varphi_2(\gamma)$ has one maximum in the region of positive values of φ_2. If damping is present the maximum value is less than π, where the maximum occurs approximately in the middle between the maximum and minimum of the amplitude frequency characteristic. The smaller the damping coefficient of the natural oscillations of liquid, the larger the phase peak. When the phase peak is larger, the greater the difference between the frequencies ω_2 and ω_λ.

The hodograph of the complex transfer number $K_1(i\omega)$ in the complex plane Z = U + iV is shown in Figure 3.5. For comparison, we shall give two hodographs, constructed for two different values of $\bar{\omega}_2$, where for Curve 2 the frequency ω_2 is larger than for Curve 1. The complex transfer number $K_1(i\omega)$ has a structure identical with that of $K_2(i\omega)$ and can be expressed by the formula

$$K_1 = \frac{\bar{\omega}_0^2 + i2\bar{\omega}_0\gamma - \gamma^2}{\bar{\omega}_1^2 + i2\bar{\omega}_1\gamma - \gamma^2} = \frac{A_1^0(\gamma)}{A_{10}(\gamma)} \exp i[\varphi_1^0(\gamma) - \varphi_{10}(\gamma)] = A_1(\gamma) e^{i\varphi_1(\gamma)}, \tag{3.32}$$

where

$$\bar{\omega}_0 = \frac{\omega_0}{\omega_2}, \quad \bar{\omega}_1 = \frac{\omega_1}{\omega_2}, \quad \bar{\omega}_0 = \frac{\omega_0}{\omega_2}, \quad \bar{\omega}_1 = \frac{\omega_1}{\omega_2}.$$

The formulas for $A_1^0(\gamma)$, $A_{10}(\gamma)$, $\varphi_1^0(\gamma)$, $\varphi_{10}(\gamma)$ can be obtained from Formulas (3.29) if one sets

$$\bar{a}_0 = \bar{a}_{20}, \quad \bar{a}_2 = \bar{a}_{10}, \quad \bar{a}_0 = \bar{a}_{10}, \quad 1 = \bar{a}_{20}.$$

When the frequencies of the system satisfy the inequality (3.30), the amplitude and the phase frequency characteristics $A_1(\gamma)$, $\varphi_1(\gamma)$ have the same form and possess the same properties as the functions shown in Figure 3.4. The minimum and maximum of the amplitude frequency characteristic occur, respectively, at $\gamma = \bar{\omega}_0$ and $\gamma = \bar{\omega}_1$.

Figure 3.6 shows graphs of $A_1(\gamma)$ and $\varphi_1(\gamma)$ for the case when the relation (3.31) holds true. Here as the frequency γ increases we first encounter a maximum, and then a minimum of the amplitude frequency characteristic. In contrast with Figure 3.4, the phase frequency characteristic $\varphi_1(\gamma)$ has no maximum in the region $\varphi_1 > 0$, and the minimum occurs in the region of negative $\varphi_1(\gamma)$. This is of principal importance in estimating the stability of motion. The form of the phase frequency characteristic $\varphi_1(\gamma)$ is determined by the relative location of zeros and poles of the transfer function. Therefore, it may be concluded that if the relative location of the zeros and poles

of the transfer function is determined by the inequality (3.30), then the function $\varphi_1(\gamma)$ is positive. If, however, the relative location of the zeros and poles is subject to (3.31), then $\varphi_1(\gamma)$ will be negative (see Figure 3.6).

The hodograph of the complex transfer number $K_1(i\omega)$ in the complex plane Z = U + iV is shown in Figure 3.7. The curves are given for the case when $\bar{\omega}_3 > \bar{\omega}_1$, where the ratio $\bar{\omega}_3/\bar{\omega}_1$ is greater for Curve 2 than for Curve 1. The entire amplitude-phase frequency characteristic is here located in the lower half-plane. If the relative position of ω_3 and ω_1, is such that $\bar{\omega}_1 > \bar{\omega}_3$ (3.30), then the amplitude-phase frequency characteristic $K_1(i\omega)$ is located in the upper half-plane.

The amplitude-phase frequency characteristics $K_1(i\omega)$, $K_2(i\omega)$ are basically identical with the frequency characteristics of simple oscillatory circuits. Just as in the case of simple oscillatory circuits, the amplitude-phase frequency characteristics undergo considerable changes within a small range of natural frequencies. For that reason the properties of the complex transfer numbers $K_1(i\omega)$ and $K_2(i\omega)$ are identified with the properties of oscillatory circuits which are formed as a result of the oscillations of liquid (or pendulums).

However, the frequency characteristics $K_1(i\omega)$ and $K_2(i\omega)$ possess properties that distinguish them from simple oscillatory circuits. These characteristics in the coordinates U, iV are represented by curves, close to circles, which are tangent to the OU axis at U = 1. Their main peculiarity is the fact that beyond the limits of a small range of natural frequencies, both for small and for large frequencies, the modulus of the complex number is close to one, and the argument close to zero.

Now let us consider the total amplitude-phase frequency characteristic $K_1(i\omega)K_2(i\omega)$. It corresponds to that part of the transfer function (3.26) which makes the transfer function of a rigid rocket with cavities partially filled with liquid different from the transfer function of an ideally rigid rocket.

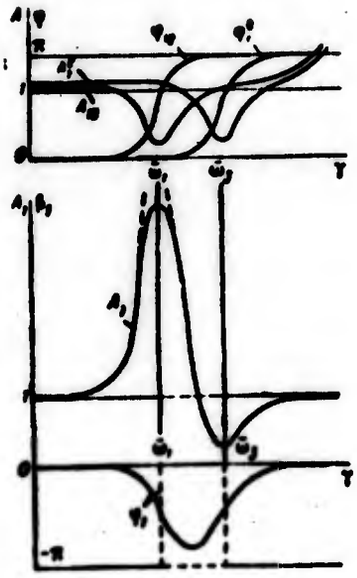

Figure 3.6

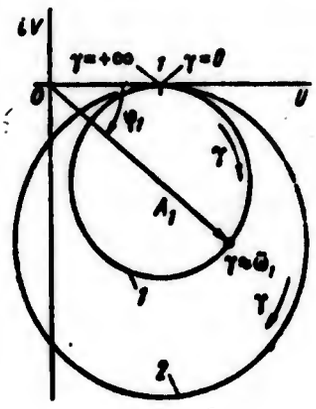

Figure 3.7

Since

$$K_1(i\omega)K_2(i\omega)=A_1(\gamma)A_2(\gamma)e^{i(\varphi_1+\varphi_2)},$$

the indicated characteristics will be easy to represent graphically if for each value of γ one multiplies the modului $A(\gamma)=A_1(\gamma)A_2(\gamma)$ and adds the arguments $\varphi(\gamma)=\varphi_1(\gamma)+\varphi_2(\gamma)$, as it was done in Figures 3.4 and 3.6. Functions $K_1(i\omega)K_2(i\omega)$ are represented in Figures 3.8 - 3.11.

Figures 3.8 and 3.9 show the frequency characteristics for the relative position of the characteristic frequencies as in (3.30), and Figures 3.10 and 3.11 — for the relative position of frequencies as in (3.31). The dotted lines show the possible versions of the characteristics.

The amplitude-phase characteristics have two maximums each which are located in the ranges containing the natural frequencies $\bar{\omega}_1$, $\bar{\omega}_2$ of the system. Depending on the relative location of the characteristic

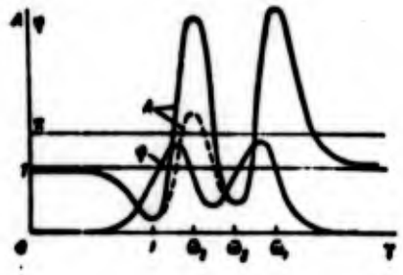

Figure 3.8

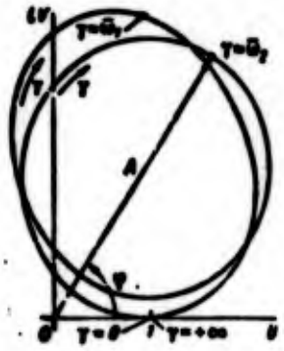

Figure 3.9

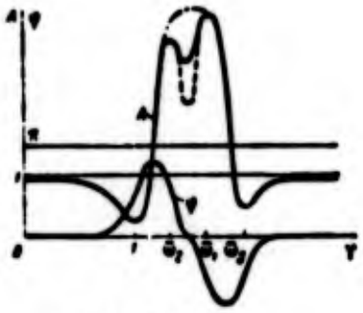

Figure 3.10

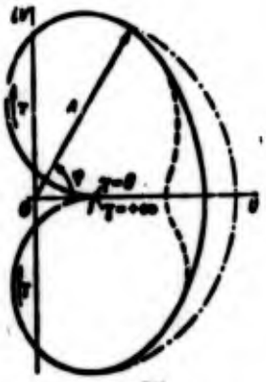

Figure 3.11

frequencies $\bar{\omega}_2, \bar{\omega}_3$, either one of the two maxima can be greater than the other. For example, as applied to Figure 3.8, the value of the $(1, \bar{\omega}_2)$ first amplitude maximum rises with an increase in the interval and gets smaller with a decrease of the interval $(\bar{\omega}_2, \bar{\omega}_3)$. The height of the second amplitude maximum will be larger, the greater $\bar{\omega}_1$ is as compared to $\bar{\omega}_3$.

The maximum values of the amplitude characteristic shown in Figure 3.10 will rise with an increase in the frequency intervals $(1, \bar{\omega}_2)$ and $(\bar{\omega}_1, \bar{\omega}_3)$. With a narrowing of the interval $(\bar{\omega}_2, \bar{\omega}_1)$, the value of $A(\gamma)$ between the two maxima increases, and the two maxima merge into one.

There is a basic difference between the amplitude-frequency characteristics shown in Figures 3.8, 3.9 and 3.10, 3.11. The difference consists in the fact that in the first two figures the entire characteristic is located in the upper half-plane of $Z = U + iV$, and in the second two it stretches over both the upper and lower half-planes. In addition to positive values $\varphi(\gamma) = \varphi_1(\gamma) + \varphi_2(\gamma)$ in the second case in the interval $(\bar{\omega}_1, \bar{\omega}_3)$, the phase frequency characteristic $\varphi(\gamma)$ assumes negative values.

As can be seen in Figures 3.8 and 3.10, the amplitude frequency and the phase frequency characteristics undergo large variations only in the narrow zone of the natural frequencies of the object. Outside of this zone the amplitude characteristic is close to unity, and the phase characteristic is close to zero. This property of the characteristics $K_1(i\omega)K_2(i\omega)$ of the oscillatory circuits derives from the fact that the amplitude of the oscillations of a liquid has a substantial value only in the resonance zone. Outside of this zone the behavior of the liquid is practically the same as the behavior of a rigid body.

Let us estimate the frequency range in which the modulus of the product $K_1(i\omega)K_2(i\omega)$ is significantly different from unity. For the purpose of the estimate, we shall use the following values of the system parameters:

$$\mu_1 = 0{,}2;\quad \mu_2 = 0{,}1;\quad \mu_3 = -0{,}05;\quad \bar{r} = \frac{r}{h} = 0{,}05;\quad \bar{l}_p = \frac{l_p}{h} = 1{,}5.$$

Then

$$\bar{\omega}_3^2 = \frac{1 + \frac{\mu_3 \bar{r}}{\bar{l}_p}}{1 - \mu_1 - \frac{\mu_2}{\bar{l}_p}} \approx 1{,}21.$$

We set

$$\bar{\omega}_1^2 \approx \frac{1}{1-\mu_1} = 1{,}25; \quad \bar{\omega}_2^2 \approx \frac{1}{1-\mu_2} = 1{,}11.$$

The characteristic frequencies satisfy the inequality in (3.30). The difference between the extreme values is

$$\bar{\omega}_1 - 1 = 0{,}12.$$

Making use of the fact that for $\gamma \leqslant 0{,}95$ and $\gamma \geqslant 1{,}05\bar{\omega}_1$ the frequency characteristics are practically constant, we shall obtain the frequency zone in which the effect of the oscillations of liquid may be considerable. This zone is located in the interval

$$0{,}95 < \gamma < 1{,}18.$$

If one takes ω_λ = 10 1/sec, then in the example just analyzed the dynamic characteristics of a rigid rocket with the oscillations of liquid taken into consideration will differ from the characteristics of an ideally rigid rocket only in the small frequency range

$$9{,}5\ 1/\text{sec} < \omega < 11{,}8\ 1/\text{sec}$$

These ranges in accordance with (3.30) and (3.31) will be, respectively,

$$0{,}95 < \gamma < 1{,}05\bar{\omega}_1;$$
$$0{,}95 < \gamma < 1{,}05\bar{\omega}_2.$$

The deviation of the product $A_1(\gamma)A_2(\gamma)$ from unity beyond the indicated frequency ranges is approximately equal to 1/N. This can be seen if we calculate $A_1(\gamma)A_2(\gamma)$, for example, for γ = 0. In so doing, on the basis of (3.27) and (3.32) we obtain

$$A_1(0)\,\bar{A}_2(0) = \frac{\bar{\omega}_2^2}{\bar{\omega}_1^2}\,\frac{1}{\bar{\omega}_2^2} \approx \frac{\left(1 + \frac{\mu_1 \bar{\sigma}}{\Gamma_0}\right)(1-\mu_1)(1-\mu_2)}{1 - \mu_1 - \frac{\mu_2}{\Gamma_0}}.$$

Inasmuch as

$$\frac{n_1\bar{r}}{l_0} \ll 1, \quad n_1^2 \ll 1,$$

we have

$$A_1(0)\,A_2(0) \approx \frac{1}{N}.$$

On the basis of this estimate, we may conclude that if the natural frequencies of the oscillations of liquid in various tanks of the rocket differ significantly from one another, then the effect of the oscillations of liquid on the amplitude-phase characteristics of the rocket can be estimated by taking these oscillations into account each time in only one tank. The natural frequency of the vibrations of the rocket with the oscillations of liquid in one tank taken into account can be calculated using Formula (3.23).

Now let us find the transfer function $\vartheta/\delta(p)$ taking account of the aerodynamic forces. We have to substitute in Equations (3.9) the expressions (3.7) for the force F_y and moments M_a and M_d. We shall limit ourselves to discussing the case where in all the tanks the natural frequency of liquid is $\omega_j = \omega_1$, and the damping coefficient is $\varepsilon_j = \varepsilon_1$.

Eliminating y_c from Equations (3.9), we bring these equations to the form

$$Q'(p)\vartheta = R'(p)\delta. \tag{3.33}$$

Here the operator polynomials Q'(p) and R'(p) have a more complicated structure than in (3.12). By analogy with (3.12) and (3.14) they can be decomposed into factors and put in the following form:

$$\begin{aligned} Q'(p) &= (a_0'p^3 + a_1'p^2 + a_2'p + a_3')(p^2 + 2\varepsilon_1'p + \omega_1'^2)\times \\ &\times (p^2 + 2\varepsilon_2'p + \omega_2'^2)(p^2 + 2\varepsilon_1 p + \omega_1^2)^{k-2}, \\ R'(p) &= -N' R_{yy}^{\delta} l_0 (p + b')(p^2 + 2\varepsilon_2'p + \omega_2'^2)(p^2 + 2\varepsilon_1 p + \omega_1^2)^{k-1}. \end{aligned} \tag{3.34}$$

where N' is a constant.

If we consider

$$\omega_0^2 = \omega_1^2 \frac{1 + \frac{\mu_2 T'}{T_p}}{1 - \mu_1 - \frac{\mu_2}{T_p}} \approx \omega_1^2,$$

then by a direct check it can be seen that $\varepsilon_3' = \varepsilon_3$, $\omega_3' = \omega_3$ and the factor (p + b') is the same as the factor appearing in the numerator of the transfer function $K_3(p)$ in (1.46) which applies to an ideally rigid rocket. In fact, if in the numerator of the transfer function $K_3(p)$ in (1.46) the coefficient c is replaced by $c_{v_y v_y}$ (1.36), ε^3 is replaced by $c_{v_y \delta}$ (1.29) and $c_{\delta\omega}$ is replaced by c_{ω_y} (1.30), we then find

$$c_{v_y \delta}(p + c_{v_y v_y}) - c_{v_y \omega} c_{\omega_y} =$$
$$= -\frac{R_{yy}^2 l_p}{I}\left[p + \frac{1}{m v_a}\frac{\rho v_a^2}{2} S\left(c_x + c_y^\alpha - \frac{l}{T_p} c_m^\alpha\right)\right].$$

On the other hand, upon transforming Equations (3.9) to the form of (3.33) and making use of (3.7), we get

$$b' = \frac{1}{m v_a}\frac{\rho v_a^2}{2} S\left(c_x + c_y^\alpha - \frac{l}{T_p} c_m^\alpha\right)\Big].$$

Thus, with the aerodynamic forces taken into account the transfer function K'(p) can be represented, just as in the case of (3.26), as a product of three transfer functions.

$$K'(p) = \frac{K'(p)}{Q'(p)} = N' K_0'(p) K_1'(p) K_2'(p). \tag{3.35}$$

where

$$K_0'(p) = -R_{yy}^2 l_p \frac{p + b'}{a_0' p^3 + a_1' p^2 + a_2' p + a_3'},$$

$$K_1'(p) = \frac{p^2 + 2\varepsilon_3' p + \omega_3'^2}{p^2 + 2\varepsilon_1' p + \omega_1'^2}, \tag{3.36}$$

$$K_2'(p) = \frac{p^2 + 2\varepsilon_1 p + \omega_1^2}{p^2 + 2\varepsilon_2' p + \omega_2'^2}.$$

When the frequency of the natural oscillations of an ideally rigid rocket in an oncoming air stream is considerably lower than the frequency of the natural oscillations of liquid in tanks, the connection between these oscillations will be weak. In this case, the transfer function $K_0'(p)$ will differ little from the transfer function of an ideally rigid rocket, $K_0(p)$ (1.46); the transfer functions $K_1'(p)$ and $K_2'(p)$ will correspond to the transfer functions $K_1(p)$ and $K_2(p)$ from (3.26). The properties of $K_0(p)$, $K_1(p)$, $K_2(p)$ have already been considered above in the present section.

5. Additional Requirements on the Angular Stability Control System

The characteristic polynomial $A'(p)$ (3.34) of the equations of the perturbed motion of a rocket with the oscillations of liquid in tanks taken into consideration has the same number of roots with a positive real part as the characteristic polynomial (1.49) for the equations of an ideally rigid rocket. When the oscillations of liquid are considered, we only get in addition complex conjugate roots with a negative real part.

In Section 4, it was shown that when the oscillations of liquid in the tanks are considered, considerable changes occur in the amplitude-phase frequency characteristic of the controlled object that take place in a small frequency range, close to the natural frequencies of the liquid. Beyond that range the characteristic is practically the same as the amplitude-phase characteristic of an ideally rigid rocket.

The logarithmic amplitude frequency characteristic of a rocket $L_{p.o}(\omega)$ with the oscillations of liquid taken into account is shown in Figure 3.12a.

If the relative position of the characteristic frequencies satisfies the inequality in (3.30)

$$1<\bar{\omega}_2<\bar{\omega}_3<\bar{\omega}_1,$$

then the phase frequency characteristic will look like the one shown in Figure 3.12b. The change in the phase frequency characteristic, due to the oscillations of liquid in tanks, as compared with the phase characteristic of an ideally rigid rocket, proceeds in the direction of phase gain ($\varphi_{p.o}>0$) .

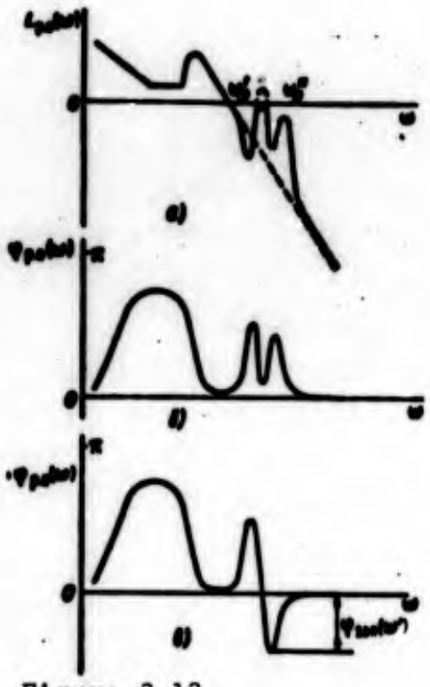

Figure 3.12

Figure 3.12, c shows the phase frequency characteristic for the relative position of the characteristic frequencies given by (3.31)

$$1<\bar{\omega}_2<\bar{\omega}_1<\bar{\omega}_3.$$

The change in the characteristic, due to the oscillations of liquid, proceeds not only in the direction of gain but also, which is very important, in the direction of lag.

Let us represent the complex transfer number of an open loop consisting of the controlled object and the stabilizer as

$$K(i\omega)=A_{p.o}(\omega)A_{AC}(\omega)$$
$$\exp i[\varphi_{p.o}(\omega)+\varphi_{AC}(\omega)]=A(\omega)\exp i\varphi(\omega).$$
$$A(\omega)=A_{p.o}(\omega)A_{AC}(\omega),$$
$$\varphi(\omega)=\varphi_{p.o}(\omega)+\varphi_{AC}(\omega).$$

In the frequency range corresponding to the natural oscillations of liquid the amplitude frequency characteristic of the controlled object has maxima that are characteristic of a significant amplification of the input signal; and therefore, the modulus of the complex

transfer number of the open loop may be greater than unity, $A(\omega)>1$ at these frequencies.

We shall formulate now the requirements that must be imposed on the phase frequency characteristic of the control system (stabilizer) to guarantee the stability of the closed system.

The process by which a rocket is stabilized by selecting an appropriate phase characteristic of the control system is called phase stabilization.

In Section 9 of Chapter I it was shown that to secure stability of an ideally rigid rocket it is necessary that the phase frequency characteristic of the control system have a phase gain in the frequency range $[0, \omega_0)$. The frequency ω_0 must be chosen such that

$$A(\omega)=A_{p.o}(\omega)A_{AC}(\omega)<1 \text{ for } \omega=\omega_0. \qquad (3.37)$$

The characteristic polynomial of an open loop with the oscillations of liquid taken into account has as many roots with a positive real part as the characteristic polynomial for the equations of an ideally rigid rocket. By the same token the requirements imposed on the phase frequency characteristic of the control system will be completely analogous. From this, however, it does not quite follow that the control system, designed for an ideally rigid rocket, will secure stability for a rocket with liquid oscillating in its tanks. If, to secure stability of an absolutely rigid rocket, it is necessary that the control system produce a phase gain, for example, up to frequency ω_0' (see Figure 3.12a), then to secure stability for a rocket with oscillating liquid, the phase gain should be produced up to a frequency ω_0''.

When the phase frequency characteristic of the controlled object is as shown in Figure 3.12b, then the phase gain of the control system

in the frequency range $[0, \omega_0'']$ is sufficient for the total phase characteristic $\varphi(\omega)$ not to cross the axis $\varphi=0$ in the negative direction for $A(\omega)\geqslant 1[L(\omega)\geqslant 0]$. In this case, the closed system will be stable.

The frequency ω_0'' will be larger than the natural frequency of the oscillations of liquid in tanks which, as we know , is inversely proportional to the square root of the tank diameter. For rockets, whose tank diameters are comparatively small, we usually have $\omega_0''>\omega_0'$. Therefore, in estimating the stability of a rocket with the oscillations of liquid in tanks taken into consideration, additional requirements are imposed on the control system in addition to those imposed on the control system of an ideally rigid rocket. These requirements consist of having to widen the frequency range in which a phase gain is to be produced from $[0, \omega_0']$ to $[0, \omega_0'']$.

If, however, the phase frequency characteristic $\varphi_{p.o}(\omega)$ has a phase lag as shown in Figure 3.12c, then the condition of phase gain up to a frequency ω_0'' is necessary but not sufficient. Still another condition has to be satisfied, namely, that at frequencies preceding ω_0'' the phase gain, produced by the control system, be greater than $\varphi_{lag}(\omega')$ i.e., that $\varphi_{AC}(\omega')>\varphi_{lag}(\omega')$. In this case, the phase characteristic of an open loop will cross the axis $\varphi=0$ in the negative direction with the condition (3.37) being satisfied, and the closed system will be stable. Sometimes the additional condition may state that the control system produce a phase lag from some frequencies. These additional conditions complicate considerably the requirements on the phase-frequency characteristics of the control system and may turn out to be impossible to satisfy.

If the requirements on the phase frequency characteristic of the control system $\varphi_{AC}(\omega)$, as formulated from the conditions for the stability of a rocket, are possible to realize, then the phase stabilization will be possible to accomplish. In this case, the controlled object is usually called structurally stable.

If the characteristic frequencies lie close together, then the phase stabilization may turn out to be impossible to accomplish, since at one frequency the control system might be required to produce a phase gain, and at another close-by frequency it might be required to produce a phase lag. In this case, the controlled object is referred to as structurally unstable.

The problem of stabilizing a liquid fuel rocket turns out to be even more complicated if in the characteristic polynomial $Q'(p)$ (3.34) there appear additional roots with a positive real part. The existence of such roots is due to the oscillations of liquid in tanks, and the existence conditions were stated in the preceding section. To secure stability of motion, it is necessary to change the dynamic properties of the controlled object in such a way that all the roots of the polynomial $Q'(p)$ that are due to the oscillations of liquid in tanks have negative real parts. The design methods of changing the dynamic properties of the controlled object to improve stability will be discussed in Section 7.

If it is impossible to secure stability by means of the phase stabilization, we then use the amplitude stabilization. The amplitude stabilization can be effected both by means of the control system and by design methods. The essence of amplitude stabilization can be stated as a requirement that in a given frequency range the inequality (3.37) be always satisfied; the phase frequency characteristic in this range may be arbitrary.

6. The Stability of a Closed System with an Ideal Control System

To simplify the process of solution, we assume that the rocket moves in air-free space. The equations of the perturbed motion of a

rocket with oscillating liquid (or a rod with pendulums) were obtained in Section 2. In air-free space they are

$$\begin{gathered} m\ddot{y}_C+\sum_{j=1}^{k} m_j^{\circ}\ddot{\lambda}_j-P_0\vartheta=R_{yp}^{\delta}\delta, \\ I\ddot{\vartheta}+\sum_{j=1}^{k} m_j^{\circ}L_j^{\circ}\ddot{\lambda}_j-g^{\circ}\sum_{j=1}^{k} m_j^{\circ}\lambda_j=-R_{yr}^{\delta}l_p\delta, \\ \ddot{\lambda}_j+\frac{g^{\circ}}{l^{\circ}}\lambda_j+L_j^{\circ}\ddot{\vartheta}+\ddot{y}_C-g^{\circ}\vartheta=0 \quad (j=1, 2,\ldots, k). \end{gathered} \tag{3.38}$$

Here we assumed that the natural frequency of all pendulums is the same: $\omega_\lambda^2=g^\circ/l^\circ$. In these equations the notation corresponds to that adopted in Section 2.

We shall assume that the control system is ideal. The differential equation of an ideal control system does not contain the derivatives $\dot{\delta}, \ddot{\delta}$, and the angle of rotation δ of the control element is determined from the equation [14].

$$\delta=k_0\vartheta+k_1\dot{\vartheta}+\frac{1}{g^{\circ}}k_2\ddot{y}_C. \tag{3.39}$$

where k_0, k_1, k_2 are the amplification coefficients of the control system.

For large frequencies the control system cannot be considered ideal. Equation (3.39) may contain important terms, proportional to $\dot{\delta}$ and $\ddot{\delta}$, that give rise to phase lag.

In estimating the stability of the closed system (3.38), (3.39), we shall make use of the technique presented in [11].

We shall assume that

$$y_C=Y_Ce^{pt}, \quad \vartheta=Ae^{pt}, \quad \lambda_j=B_je^{pt}.$$

Then the characteristic equation of the closed system (3.38), (3.39) will be

$$p^2(p^2+\omega_\lambda^2)^{k-2}(a_0p^6+a_1p^5+a_2p^4+a_3p^3+a_4p^2+a_5p+a_6)=0. \tag{3.40}$$

The roots of this equation that are the solution of $p^2 \equiv 0$ correspond to that perturbed motion in which $\vartheta = \lambda_j = 0$, and $y_c = (y_c)_0 + t(v_c)_0$. This is a steady-state translational motion of the rod with attached pendulums with constant velocity $(v_c)_0$. This is possible because the control system does not react to velocity $\dot{y}_c$. The resulting mismatch in displacement (velocity) $y_c(\dot{y}_c)$ must be eliminated by the channel controlling the lateral stability or the center of mass.

Here we shall determine only those conditions for which the closed system will be stable in the coordinates ϑ and λ_j.

The notation as before will be

$$\mu_1 = \frac{1}{m}\sum_{j=1}^{k} m_j^*, \quad \mu_2 = \frac{1}{I}\sum_{j=1}^{k} m_j^* L_j^{*2}, \quad \mu_3 = \frac{1}{m_0}\sum_{j=1}^{k} m_j^* L_j^*,$$
$$\frac{l_2}{h} = \bar{l}_p, \quad \omega_0 = \sqrt{\frac{\bar{I}}{m}}, \quad \bar{\rho} = \frac{\rho_0}{\rho}. \tag{3.41}$$

In addition, we set $R_{yp}^* = \sigma P_{ef}$, where σ is some coefficient less than one.

Then the coefficients of the third factor in the characteristic Equation (3.40) can be expressed by the following formulas:

$$a_0 = \bar{\rho}^2 \{(k_2/\sigma)(\bar{l}_p\mu_3 + \mu_2 - 1) + [(1-\mu_1)(1-\mu_2) - \mu_3^2]\},$$
$$a_1 = \omega_\lambda^2 (k_1/\sigma)\bar{\rho}[-\mu_3 + \bar{l}_p(1-\mu_1)],$$
$$a_2 = \omega_\lambda^2 \bar{\rho}\{\mu_3 + 2\bar{\rho} - \bar{\rho}\mu_1 - \bar{\rho}\mu_2 + (k_2/\sigma)(\bar{l}_p - \bar{l}_p\mu_1 - 2\mu_3 + \bar{\rho}\mu_2 + \bar{\rho}\bar{l}_p\mu_3 - 2\bar{\rho}) + (k_0/\sigma)(\bar{l}_p - \bar{l}_p\mu_1 - \mu_3)\},$$
$$a_3 = \omega_\lambda^4 (k_1/\sigma)(\mu_1 + 2\bar{l}_p\bar{\rho} - \bar{\rho}\bar{l}_p\mu_1 - \bar{\rho}\mu_2),$$
$$a_4 = \omega_\lambda^4 [\bar{\rho}^2 + \mu_2\bar{\rho} + (k_2/\sigma)(\mu_1 + 2\bar{l}_p\bar{\rho} - 2\bar{\rho}\mu_3 - \bar{l}_p\bar{\rho}\mu_1 - \bar{\rho}^2) + (k_0/\sigma)(\mu_1 + 2\bar{l}_p\bar{\rho} - \bar{\rho}\mu_3 - \bar{l}_p\bar{\rho}\mu_1)],$$
$$a_5 = \omega_\lambda^6 (k_1/\sigma)(\bar{l}_p\bar{\rho} + \mu_1),$$
$$a_6 = \omega_\lambda^6 (\bar{l}_p\bar{\rho} + \mu_1)[(k_2/\sigma) + (k_0/\sigma)].$$

We assume that

$$k_0 > 0, \ k_1 > 0, \ k_2 \geq 0, \ \sigma > 0, \ l_p > 0,$$
$$0 < \mu_1 < 1, \ 0 < \mu_2 < 1, \ -1 < \mu_3 < 1, \ 0 < \bar{\rho} < \infty.$$

To estimate the stability of motion and determine the boundaries of the stability regions, we shall make use of the Routh-Hurwitz stability criterion. According to the Hurwitz theorem [13], the necessary and sufficient condition for a polynomial of n^{th} degree Q(p) to have all roots with negative real parts is that the following inequality be satisfied

$$\Delta_1>0;\ \Delta_2>0,\ldots;\ \Delta_n>0, \tag{3.43}$$

where $\Delta_1, \Delta_2, \ldots, \Delta_n$ are the diagonal minors of the Hurwitz determinant.

The Hurwitz determinant and the diagonal minors have the following forms

$$\begin{vmatrix} a_1 & a_0 & 0 & 0 & 0 & 0 \\ a_3 & a_2 & a_1 & a_0 & 0 & 0 \\ a_5 & a_4 & a_3 & a_2 & a_1 & a_0 \\ 0 & a_6 & a_5 & a_4 & a_3 & a_2 \\ 0 & 0 & 0 & a_6 & a_5 & a_4 \\ 0 & 0 & 0 & 0 & 0 & a_6 \end{vmatrix},$$

$$\Delta_1=a_1,\ \Delta_2=\begin{vmatrix} a_1 & a_0 \\ a_3 & a_2 \end{vmatrix},\ \ldots,\ \Delta_6=a_6\Delta_5,$$

$$\Delta_5=\begin{vmatrix} a_1 & a_0 & 0 & 0 & 0 \\ a_3 & a_2 & a_1 & a_0 & 0 \\ a_5 & a_4 & a_3 & a_2 & a_1 \\ 0 & a_6 & a_5 & a_4 & a_3 \\ 0 & 0 & 0 & a_6 & a_5 \end{vmatrix}.$$

From inequalities (3.43), it follows in particular that all the coefficients of the polynomial Q(p) should be of the same sign, for example, $a_0>0, a_1>0, \ldots, a_6>0$.

Let us find the boundaries of the stability regions, determined by the roots of the third factor in Equation (3.40). These boundaries will be defined by the equations

$$a_0=0,\ \Delta_5=0.$$

An analysis of the coefficients shows that in our case the determinant Δ_5 can be represented as a product of four functions

$$\Delta_5 = C\psi_0\psi_1\psi_2\psi_3,$$

where C is a positive constant.

$$\begin{aligned}
\psi_0 &= \bar{l}_p\bar{\rho} + \mu_1,\\
\psi_1 &= \mu_1\mu_2 - \mu_3^2,\\
\psi_2 &= (k_2/\sigma)(\mu_1 + \bar{\rho}\mu_2 + \bar{l}_p\bar{\rho}\mu_1) + \mu_1^2 - \mu_1 - \bar{\rho}\mu_2,\\
\psi_3 &= -\bar{l}_p^2\bar{\rho}\mu_3 + \bar{l}_p(\bar{\rho}\mu_1 - \bar{\rho}\mu_2 - \mu_3) - (\mu_1\mu_2 - \mu_1 - \bar{\rho}\mu_3 - \mu_3^2).
\end{aligned} \tag{3.44}$$

The conditions $\psi_0>0$ and $\psi_1>0$ are always satisfied, and therefore, the boundaries of the stability regions are determined by setting to zero any one of the quantities ψ_2, ψ_3, a_0. In view of (3.44), utilizing notations of (3.41) and (3.42) these conditions can be written as

$$\frac{k_2}{\sigma}\left[\bar{\rho}\sum_{j=1}^{n}\bar{m}_jL_j + (1+\bar{l}_p\bar{\rho})\sum_{j=1}^{n}\bar{m}_j\right] + \left(\sum_{j=1}^{n}\bar{m}_j - 1\right)\sum_{j=1}^{n}\bar{m}_j - \bar{\rho}\sum_{j=1}^{n}\bar{m}_jL_j = 0, \tag{3.45}$$

$$\left(\sum_{j=1}^{n}\bar{m}_j + \bar{l}_p\right)\sum_{j=1}^{n}\bar{m}_jL_j^2 + \left(\bar{l}_p\bar{\rho} + \bar{l}_p - \bar{\rho} - \sum_{j=1}^{n}\bar{m}_jL_j\right)\sum_{j=1}^{n}\bar{m}_jL_j - (\bar{l}_p\bar{\rho}+1)\sum_{j=1}^{n}\bar{m}_j = 0, \tag{3.46}$$

$$\frac{k_2}{\sigma}\left(\sum_{j=1}^{n}\bar{m}_jL_j^2 + \bar{l}_p\sum_{j=1}^{n}\bar{m}_jL_j - 1\right) + \left(\sum_{j=1}^{n}m_j - 1\right)\sum_{j=1}^{n}\bar{m}_jL_j^2 - \left(\sum_{j=1}^{n}\bar{m}_jL_j\right)^2 - \sum_{j=1}^{n}\bar{m}_j + 1 = 0. \tag{3.47}$$

Here $L_j = L_j^*/\rho_0$, $\bar{m}_j = m_j^*/m$. The condition $a_3>0$ will be satisfied if $a_1>0$. The condition $a_0>0$ follows from the condition $k_1>0$ which was assumed earlier.

If in the third factor of the characteristic Equation (3.40) we set $p = i\omega$ and construct the real and imaginary parts of the Mikhaylov function [5], then in view of the fact that the roots of the real and imaginary parts of the function alternate it follows that the following inequality should be satisfied.

$$\mu_3(\bar{l}_p\bar{\rho}+1)+\mu_4\bar{m}_p>0,$$

which must be considered if $\mu_3<0$.

In the region of stability one should have: $a_0>0, \psi_2>0, \psi_3>0$ or $a_0<0, \psi_2<0, \psi_3<0$.

The boundaries of the stability regions, defined by (3.45) - (3.47) are conveniently considered as surfaces in a k-dimensional space spanned by $\bar{L}_j$. The quantities $\bar{\rho}, \bar{m}_p, \bar{l}_p$ are fixed parameters. It is important to note that the equations of these surfaces do not contain k_0 and k_1. These surfaces depend on the parameter k_2, i.e., on the amplification coefficient multiplying $\ddot{y}_c$ in the equation of the control system (3.39).

A detailed analysis of the surface Equations (3.45) - (3.47) shows that there is a surface which does not move with a change in k_2 and space of $\bar{L}_j$. This surface is determined by Equation (3.46). The surface defined by Equation (3.47) determines the family of second-order surfaces with the same parameter k_2. Changing the amplification coefficient k_2, one can considerably deform the stability regions of the system.

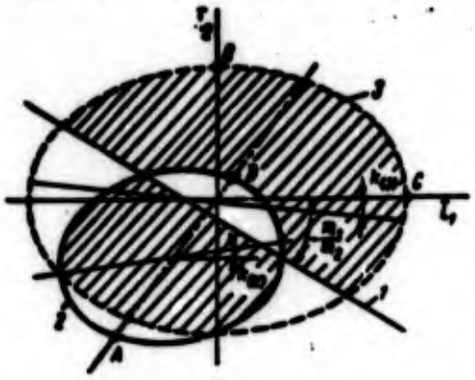

Figure 3.13

Let us consider in more detail the case when the rocket has two tanks. In this case the space of $\bar{L}_j$ degenerates into a plane, and the boundaries of the stability regions become plane curves. The stability boundaries in the coordinates L_1 and $L_2 = 2$ and

$k_2 = 2$ are shown in Figure 3.13. The regions of stability are shaded.

The condition (3.45) gives the following equation for the straight line 1 (see Figure 3.13):

$$L_2 = -\frac{\bar{m}_1}{\bar{m}_2} L_1 - \left[\left(\bar{m}_1 \bar{\rho} \bar{m}_2 + \frac{1}{\bar{\rho}}\right) - \frac{(\bar{m}_1 + \bar{m}_2)^2}{\bar{\rho} \bar{m}_2}\right].$$

The condition (3.46) gives an equation for Ellipse 2 with the coordinates of the center

$$L_1 = L_2 = \frac{\bar{\rho} - \bar{T}_p - T_p^2 \bar{\rho}}{2 \bar{T}_p}.$$

The major axis of this ellipse has an angular slope coefficient

$$k_{(2)} = \frac{1}{2\bar{m}_1 \bar{m}_2}\left[\bar{T}_p (\bar{m}_2 - \bar{m}_1) + \sqrt{\bar{\rho}^2 T_p^2 (\bar{m}_2 - \bar{m}_1)^2 + 4\bar{m}_1 \bar{m}_2}\right].$$

The condition (3.47) gives an equation for Ellipse 3 with the center at the origin of the coordinates and with the angular coefficient of the major axis

$$k_{(3)} = \frac{1}{2\bar{m}_1 \bar{m}_2}\left[(\bar{m}_2 - \bar{m}_1) - \sqrt{(\bar{m}_1 - \bar{m}_2)^2 + 4\bar{m}_1 \bar{m}_2}\right].$$

The coordinates of the characteristic points A, B, C, D have the following values:

$$A\left(-\frac{1 + T_p \bar{\rho}}{\bar{\rho}}, -\frac{1 + T_p \bar{\rho}}{\bar{\rho}}\right), \quad B\left(0, \sqrt{\frac{1 - \bar{m}_1 - \bar{m}_2}{\bar{m}_2 (1 - \bar{m}_1)}}\right),$$

$$C\left(\sqrt{\frac{1 - \bar{m}_1 - \bar{m}_2}{\bar{m}_1 (1 - \bar{m}_2)}}, 0\right), \quad D\left(\frac{1}{T_p}, \frac{1}{T_p}\right).$$

In particular, when the pendulum masses are identical, i.e., when $\bar{m}_1 = \bar{m}_2 = \bar{m}_0$, the expressions for the angular coefficients become simplified. Then

$$L_2 = -L_1 + \frac{2}{\bar{\rho}}, \quad k_{(2)} = 1, \quad k_{(3)} = -1.$$

The slope angle of the straight line 1 turns out to be $-\pi/4$, and the two ellipses diverge also at an angle of $-\pi/4$.

The squares of the ellipse semiaxes will be:
for Ellispe 2

$$a^2=\frac{(\bar{I}_0+\bar{T}_0^2\bar{\rho}+\bar{\rho})^2}{2\bar{\rho}\bar{I}_0(\bar{\rho}\bar{I}_0+2\bar{m}_0)},\quad b^2=\frac{(\bar{I}_0+\bar{T}_0^2\bar{\rho}+\bar{\rho})^2}{2\bar{\rho}^2\bar{T}_0^2};$$

for Ellipse 3

$$a^2=\frac{1}{\bar{m}_0},\quad b^2=\frac{1-2\bar{m}_0}{\bar{m}_0}.$$

If the amplification coefficient $k_2 \neq 0$, then to Equation (3.45) there will correspond a family of straight lines 1, to Equation (3.46)- Ellipse 2, and to Equation (3.47) — a family of Curves 3 of second order.

For the case when

$$\frac{\bar{\rho}_2}{\bar{\rho}}-1-\bar{m}_1-\bar{m}_2<0,$$

the curves plotted in the $\bar{L}_1$, $\bar{L}_2$ - coordinates are shown in Figure 3.14. The stability regions are shaded. We remember that L_1^* is the distance between the center of mass of the system and mass m_1^* of the first (upper) pendulum; $\bar{L}_2^*$ is the distance between the center of mass of the system and the mass m_2^* of the other (lower) pendulum. If the mass m_2^* is located below the center of mass, then $L_2^\circ<0$. When the position of pendulums on the rod is such that a point with coordinates $(L_1^\circ/\rho_0, L_2^\circ/\rho_0)$ is located in the shaded region, then the closed system (3.38), (3.39) will be stable.

An estimate of the stability of motion of the rod with pendulums, assuming the properties of the control system are given analytically, can be made using a method worked out by B. I. Rabinovich [6]. This method is based on an analysis of the geometric properties of the

hodographs for complex transfer numbers of an open loop $K(i\omega)$, consisting of the controlled object $K_{p.o}(i\omega)$ and the stabilizer $K_{AC}(i\omega)$, and on applying the Nyquist frequency criterion.

In contrast to Section 5, where the transfer function of the controlled object (rocket) with the oscillating liquid is represented as a product of transfer functions, in [6] it is shown that in the neighborhood of the roots of the characteristic equation of the controlled object, the transfer function of an open loop can be decomposed into a sum of simple fractions

$$K(p)=\sum_{s=0}^{s_0}\frac{2\alpha_s-\beta_s\Omega_s}{p^2+2\alpha_s p+\Omega_s^2}, \qquad (3.48)$$

where α_s, Ω_s are the damping coefficient and the frequency of the natural oscillations of an s^{th} oscillator; α_s and β_s are some coefficients. An oscillator is usually defined as a system (circuit) whose natural oscillations are described by the equation

$$\ddot{x}+2\alpha\dot{x}+\omega^2 x=0.$$

According to this decomposition, the block diagram of a closed system can be constructed of parallel circuits — each consisting of two transfer functions, the transfer function of the controlled object $[K_{p.o}(p)]_s$ and the transfer function of the stabilizer $[K_{AC}(p)]_s$, $s = 0, 1, 2, \ldots, s_0$. Such a block diagram is shown in Figure 3.15.

As before we shall select a characteristic point C (1,i0) in the complex plane. Then the characteristic equation of the closed system for an s^{th} circuit will be

$$K_s(p)-1=0.$$

In view of (3.48) we get

$$p^2+2(\alpha_s-\alpha_s)p+\omega_s^2+\beta_s\alpha_s=0 \quad (s=0, 1, 2,\ldots s_0).$$

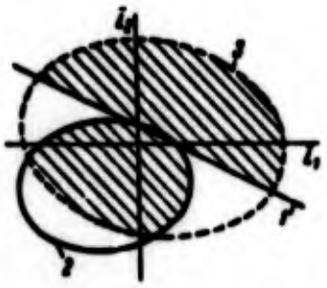

Figure 3.14

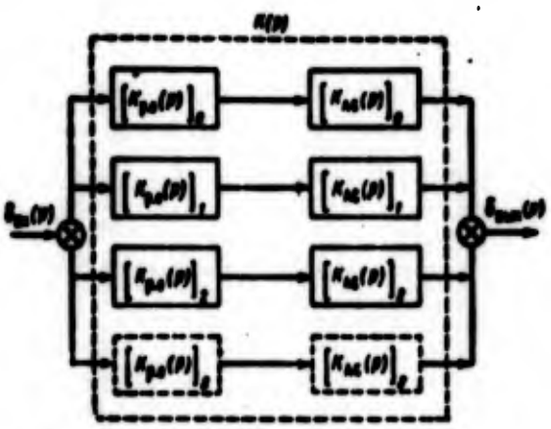

Figure 3.15

The roots of this equation are

$$p_{1,2} = -\varepsilon_0\left(1-\frac{\alpha_1}{\varepsilon_0}\right) \pm i\omega_0\sqrt{1+\frac{\lambda_1}{\omega_0}}.$$

If the stability of each circuit in the block diagram can be considered independently, then the stability conditions of the closed system will be

$$\begin{aligned} &\frac{\alpha_1}{\varepsilon_0} < 1 \quad \text{for} \quad \varepsilon_0 > 0, \\ &\frac{\alpha_1}{\varepsilon_0} > 1 \quad \text{for} \quad \varepsilon_0 < 0 \end{aligned} \tag{3.49}$$

For a given object of control, α_0/ε_0 can be changed only by modifying the properties of the control system; therefore, conditions (3.49) can be viewed as requirements that are imposed on the phase frequency and amplitude frequency characteristics of the control system. If these requirements can be satisfied by selecting the phase frequency characteristic $\varphi_{AC}(\omega)$ for all s = 0, 1, 2, ..., s_0 then the phase stabilization is possible to accomplish. The controlled object will be in this case structurally stable.

Methods of constructing regions of the system parameters where the system is either stable or unstable are presented in [10, 11, 12].

7. Structural Methods of Improving Stability

Section 5 showed that sometimes it is difficult to secure stability of a liquid-fuel rocket. In such cases amplitude stabilization is used which requires that (3.37) be satisfied in some frequency range

$$A(\omega)=A_{p.o}(\omega)A_{AC}(\omega)<1.$$

If $\omega_1>\omega_0$, where ω_0 is the frequency at which the phase lag of the control system is zero, then (3.37) should be satisfied for $\omega>\omega_1$. In other words, for $\omega_1>\omega_0$ it is necessary that in the natural frequency range of the liquid the modulus of the complex transfer number of the entire open loop $A(\omega)$ be less than one. In this situation no restrictions are imposed on the phase frequency characteristic for $\omega>\omega_0$.

Let us consider structural methods of lowering $A_{p.o}(\omega)$ in the frequency range of natural oscillations of a liquid. The methods can be based on solving and analyzing the hydrodynamic equations and consist mainly of modifying the design of fuel tanks.

All structural modifications to secure a better stability of a liquid-fuel rocket seek to fulfill three objectives: 1) to increase the dissipation of energy from the oscillating liquid; 2) to decrease the reduced mass in order to weaken the total dynamic effect on the oscillations even with small dissipation of energy. Usually a decrease in reduced mass is accompanied by an increase in the natural frequency of the oscillations of liquid; 3) to change the natural frequency of the oscillations of the liquid.

An increase in the energy dissipation from the oscillating liquid can be achieved by means of various devices in the form of floats that are placed on the free surface of the liquid. The floats

usually are in the shape of rings (toruses). They break up the free surface into small segments thus, intensifying the energy dissipation from the oscillating liquid. The energy is dissipated when the liquid moves against the walls of the floats.

As an example Figure 3.16 shows the plots of the calculated and experimental values of the amplitude of the lateral force F_y^0, due to the forced transverse oscillations of the cylindrical tank having an amplitude y_c, versus the frequency. The plots are taken from [14]. The experimental values are shown as dots for two different dampers floating on the surface: one being a ring and the other being a body with a large number of openings. The calculated curves were obtained for different values of the relative damping coefficient ξ:

$$\ddot{\lambda} + 2\varepsilon_1\dot{\lambda} + \omega_1^2\lambda = y_c \sin pt.$$

The same figure for comparison shows a graph of the force that would appear if the liquid were to be considered "frozen".

$$\left|\frac{F_y^0}{y_c}\right| = p^2 m.$$

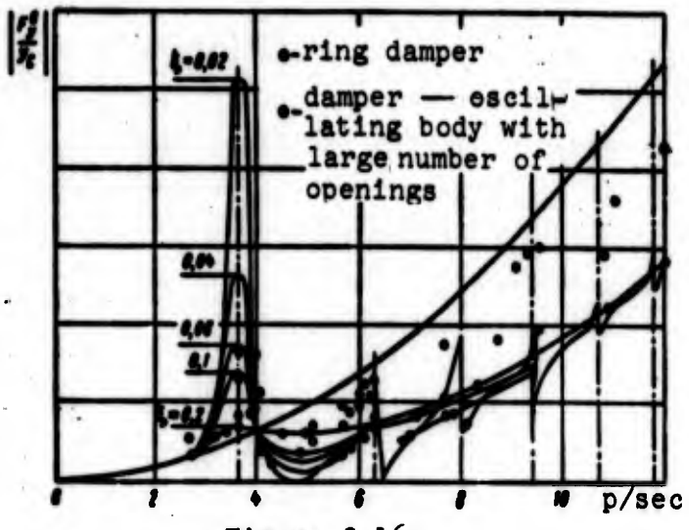

Figure 3.16

As we see at $\xi \approx 0.2$ for the resonance frequency of the first tone, the amplitude of the force is limited by a number slightly exceeding the force due to the "frozen" liquid. Thus, when effective floating dampers are used the amplitude frequency characteristics of a liquid-fuel rocket will hardly differ from the frequency characteristics of an ideally rigid rocket.

The value of the reduced mass of the oscillating liquid and its distribution depend on the geometry of the tank and the submerged height. The Formulas (2.62) and (2.43) for the reduced mass and the natural frequency of the liquid imply that, as the radius of the tank decreases, the mass also gets smaller, and at the same time the natural frequency of the liquid rises.

A decrease in the reduced mass of the oscillating liquid leads to a lowering of the dynamic effect that the liquid has on the fuselage of the rocket, and other conditions being equal, the diameter of the circle of the amplitude-phase frequency characteristic will be smaller. Thus, more suitable conditions are created for an amplitude stabilization.

An increase in the natural frequency of the liquid and the accompanying change in the frequency of the system may make phase stabilization more difficult. Therefore, even with a change in the geometry of the tanks optimum results may not always be achieved. A change in the amplitude-phase frequency characteristic may be advantageous in one area and disadvantageous in another.

Some suggestions for changing the design of fuel tanks to improve the stability of liquid-fuel rockets are presented in [14].

The geometry of the tank can be modified in several ways: 1) a tank with a large diameter may be replaced by several tanks with smaller diameters, 2) inside a tank of a large diameter we can set up cylindrical partitions — make a tank inside a tank, 3) the tank might be subdivided into separate compartments by means of radial or radial and cylindrical partitions creating a sectored tank (see Figures 2.14, 2.17).

If, for example, a cylindrical tank of radius r_0' is replaced by four tanks of radius r_0'' with the same total cross section ($r_0'' = r_0'/2$), then the reduced mass of liquid in all four tanks will be twice as small as that in one tank of radius r_0'. The natural frequency of liquid is in this case increased 1.41 times.

Subdividing the tank into k identical tanks, the natural frequency of liquid increases basically proportionally to the fourth-degree root of the number of tanks

$$\frac{\omega_n^{(k)}}{\omega_n^{(1)}} = \sqrt[4]{k} \sqrt{\frac{\operatorname{th}\left(\zeta_n \sqrt{k} \frac{h}{r_0}\right)}{\operatorname{th}\left(\zeta_n \frac{h}{r_0}\right)}}.$$

and the reduced mass of the oscillating liquid decreases inversely proportionately to the square root of the number of tanks

$$\frac{m_n^{(k)}}{m_n^{(1)}} = \frac{1}{\sqrt{k}} \sqrt{\frac{\operatorname{th}\left(\zeta_n \sqrt{k} \frac{h}{r_0}\right)}{\operatorname{th}\left(\zeta_n \frac{h}{r_0}\right)}}.$$

If the tank is subdivided by means of a circular cylindrical partition, then the oscillations of liquid will have their smallest effect in the case when the reduced masses in the ring-like and the circular (internal) tanks are approximately equal, and the phases of their forced oscillations are opposite. In this case, the dynamic action of liquid on the ring-like and circular tanks is mutually balanced. When the ratio of the diameters of the internal and external cylinders is $\beta = 0.77$, the reduced masses are approximately equal. However, the natural frequencies of the liquid in tanks are such that the phases of the forced oscillations of the reduced masses of liquid are not very advantageous. Mutual balance is not achieved. When the ratio of the diameters is $\beta = 0.5$, the phases of forced oscillations are favorable, but the reduced masses of the oscillating liquid are in the ratio 1:5.

It is much more convenient to subdivide the tank by means of radial partitions. Figure 3.17 shows for comparison graphs of the reduced masses of the oscillating liquid for three forms of cylindrical tanks. A tank with a circular cross section is one that is most disadvantageous. In this case, the reduced mass for the first tone is $1.43\ \rho r_0^3$ which approximately corresponds to a mass of liquid in a cylindrical tank of height $0.5\ r_0$. When a concentric partition is used with a diameter equal to one-half of the diameter of the tank ($\beta = 0.5$), the reduced mass is $\sim 0.96\ \rho r_0^3$ if only the external tank is filled, and $1.14\ \rho r_0^3$ if both tanks are filled. If use is made of radial partitions (four-sectored tank) the reduced mass for the first tone is only $0.46\ \rho r_0^3$. If the reduced masses for the first tone in all four sectors are put together and compared with the reduced mass m_n for the first tone of oscillations in a cylindrical tank with a circular cross section, then the sum would amount to less than one-half of m_n.

In the case of a four-sectored tank the reduced mass, corresponding to the second natural frequency, amounts to almost one-half of the reduced mass for the first tone, and must be taken into consideration in analyzing the stability of motion.

To increase the dissipation of energy from the oscillating liquid, the tanks are usually subdivided by means of perforated partitions rather than solid ones, i.e., partitions with a large number of holes. As a result of a pressure drop between separate sectors of the tank, the drop being due to oscillations, the liquid flows through the perforated partitions, and thus the kinetic energy of the liquid is dissipated.

When perforated partitions are set up the natural frequency and the reduced mass of the oscillating liquid are modified. However, the main effect of the perforated partitions consists in a significant increase of the damping coefficient.

Sometimes the stabilization of liquid fuel in tanks by means of the control system is hard to achieve only for a small time segment.

In such cases stabilization is facilitated very easily by structural means. For this purpose it is necessary to set up in a tank a partition with holes — an intermediate perforated bottom — perpendicular to the longitudinal axis of the tank. As the free surface of liquid fuel approaches the intermediate bottom, the reduced mass and the natural frequency rapidly decrease, and the energy dissipation from the fluid increases. Within a small time interval the effect of the oscillations of the free surface can be practically reduced to zero.

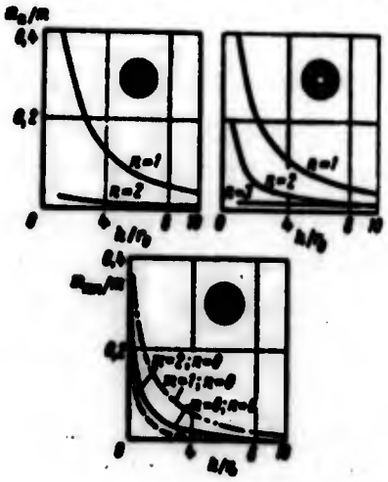

Figure 3.17

8. Auto-oscillations of the Rocket

In Section 5 we formulated additional requirements on the control system to help in stabilizing the closed system. The amplitude-phase frequency characteristic of an open loop, shown in Figure 3.18a, corresponds to a stable closed system. The characteristic of a statically stable rocket has such a form.

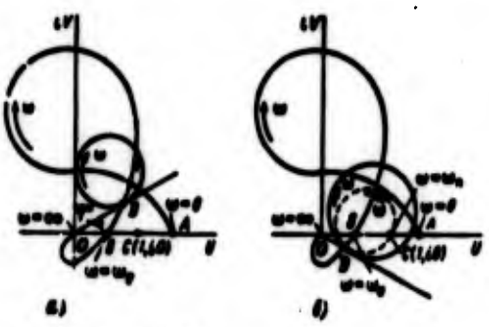

Figure 3.18

In view of the fact that the characteristic polynomial Q(p) of a statically stable rocket has one positive root, point A ($\omega = 0$) is located to the right of point C(1,i0), and point B($\omega = \omega_0$) is located to

the left of point C. The frequency characteristic encircles point C half way in the positive direction; the closed system is stable.

Point D on the frequency characteristic lies in the frequency interval in which the dynamic properties of the oscillating liquid appear. In this interval the natural frequency of the oscillations of liquid in tanks is located. Instead of two rings, as shown in Figure 3.9, here (not to obscure the diagram) we only have one ring of the frequency characteristic, corresponding to the relative position of frequencies in (3.30). At the natural frequency of liquid for such a position of frequencies, a gain in phase φ^* does not decrease.

Figure 3.18,b, shows the amplitude-phase frequency characteristic of an open loop, corresponding to an unstable closed system. The frequency characteristic crosses the real axis in the negative direction to the right of point C (1,i0). This is due to the fact that in this case the additional requirement on the control system is not satisfied. The control system is supposed to secure a phase gain up to higher frequencies than the natural frequency of the liquid. The given frequency characteristic does not satisfy this requirement, since the frequency at D is larger than the frequency at $B(\omega=\omega_1)$.

Suppose that the system we are discussing is unstable (see Figure 3.18b). Random oscillations of the system will begin to increase, and nonlinear effects will appear that may be due to the control actuator and the oscillations of the liquid itself. When the amplitude of oscillations increases, the amplification coefficient of the control actuator is lowered, and the equivalent damping coefficient of natural oscillations of liquid is increased. This means that, as the amplitude of oscillations increases, the modulus of the complex transfer number of an open loop will decrease until the frequency characteristic passes through point C(1,i0) (limiting cycle). Further increase of the amplitude does not occur, and in the system stationary

periodic oscillations are set up with frequency ω_p and amplitude a_p (auto-oscillations). The frequency of periodic oscillations ω_p lies in the frequency interval of point D, and therefore differs little from the natural frequency of liquid ω_λ.

For small perturbations the stationary oscillations of liquid with amplitude a_p are stable. In fact if the system is acted upon in such a way that the amplitude becomes greater than a_p, then the energy dissipation from the oscillations intensifies, and the amplification coefficient of the control actuator decreases. There will be a decrease in the modulus of the complex transfer number, and the frequency characteristic in the neighborhood of ω_λ will not cross the real axis to the right of point C(1,i0). The system will become stable, the amplitude will start decreasing, and the modulus of the complex transfer number will increase until the ring of the frequency characteristic passes through point C(1,i0) corresponding to periodic oscillations.

In auto-oscillations all loops of the oscillating system execute oscillations with the same frequency ω_p. The amplitudes of the oscillations in various loops (generalized coordinates) such as the control current, control elements, the fuselage, and liquid in tanks are different and can be determined only if the nonlinear properties of the system are taken into consideration. This is usually done on analog computers. The amplitudes of the fuselage vibrations are small. The question, however, whether the auto-oscillations should be allowed can only be answered if the fuselage strength is taken into consideration.

REFERENCES

1. Abramsov, Gartsa, Kana. Motion of liquid in cylindrical tanks subdivided into compartments. Raketnaya tekhnika, No. 6, 1962.

2. Kolesnikov, K. S. On the peculiar properties of a certain pendulum system. PMM. Iadatel'stvo AN SSSR, No. 4, 1962.

3. Kolesnikov, K. S. Oscillations of liquid in a cylindrical vessel.

4. Lyukens. Methods of analyzing the control system of a large elastic rocket, Voprosy raketnoy tekhniki, No. 9, 1961.

5. Popov, Ye. P. Dinamika sistem avtomaticheskogo regulirovaniya (The dynamics of the control system.) Gostekhizdat, 1954.

6. Rabinovich, B. I. A study of the stability of mechanical systems with a large number of the degrees of freedom. Izv. AN SSSR, Tekhnicheskaya Kibernetika, No. 4, 1964.

7. Rabinovich, B. I. Dokuchayev, L. V. and Z. M. Polyakova. On calculating the coefficients of the equations of the perturbed motion of a rigid body with cavities partially filled with liquid. Kosmicheskiye issledovaniya, Izdatel'stvo Nauka, Vol. III, No. 2, 1965.

8. Rapoport, I. M. Dinamika uprugogo tela, chastichno sapolnennogo zhidkost'yu (Dynamics of an elastic body partically filled with liquid). Mashgiz, 1967.

9. Rumyantsev, V. V. Equations of motion of a rigid body with cavities partially filled with liquid. PMM, Vol. 18, No. 6, 1954.

10. Sidorov, I. M. and I . P. Korotayeva. The stability of mechanical systems with many degrees of freedom and a presence of a control system. Izv. AN SSSR, Tekhnicheskaya Kibernetika, No. 4, 1965.

11. Tsurikov, Yu. A. On the stability of the motion of a rod with pendulums. Izdatel'stvo AN SSSR, Mekhanika tverdogo tela. No. 3, 1966.

12. Cheremnykh, S. V. Some problems of the stability of the rigid body with a liquid filler. Izdatel'stvo An SSSR, Mekhanika tverdogo tela, No. 3, 1966.

13. Chetayev, N. G. Ustoychivost' dvizheni (Stability of motion). Gostekhizdat, 1955.

14. Bauer, H. F. Fuel oscillations in rocket tanks and their effect on the total stability. Zeitschrift fur Flugwissenschaften, Vol. 12, No. 3, 1964.

CHAPTER IV

LATERAL VIBRATIONS OF A ROCKET AS AN INHOMOGENEOUS ELASTIC ROD

For the sake of analyzing the lateral vibrations, the fuselage of the rocket is usually replaced by a straight inhomogeneous elastic rod. The main goal of the present chapter is to study forced vibrations of a rod that are determined by particular solutions of equations. The actual solution of the problem is usually preceded by determining the modes and frequencies of the natural vibrations.

1. An Equation of the Lateral Vibrations of a Straight Inhomogeneous Rod.

Let EJ(x) denote the bending stiffness, m(x)-the linear mass, l-the length of the rod. Neglecting displacements along the longitudinal axis and assuming that the vibrations take place in the plane of symmetry of the rod, we shall set up the equation of the lateral motion of a rod element of length dx in a fixed frame of reference xOy (Figure 4.1). We obtain

$$m(x)\frac{\partial^2 y}{\partial t^2} = -\frac{\partial Q}{\partial x} + q(x, t),$$

where q(x,t) is the intensity of the external lateral distributed force acting on the rod in the xOy plane; y(x,t) is a displacement in the Oy direction perpendicular to the undeformed axis of the rod; Q is the lateral force at a cross section whose abscissa is x.

Neglecting the rotational inertia of a rod element we write an equation of the moment of force, acting on a separated element. Retaining only first-order infinitesimals, we get

$$\frac{\partial M}{\partial x}dx = Qdx. \tag{4.1}$$

Here M is the bending moment at a cross section whose abscissa is x.

Let us use the Voigt hypothesis [1] according to which tension c depends not only on the strain ε but also on the rate of strain $\partial\varepsilon/\partial t$, i.e.

$$\sigma = E\left(\varepsilon + h\frac{\partial \varepsilon}{\partial t}\right).$$

Here h is the friction coefficient.

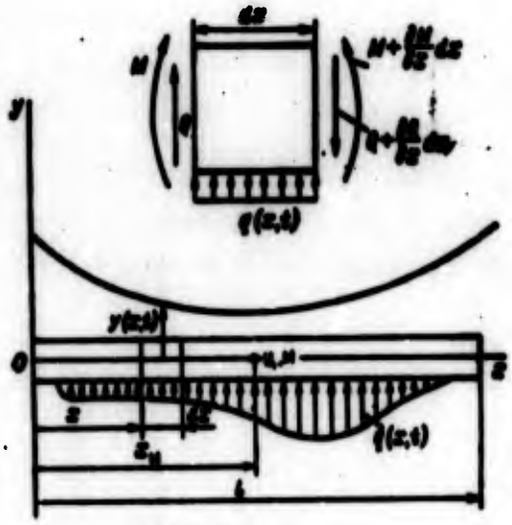

Figure 4.1

Bending strain is

$$\varepsilon = -\tilde{y}(x)\frac{\partial^2 y(x,t)}{\partial x^2},$$

where $\tilde{y}(x)$ is the distance between the neutral rod axis and the fiber in question. Then

$$\sigma = -E\left(1 + h\frac{\partial}{\partial t}\right)\tilde{y}(x)\frac{\partial^2 y(x,t)}{\partial x^2}.$$

We shall assume that h = const. The bending moment is

$$M = -\int_F \sigma\tilde{y}(x)dF = \left(1 + h\frac{\partial}{\partial t}\right)EJ(x)\frac{\partial^2 y(x,t)}{\partial x^2}. \tag{4.2}$$

Eliminating the lateral force Q and the bending moment M, we obtain the differential equation of the lateral vibrations of the rod

$$\left(1 + h\frac{\partial}{\partial t}\right)\frac{\partial^2}{\partial x^2}\left[EJ(x)\frac{\partial^2 y}{\partial x^2}\right] + m(x)\frac{\partial^2 y}{\partial t^2} = q(x,t). \tag{4.3}$$

Let us first consider the case when q(x,t) = 0. A general solution of Equation (4.3) can be represented in the form

$$y(x,t)=\sum_{n=1}^{\infty} f_n(x)q_n(t), \tag{4.4}$$

where $f_n(x)q_n(t)$ are particular solutions of Equation (4.3) which can be determined by the Fourier method. Substituting (4.4) into (4.3) and separating the variables, we get

$$\frac{[EJ(x)f_n'']''}{m(x)f_n}=-\frac{\ddot{q}_n}{q_n+h\dot{q}_n}=-\omega_n^2 \quad (n=1,2,\ldots)$$

or

$$\ddot{q}_n+2\varepsilon_n\omega_n\dot{q}_n+\omega_n^2q_n=0 \quad (n=1,2,\ldots), \tag{4.5}$$

$$(EJ(x)f_n'')''-\omega_n^2m(x)f_n=0 \quad (n=1,2,\ldots). \tag{4.6}$$

where

$$\frac{d}{dx}(\ )=(\ )', \quad h\omega_n=2\varepsilon_n.$$

At either end of a free rod the bending moment M and the lateral force Q are zero. Therefore, on the basis of (4.1), (4.2), and (4.4) functions $f_n(x)$ should satisfy the following boundary conditions:

$$f_n''(0)=0; \quad [EJ(x)f_n''(x)]'_{x=0}=0, \tag{4.7}$$

$$f_n''(l)=0, \quad [EJ(x)f_n''(x)]'_{x=l}=0. \tag{4.8}$$

Conditions (4.8) can be put in another form. In view of (4.7) and (4.8), we get

$$\int_0^l (EJ(x)f_n'')''\,dx=0, \quad \int_0^l (EJ(x)f_n'')''(x-x_m)\,dx=0, \tag{4.9}$$

where x_M is the coordinate of the center of mass of the rod.

From Equation (4.6) and also considering (4.9), we find

$$\int_0^l m(x) f_n dx = 0, \quad \int_0^l m(x) f_n(x - x_m) dx = 0. \tag{4.10}$$

The equations in (4.10) correspond to the two boundary conditions (4.8). The physical meaning of these equations is that the resultant of all forces of inertia and the moment of these forces for vibrations of form $f_n(x)$ are equal to zero.

Equation (4.6) is an ordinary differential equation for the bending of a rod under a distributed load $\omega^2_n m(x) f_n$, equal to the forces of inertia on the mass of the rod. To obtain nontrivial solutions of Equation (4.6), satisfying the boundary conditions (4.7) and (4.8) is equivalent to solving the classical Sturm-Liouville problem.

Equation (4.5) shows that the natural vibrations of a rod, when internal friction is present, are damped everywhere.

The Voigt hypothesis is, generally speaking, not confirmed by experiment, but it is convenient for a qualitative analysis of the behavior of the system.

The energy dissipation in elastic vibrations of structures takes place mainly as a result of friction between the adjoining parts of the structure . Ye. S. Sorokin [1] proposed a hypothesis to take care of structural friction in the differential equations. According to this hypothesis the internal friction in elastic harmonic vibrations is proportional to the elastic restoring force, but is out of phase by the angle $\pi/2$. If the complex representation of simple harmonic motion is used, then instead of (4.2) the bending moment can be expressed by the following formula:

$$M = \left(1 + i\frac{\psi}{2\pi}\right) EJ(x) \frac{\partial^2 y}{\partial x^2}, \tag{4.2a}$$

where ψ is the coefficient of energy absorption due to vibrations, equal to the ratio of energy absorbed during one cycle, ΔW, to the total energy of the system, W. In harmonic oscillations, the

absorption coefficient is equal to twice the decrement, δ of free oscillations [1], so that

$$\psi = \frac{\Delta W}{W} = 2\delta.$$

Formula (4.2a) turns out to be accurate enough if ψ is small. The region of application of this formula should, apparently, be limited to oscillations induced by a harmonic force.

The differential equation of lateral vibrations of the rod with Sorokin's hypothesis taken into account will instead of (4.3) have the following form

$$\left(1+i\frac{\psi}{2\pi}\right)\frac{\partial^2}{\partial x^2}\left[EJ(x)\frac{\partial^2 y}{\partial x^2}\right]+m(x)\frac{\partial^2 y}{\partial t^2}=p(x)e^{i\omega t}. \qquad (4.3a)$$

The question of the forces of internal friction will be discussed in more detail in Section 5, Chapter 5.

2. The Properties of the Modes and the Frequencies of Natural Vibrations

In theory of vibrations the eigenfunctions of problems (4.6) - (4.8) are often called natural vibrational modes, and the eigenvalues are referred to as natural frequencies. Let us formulate shortly the most important properties of the eigenfunctions and eigenvalues (for proofs see [9, 16]).

1. There exists an infinite set of various natural frequencies $\omega_N (N = \mathrm{I}, \mathrm{II}, \mathrm{II}+n, n = 1, 2, \ldots)$. For a free rod among this set of frequencies there are two zero frequencies: $\omega_{\mathrm{II}}=0$ and $\omega_{\mathrm{I}}=0$ that are characteristic of a rod as a rigid body.

Integrating Equation (4.6) for $\omega^2_{\mathrm{II}}=0$ and boundary conditions (4.7) and (4.8), we obtain up to a multiplicative constant the following eigenfunctions

$$f(x)=f_{\mathrm{I}}(x)+f_{\mathrm{II}}(x), \quad f_{\mathrm{I}}(x)=1, \quad f_{\mathrm{II}}(x)=\frac{1}{x_m}(x-x_m). \qquad (4.11)$$

The frequencies ω_n ($n = 1, 2, \ldots$) are characteristic of rod vibrations. All these frequencies are real and positive, and $\omega_n \neq \omega_m$ if $n \neq m$. Each of the frequencies ω_n has a natural vibrational mode $f_n(x)$.

2. All natural vibrational modes are orthogonal, with a weight function $m(x)$. This is not hard to show using Equation (4.6) and the boundary conditions (4.7) and (4.8).

Integration by parts gives

$$\int_0^l (EJ(x) f_n'')'' f_m \, dx = \int_0^l EJ(x) f_n'' f_m'' \, dx. \tag{4.12}$$

Let us choose two arbitrary natural mnumbers n and m, where $n \neq m$. We write Equation (4.6) for a fixed index n. Let us multiply this equation by a function $f_m(x)$. Then we write Equation (4.6) for index m and multiply it by $f_n(x)$. Now let us subtract the second equation from the first and integrate over x between 0 and l. Then, in view of (4.12), we obtain

$$(\omega_m^2 - \omega_n^2) \int_0^l m(x) f_n f_m \, dx = 0.$$

In asmuch as for $n \neq m$ the frequency $\omega_n \neq \omega_m$, we have

$$\int_0^l m(x) f_n f_m \, dx = 0 \quad (n \neq m). \tag{4.13}$$

This is indeed the orthogonality condition for natural vibrational modes.

The conditions for the orthogonality of $f_I(x)$ and $f_{II}(x)$ with each of $f_n(x)$ will be expressed by (4.11) and (4.13) Formulas (4.10). The fact that f_I and f_{II} are orthogonal can be shown directly

$$\int_0^l m(x) f_I f_{II} \, dx = \frac{1}{x_n} \int_0^l m(x)(x - x_n) \, dx = 0, \tag{4.14}$$

since the static moment of the rod relative to the center of mass is zero. The physical meaning of the orthogonality conditions is the following: the total work of the forces of inertia, arising in vibrations of any particular mode, say $f_n(x)$, along the displacement of any other mode, say $f_m(x)$, is zero.

On the basis of the orthogonality conditions (4.10) it can be established that vibrations of a free rod of mode $f_n(x)$ corresponding to nontrivial eigenvalues, are self-balanced. They do not cause a displacement of the center of mass of the rod or a rotation of the rod about the center of mass, but it must be kept in mind that when bending vibrations are present the center of mass does not lie on the elastic axis of the rod.

3. The set of functions

$$f_I(x),\ f_{II}(x),\ f_n(x)\quad (n=1, 2, 3\ldots)$$

forms the so-called complete system of orthogonal eigenfunctions with a weight function m(x).

An arbitrary continuous function p(x) can be represented in the interval [0, l] by an infinite series

$$p(x)=\sum_{N=I}^{I} a_N f_N(x)\quad (N=I, II, n;\ n=1, 2, \ldots), \tag{4.15}$$

that converges in the mean. The numbers a_N are called the Fourier coefficients of p(x).

Let us multiply (4.15) by $m(x)f_N(x)$, where N is a constant, and integrate between 0 and l. In view of (4.13), we get

$$a_N=\frac{\int p(x)\,m(x)\,f_N dx}{\int m(x)\,f_N^2 dx}. \tag{4.16}$$

Thus, for a free rod a solution of Equation (4.3) for q(x,t) = 0 by (4.4) and (4.11) can be written as

$$y(x, t)=\sum_{N=1}^{\infty} f_N(x) q_N(t) \quad (N=1, II, n;\ n=1, 2, \ldots). \quad (4.17a) \qquad (4.17a)$$

Denoting the generalized coordinates as

$$q_1(t)=y_n(t), \quad \frac{q_{II}(t)}{x_n}=\theta(t),$$

we obtain

$$y(x, t)=y_n(t)+\theta(t)(x-x_n)+\sum_{n=1}^{\infty} f_n(x) q_n(t). \qquad (4.17)$$

4. The number of sign changes of an N^{th} natural vibrational mode is N-1 [1]. In other words, the nodes of an N^{th} vibrational mode divide the interval [0, l] into N parts.

5. Under homogeneous boundary conditions between two zeros of an N^{th} vibrational mode there must be one zero of an $N + 1^{st}$ vibrational mode [1].

3. Determination of the Modes and Frequencies of the Natural Oscillations of an Inhomogeneous Rod by Successive Approximations

One of the principal problems in an analysis of the vibrations of systems with distributed parameters, including rods, is to determine the modes and frequencies of natural vibrations. Let us study this problem in more detail as applied to a free rod. First, we shall present the method of successive approximations which is most suitable for calculating the first vibrational modes.

To determine the modes and frequencies of natural oscillations, one has to integrate Equation (4.6) with variable coefficients

$$(EJ_0(x)f_n')' = \omega_n^2 m(x) f_n. \qquad (4.18)$$

The solution should satisfy the boundary conditions (4.7) and (4.8). Instead of (4.8) we shall use (4.10).

If the coefficients of Equation (4.18) are constant, i.e.,

$$EJ(x) = EJ_0 = \text{const}, \quad m(x) = m_0 = \text{const},$$

then, as we know, the general solution of Equation (4.18) with boundary conditions (4.7) and (4.8) will be

$$f_n = C[(\sin \alpha_n x + \operatorname{sh} \alpha_n x) A_n + (\cos \alpha_n x + \operatorname{ch} \alpha_n x)],$$

$$\alpha_n = \frac{\lambda_n}{l}, \quad A_n = \frac{\operatorname{ch} \alpha_n l - \cos \alpha_n l}{\sin \alpha_n l - \operatorname{sh} \alpha_n l},$$

where the eigenvalues λ_n are the nondegenerate roots of the equation

$$\cos \alpha_n l \operatorname{ch} \alpha_n l - 1 = 0;$$

$$\lambda_1 = 4{,}73; \quad \lambda_2 = 7{,}85; \quad \lambda_3 = 11{,}0; \ldots$$

The first three vibrational modes of a homogeneous rod are shown in Figure 4.2

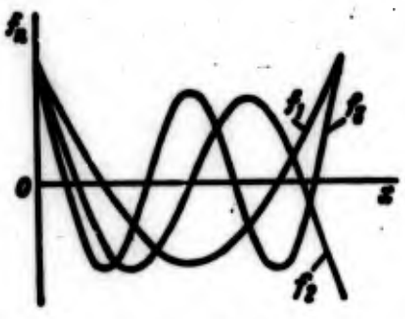

Figure 4.2

The natural frequencies are calculated from

$$\omega_n = \alpha_n^2 \sqrt{\frac{EJ_0}{m_0}} = \left(\frac{\lambda_n}{l}\right)^2 \sqrt{\frac{EJ_0}{m_0}} = \lambda_n^2 \sqrt{\frac{EJ_0}{m_0 l^4}}. \qquad (4.19)$$

Now let us consider Equation (4.18) with variable coefficients. Let us integrate it twice with respect to x. In view of the boundary conditions (4.7), we get

$$(EJ(x)f_n')' = \omega_n^2 \int_0^x m(x) f_n dx, \tag{4.20}$$

$$EJ(x)f_n' = \omega_n^2 \int_0^x \int_0^x m(x) f_n dx^2. \tag{4.21}$$

We assume

$$M_x = \omega_n^2 M_{1x}, \quad M_{1x} = \int_0^x \int_0^x m(x) f_n dx^2. \tag{4.22}$$

Further integration gives

$$f_n' = \omega_n^2 \left(\int_0^x \frac{M_{1x}}{EJ(x)} dx + D_1 \right), \tag{4.23}$$

$$f_n = \omega_n^2 \left(\int_0^x \int_0^x \frac{M_{1x}}{EJ(x)} dx^2 + D_1(x - x_m) + D_2 \right) \tag{4.24}$$

For simplicity of notation we let

$$\psi(x) = \int_0^x \int_0^x \frac{M_{1x}}{EJ(x)} dx^2, \tag{4.25}$$

$$f_n = \omega_n^2 \bar{f}_n, \quad \bar{f}_n = \psi(x) + D_1(x - x_m) + D_2. \tag{4.26}$$

The integration constants D_1 and D_2 will be calculated from (4.10). Substituting (4.26) into the first equation in (4.10) and keeping in mind that the static moment of the rod relative to the center of mass is zero, we find

$$D_2 = -\frac{1}{m} \int_0^l m(x) \psi(x) dx. \tag{4.27}$$

Here m is the mass of the rod

$$m = \int_0^l m(x) dx. \tag{4.28}$$

From the second equality in (4.10) we get

$$D_1 = -\frac{1}{I} \int_0^l m(x) \psi(x) (x - x_m) dx, \tag{4.29}$$

where I is the mass moment of inertia of the rod relative to a lateral axis through the center of mass:

$$I=\int_0^l m(x)(x-x_m)^2\,dx. \tag{4.30}$$

The method of successive approximations for determing the first vibrational mode consists of the following. As the input function we take any self-balancing vibrational mode f, and for a distributed load m(x)f a function $\bar{f}_1$ (4.26) is calculated. If the ratio $f/\bar{f}_1$ does not turn out to be constant for all cross sections of the rod, then the calculation must be repeated, using f_1 as a new starting function. Continuing the calculation in that order, we can achieve an arbitrarily small difference between the two consecutive approximations and obtain an eigenfunction of a required degree of accuracy. The closer the starting function was to the vibrational mode sought, the smaller the number of steps required to achieve the desired accuracy. In the majority of cases the solution can be obtained faster if, as a starting function, one takes an actual first vibrational mode for a free homogeneous rod f_1^0. To improve the convergence to f_1^0 it is advisable to introduce a correction to make the starting vibrational mode self-balanced

$$f_1=f_1+D_1(x-x_m)+D_2.$$

The coefficients D_1 and D_2 can be determined from (4.27) and (4.29), in which instead of $\psi(x)$, f_1^0 must be substituted.

This method allows us to calculate only the first vibrational mode. In determining higher vibrational modes it is necessary in addition to make sure that the orthogonality conditions are satisfied (4.13).

Let us first consider the procedure to calculate the second vibrational mode f_2. We take f_2 to be a sum of functions

$$f_2=f_2+\Delta_m f_1+D_1(x-x_m)+D_2, \tag{4.31}$$

where f_2^0 is the second vibrational mode for a homogeneous free rod; Δ_{21} is a coefficient, as yet unknown, with which the function f_1 was introduced, f_1 being known from the previous calculation.

Let us substitute (4.31) into condition (4.13) and find the value of Δ_{21}

$$\Delta_{21}=-\frac{1}{m_1}\int_0^l m(x)f_2f_1^2dx,\quad m_1=\int_0^l m(x)f_1^2dx. \tag{4.32}$$

The definite integrals, appearing in (4.32), are easy to evaluate using tables, since the integrands are known. In many cases the accuracy obtained is sufficient to solve practical problems. However, in case of necessity, function f_2 found from (4.31) and (4.32) can be determined more exactly using the method of successive approximations, i.e., the same method that was recommended for improving the accuracy of the first vibrational mode. In order not to violate the orthogonality condition, after each approximation it is necessary again to introduce a correction according to (4.31), taking in the calculation of Δ_{21} instead of f_2^0 the function f_2 obtained in the latest approximation.

Having determined f_1 and f_2 with the desired degree of accuracy, we can proceed to determine f_3. Assume f_3 is given as the following sum

$$f_3=f_3^0+\Delta_{31}f_1+\Delta_{32}f_2+D_1(x-x_0)+D_2,$$

where f_3^0 is the third vibrational mode for a homogeneous free rod.

The unknown coefficients Δ_{31} and Δ_{32} can be determined from the orthogonality conditions (4.13)

$$\int_0^l m(x)f_3f_1dx=0,\quad \int_0^l m(x)f_3f_2dx=0.$$

We get

$$\Delta_{31}=-\frac{1}{m_1}\int_0^l m(x)f_3^0f_1dx,\quad \Delta_{32}=-\frac{1}{m_2}\int_0^l m(x)f_3^0f_2dx,$$

$$m_2=\int_0^l m(x)f_2^2dx.$$

More accurate approximations to f_3 are obtained using the same procedure as for f_1 and f_2. A numerical method of calculating the modes and frequencies of natural oscillations from Equations (4.18) - (4.32) was investigated in detail by Yu. A. Shimanskiy [22].

Now we shall obtain a formula for determining the natural frequencies. If the ratio $f_n/\bar{f}_n$ is constant for all cross sections of the rod, then by (4.26)

$$\omega_n^2 = \frac{f_n}{\bar{f}_n}$$

It is more convenient to calculate the natural frequency from the condition that for a conservative system the maximum value of the kinetic energy of natural oscillations is equal to the maximum value of the potential energy. We have $T_{max} = U_{max}$, where

$$T_{max} = \frac{1}{2}\int_0^l m(x)(f_n \dot{q}_{n\,max})^2\,dx = \frac{1}{2}\omega_n^2 (q_n^2)_{max}\, m_n,$$

$$U_{max} = \frac{1}{2}\int_0^l EJ(x)(f_n'' q_{n\,max})^2\,dx = \frac{1}{2} k_n (q_n^2)_{max},$$

with

$$m_n = \int_0^l m(x) f_n^2\,dx, \quad k_n = \int_0^l EJ(x) f_n''^2\,dx. \tag{4.33}$$

Here m_n is the effective mass of the rod, k_n is the effective rigidity of the rod.

From $T_{max} = U_{max}$ we get Rayleigh's formula

$$\omega_n^2 = \frac{k_n}{m_n}. \tag{4.34}$$

An expression for k_n can be obtained which is more convenient in practical calculations if we use (4.21) and (4.22):

$$k_n = \int_0^l \frac{M_{nx}^2}{EJ(x)}\,dx = \omega_n^4 k_n', \quad k_n' = \int_0^l \frac{M_{1x}^2}{EJ(x)}\,dx. \tag{4.35}$$

Then instead of (4.34) we obtain

$$\omega_n^2 = \frac{m_n}{k_n'}. \tag{4.36}$$

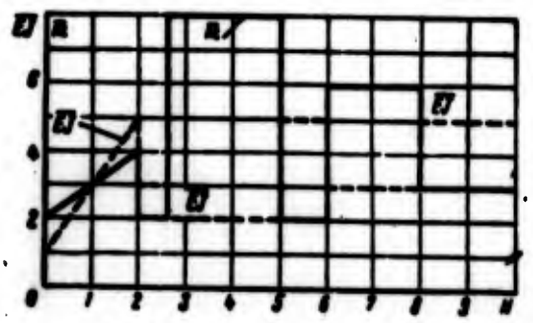

Figure 4.3

The last formula has an advantage because the expression for k_n' does not contain a second derivative. We note that the coefficients m_n, k_n and k_n' should only be calculated for modes close to the natural modes $f_n(x)$.

Let us illustrate the method presented here with a numerical example. The starting data for the calculation will be supplied by diagrams of mass distribution m(x) and rigidity EJ(x) versus the length of the rod, and the first vibrational mode f_1^0 of a homogeneous free rod.

For convenience in calculations it is common to introduce bending rigidity and mass units

$$EJ(x) = \overline{EJ} \cdot EJ_0, \quad m(x) = \bar{m} \cdot m_0.$$

The running mass $\bar{m}$ and bending rigidity $\overline{EJ}$ of the rod are shown in Figure 4.3, where N = 0, 1, 2,... is the cross section number; the length of the rod is l = 25 m. In order not to make the computational table too cumbersome, we assume the number of segments to be k = 10, and, consequently, the length of a segment is Δ = 2.5m.

The entire computation is tabulated in Tables 4.1 and 4.2. The starting data are the ordinates of functions $\bar{m}$ and $\overline{EJ}$ obtained from the graph in Figure 4.3 for each cross section. If in any cross

section the ordinate of $\overline{EJ}$ or $\bar{m}$ has two limiting values, then it is required to take the mean value of the ordinates. The definite integrals are evaluated from the table using the trapezoidal method.

Table 4.1 is auxiliary. In columns 3-9 we have the cross section N_M in which the center of mass of the rod is located, and the moment of inertia in the scale $\Delta^2\Delta_1 m_0$ $(\Delta_1=\Delta/2)$ is calculated

$$N_M=\frac{\sum_0^k \bar{m}N}{\sum_0^k \bar{m}}=4{,}979; \qquad I=\sum_0^k (8).$$

Inasmuch as the vibrational mode f_1^0 is not self-balanced for an inhomogeneous rod, we have to introduce a correction in it, and therefore,

$$f_1=f_1^0+D_1(N-N_M)+D_2.$$

The coefficients D_1 and D_2 can be calculated from (4.27) and (4.29). Using the data in Table 4.1, we get

$$D_1=-\frac{\sum_0^k (11)}{\sum_0^k \bar{m}}, \quad D_2=-\frac{\sum_0^k (13)}{\sum_0^k (6)}.$$

In the last column of Table 4.1, we have the self-balanced vibrational mode f_1 which was put in column four of Table 4.2 as a starting function for the last calculation.

Due to error accumulation the value of $\sum_0^k (6)$ in column 7 and k^{th} row in Table 4.2 differs from zero. Therefore, to satisfy the boundary condition at the right end of the rod [M(l) = 0], a correction must be introduced. This correction can be considered to be linearly dependent on the length and may be determined from the formula

$$\Delta_M=-\frac{N}{k}\sum_0^k (6).$$

The correction was entered in column 8 of Table 4.2.

Column 12 contains a function $\psi(x)$. Now let us determine the coefficients D_1 and D_2. According to (4.27) and (4.29)

$$D_2 = -\frac{\sum_0^k (13)}{\sum_0^k =}, \quad D_1 = -\frac{\sum_0^k (16)}{l}.$$

Column 21 contains the vibrational mode f_1 that has been normalized to unity in a zero corss section. This concludes a calculation of the vibrational mode to a first approximation. But this usually turns out to be insufficient, since the obtained mode will considerably differ from the starting one. Beginning with column 4, the calculation must be repeated using for the starting function the vibrational mode obtained in the previous approximation. In columns 22 and 23 the values of the vibrational mode f_1 are given that were obtained in the second and third approximation.

Assuming conditionally that the third approximation has the required accuracy, let us calculate the bending moments. The results are shown in Column 28.

Let us determine the natural frequency of the first mode. According to (4.33) - (4.36) where we take into consideration the units of mass m_0, bending rigidity EJ_0, and the length of a rod segment Δ, we have

$$\omega_1^2 = \frac{m_0 \Delta_1 \sum_0^k \bar{m} f_1^2}{\frac{(m_0 \Delta_1)^2}{EJ_0} \Delta_1 \sum_0^k (30)} = \frac{EJ_0}{m_0 \Delta_1^4} \frac{\sum_0^k \bar{m} f_1^2}{\sum_0^k (30)} = 0{,}00278 \frac{EJ_0}{m_0 \Delta_1^4}.$$

where $\Delta_1 = \Delta/2$. . In our case Δ_1 = 1.25 m.

TABLE 4.1

Table 4.1

№	$\bar{m}$	$\bar{m}N$	$\sum_0^N \bar{m}$	$\sum_0^N \bar{m}N$	$N-N_u$	$(N-N_u)^2$	(2)·(7)*	$\sum_0^N$(8)	f_1^0
1	2	3	4	5	6	7	8	9	10
0	2	0	0,00	0,00	—4,979	24,790	49,58	0,000	1,000
1	3	3	5,00	3	—3,979	15,832	47,496	97,076	0,537
2	3	6	11,00	12	—2,979	8,874	26,622	171,194	0,097
3	8	24	22,00	42	—1,979	3,916	31,328	229,144	—0,272
4	8	32	38,00	98	—0,979	0,958	7,664	268,136	—0,520
5	5	25	51,00	155	0,021	0,0004	0,002	275,802	—0,607
6	4	24	60,00	204	1,021	1,042	4,168	279,972	—0,520
7	6	42	70,00	270	2,021	4,084	24,504	308,644	—0,272
8	4,5	36	80,50	348	3,021	9,126	41,067	374,215	0,097
9	3	27	86,00	411	4,021	16,168	48,504	463,786	0,537
10	3	30	94,00	468	5,021	25,210	75,630	587,920	1,000

CONTINUATION

$\bar{m}f_1^0$	$\sum_0^N$(11)	(6)·(11)	$\sum_0^N$(13)	D_1·(6)	D_2+(15)	f_1^0+(16)	$\frac{f_1=}{(17)_{N=0}}$ (17)
11	12	13	14	15	16	17	18
2	0,000	—9,958	0.000	0,101	0,242	1,242	1,000
1,611	3,611	—6,410	—16,368	0,081	0,222	0,759	0,611
0,291	5,513	—0,867	—23,645	0,060	0,201	0,298	0,240
—2,176	3,628	4,306	—20,206	0,040	0,181	—0,091	—0,073
—4,160	—2,708	4,073	—11,827	0,020	0,161	—0,359	—0,289
—3,035	—9,903	—0,0637	—7,818	—0,000	0,141	—0,466	—0,375
—2,080	—15,018	—2,124	—10,005	—0,021	0.120	—0.4	—0,322
—1,632	—18,730	—3,298	—15,427	—0,041	0,100	—0,172	—0,138
0,436	—19,926	1,317	—17,408	—0,061	0,080	0,177	0.142
1,611	—17,879	6,478	—9,613	—0,082	0,059	0,396	0,480
3	—13,268	15,063	11,928	—0.102	0,039	1,039	0,836

* Numbers in parentheses denote column numbers in the Table.

TABLE 4.2

Table 4.2

№	$\overline{EJ}$	$\bar{m}$	f_1	$\bar{m}f_1$	$\sum_0^N \bar{m}f_1$	$\sum_0^N (6)$	Correction Δ_M	$M_{1s}=(7)+(8)$	$\frac{M_{1s}}{\overline{EJ}}$
1	2	3	4	5	6	7	8	9	10
0	1	2	1,000	2	0,000	0,000	0	0	0
1	3	3	0,611	1,833	3,833	3,833	—0,032	3,781	1,260
2	4	3	0,240	0,720	6,386	14,052	—0,105	13,947	3,487
3	2	8	—0,073	—0,584	6,522	26,960	—0,157	26,803	13,402
4	2	8	—0,289	—2,312	3,626	37,108	—0,210	36,898	18,449
5	3,5	5	—0,375	—1,875	—0,361	40,173	—0,262	39,911	11,403
6	4	4	—0,322	—1,288	—3,724	35,888	—0,314	35,574	8,894
7	3	6	—0,138	—0,828	—5,840	26,324	—0,367	25,953	8,652
8	4	4,5	0,142	0,639	—6,029	14,455	—0,419	14,036	3,509
9	5	3	0,480	1,44	—3,950	4,476	—0,472	4,004	0,801
10	5	3	0,836	2,508	—0,002	0,524	—0,524	0	0

CONTINUATION

$\sum_0^N (10)$	$\psi(x)=-\sum_0^N (11)$	$\bar{m}f(x)$	$\sum_0^N (13)$	$N-N_M$	(13)·(15)	$\sum_0^N (16)$	$D_1(15)$
11	12	13	14	15	16	17	18
0	0	0	0	—4,979	0	0	790,32
1,260	1,260	3,780	3,370	—3,979	—15,04	—15,04	631,59
6,007	8,527	25,581	33,141	—2,979	—76,21	—103,29	472,86
22,996	37,43	299,44	358,16	—1,979	—592,59	—775,09	314,13
84,747	115,07	920,56	1578,16	—0,979	—901,23	—2268,91	155,40
84,599	254,42	1272,10	3770,82	0,021	26,71	—3143,43	—3,333
104,996	443,91	1775,64	6818,56	1,021	1812,93	—1303,79	—162,06
122,44	671,25	4027,50	12621,7	2,021	8139,58	8648,72	—320,79
134,60	926,29	4177,30	20826,5	3,021	12619,6	29407,9	—479,52
138,91	1201,80	3605,40	28609,2	4,021	14497,3	56524,8	—638,25
139,71	1480,42	4441,26	36655,9	5,021	22299,6	93321,7	—796,98

TABLE 4.2 (continuation)

CONTINUATION

D_i	$\bar{f}_i = (12)+(18)+(19)$	$f_i = \frac{(20)}{\sum(20)}$	f_i	f_i	$\bar{m}f_i$	$\sum_0^N \bar{m}f_i$	$\sum_0^N(25)$
19	20	21	22	23	24	25	26
—389,95	400,37	1,000	1,000	1,000	2	0	0
	242,90	0,607	0,605	0,605	1,815	3,815	3,815
	91,44	0,228	0,225	0,225	0,675	6,305	13,935
	—38,39	—0,096	—0,099	—0,099	—0,793	6,187	26,427
	—119,48	—0,298	—0,298	—0,299	—2,392	3,002	35,616
	—138,86	—0,347	—0,343	—0,343	—1,715	—1,105	37,513
	—108,10	—0,270	—0,263	—0,263	—1,052	—3,872	32,536
	—39,49	—0,099	—0,093	—0,092	—0,554	—5,478	23,186
	58,82	0,147	0,148	0,148	0,666	—3,366	12,342
	173,60	0,434	0,426	0,426	1,278	—3,422	3,554
	293,49	0,733	0,717	0,716	2,148	0,004	0,136

CONTINUATION

Correction Δ_M	$M_{1z} = (26)+(27)$	Δl^2_{1z}	$\frac{\Delta l^2_{1z}}{EJ}$	$\sum_0^N(30)$	f_i^2	$\bar{m}f_i^2$	$\sum_0^N \bar{m}f_i^2$
27	28	29	30	31	32	33	34
0	0	0	0	0	1	2	0
—0,0136	3,801	14,448	4,816	4,816	0,366	1,098	3,098
—0,0272	13,908	193,43	48,36	57,99	0,051	0,153	4,349
—0,0408	26,386	696,22	348,11	454,46	0,0098	0,079	4,581
—0,0544	35,562	1264,6	632,30	1434,9	0,0894	0,715	5,374
—0,068	37,445	1402,13	400,61	2467,8	0,118	0,590	6,679
—0,0816	32,454	1053,3	263,32	3131,7	0,0692	0,277	7,546
—0,0952	23,091	533,19	177,73	3572,8	0,0085	0,0511	7,874
—0,109	12,233	149,65	37,41	3787,9	0,0219	0,099	8,024
—0,122	3,432	11,779	2,356	3827,7	0,181	0,543	8,666
—0,136	0	0	0	3830,0	0,513	1,539	10,748

4. A Calculation of the Modes and Frequencies of Natural Oscillations using the Initial-Parameter Method

In addition to the method of successive approximations, there are other methods of solving numerically differential equations of boundary-value problems. Let us consider now the method of initial parameters which is suitable for solving problems numerically on digital computers.

The idea behind the method is that at one end of the rod we are given the values of a function and its derivatives. Some of these values are determined from the boundary conditions, and the remaining ones are given as arbitrary initial parameters. The conditions imposed on the function at one end of the rod together with the differential equation completely determine behavior of an elastic system. In numerical calculations the initial parameters are given as numbers, and to satisfy boundary conditions at the other end of the rod one has to make several approximations. The method of initial parameters is used in construction engineering in various modified forms proposed in various years by Clebsch, A. N. Krylov, Sh. Ye. Mikeladze, N. I. Bezukhov, et al. Some of those methods are discussed in [21].

In contrast with static problems, when making calculations in the area of elastic vibrations the natural frequency must also be given so that the coefficients of the differential equation will be known.

Let us divide the rod into k segments. For each of these segments the coefficients

$$EJ(x)=EJ(x)_i,\ m(x)=m(x)_i$$

are considered constant.

The differential Equation (4.18) for an i^{th} segment will have constant coefficients

$$f_{ni}^{IV} - a_{ni}^4 f_{ni} = 0, \quad a_{ni}^4 = \frac{m(x)_i}{EJ(x)_i}\omega_n^2, \tag{4.37}$$

where ω_n is an arbitrary initial parameter.

Equation (4.37) has an exact solution

$$f_{ni} = C_{1i}\sin a_{ni}x_i + C_{2i}\cos a_{ni}x_i + C_{3i}\operatorname{sh} a_{ni}x_i + C_{4i}\operatorname{ch} a_{ni}x_i \tag{4.38}$$

and its arbitrary constants can be determined in terms of arbitrary integration constants of the previous segment from the adjoint bour iary conditions at $x_i = l_i$ and $x_{i+1} = 0$ (here l_i is the length of an i^{th} segment of the rod).

At the boundary of the i^{th} and $(i + 1)^{st}$ segments we have adjoining boundary conditions

$$\begin{aligned} f_{ni} &= f_{n(i+1)}, \\ f'_{ni} &= f'_{n(i+1)}, \\ (EJf''_n)_i &= (EJf''_n)_{i+1}, \\ (EJf'''_n)_i &= (EJf'''_n)_{i+1}. \end{aligned} \tag{4.39}$$

Substituting here (4.38) for the i^{th} and $(i + 1)^{st}$ segments, we obtain four equations from which we shall find the relationship between the constants of the $(i + 1)^{st}$ segments and the constants of the i^{th} segment:

$$\begin{aligned} C_{1(i+1)} &= \frac{1}{2}\gamma_i[C_{1i}(1+\gamma_i^2\beta_i)\cos a_{ni}l_i - C_{2i}(1+\gamma_i^2\beta_i)\sin a_{ni}l_i + \\ &+ C_{3i}(1-\gamma_i^2\beta_i)\operatorname{ch} a_{ni}l_i + C_{4i}(1-\gamma_i^2\beta_i)\operatorname{sh} a_{ni}l_i], \\ C_{2(i+1)} &= \frac{1}{2}[C_{1i}(1+\gamma_i^2\beta_i)\sin a_{ni}l_i + C_{2i}(1+\gamma_i^2\beta_i)\cos a_{ni}l_i + \\ &+ C_{3i}(1-\gamma_i^2\beta_i)\operatorname{sh} a_{ni}l_i + C_{4i}(1-\gamma_i^2\beta_i)\operatorname{ch} a_{ni}l_i], \end{aligned} \tag{4.40}$$

(Equation continued on next page)

(Equation continued from preceding page)

$$C_{3(i+1)}=\frac{1}{2}\gamma_i\left[C_{1i}(1-\gamma_i^2\beta_i)\cos\alpha_{ni}l_i-C_{2i}(1-\gamma_i^2\beta_i)\sin\alpha_{ni}l_i+\right.$$
$$\left.+C_{3i}(1+\gamma_i^2\beta_i)\operatorname{ch}\alpha_{ni}l_i+C_{4i}(1+\gamma_i^2\beta_i)\operatorname{sh}\alpha_{ni}l_i\right],$$
$$C_{4(i+1)}=\frac{1}{2}\left[C_{1i}(1-\gamma_i^2\beta_i)\sin\alpha_{ni}l_i+C_{2i}(1-\gamma_i^2\beta_i)\cos\alpha_{ni}l_i+\right. \qquad (4.40)$$
$$\left.+C_{3i}(1+\gamma_i^2\beta_i)\operatorname{sh}\alpha_{ni}l_i+C_{4i}(1+\gamma_i^2\beta_i)\operatorname{ch}\alpha_{ni}l_i\right],$$

where

$$\gamma_i=\sqrt{\frac{m(x)_i}{m(x)_{i+1}}\frac{EJ(x)_{i+1}}{EJ(x)_i}},\quad \beta_i=\frac{EJ(x)_i}{EJ(x)_{i+1}}.$$

Making use of the two boundary conditions at the left end of the first segment of the rod

$$(f_{n1}')_{x_1=0}=0,\quad (f_{n1}'')_{x_1=0}=0$$

and letting, in addition, $(f_{n1})_{x=0}=1$, we shall express all the arbitrary constants of the solution (4.38) for the first segment in terms of any one arbitrary constant, say C_{11}:

$$f_{n1}=C_{11}(\sin\alpha_{n1}x_1+\operatorname{sh}\alpha_{n1}x_1)+\frac{1}{2}(\cos\alpha_{n1}x_1+\operatorname{ch}\alpha_{n1}x_1).$$

Thus, the coefficients C_i for all segments will be expressed in terms of C_{11} by means of Formulas (4.40).

There are two additional boundary conditions at the right end of the last segment:

$$f_{nk}'(l_k)=0,\quad f_{nk}''(l_k)=0$$

They are used to determine the last constant (in our case C_{11}) and to check the correctness of the given frequency ω_n. If the frequency ω_n assumed in the calculations is a natural frequency of the rod, then both conditions will be satisfied at the right-hand end of the rod, and the calculation of the elastic vibrational modes can be considered exact.

However, in view of the fact that the frequency ω_n is first given in a tentative fashion, one of the boundary conditions for example, the second will clearly not be satisfied, and

$$f_{n2}^{*}(l_2) = \varphi(\omega_n) = \alpha_{n2}^{3}(-C_{12}\cos\alpha_{n2}l_2 + C_{22}\sin\alpha_{n2}l_2 + C_{32}\operatorname{ch}\alpha_{n2}l_2 + C_{42}\operatorname{sh}\alpha_{n2}l_2) \neq 0.$$

In this case the calculation is repeated for several close values of frequency ω_n, and by trial and error values of frequency are found for which the equality $\varphi(\omega_n) \approx 0$ is satisfied with sufficient accuracy.

In an initial calculation the frequency ω_n is taken to be the frequency of a homogeneous rod that is close to the given rod in its parameters. After determining the natural freqeuecy ω_n and all the coefficients C_1, the vibrational modes are determined successively for all segments from Equations (4.38).

In conclusion, it is advisable to verify the self-balancing of the vibrational modes. For this purpose the self-balanced vibrational mode of the rod will be represented as a sum

$$f_n = f_n^{*} + D_1(x - x_n) + D_2,$$

where f_n^{*} is a vibrational mode obtained from calculations. The coefficients D_1 and D_2 here have the same meaning as in Equation (4.26). In calculating these coefficients from (4.27) - (4.29), in which instead of functions $\psi(x)$ one must use function f_n^{*}, one gets values approaching zero.

The method of initial parameters can be used to calculate the mode and frequency of the natural oscillations for any mode number without first calculating the vibrational modes for preceding mode numbers. However, it is not always possible to say for which mode number the natural frequency has been determined. To supply an answer it is necessary to construct a vibrational mode and find the number of nodes, i.e., the number of points on the rod axis at which $f_n(x) = 0$.

Consider a numerical example. We shall calculate using the method of initial parameters the vibrational modes and frequencies for the first two mode numbers of a straight inhomogeneous rod. The diagrams showing the mass and bending rigidities for the rod are shown in Figure 4.3. The length of the rod, units of mass and rigidity will be taken to be the same as those used in the numberical calculations done by the method of successive approximations, i.e., $l = 25$ m, $m_0 = 15$ kgf $\cdot$ sec^2/m^2, $EJ_0 = 10.5 \cdot 10^6$ kgf$\cdot$m^2.

At the left end of the rod the running mass and bending rigidity change in a linear fashion. For the sake of the computation this end of the rod will be replaced by two segments of the same length with constant mass and rigidity; the mass and rigidity will be assumed to be equal to their mean values. On the basis of the graphs of functions $\bar{m}$ and $\overline{EJ}$ the rod will be divided into seven segments ($k = 7$) whose parameters are given in Table 4.3.

TABLE 4.3

i	1	2	3	4	5	6	7
$\bar{m}_i$	2,5	2,5	2,0	6,0	2,0	6,0	3,0
$\overline{EJ}_i$	2,0	4,0	3,0	2,0	5,0	3,0	5,0
$\frac{m_0 \bar{m}_i}{EJ_0 \overline{EJ}_i}$	$0,179 \cdot 10^{-5}$	$0,125 \cdot 10^{-5}$	$0,0864 \cdot 10^{-5}$	$0,572 \cdot 10^{-5}$	$0,0572 \cdot 10^{-5}$	$0,286 \cdot 10^{-5}$	$0,0858 \cdot 10^{-5}$
$l_i \cdot m$	2,5	2,5	1,25	6,25	2,5	5,0	5,0

TABLE 4.4

$\frac{x}{l}$	0	0,1	0,2	0,3	0,4	0,5	0,6	0,7	0,8	0,9	1,0
$f_1(x)$	1,000	0,994	0,921	−0,114	−0,981	−0,353	−0,358	−0,092	0,167	0,450	0,740
$f_2(x)$	1,000	0,879	−0,168	−0,479	−0,305	0,147	0,548	0,636	0,308	−0,509	−1,306
$f_3(x)$	1,000	0,127	−0,468	−0,445	0,250	0,534	0,158	−0,302	−0,327	0,105	0,665

The first three vibrational modes, calculated using the method presented here, are given in Table 4.4. The form of the function $\varphi(\omega_n)$ is shown in Figure 4.4. The natural frequencies (1/sec) are as follows:

$$\omega_1 = 25{,}23; \quad \omega_2 = 64{,}78; \quad \omega_3 = 132{,}5.$$

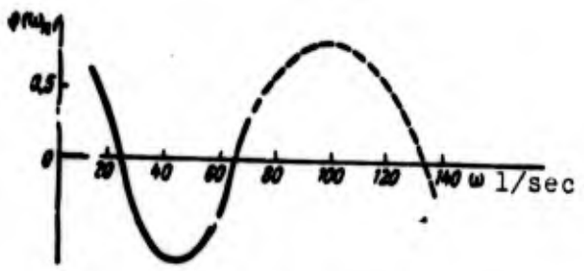

Figure 4.4

5. A Determination of the Modes and Frequencies of the Natural Oscillations of a Rod with Elastically Suspended Masses

A straight inhomogeneous rod is the simplest model in calculating the modes and frequencies of lateral vibrations. In this case the liquid in tanks is arbitrarily assumed to be "solidified" in the sense that in executing oscillations it does not move against the walls of the tank and it does not contribute to the bending rigidity of the rocket fuselage. The "solidified" liquid can be visually represented as sand or a large number of ideally elastic rods continuously filling the cavity of the tank from the bottom to the free surface level.

A straight inhomogeneous rod with elastically suspended masses can serve as the next approximation to a liquid-propellant rocket (Figure 4.5). Each mass suspended from a spring is a mechanical analog

of one oscillation mode. In calculating the modes and frequencies of the natural oscillations of the fuselage the replacement of the oscillating liquid with elastically suspended masses is inherently inaccurate, since the system of forces distributed along the length is then replaced by an equivalent but concentrated force.

We assume that each spring-mass system is a mechanical analog of the first oscillation mode. For the j^{th} cylindrical tank the mass m_j can be calculated from (2.73) with n = 1

$$m_j = \pi r_{0j}^3 \rho \frac{2 \operatorname{th}\left(\zeta_n \frac{h_j}{r_{0j}}\right)}{\zeta_n (\zeta_n^2 - 1)} \quad (n=1). \tag{4.41}$$

The rigidity coefficient (or simply the rigidity), k_j, of a spring is chosen so that the natural frequency of the mass m_j is equal to the natural oscillation frequency in a stationary tank:

$$k_j = m_j \omega_j^2, \quad \omega_j^2 = \frac{g \zeta_n \operatorname{th}\left(\zeta_n \frac{h_j}{r_{0j}}\right)}{r_{0j}} \quad (n=1) \tag{4.42}$$

The distance from the undisturbed free surface to the center of mass of m_j on the basis of (2.67) is

$$x_j^* = \frac{2 r_{0j}}{\zeta_n} \operatorname{th}\left(\zeta_n \frac{h_j}{2 r_{0j}}\right) \quad (n=1).$$

If the distance from the upper tip of the fuselage to the undisturbed free surface of a j^{th} tank is denoted by l_j, then the distance from the same point to an elastically suspended mass will be

$$x_j = l_j + x_j^*. \tag{4.43}$$

Part of the liquid mass forms a suspended mass m_j, and therefore, the graph of the mass of the rod should not include the mass of the liquid after a certain length. However, the mass m_j can be included into the mass of the rod and only those forces can be considered that arise due to the movement of the mass m_j relative to the rod. This is precisely what we shall do below.

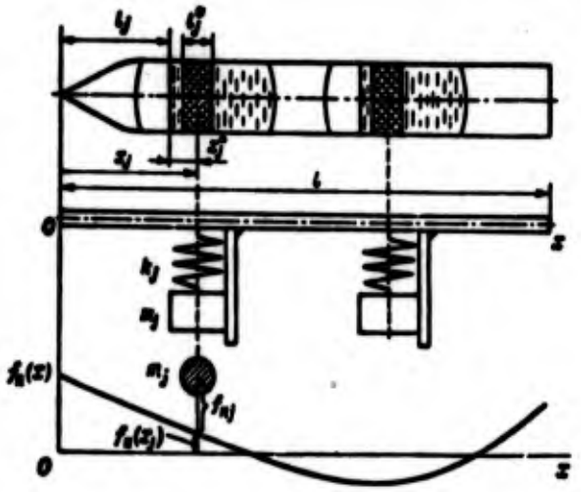

Figure 4.5

Let us analyze the distinctive features in the computation of natural vibrational modes by a method of initial parameters. In contrast to Section 4 here one has to consider at each cut $x = x_j$ the additional concentrated forces caused by the movement of the elastically suspended masses relative to the rod.

Let $f_n(x)$ represent the unknown lateral vibrational modes of the rod. $f_n(x_j)$ will then stand for the vibrational mode of the rod at x_j, and f_{nj} will denote the deflection of mass m_j from the bent axis of the rod (see Figure 4.5). Assuming that the lateral vibrations are harmonic with frequency ω_n, we find

$$f_{nj} = f_n(x_j)\beta_j\omega_n^2, \quad \beta_j = \frac{1}{\omega_j^2 - \omega_n^2}, \ (\omega_j \neq \omega_n), \ \omega_j^2 = \frac{k_j}{m_j}.$$

The additional concentrated force at $x = x_j$ is

$$m_j f_{nj}\omega_n^2 = m_j f_n(x_j)\omega_n^4\beta_j. \tag{4.44}$$

This force depends on the ratio of the partial frequency ω_j and the natural frequency of the system, ω_n.

When coupling separate segments of the rod at the locations of concentrated masses, one must take into account an additional concentrated force (4.44). The magnitude and direction of the concentrated force are shown in Figure 4.6. Then in order to couple segments lying to the left and right of x_j, instead of Equation (4.39), we shall have

$$\begin{aligned} f_{ni}(l_i) &= f_{n(i+1)}(0), \\ f'_{ni}(l_i) &= f'_{n(i+1)}(0), \\ [EJ(l)f''_n(l)]_i &= [EJ(0)f''_n(0)]_{i+1}, \\ [EJ(l)f'''_n(l)]_i + m_j f_n(x_j)\beta_j\omega_n^4 &= [EJ(0)f'''_n(0)]_{i+1}. \end{aligned} \tag{4.45}$$

In other respects the computation procedure is completely analogous to that presented in the preceding section.

Let us consider a numerical example. We shall determine the first vibrational mode and its frequency for a rod with elastically suspended masses. For the purposes of the calculation, we shall consider the rod whose parameters are given in Table 4.3. The segments i = 4 and i = 6 will be assumed to represent the cylindrical tanks containing liquid fuel, and the initial points of these segments will be considered to coincide with the undisturbed free surface of the liquid. Supposed the upper tank (i = 4) contains an oxidant of specific gravity γ_A = 1140 kgf/m^3, and the lower tank (i = 6) - fuel of γ_B = 800 kgf/m^3. The radii of the tanks will be assumed identical (r_0 = 0.75m).

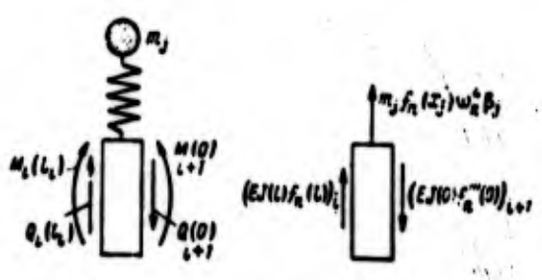

Figure 4.6

Considering only the first oscillation mode, we find from (4.41) that the values of the elastically suspended masses m_j for the oxidant-containing tank (j = A) and for the fuel-containing tank (j = B) are the following:

$$m_A = 68 \text{ kgf} \cdot \text{sec}^2/\text{m}, \quad m_B = 48 \text{ kgf} \cdot \text{sec}^2/\text{m}.$$

An acceleration $g^* = 100$ m/sec^2 will be used in the calculations. Then from (4.42) we shall obtain the natural frequencies and the rigidity coefficients of the springs

$$\omega_A^2 = \omega_b^2 = 248 \text{ 1/сек}^2, \quad k_A = 16864 \text{ кГ/м}, \quad k_b = 11904 \text{ кГ/м}.$$

The distance between the undisturbed free surface of the liquid and an elastically suspended mass is

$$x_j^* = \frac{2r_{0j}}{\zeta_n} \text{th}\left(\zeta_n \frac{h_j}{2r_{0j}}\right).$$

This means that for n = 1 the distances are $x_A^* = x^*_B = 0.81$ m.

Each of the segments i = 4 and i = 6 of Table 4.3 must now be divided into two segments — to the left and to the right of the mass at the center. In all we obtain 9 segments for which the values of m_i, EJ_i, l_i are given in Table 4.5. Between the segments 4 and 5, 7 and 8 lie the lumped masses $\bar{m}_j = m_0$ (j = A, B).

The first vibrational mode calculated using the method of initial parameters is given in Table 4.6. The frequency of the first mode for a rod with elastically suspended masses is $\omega_1 = 25.36$ 1/sec. This frequency is slightly higher than the frequency of the first vibrational mode of an inhomogeneous rod without elastically suspended masses ($\omega_1 = 25.23$ 1/sec, see Section 4).

Since the natural frequency of elastically suspended masses, ω_j, is less than the frequency of the natural oscillations of the system, ω_1, then (4.44) $\beta_j < 0$, and the displacements of elastically suspended masses, f_{nj}, and those of the rod, $f_n(x_j)$, will proceed in opposite directions, which also follows from Table 4.6. A comparison of Tables 4.4 and 4.6 clearly shows that as a result of a displacement of masses m_j the vibrational mode of the rod is also slightly modified.

TABLE 4.5

i	1	2	3	4		5	6	7		8	9
$\bar{m}_i$	2,5	3,5	2,0	8,0		8,0	2,0	6,0		6,0	3,0
$\overline{EJ}_i$	2,0	4,0	3,0	2,0		2,0	5,0	3,0		3,0	5,0
$\frac{m_0\bar{m}_i}{EJ_0\overline{EJ}_i}$	$0,179\cdot10^{-5}$	$0,125\cdot10^{-5}$	$0,0834\cdot10^{-5}$	$0,572\cdot10^{-5}$		$0,572\cdot10^{-5}$	$0,0572\cdot10^{-5}$	$0,191\cdot10^{-5}$		$0,286\cdot10^{-5}$	$0,0858\cdot10^{-5}$
$l_i = x$	2,5	2,5	1,25	10,81		5,44	2,5	0,81		4,19	5,0
$\hat{m}^0_{jm_0}$					68				48		

TABLE 4.6

$\frac{x}{l}$	0	0,1	0,2	0,282	0,3	0,4	0,5	0,6	0,632	0,7	0,8	0,9	1,0
$f_1(x)$	1,000	0,500	0,211	−0,0765	−0,129	−0,241	−0,372	−0,275	−0,225	−0,094	0,102	0,451	0,749
f_{nA}				0,0247									
f_{nE}									0,729				

The above example implies that the effect of the suspended masses on the mode and frequency of the natural oscillations of the system will be slight if the frequency of the elastically suspended masses significantly differs from the partial frequency of the rod. If these frequencies lie closeby, then it may be expected that the influence of the masses will be considerable.

6. Forced Oscillations of a Free Elastic Rod

Let us assume that in Equation (4.3) the intensity of the external distributed force q(x,t) can be represented as a product

$$q(x, t)=q(t)p(x).$$

Forced oscillations of the rod y(x,t) will be represented as a series (4.17) in vibrational modes

$$y(x, t)=y_0(t)+\theta(t)(x-x_0)+\sum_{n=1}^{\infty} f_n(x)q_n(t). \tag{4.46}$$

Let us substitute in Equation (4.3) the expression (4.46) for y(x,t). We obtain

$$\begin{aligned}(q_n+h\dot{q}_n)\left[EJ(x)\sum_{n=1}^{\infty} f_n^{\cdot}\right]+m(x)\left[\ddot{y}_0+\ddot{\theta}(x-x_0)+\right.\\ \left.+\sum_{n=1}^{\infty} f_n\ddot{q}_n\right]=q(t)p(x).\end{aligned} \tag{4.47}$$

Let us integrate this equation with respect to x from 0 to l. Then let us multiply Equation (4.47) by $(x-x_M)$, and integrate again with respect to x over the same interval. Finally, let us multiply Equation (4.47) by $f_n(x)$, where n is any natural number, and integrate with respect to x from 0 to l. In view of (4.7), (4.8), (4.9) - (4.12) and (4.28) - (4.34) we shall obtain the following system of ordinary differential equations with constant coefficients to determine the generalized coordinates y_m, $\theta(t)$, $q_n(t)$:

$$m\ddot{y}_u = q(t)\int_0^l p(x)\,dx,$$

$$I\ddot{\theta} = q(t)\int_0^l p(x)(x-x_u)\,dx,$$

$$\ddot{q}_n + 2k_n\omega_n\dot{q}_n + \omega_n^2 q_n = q(t)\frac{\int_0^l p(x) f_n dx}{m_n}, \quad (n=1, 2, \ldots) \tag{4.48}$$

where

$$2k_n = h\omega_n, \quad m_n = \int_0^l m(x) f_n^2 dx.$$

The first two equations are the equations of motion of the center of mass, and of rotation about the lateral axis through the center of mass of an absolutely rigid rod. From the last group of equations with given external forces q(t)p(x), one can find the generalized coordinates $q_n(t)$ of the lateral oscillations of the rod.

Below we shall mainly investigate steady-state harmonic oscillations which are determined by the particular solutions of Equations (4.48) under the condition that q(t) is harmonic. If the initial conditions are given as

$$y(x, 0) = \varphi(x), \quad \frac{\partial y(x, 0)}{\partial t} = \psi(x),$$

where $\varphi(x), \psi(x)$ are continuous functions, and it is required to find general solutions of Equations (4.48), then to determine the arbitrary integration constants the initial conditions should be expanded into a series in eigenfunctions

$$\varphi(x) = y_u(0) + \theta(0)(x-x_u) + \sum_{n=1}^{\infty} f_n(x) q_n(0),$$

$$\psi(x) = \dot{y}_u(0) + \dot{\theta}(0)(x-x_u) + \sum_{n=1}^{\infty} f_n(x)\dot{q}_n(0).$$

The expansion coefficients can be determined from the following formulas [16]:

$$y_n(0)=\frac{1}{m}\int_0^l m(x)\varphi(x)\,dx,\quad \dot{y}_n(0)=\frac{1}{m}\int_0^l m(x)\psi(x)\,dx,$$

$$\theta(0)=\frac{1}{I}\int_0^l m(x)\varphi(x)(x-x_m)\,dx,\quad \dot{\theta}(0)=\frac{1}{I}\int_0^l m(x)\psi(x)(x-x_m)\,dx,$$

$$q_n(0)=\frac{1}{m_n}\int_0^l m(x)\varphi(x)f_n(x)\,dx,\quad \dot{q}_n(0)=\int_0^l m(x)\psi(x)f_n(x)\,dx.$$

We assume

$$Q_n(t)=q(t)\int_0^l p(x)f_n\,dx.$$

The quantity $Q_n(t)$, appearing on the right-hand side of the third equation in (4.48), is a generalized force. When the rod is acted upon by a system of lateral forces, as, for example, shown in Figure 4.7, the right-hand side of Equation (4.47) can be written as [21]

$$q(x,t)=q_1(t)p(x)+\sum_{(r)}q_{r1}(t)Q_r\Delta(x-x_r)-$$
$$-\frac{dM(x)}{dx}q_2(t)-\sum_{(s)}q_s(t)M_s[\Delta'(x-x_s)],$$

where $\Delta(x-l)$ is the Dirac delta function which has the following properties:

$$\int_0^l\varphi(x)\Delta(x-l)\,dx=\begin{cases}\varphi(l) & x\geqslant l,\\ 0 & x<l,\end{cases}$$

$$\int_0^l\varphi(x)\Delta'(x-l)\,dx=\begin{cases}-\varphi'(l) & x\geqslant l,\\ 0 & x<l.\end{cases}$$

Upon evaluating the integral

$$\int_0^l q(x,t)f_n(x)\,dx,$$

we shall obtain the generalized force

$$Q_n(t)=q_1(t)\int_0^l p(x)\,f_n\,dx+\sum_{(r)}q_r(t)Q_r(x_r)f_n(x_r)+$$
$$+q_2(t)\int_0^l \mathfrak{M}(x)f_n'(x)\,dx+\sum_{(s)}q_s(t)M_sf_n'(x_s). \tag{4.49}$$

The advantage of this method of determining the forced vibrations of the rod is the clarity of the solving technique and the simplicity of interpreting the solution. The forced oscillations of the system with distributed parameters are represented as infinite sums of the oscillations of simple oscillators.

Now consider Equation (4.3a) in which the internal friction is accounted for by means of the hypothesis of Sorokin:

$$\left(1+i\frac{\psi}{2\pi}\right)\frac{\partial^2}{\partial x^2}\left[EJ(x)\frac{\partial^2 y}{\partial x^2}\right]+m(x)\frac{\partial^2 y}{\partial t^2}=p(x)e^{ipt},$$

where p is the frequency of the oscillations of the external force.

For steady-state forced oscillations we take

$$y(x,\,t)=\phi(x,\,p)e^{ipt},$$

where $\phi(x,p)=U(x,p)+iV(x,p)$ may be called the complex form of forced oscillations. The form is determined by the set of functions U(x,p) and V(x,p). The function $\phi(x,\,p)$ should satisfy the equation

$$\left(1+i\frac{\psi}{2\pi}\right)[EJ(x)\phi''(x,\,p)]''-m(x)p^2\phi(x,\,p)=p(x). \tag{4.50}$$

We set in this equation

$$\phi(x,\,p)=\sum_{N=1}^{\infty}b_N(p)f_N(x)\quad(N=1,\,11,\,n;\;n=1,\,2,\ldots), \tag{4.51}$$

where $f_N(x)$ are the vibrational modes of a free rod, satisfying Equation (4.6) and the boundary conditions (4.7) and (4.8).

Since

$$[EJ(x)f_N'(x)]''=\omega_N^2m(x)f_N(x),$$

then from Equation (4.50) we get

$$\sum_{N=1}^{\infty} b_N(p)\left[\left(1+i\frac{\psi}{2\pi}\right)\omega_N^2-p^2\right]m(x)f_N(x)=p(x). \tag{4.52}$$

Let us multiply both sides of Equation (4.52) by $f_N(x)$, and integrate it with respect to x from 0 to l. Making use of the orthogonality conditions for the natural oscillations $f_N(x)$, we obtain

$$b_N(p)\left[\left(1+i\frac{\psi}{2\pi}\right)\omega_N^2-p^2\right]\int_0^l m(x)f_N^2(x)=\int_0^l p(x)f_N(x)\,dx$$

$$(N=\mathrm{I},\ \mathrm{II},\ n;\quad n=1,2,\ldots).$$

Hence, we shall find the formulas to determine the coefficients

$$b_N(p)=\frac{a_N}{(\omega_N^2-p^2)+i\omega_N^2\frac{\psi}{2\pi}},\quad a_N=\frac{\int_0^l p(x)f_N(x)\,dx}{\int_0^l m(x)f_N^2\,dx}. \tag{4.53}$$

The first two terms of the series in (4.51) express the forced vibrational modes of a rod as a rigid body. The vibrational modes, corresponding to the trivial frequency $\omega_N=0$, are by (4.11) equal to

$$f_{\mathrm{I}}=1,\quad f_{\mathrm{II}}=\frac{1}{x_u}(x-x_u).$$

Therefore, the coefficients are

$$b_{\mathrm{I}}=-\frac{1}{p^2m}\int_0^l p(x)\,dx,\quad b_{\mathrm{II}}=-\frac{x_u^2}{p^2I}\int_0^l p(x)(x-x_u)\,dx. \tag{4.54}$$

The formulas for the coefficients $b_n(p)$ and a_n, corresponding to the elastic vibrational modes of the rod, are the following:

$$b_n(p)=\frac{a_n}{(\omega_n^2-p^2)+i\omega_n^2\frac{\psi}{2\pi}},\quad a_n=\frac{1}{m_n}\int_0^l p(x)f_n\,dx. \tag{4.55}$$

The expression for the coefficients $b_n(p)$ can also be represented as

$$b_n=\frac{a_n}{\omega_n^2\sqrt{(1-\gamma_n^2)^2+\left(\frac{\psi}{2\pi}\right)^2}}e^{i\varphi_n}, \tag{4.56}$$

where

$$\operatorname{tg}\varphi_n = -\frac{\frac{\psi}{2\pi}}{1-\gamma_n^2}, \quad \gamma_n = \frac{p}{\omega_n}. \tag{4.57}$$

In this case the forced steady-state elastic oscillations of any mode number will be

$$y_n(x, t) = b_n f_n(x) e^{i(pt+\varphi_n)} = f_n(x) \frac{a_n}{\omega_n^2 \sqrt{(1-\gamma_n^2)^2 + \left(\frac{\psi}{2\pi}\right)^2}} e^{i(pt+\varphi_n)}. \tag{4.58}$$

If in Equations (4.48) we set $q(t) = e^{ipt}$, then the particular solutions of these equations can be written as

$$\begin{aligned} y_n(t) &= b_1 e^{ipt}, \\ \theta(t) &= \frac{b_{11}}{x_{11}} e^{ipt}, \\ q_n(t) &= \frac{a_n e^{i(pt+\varphi_n)}}{\omega_n^2 \sqrt{(1-\gamma_n^2)^2 + (2\varepsilon_n\gamma_n)^2}}. \end{aligned} \tag{4.59}$$

where

$$\operatorname{tg}\varphi_n = -\frac{2\varepsilon_n\gamma_n}{1-\gamma_n^2}.$$

A comparision of (4.54) and (4.56) with (4.59) shows that the solutions of equations for the elastic vibrations are slightly different from each other. For small friction coefficients this difference is practically insignificant.

The problem of forced oscillations can be solved, including the case when the external force P(t) is nonharmonic, using the operational methods. To illustrate this method we shall consider forced oscillations of a homogeneous rod with a lateral force P(t) applied to its right-hand end.

On the basis of (4.3) the differential equation of the lateral vibrations will be

$$\left(1+h\frac{\partial}{\partial t}\right)EJ_0\frac{\partial^4 y(x,t)}{\partial x^4}+m_0\frac{\partial^2 y(x,t)}{\partial t^2}=0. \tag{4.60}$$

The function y(x,t) should satisfy the following boundary conditions:

$$\frac{\partial^2 y(0,t)}{\partial x^2}=0,\quad \frac{\partial^2 y(0,t)}{\partial x^2}=0,$$
$$\frac{\partial^2 y(l,t)}{\partial x^2}=0,\quad -\left(1+h\frac{\partial}{\partial t}\right)EJ_0\frac{\partial^3 y(l,t)}{\partial x^3}=P(t). \tag{4.61}$$

Applying the Laplace transform [10] to Equation (4.60) and to the boundary conditions (4.61), we obtain a differential equation for the transform

$$c_0^2(1+hs)\frac{d^4Y(x,s)}{dx^4}+s^2Y(x,s)=0 \tag{4.62}$$

and its boundary conditions

$$\frac{d^2Y(+0,s)}{dx^2}=0,\quad \frac{d^2Y(+0,s)}{dx^2}=0,$$
$$\frac{d^2Y(l-0,s)}{dx^2}=0,\quad c_0^2(1+hs)\frac{d^3Y(l-0,s)}{dx^3}=a_1(s), \tag{4.63}$$

where s is a parameter;

$$c_0^2=\frac{EJ_0}{m_0};\quad a_1(s)=\frac{1}{m_0}\int_0^\infty P(t)e^{-st}dt.$$

The homogeneous Equation (4.62) is solved using the usual technique: a substitution $Y(x,s)=Ce^{\alpha x}$ is made which leads to the characteristic equation

$$(1+hs)c_0^2\alpha^4+s^2=0.$$

Calculating the four roots $\alpha_1(s),\ldots,\alpha_4(s)$ of this equation, we obtain the total integral

$$Y(x,s)=C_1e^{\alpha_1 x}+C_2e^{\alpha_2 x}+C_3e^{\alpha_3 x}+C_4e^{\alpha_4 x}.$$

The arbitrary constants $C_1, \ldots, C_4$ are determined in such a way that the conditions (4.63) are satisfied. When this is done it remains to determine the original function $y(x,t)$ corresponding to the transform $Y(x,s)$. For this, one usually consults handbooks [5].

If the external force is harmonic, then the forced oscillations of the rod in a closed form, without an expansion into a series in eigenfunctions, can also be found without using the Laplace transform. Let us illustrate the method of solution using the example of Equation (4.60) with the boundary conditions (4.61).

We take $P(t)=P_0e^{ipt}$. The solution of Equation (4.60) will be assumed to have the form

$$y(x, t)=\phi(x)e^{ipt}. \tag{4.64}$$

Substituting (4.64) into (4.60), we obtain an ordinary differential equation for $\phi(x)$

$$(1+ikp)c_0^2\phi^{IV}-p^2\phi=0. \tag{4.65}$$

We shall use the substitution $\phi(x)=e^{rx}$. From the characteristic equation

$$(1+ikp)c_0^2r^4-p^2=0,$$

in which p is the frequency of the external force, we find four roots of r:

$$r_m=\sqrt[4]{Q}e^{i\varphi_m} \quad (m=1, 2, 3, 4),$$

where

$$Q=\frac{p^2}{c_0^2\sqrt{1+k^2p^2}}, \quad \varphi_m=\frac{\varphi+2\pi m}{4},$$

$$\operatorname{tg}\varphi=-kp, \quad -\frac{\pi}{2}<\varphi<0.$$

The total integral of Equation (4.65) will consist of a sum of four partial solutions:

$$\phi(x)=C_1e^{\alpha_1 x}+C_2e^{\alpha_2 x}+C_3e^{\alpha_3 x}+C_4e^{\alpha_4 x}. \tag{4.66}$$

On the basis of (4.61) and (4.64) the boundary conditions for the function $\phi(x)$ will be

$$\begin{gathered}\phi''(0)=0,\quad \phi'''(0)=0,\\ \phi''(l)=0,\quad -(1+ihp)\phi'''(l)=\frac{P_0}{EJ_0}.\end{gathered} \tag{4.67}$$

Using these conditions in the solving (4.66) we shall find the arbitrary constants $C_1, \ldots, C_4$. The function $\phi(x)$ is complex and depends on the frequency of the external force. The phase lag between the movement of the rod and the external force is included in $\phi(x)$, and not in the functions of time, $q_n(t)$, as was the case in Equations (4.48). The complex function

$$\phi(x, p)=U(x, p)+iV(x, p)$$

depends on the frequency p.

Let us solve the differential Equation (4.65) for the case h = 0. Let $p^2/c_0^2=\alpha^4$. Then the total integral of Equation (4.65) will be

$$\phi(x)=C_1\sin\alpha x+C_2\cos\alpha x+C_3\operatorname{sh}\alpha x+C_4\operatorname{ch}\alpha x.$$

In view of the boundary conditions (4.67) we obtain

$$\begin{gathered}\phi(x)=C_1(\sin\alpha x+\operatorname{sh}\alpha x)+C_2(\cos\alpha x+\operatorname{ch}\alpha x),\\ C_1=\frac{P_0}{D\alpha^2EJ_0}(\cos\alpha l-\operatorname{ch}\alpha l),\\ C_2=\frac{P_0}{D\alpha^2EJ_0}(-\sin\alpha l+\operatorname{sh}\alpha l),\\ D=\cos\alpha l\operatorname{ch}\alpha l-1\neq 0.\end{gathered}$$

The parameter α is known; it depends on the frequency of the external force p. For a certain value of p, D may be zero. This means that the frequency of the external force coincides with one of the

natural frequencies of the rod, and the system will be found in the resonance mode.

The function

$$\frac{\phi(x) EJ_0}{P_0 l^3} = \phi_1(x)$$

may be called the forced lateral vibrational mode of the rod. Figure 4.8 shows such modes of oscillation for three different values of frequency p (see curves 1, 2, 3, respectively):

$$p/\omega_1 = 0{,}2; \quad p/\omega_1 = 0{,}95; \quad p/\omega_1 = 1{,}05.$$

Here

$$\omega_1 = \left(\frac{4{,}73}{l}\right)^2 \sqrt{\frac{EJ_0}{m_0}}$$

is the frequency of the first vibrational mode of the rod.

For $p/\omega_1 = 0{,}2$ the elastic vibrations are insignificant; the rod moves essentially as a rigid body. When $p/\omega_1 = 0{,}95$ or 1.05 the first elastic vibrational mode is preponderant, and therefore, the forced vibrational modes are close to the first natural vibrational mode. In view of the fact that the first vibrational mode of frequency $p/\omega_1 = 0{,}95$ occurs up to resonance, and the one of frequency $p/\omega_1 = 1{,}05$ — after the resonance, the forced vibrational modes, as it was to be expected, have different signs.

In contrast with the natural vibrational mode $f_n(x)$, the forced vibrational modes $\phi(x)$ is not self-balanced, and therefore, its use in the analysis of the dynamic properties of rockets is sometimes inconvenient. To avoid these inconveniences we shall separate from $\phi(x)$ the linear function characterizing the motion of a rod as a rigid body. For this purpose, we set

$$y(x, t) = \phi(x, p) e^{ipt} = [Y_n(p) + \vartheta(p)(x - x_n) + Y(x, p)] e^{ipt}, \qquad (4.68)$$

where x_M is the coordinate of the center of mass of the rod. We choose $Y_M(p)$ and $\Phi(p)$ so that the first two terms would express the forced vibrations of the rod as a rigid body under the influence of the external harmonic force $P_0 e^{ipt}$. Then we get

$$-p^2 Y_M(p)\int_0^l m_0 dx = -p^2 Y_M(p) m = P_0,$$
$$-p^2\Phi(p)\int_0^l m_0(x-x_M)^2 dx = -p^2\Phi(p) I = P_0(l-x_M). \tag{4.69}$$

Here $Y_M(p)$ and $\Phi(p)$ are the amplitude of the oscillations of the center of mass and the angle of rotation of the rod as a rigid body in forced oscillations of frequency p.

Integrating the differential equation

$$EJ_0\varphi^{IV}(x) - p^2 m_0\varphi(x) = 0$$

with the boundary conditions (4.67), letting h = 0, we find

$$-p^2\int_0^l m_0\varphi(x)\,dx = P_0,$$
$$-p^2\int_0^l m_0\varphi(x)(x-x_M)\,dx = P_0(l-x_M). \tag{4.70}$$

On the basis of (4.68) - (4.70), we get

$$-p^2\int_0^l Y(x, p) m_0 dx = 0,$$
$$-p^2\int_0^l m_0 Y(x, p)(x-x_M)\,dx = 0.$$

The resultant of the forces of inertia and the moment of the forces of inertia in lateral vibrations of the form Y(x,p) are zero, i.e., the vibrations of that form are self-balanced. The separation of $\varphi(x,p)$ into three functions (4.68) is schematically shown in Figure 4.9.

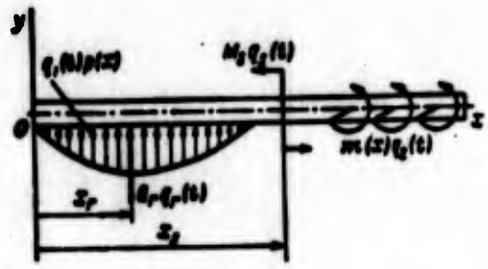

Figure 4.7

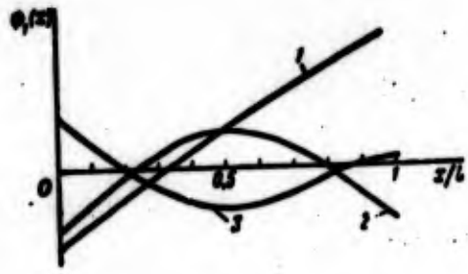

Figure 4.8

Let us now compare the two different representations of forced vibrations, (4.46) and (4.68). In both cases the forced lateral vibrations are shown in the form of a sum of three vibrations — the vibrations of the center of mass, vibrations relative to the center of mass, and the bending self-balanced vibrations. This is where the similarity of the solutions lies. The difference between them is that in (4.46) the elastic vibrations are represented in the form of an infinite series in eigenfunctions, and in (4.68) they are characterized by one function Y(x,p) which is a function of the coordinate and the frequency of the external force.

Below we shall be interested in the values of the elastic displacements at the locations of the control system sensors. This includes such quantities as the slope angle of the tangent line at the location of the gyroscope, the angular velocity, etc.

The slope angle of the tangent line at the location of the gyroscope is

$$y'(x_r, t) = \varphi'(x_r, p)e^{ipt} = [\vartheta(p) + Y'(x_r, p)]e^{ipt}.$$

The complex transfer number for the angles of the rotation of cross sections as a result of bending vibrations will be

$$\frac{\varphi'(x, p)}{P_0} = U(p) + iV(p) = A(p)e^{i\psi(p)}.$$

The hodograph of this complex number as a function of the frequency p and h ≠ 0 is plotted in the complex plane Z = U + iV (Figure 4.10). At the natural frequencies the modulus of the complex number attains a maximum.

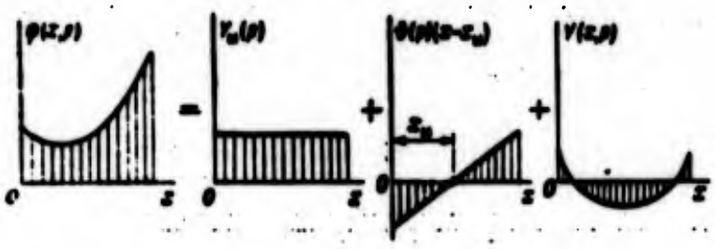

Figure 4.9

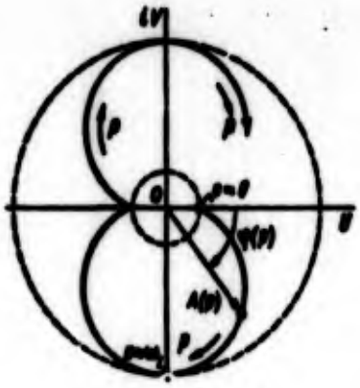

Figure 4.10

The method of initial parameters, presented in Section 4, will now be used to determine the forced oscillatory modes of an inhomogeneous rod. For any i^{th} segment of the rod we shall have a differential equation with constant coefficients (4.37)

$$\varphi_i^{IV}(x)+\alpha_i^4\varphi_i(x)=0,\quad \alpha_i^4=\frac{m(x)_i}{EJ(x)_i}p^2\quad (i=1,\ 2,\ldots\ k). \tag{4.71}$$

The principal difference between Equations (4.37) and Equations (4.71) is that in Equations (4.37) the coefficients α_i depend on the unknown natural frequency ω_n, and in Equations (4.71) they depend on the frequency of forced vibrations p, and therefore are known.

The solution of the equation for an i^{th} segment of the rod will be

$$\varphi_i(x)=C_{1i}\sin z_ix_i+C_{2i}\cos z_ix_i+C_{3i}\operatorname{sh} z_ix_i+C_{4i}\operatorname{ch} z_ix_i. \tag{4.72}$$

The arbitrary constants for a following segment are determined by the constants of the preceding segment by virtue of equations that are analogous to (4.39):

$$\begin{aligned}
\phi_i(l_i) &= \phi_{i+1}(0), \\
\phi_i'(l_i) &= \phi_{i+1}'(0), \\
[EJ\phi''(l)]_i &= [EJ\phi''(0)]_{i+1}, \\
[EJ\phi'''(l)]_i &= [EJ\phi'''(0)]_{i+1}.
\end{aligned} \tag{4.73}$$

The first two boundary conditions in (4.67) yield two arbitrary constants of the first segment, for example C_{31} and C_{41}. The other two arbitrary constants C_{11} and C_{21}, in terms of which the arbitrary constants of all segments will be expressed by means of (4.40), are determined by the second two boundary conditions in (4.67). Thus, a solution (4.72) for all segments of the rod will be found, and $\phi(x)$ for an inhomogeneous rod will become known.

Let us note the characteristic features of the method of initial parameters as applied to the case when the external force is applied not at the end of the rod but at a certain cross section x_p (Figure 4.11). These characteristics are manifested only when coupling various segments of the rod, and at the point of application of force P_0.

The cross section $x = x_p$ is included into an independent segment of infinitesimal length whose mass can be neglected, and the bending rigidity can be considered infinitely large. Then in order to couple segments, lying to the left and right of x_p the last equation in (4.73) can be replaced by the following:

$$[EJ\phi''(l)]_i + P_0 = [EJ\phi''(0)]_{i+1}. \tag{4.74}$$

At the right-hand end of the last k^{th} segment boundary conditions will be

$$\phi''(l_k) = 0, \quad \phi'''(l_k) = 0. \tag{4.75}$$

The same method can be used to solve a problem of forced lateral vibrations when at certain cross sections x_j there are masses m_j suspended elastically from the rod (see Figure 4.3). In this case,

for the purpose of coupling segments lying to the left and right of x_j, the last equation in (4.73) is replaced by the following:

$$[EJ(l)\phi'''(l)]_i + m_j\phi(x_j)\beta_j p^4 = [EJ(0)\phi'''(0)]_{i+1}. \qquad (4.76)$$

where

$$\beta_j = \frac{1}{\omega_j^2 - p^2}. \qquad (4.77)$$

Thus, the problem of forced harmonic vibrations of the rod has been solved using two methods. In one method the external forces and forced vibrations are expanded into a series in eigenfunctions of an inhomogeneous rod (4.46). First, the problem of natural vibrations is solved, and eigenfunctions and natural frequencies are found. This method allows us to see clearly the effect that the distributions of m_x and EJ(x) have on the frequencies and modes of natural vibrations. Also in stability analysis this method permits us to estimate their effect on the stability of a system which is very important when designing a rocket and its control system. The method is most suitable when the natural frequencies of the vibrations of a rocket fuselage significantly differ from one another, and the stability analysis can be conducted separately for each vibrational mode.

According to the second method, the external harmonic force is included in the boundary conditions, and the forced vibrations are sought in the form of the function $\phi(x, p)e^{ipt}$ without expanding it into a series in eigenmodes. Here instead of a series only one function $\phi(x, p)$ is needed to characterize forced vibrations of a rod. This method gives an exact solution expressed as a single function which is advantageous in analyzing the stability of motion when the frequencies of some fuselage vibrational modes are close to one another. This method is also most suitable in final design stages when the rocket has already been designed insofar as it is an object of control, and built, and one is required to verify its stability and obtain certain quantitative estimates.

7. Lateral Vibrations of an Elastic Rod Loaded With an Axial Slave Force

A force P whose direction always coincides with a tangent to the bent axis of the rod has come to be called a slave force. To a first approximation we can consider that this property is possessed by the thrust force of a rocket engine rigidly attached to the rocket. Therefore, a straight inhomogeneous elastic rod with a slave compressing force attached to an end can be taken as a model for studying the lateral vibrations of an elastic fuselage of the rocket. An

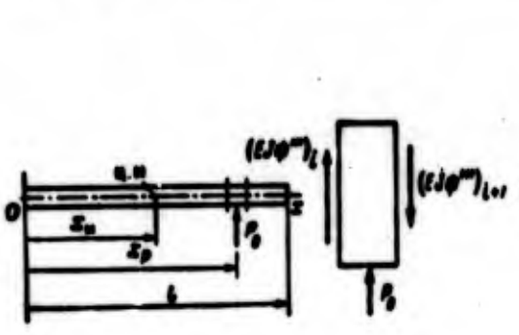

Figure 4.11

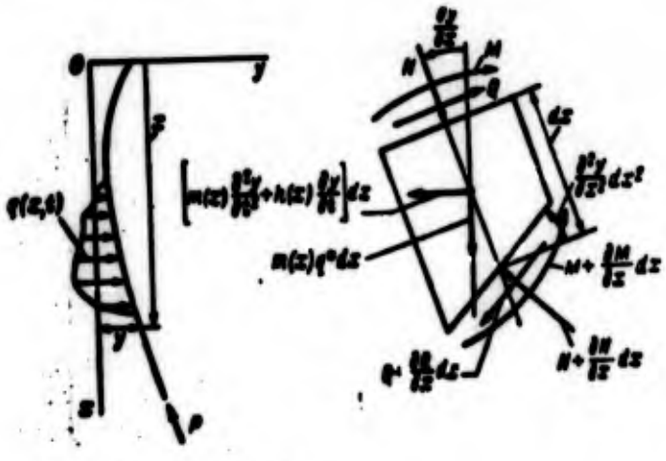

Figure 4.12

elastic rod with a slave force is a nonconservative system. As a result of the action of a compressing force, the dynamic characteristics of the rod (frequencies and natural vibrational modes) may become slightly modified. For a force P that exceeds a certain critical value, a dynamic instability may be a result.

Figure 4.12 shows an inhomogeneous rod in a bent state loaded with an axial slave force P; the same figure also shows a rod element of length dx at a cross section x with forces acting on it. The force of friction is assumed to be proportional to the first power of velocity. Here m(x), h(x), are the running mass and the coefficient

of viscous friction, q(x,t) is an external distributed force, N is a normal force at a cross section, g^* is an acceleration characterizing the intensity of mass forces in the direction of the Ox axis.

In studying the lateral vibrations of a rod acted on by an axial slave force, we shall not impose any restrictions on the motion of the center of mass of the rod in the directions of stationary coordinate axes Ox, Oy. However, the angular quantities $\partial^2 y/\partial x$, $\partial^2 y/\partial x^2$ will be assumed small, and this will be the basis for linearizing equations.

Applying d'Alambert's principles, we shall set up equations of equilibrium for the rod elements of length dx shown in Figure 4.12. Projecting the acting forces on the stationary coordinate axes and summing the moments of all forces relative to the center of mass of the element, we get

$$\begin{aligned} &-N'(x)dx+m(x)g^*dx+Q\frac{\partial^2 y}{\partial x^2}dx=0,\\ &-\frac{\partial Q}{\partial x}dx-\frac{\partial N}{\partial x}dx\frac{\partial y}{\partial x}-N(x)\frac{\partial^2 y}{\partial x^2}dx-\\ &-\left[m(x)\frac{\partial^2 y}{\partial t^2}+h(x)\frac{\partial y}{\partial t}\right]dx+q(x,t)dx=0,\\ &\frac{\partial M}{\partial x}dx+Qdx=0. \end{aligned} \tag{4.78}$$

In view of (4.2) we have

$$EJ(x)\frac{\partial^2 y}{\partial x^2}=M.$$

From the second and third equation in (4.78) we shall find

$$\frac{\partial^2}{\partial x^2}\left[EJ(x)\frac{\partial^2 y}{\partial x^2}\right]+\frac{\partial}{\partial x}\left(N(x)\frac{\partial y}{\partial x}\right)+m(x)\frac{\partial^2 y}{\partial t^2}+h(x)\frac{\partial y}{\partial t}=q(x,t). \tag{4.79}$$

The term

$$Q\frac{\partial^2 y}{\partial x^2}=\frac{\partial}{\partial x}\left[EJ(x)\frac{\partial^2 y}{\partial x^2}\right]\frac{\partial y}{\partial x}$$

in the first equation of (4.78) can be neglected since compared to the remaining terms it is an infintesimal of a higher order.

Then

$$\frac{\partial N(x)}{\partial x}=g^*m(x).$$

An x derivative of the normal compressing force is equal to the mass forces acting in the direction of the Ox axis.

The boundary conditions for the normal force will be

$$N(0)=0, \quad N(l)=P. \tag{4.80}$$

Consequently,

$$N(x)=g^*\int_0^x m(x)dx, \quad g^*=\frac{P}{m}, \quad m=\int_0^l m(x)dx. \tag{4.81}$$

Hence, we see in particular it is clear that the value of the acceleration g*, characterizing the intensity of mass forces, does not depend on small bending strains of the rod.

Equation (4.79), expressing the lateral vibrations of the rod, does not depend on the first equation in (4.78), the latter characterizing the longitudinal motion. In other words, small lateral vibrations of the rod can be considered independent of the longitudinal motion, assuming that the rod is acted upon by the acceleration of mass forces g* = P/m along the Ox axis. We can consider that the rod does not move, as it were, in the Ox direction, and the Ox component of P is always balanced by the forces of inertia of the rod, i.e., always P = mg*.

Equation (4.79) will be solved for the case

$$\frac{h(x)}{m(x)}=2\varepsilon=\text{const}$$

and when the external distributed force is

$$q(x, t)=0.$$

A general solution of Equation (4.79) can be written as

$$y(x, t)=\sum_{n=1}^{\infty}\varphi_n(x)q_n(t), \tag{4.82}$$

where $\varphi_n(x)q_n(t)$ are partial solutions of Equation (4.79) which can be obtained by the method of separation of variables. Substituting (4.82) into (4.79) and separating the variables, we get

$$\ddot{q}_n + 2\varepsilon_n\omega_n\dot{q}_n + \omega_n^2 q_n = 0, \quad (\varepsilon = \xi_n\omega_n), \tag{4.83}$$

$$[EJ(x)\varphi_n'']'' + (N(x)\varphi_n')' - \omega_n^2 m(x)\varphi_n = 0 \quad (n = 1, 2, \ldots). \tag{4.84}$$

The functions $\varphi_n(x)$ should satisfy the following boundary conditions:

$$\varphi_n'(0) = 0, \quad [EJ(x)\varphi_n''(x)]'_{x=0} = 0. \tag{4.85}$$

$$\varphi_n'(l) = 0, \quad [EJ(x)\varphi_n''(x)]'_{x=l} = 0. \tag{4.86}$$

The functions $\varphi_n(x)$ that are solutions of Equation (4.84) and satisfy the boundary conditions (4.86) are not orthogonal. In fact let us fix in Equation (4.84) an index n, and let us multiply this equation by $\varphi_m(x)$, where $n \neq m$, and finally let us integrate it with respect to x from 0 to l. Now let us write Equation (4.84) for an index m, multiply it by $\varphi_n(x)$, and also integrate it with respect to x over the interval [0, l]. Subtracting the second equation from the first, we get

$$(\omega_n^2 - \omega_m^2)\int_0^l m(x)\varphi_n\varphi_m\,dx = P[\varphi_n'(l)\varphi_m(l) - \varphi_m'(l)\varphi_n(l)]$$

$$(m, n = 1, 2, \ldots; n \neq m).$$

The difference of work done by forces of inertia in lateral vibrations is equal to the difference of work done by the lateral components of force P. The forces of inertia, arising in the presence of oscillatory modes $\varphi_n(x)$, are not self-balanced; they are balanced by a lateral component of force P. This can be seen by integrating Equations (4.84) with respect to x over the interval [0,l]. In view of the conditions (4.80), (4.85) and (4.86) we have

$$\omega_n^2\int_0^l m(x)\varphi_n(x)\,dx = P\varphi_n'(l). \tag{4.87}$$

Multiplying Equation (4.84) by $(x - x_M)$, and integrating it with respect to x over $[0,l]$, we get

$$\omega_n^2 \int_0^l m(x)\varphi_n(x-x_M)\,dx = \\ = P[\varphi_n'(l)(l-x_M)-\varphi_n(l)] + \frac{P}{m}\int_0^l m(x)\varphi_n\,dx. \tag{4.88}$$

The moment of the forces of inertia arising in the lateral vibrations, relative to the center of mass, is balanced by the moment of force P, and the moment of the forces of inertia which are proportional to the longitudinal acceleration $g^* = P/m$.

Equation (4.84) for a homogeneous rod will be put in the form

$$v_n^{IV} + \beta[tv_n']' - \lambda_n^2 v_n = 0, \tag{4.89}$$

where

$$\beta = \frac{Pl^2}{EJ_0}, \quad \lambda_n^2 = \omega_n^2 \frac{m_0 l^4}{EJ_0}, \quad t = \frac{x}{l}, \quad v_n = \frac{\varphi_n}{l}.$$

The boundary conditions (4.85) and (4.86) can be written as

$$v_n'(0) = v_n''(0) = v_n'(l) = v_n''(l) = 0.$$

The solution of Equation (4.89) is given in [4, 7, 19]. It is written in the form of a power series

$$v_n(t) = \sum_{k=0}^{\infty} C_k t^k.$$

It follows from the boundary conditions that

$$C_1 = C_2 = 0, \quad \sum_{k=3}^{\infty} C_k k(k-1)(k-2) = 0, \\ \sum_{k=3}^{\infty} C_k k(k-1) = 0. \tag{4.90}$$

The following recurrence formula is used to determine the coefficients of the series

$$C_k = \frac{\phi(\lambda_n, \beta)}{k(k-1)(k-2)(k-3)},$$

where

$$\phi(\lambda_n, \beta) = \lambda_n^2 C_{k-1} - \beta C_{k-3}(k-3)^2.$$

The coefficients C_0 and C_1 remain undetermined . They enter linearly in (4.90) which can be rewritten as

$$A_0 C_0 + A_1 C_1 = 0, \quad B_0 C_0 + B_1 C_1 = 0.$$

The conditions for the existence of a nonzero solution gives

$$A_0 B_1 - A_1 B_0 = 0.$$

Figure 4.13, taken from [19], shows the mode and dimensionless frequency of natural oscillations for the first and second mode number versus the parameters β. The dimensionless frequency of oscillations λ is connected with the dimensioned natural frequency by the relation

$$\omega = \lambda_n \sqrt{\frac{EJ_0}{\rho F l^4}}.$$

For β = 0 for the first oscillatory mode $\lambda_1 = 4{,}73^2 = 22{,}37$; and for the second oscillatory mode $\lambda_2 = 7{,}85^2 = 61{,}62$. A critical state occurs for β_{cr} = 109.69 which corresponds to the critical force P_{cr} exceeding approximately 11 times the Euler critical force $P_{cr} = \pi^2 EJ_0/l^2$ for a rod hinged and subjected to a compressing axially centered force. It will be noted that for a rod hinged and loaded with dead weight (which corresponds to the case when the force at the end of the rod does not follow its bent axis) the coefficient of the critical force is β_{cr} = 18.6 [17].

A further increase of force P leads to the situation where the equation to determine natural frequencies has a complex root. This means that the oscillatory motion has an increasing amplitude.

Figure 4.14 shows a graph of the natural frequency versus the parameter β for the first eight mode numbers [2]. In this case $\omega=\omega_n/\omega_1^0$, where ω_1^0, which is the natural frequency for the first mode number of a rod not loaded with an axial force, is equal to $4{,}73^2\sqrt{\frac{EJ_0}{m_0 l^4}}$. For $\beta=405$ the frequencies corresponding to the third and fourth natural oscillatory modes merge together, whereas the frequencies corresponding to the two subsequent higher modes of natural oscillations* depend on the parameter β for the first eight mode numbers [2]. It can be assumed that stability losses for higher oscillatory modes will correspond to a pairwise merging of the natural oscillations of the system.

We note that for rockets the coefficient β usually does not exceed several units, and therefore the phenomenon of instability occuring at $\beta_{cr}=109{,}69$ is only of theoretical interest. By analogy with (4.68) we can separate from the function $\varphi_n(x)$ a linear function of x, so that the remaining part $f_n(x)$ will be a self-balanced mode characterizing the bending vibrations

$$\begin{gathered}\varphi_n(x)=f_{Mn}+\theta_n(x-x_M)+f_n(x),\\ \int_0^l m(x)f_n(x)\,dx=0,\\ \int_0^l m(x)f_n(x)(x-x_M)\,dx=0.\end{gathered}\tag{4.91}$$

In order to make the last two equations valid, the numbers f_{Mn} and θ_n must be determined from the following equations:

$$\begin{aligned}-\omega_n^2 f_{Mn}m&=P\varphi_n'(l)=P[\theta_n+f_n'(l)],\\ -\omega_n^2\theta_n J&=P[f_n'(l)(l-x_M)-f_n(l)].\end{aligned}\tag{4.92}$$

*Translator's note: There is apparently text missing here in the original Russian material.

TABLE 4.7

First Mode

β \ x/l	0	0,1	0,2	0,3	0,4	0,5	0,6	0,7	0,8	0,9	1,0	λ_1^2
0	1,000	0,537	0,097	−0,272	−0,520	−0,607	−0,520	−0,272	0,097	0,537	1,000	22,37
10	1,000	0,541	0,104	−0,267	−0,520	−0,616	−0,532	−0,283	0,095	0,547	1,024	20,975
20	1,000	0,546	0,111	−0,262	−0,522	−0,624	−0,546	−0,295	0,091	0,558	1,051	19,529
30	1,000	0,550	0,119	−0,256	−0,523	−0,634	−0,562	−0,310	0,087	0,571	1,083	18,043
50	1,000	0,562	0,136	−0,242	−0,524	−0,662	−0,608	−0,347	0,077	0,611	1,170	15,024

Second Mode

β \ x/l	0	0,1	0,2	0,3	0,4	0,5	0,6	0,7	0,8	0,9	1,0	λ_2^2
0	1,000	0,228	−0,366	−0,662	−0,483	0,000	0,483	0,662	0,366	−0,228	−1,000	61,62
10	1,000	0,221	−0,410	−0,677	−0,491	0,011	0,517	0,708	0,417	−0,264	−1,094	59,767
20	1,000	0,213	−0,427	−0,697	−0,500	0,027	0,560	0,754	0,442	−0,287	−1,119	57,775
30	1,000	0,200	−0,449	−0,722	−0,511	0,049	0,616	0,819	0,472	−0,331	−1,224	55,662
50	1,000	0,158	−0,525	−0,808	−0,537	0,127	0,798	1,025	0,564	−0,474	−1,754	51,108

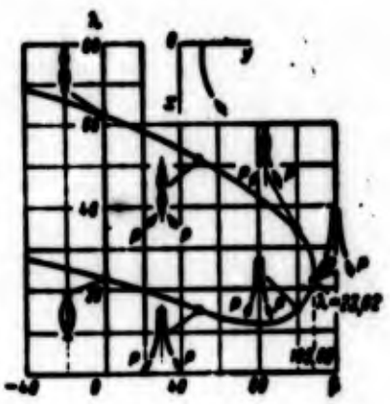

Figure 4.13

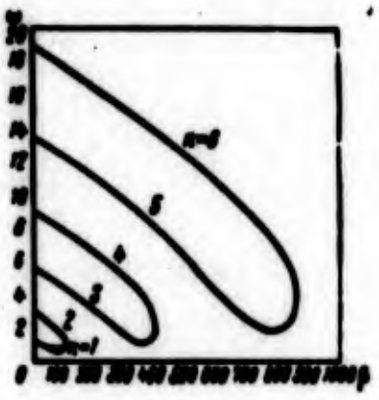

Figure 4.14

obtained from (4.87) and (4.88)

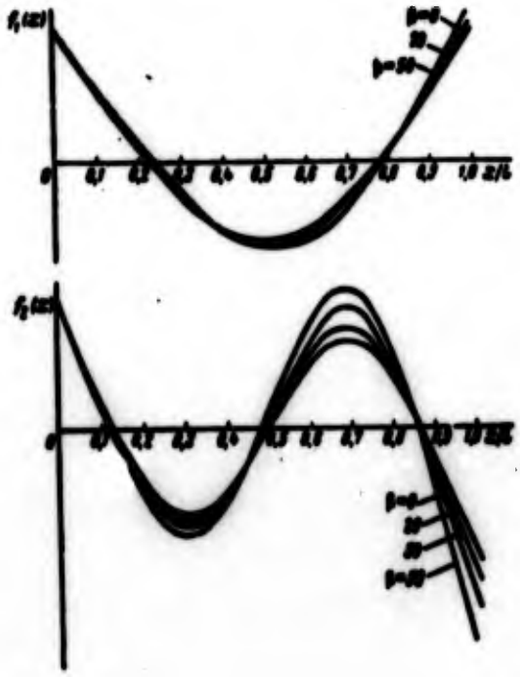

Figure 4.15

Table 4.7, composed on the basis of solving Equations (4.89), (4.91), shows for comparison the values of functions $f_n(x)$ and the dimensionless frequencies λ_n for the first and second oscillatory modes of a homogeneous rod for values of β. The graphs of $f_n(x)$ are also shown for comparison in Figure 4.15.

For small values of β, the functions $f_n(x)$ representing the first oscillatory modes of a rod subject to a slave force, do not differ much from the natural oscillatory modes of a rod ($\beta = 0$). The natural frequencies can be considered to decrease proportionally to β. Therefore, as a rough approximation of the first two oscillatory modes one can recommend a use of the natural oscillatory modes of a rod without a slave force, and the effect of a slave force on the natural frequency for $\beta < 20$ can be estimated by a linear correction

$$\omega_n = (1 - \mu_n^0 \beta)\,\omega_n^0, \quad \beta = \frac{Pl^2}{EJ_0}, \quad 0 < \beta < 20. \tag{4.93}$$

Here ω_n^0 is the natural frequency calculated for P = 0, i.e., without a slave force. On the basis of Table 4.7 we can take $\mu_1^0 \approx 0{,}14$; $\mu_2^0 \approx 0{,}2$. The quantity P/EJ_0 entering the parameter β can be approximately calculated by decomposing the rod into k segments with constant masses m_i and the bending rigidity EJ_i. Then we get

$$\frac{P}{EJ_0} = \left(\sum_{i=1}^{k} \frac{r_i}{\sqrt{EJ_i}}\right)^2. \tag{4.94}$$

A use of the natural oscillatory modes of a rod, not loaded with a slave force, in solving the problem of the vibrations of a rod loaded with a slave force will be considered in the following section.

8. An Application of the Bubnov-Galerkin Method to the Problem of the Lateral Vibrations of a Rod Loaded by an Axial Slave Force.

As already noted in the previous section, the functions characterizing the lateral vibrations of a rod with an axial slave force are not orthogonal. As a consequence, the equations of forced vibrations for all generalized coordinates $q_n(t)$ turn out to be interrelated. This complicates immensely the solution of the problem. Even the problem of determining the modes and frequencies of the natural oscillations of the rod loaded with an axial slave force is sufficiently time-consuming.

In this section we present an approximation method proposed by Bubnov-Galerkin [2, 14] for solving the problem of the forced lateral vibrations of an inhomogeneous rod subject to a slave force.

The forced lateral vibrations $y(x, t)$, defined by Equations (4.79), will be written as a series (4.17),

$$y(x,t)=y_M(t)+\varphi(t)(x-x_M)+\sum_{n=1}^{\infty} f_n(x)q_n(t), \tag{4.95}$$

where $y_M(t)$ and $\varphi(t)$ are the generalized coordinates of a rod as a rigid body; $q_n(t)$ is the generalized coordinate corresponding to the function $f_n(x)$; x_M is the coordinate of the center of mass of the rod; x is the coordinate of an arbitrary cross section of the rod.

The functions $f_n(x)$ are represented by the natural oscillatory modes of a rod with free ends without the slave force ($P = 0$). Thus, the functions $f_n(x)$ satisfy the differential Equations (4.6)

and the boundary conditions (4.7) and (4.8). In Equation (4.6) ω_n is the natural frequency of an n^{th} mode of a rod with free ends for $P = 0$.

It will be noted that all boundary conditions (4.85) and (4.86) satisfy each of the functions appearing in the series (4.95) which is a necessary condition for applying the Bubnov-Galerkin method. This method allows us to go from Equation (4.79) to a system of ordinary differential equations which usually can be solved using only a finite number of terms in (4.95).

A substitution of (4.95) into Equation (4.79) is of necessity accompanied by a certain error, inasmuch as (4.95) is not a solution of (4.79). In accordance with the Bubnov-Galerkin method this error must be multiplied by each of the approximating functions in (4.95), integrated with respect to x from 0 to l, and the value of the integral set equal to 0. As a result we obtain the following system of equations:

$$\begin{gathered}
\int_0^l \left\{ \frac{\partial^2}{\partial x^2}\left(EJ(x)\frac{\partial^2 y}{\partial x^2}\right) + \frac{\partial}{\partial x}\left(N(x)\frac{\partial y}{\partial x}\right) + m(x)\frac{\partial^2 y}{\partial t^2} + \right. \\
\left. + h(x)\frac{\partial y}{\partial t} - q(x,t) \right\} dx = 0, \\
\int_0^l \left\{ \frac{\partial^2}{\partial x^2}\left(EJ(x)\frac{\partial^2 y}{\partial x^2}\right) + \frac{\partial}{\partial x}\left(N(x)\frac{\partial y}{\partial x}\right) + m(x)\frac{\partial^2 y}{\partial t^2} + \right. \\
\left. + h(x)\frac{\partial y}{\partial t} - q(x,t) \right\} (x - x_w)\, dx = 0, \\
\int_0^l \left\{ \frac{\partial^2}{\partial x^2}\left(EJ(x)\frac{\partial^2 y}{\partial x^2}\right) + \frac{\partial}{\partial x}\left(N(x)\frac{\partial y}{\partial x}\right) + \right. \\
\left. + m(x)\frac{\partial^2 y}{\partial t^2} + h(x)\frac{\partial y}{\partial t} - q(x,t) \right\} f_n(x)\, dx = 0. \\
(n = 1, 2, \ldots, n^0)
\end{gathered} \tag{4.96}$$

Here instead of y(x,t), one must substitute a finite number of terms from (4.95) into the expressions appearing in the parentheses.

In order to make it easier to obtain the final equations we shall write out certain intermediate integration results.

On the basis of (4.11) we have

$$\int_0^l \frac{\partial^2}{\partial x^2}\left(EJ(x)\frac{\partial y}{\partial x^2}\right)dx=0, \quad \int_0^l \frac{\partial^2}{\partial x^2}\left(EJ(x)\frac{\partial y}{\partial x^2}\right)(x-x_u)\,dx=0.$$

Integrating by parts and keeping in mind (4.7) and (4.8), we find

$$\int_0^l \frac{\partial^2}{\partial x^2}\left(EJ(x)\frac{\partial y}{\partial x^2}\right)f_n(x)=q_n(t)\int_0^l EJ(x)f_n''^2\,dx.$$

The forces of viscous friction, arising only during elastic vibrations of a rod, will be taken into consideration. In addition the relation $h(x)/m(x)=2\varepsilon$, used in the previous section, will be assumed valid. Then in view of (4.10), (4.12), and (4.14) we shall obtain

$$\int_0^l h(x)\frac{\partial y}{\partial t}dx=\int_0^l h(x)\frac{\partial y}{\partial t}(x-x_u)\,dx=0,$$

$$\int_0^l h(x)\frac{\partial y}{\partial t}f_n(x)\,dx=\dot{q}_n\int_0^l h(x)f_n^2dx=\dot{q}_nh_n,$$

$$\int_0^l m(x)\frac{\partial y}{\partial t^2}(x-x_u)\,dx=\ddot{\theta}\int_0^l m(x)(x-x_u)^2dx=\ddot{\theta}I,$$

$$\int_0^l m(x)\frac{\partial y}{\partial t^2}dx=\ddot{y}_u\int_0^l m(x)\,dx=\ddot{y}_um,$$

$$\int_0^l m(x)\frac{\partial y}{\partial t^2}f_n(x)\,dx=\ddot{q}_n\int_0^l m(x)f_n^2dx=\ddot{q}_nm_n.$$

Integrating by parts, and using (4.80) and (4.81) we shall find

$$\int_0^l \frac{\partial}{\partial x}\left(N(x)\frac{\partial y}{\partial x}\right)dx=P\left(\theta+\sum_{n=1}^{n^0}f_n'(l)q_n\right).$$

$$\int_0^l \frac{\partial}{\partial x}\left(N(x)\frac{\partial y}{\partial x}\right)(x-x_u)\,dx=P\sum_{n=1}^{n^0}q_n\left[f_n'(l)(l-x_u)-f_n(l)\right],$$

$$\int_0^l \frac{\partial}{\partial x}\left(N(x)\frac{\partial y}{\partial x}\right)f_n(x)\,dx=Pf_n(l)\sum_{n=1}^{n^0}f_n'(l)q_n-$$

$$-\frac{P}{m}\int_0^l f_n'(x)\sum_{n=1}^{n^0}f_n'(x)q_n\int_0^x m(x)\,dx^2.$$

Combining all the intermediate integration results and introducing the notation, we obtain the following n^0+2 ordinary differential equations in generalized coordinates y_u, θ, q_n :

$$m\ddot{y}_u+P\theta+P\sum_{n=1}^{n^0}f_n'(l)q_n=\int_0^l q(x,t)\,dx,$$

$$I\ddot{\theta}+P\sum_{n=1}^{n^0}A_nq_n=\int_0^l q(x,t)(x-x_u)\,dx,$$

$$m_n\ddot{q}_n+h_n\dot{q}_n+k_nq_n+P\sum_{\substack{m=1\\m\neq n}}^{n^0}B_{nm}q_m= \tag{4.97}$$

$$=\int_0^l q(x,t)f_n(x)\,dx\quad(n,m=1,2,\ldots,n^0).$$

Here

$$A_n=f_n'(l)(l-x_u)-f_n(l),$$

$$B_{nm}=f_n(l)f_m'(l)-\frac{1}{m}\int_0^l f_n'(x)f_m'(x)\int_0^x m(x)\,dx^2,\quad n\neq m. \tag{4.98}$$

The effective mass, the effective friction coefficient, and the effective rigidity are

$$m_n=\int_0^l m(x)f_n^2dx,$$

$$h_n=\int_0^l h(x)f_n^2dx, \tag{4.99}$$

$$k_n=\int_0^l EJ(x)f_n''^2dx+Pf_n'(l)f_n(l)-\frac{P}{m}\int_0^l f_n'^2(x)\int_0^x m(x)\,dx^2.$$

The formulas for the effective mass coefficients are the same as those for the case of a rod not loaded with an axial slave force. The formulas for the effective rigidity coefficients turn out to be different. According to (4.33), the effective rigidity coefficient is equal to twice the value of the potential energy of a bent rod for the amplitude $q_n = 1$. In case of a rod loaded with an axial slave force the effective rigidity coefficient consists of three terms: the potential energy of bending, the work done by the lateral component of force $Pf_n'(l)$ over a distance $f_n(l)$, and the work (with a negative sign) done by the axial compressing forces over displacements caused by lateral bending:

$$\frac{P}{m}\int_0^l f_n'^2(x)\int_0^x m(x)\,dx=\int_0^l N(x)f_n'^2\,dx.$$

Calculations show that the work of compressing forces is greater than the work done by the lateral component; and therefore the natural frequency of the lateral vibrations of the rod subject to axial slave force is lower than the natural frequency of a rod not subject to a slave-force.

The right-hand sides of Equations (4.97) represent generalized forces acting on the rod. The force P is not included in the generalized forces, it is in this case a part of the system — the rod with the slave force.

The equation of elastic vibrations in (4.97) does not depend on the first and second equations, and forms a system of n^0 equations. This system can be more compactly represented by one matrix equation

$$[\ddot{q}_k]+[H_{jk}][\dot{q}_k]+[G_{jk}][q_k]=[F_k]. \tag{4.100}$$

where

$$[q_k]=\begin{bmatrix} q_1 \\ q_2 \\ \vdots \\ q_{n^0} \end{bmatrix}, \quad [F_k]=\begin{bmatrix} F_1 \\ F_2 \\ \vdots \\ F_{n^0} \end{bmatrix}$$

$[H_{jk}]$ and $[G_{jk}]$ are square matrices of order n^0. The expressions for the matrix elements $[H_{jk}]$, $[G_{jk}]$, and $[F_k]$ are as follows

$$H_{jk}=\frac{h_j}{m_j}\delta_{jk} \quad (j, k=1, 2, \ldots, n^0),$$

$$G_{jk}=\frac{h_j}{m_j}\delta_{jk}+\frac{P}{m}\left[f_j(l)f_k'(l)-\frac{1}{m}\int_0^l f_j'(x)f_k'(x)\int_0^x m(x)\,dx^2\right], \tag{4.101}$$

$$(j, k=1, 2, \ldots, n^0),$$

$$F_k=\frac{1}{m_k}\int_0^l q(x, t)f_k(x)\,dx \quad (k=1, 2, \ldots, n^0).$$

Here δ_{jk} is the Kronecker symbol ($\delta_{jk}=1$ for $j = k$; $\delta_{jk}=0$ for $j \neq k$). Solving the system (4.100), and substituting the results into the first and second equations of (4.97) we shall find the lateral acceleration of the center of mass of the rod $\ddot{\bar{y}}_M$ and the angular acceleration $\ddot{\theta}$.

The Bubonov-Galerkin method makes it possible to study the lateral vibrations of a rod subject to an axial slave force for the case when q(x,t) - 0. For this purpose one must set $F_k = 0$ in Equation (4.100). For simplicity, one can in addition let all $H_{jk} = 0$.

Assuming

$$[q_k] = [\bar{q}_k] e^{i\omega t}, \tag{4.102}$$

where $[\bar{q}_k]$ is a column matrix of constant coefficients, and substituting (4.102) into (4.100), we get a system of linear homogeneous algebraic equations. In order to obtain nontrivial solutions to these equations one must set to zero the determinant of the coefficients multiplying $\bar{q}_k$. As a result we obtain

$$\det \| [G_{jk}] - \omega^2 [E] \| = 0, \tag{4.103}$$

where [E] is a unit matrix. The characteristic equation (4.103) is an algebraic equation in ω^2. For the stability of each vibrational mode of the system it is necessary that all roots ω^2 of Equation (4.103) be real and possitive. The presence of negative or complex roots shows that there exists at least one unstable mode.

A detailed analysis of Equation (4.97) shows that for $q(x,t) = 0$ for all values of $P \neq 0$ there exist two natural oscillatory modes with a zero frequency. One of these modes is associated with a translational motion of a rod as a rigid body in the lateral direction, without rotation. The second oscillatory mode corresponds to a rotational motion of the rod as a rigid body with a constant angular velocity. These modes, strictly speaking, are unstable, so that the system is unstable irrespective of whether the elastic vibrations of the rod are stable or not. Below we shall assume, having in mind guided missiles, that the stability of motion of a rod as a rigid body is always secured by a controlled system, and therefore attention will be mostly given to the stability of the elastic vibrations of the rod.

Reference [2] gives the results of calculations done using the Bubonv-Galerkin methods. The solutions of Equation (4.103) were found for gradually increasing values for force P. The computation was repeated for several different values of n^0 in order to determine what number of the oscillatory modes should be used to correctly evaluate the character of frequency change. If one takes $n^0 = 1$, then the fundamental and single natural frequency vanishes for $\beta = Pl^2/EJ_0 = 81.4$. For $n^0 \geqslant 2$ the first root, corresponding to instability, appears as a result of the first and second characteristic frequencies being merged. The graph of these frequencies versus parameter β is shown in Figure 4.16 for values $n^0 = N = 1, 3, 3, 4, 5$, where the quantity $\omega = \omega_n/\omega_1^0$ is plotted on the ordinate axis, and ω_1^0 is the first natural frequency for $\beta = 0$.

Figure 4.16 shows that the natural oscillatory modes corresponding to Equation (4.6) - (4.8) give good results in determining the first and second natural frequency of the vibrations of a rod subject to a slave force. For $\beta \leqslant 20$ it is sufficient to only use one or two terms of the series.

If among the natural frequencies there are any adjacent frequencies, then in studying the forced vibrations of a rod it is advisable to use the method of initial parameters. We shall present the procedure for solving the problem in case when the rod is subject to a lateral harmonic force $P(t) = P_0 e^{i\nu t}$, applied at $x = x_p$ as well as the slave force (see Figure 4.11).

Let us subdivide the rod into case segments for each of which the quantities EJ(x), N(x), m(x) will be assumed constant.

The forced harmonic vibrations of each i^{th} segment of the rod will be sought in the form

$$y_i(x, t) = \phi_i(x_i, p) e^{i\nu t}.$$

Then for any i^{th} segment of the rod Equation (4.79) for $h(x) \equiv 0$, $q(x,t) \equiv 0$ becomes an equation with constant coefficients.

$$\varphi_i^{IV} + v_i^2 \varphi_i'' - a_i^4 \varphi_i = 0 \quad (i = 1, 2, \ldots, k). \tag{4.104}$$

in which

$$v_i^2 = \frac{N_i}{EJ_i}, \quad a_i^4 = p^2 \frac{m_i}{EJ_i}.$$

Assuming the partial solution Equation (4.104) to have the form

$$\varphi_i = e^{rx_i},$$

we get

$$r_i^4 + v_i^2 r_i^2 - a_i^4 = 0.$$

Whence,

$$(r_{1,3})_i = \pm k_i, \quad (r_{2,4})_i = \pm \eta_i,$$

$$k_i = \frac{1}{\sqrt{2}} \sqrt{v_i^2 + \sqrt{v_i^4 + a_i^4}}, \quad \eta_i = \frac{1}{\sqrt{2}} \sqrt{-v^2 + \sqrt{v_i^4 + a_i^4}}.$$

The general solution of Equation (4.104) will be

$$\varphi_i(x_i, p) = C_{1i} \sin k_i x_i + C_{2i} \cos k_i x_i + C_{3i} \operatorname{sh} \eta_i x_i + C_{4i} \operatorname{ch} \eta_i x_i. \tag{4.105}$$

At the boundary of the i^{th} and $(i+1)^{st}$ segments we have the coupling conditions (4.73). At the boundary of the segments to the left and right of x_p the last equation in (4.73) is replaced by (4.74). At the left-hand end of the first segment and the right-hand end of the last k^{th} segment the boundary conditions will be

$$\varphi_1(0) = 0, \quad \varphi_1''(0) = 0, \quad \varphi_k(l_k) = 0, \quad \varphi_k''(l_k) = 0.$$

Thus, to determine 4k coefficients we have 4k boundary conditions, out of which one is not a zero boundary condition. Continuing all the solutions ϕ_1 from the first to the last segment we get a function $\phi(x, p)$, characterizing the forced vibrations of the entire inhomogeneous rod. The method of initial parameters gives satisfactory results only for small values of $\beta = Pl^2/EJ_0$.

From the function $\phi(x, p)$ one can separate a self-balanced function Y(x, p) characterizing the elastic vibrations of the rod:

$$Y(x, p) = \phi(x, p) - Y_M(p) - \theta(p)(x - x_M),$$

$$\int_0^l m(x) Y(x, p)\, dx = 0,$$

$$\int_0^l m(x) Y(x, p)(x - x_M)\, dx = 0.$$

The vibration amplitudes $Y_M(p)$ and $\theta(p)$ are in this case determined by the following two equations:

$$-p^2 Y_M(p) m = P_0 - P[\theta(p) + Y'(l, p)],$$
$$-p^2 \theta(p) J = P_0(x_P - x_M) - P[Y'(l, p)(l - x_M) - Y'(l, p)].$$

These equations determine the amplitudeof the forced vibrations of a rod as a rigid body relative to which the elastic vibrations governed by Y(x,P) will be self-balanced. In contrast to a rod not subject to the slave force (4.69), here the vibrations of the center of mass with an amplitude $Y_M(p)$ occur as a result of the action of two forces — the lateral force P_0 and the slave force P.

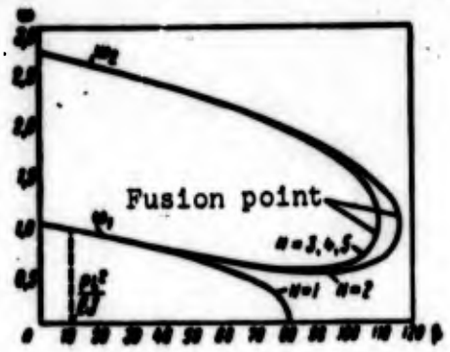

Figure 4.16

REFERENCES

1. Babakov, I. M. Teoriya kolebaniy (Theory of Oscillations) Gostekhizdat, 1958.

2. Bil, Dynamic Stability of an Elastic Rocket Subject to Constant and Pulsating forces fo Thrust, Raketnaya tekhnika i kosmonavtika. No. 3, 1965.

3. Bolotin, V. V. Nekonservativnyye zadachi teorii uprugoy ustoychivosti (Nonconservative problems in Theory of Elastic Stability). Fizmatgiz, 1961.

4. Goroshko, O. A. Dinamika uprugoy konstruktsii v usloviyakh svobodnogo poleta (Dynamics of an Elastic Structure Under the Conditions of Free Flight) Izdatel'stvo "Naukova dumka", Kiev, 1965.

5. Ditkin, V. A. and A. P. Prudnikov. Spravochnik po operatsionnomu ischisleniya (Manual of Operational Calculus) Izdatel'stvo "Vysshaya shkola', 1965.

6. Kamke, E. Spravochnik po obyknovennym differentsial'nym uravneniyam (Manual of Ordinary Differential Equations) Izdatel'stvo "Nauka", 1965.

7. Kenig, The Effect of the Reactive Force on the Bending Mechanical Characteristics of a Rocket. Voprosy raketnoy tekhniki, No. 5, 1965.

8. Kolesnikov, K. S. Oscillations of a Liquid in a Cylindrical Container.

9. Courant, R. and D. Hilbert. Methods of Mathematical Physics, Gostekhizdat, Vol. I, II, 1951.

10. Lur'ye, A. I. Operational Calculus in Applications to Mechanical Problems, GITTL, 1938.

11. Lukens, Methods of Analyzing the control Systems of a Large Elastic Rocket. Voprosy raketnoy tekhniki, No. 9, 1961.

12. Nudel'man, Ya. L. Metody opredeleniya sobstvennykh chastot i kriticheskikh sil dlya sterzhnevykh sistem (Methods of Determining the Natural Frequencies and Critical Forces for Rod Systems) Gostekhizdat, 1949.

13. Panovko, Ya. G. and I. I. Gubanov. Ustoychivost' i kolebaniya uprugikh sistem (Stability and the Oscillations of Elastic Systems). Izdatel'stvo "Nauka", 1964.

14. Pomomarev, S. D., V. L. Biderman, K. K. Likharev, V. M. Makushin, N. N. Malinin, and V. I. Feodos'yev. Raschety na prochnost' v mashinostroyenii (Strength Calculations in Mechanical Engineering, Mashgiz, Vol. III, 1959.

15. Rayleigh, Theory of Sound, Gostekhizdat, Vols. I, II, 1955.

16. Sobolev, S. L. Uravneniya matematicheskoy fiziki (Equations of Mathematical Physics, Gostekhizdat, 1950.

17. Timoshenko, S. P. Ustoychivost' uprugikh sistem (Stability of Elastic Systems, Gostekhizdat, 1955.

18. Timoshenko, S. P. Kolebaniya v inzhenernom dele (Oscillations in engineering) Fizmatgiz, 1959.

19. Feodos'yev, V. I. On a certain problem in stability, Vol. 29, No. 2, 1965.

20. Kharti, A Dynamic Analysis of Structures, Based on an Analysis of the Oscillatory Modes of Separate Elements. Raketnaya tekhnika i kosmonavtika No. 4, 1965.

21. Chuvikovskiy, V. S., O. M. Paliy and V. Ye. Spiro. Obolochki sudovykh konstruktsiy (Shells in Container Structures) "Sudostroyeniye" Leningrad, 1966.

22. Shimanskiy, Yu. A. Dinamicheskiy raschet sudovykh skonstruktsiy (dynamic Calculations of Container Structures) Sudpromgiz, 1963.

CHAPTER V

THE EFFECT OF THE ELASTIC PROPERTIES OF THE FUSELAGE ON THE STABILITY OF ROCKET MOTION

1. Preliminary Remarks

The elastic properties of the fuselage have a strong effect on the dynamic stability of guided rockets, especially when the rocket is very long. This problem assumes a great importance for large multi-stage booster rockets which are used to launch and accelerate space-craft. In the powered stage a rocket passes through dense atmospheric layers where it is strongly influenced by the aerodynamic forces acting on its fuselage.

In the case where the fuselage is nonrigid, problems arise out of which the most important ones are: a stabilization of the elastic lateral vibrations of the fuselage, the problem of accounting for the effect of the elastic wiring and the elastic suspension of the power plant on the rocket stability, a compensation for the navigational errors caused by a rotation of the thrust vector. Figure 5.1 shows a three-stage rocket in a deformed state.

To make the flight of a rocket along the calculated trajectory possible, a program mechanism (a computer) of the control system specifies the angle of turn of the thrust vector as a function of

time. The angular control system computes errors in the angular possition, and produces opposing control forces. When elastic lateral vibrations of the fuselage are present, the error in the angular position of the rocket, θ_1, determined by the control system, consists of two parts:

$$\theta_1 = \theta + \left(\frac{\partial y_{n2}}{\partial x}\right)_{x=x_r},$$

where $\left(\frac{\partial y_{n2}}{\partial x}\right)_{x=x_g}$ is the angle between the tangent to the bent axis of the fuselage at the location of the gyroscope, and the fuselage axis for the case when the rocket represents an ideally rigid body.

This error will be reduced to zero by the control system, and the deflection imparted to the rocket by the control units will depend on the angle θ_1, which differs from the angle θ by

$$\left(\frac{\partial y_{n2}}{\partial x}\right)_{x=x_r}.$$

Due to the bending of the fuselage the thrust vector will be rotated by an angle

$$\theta + \left(\frac{\partial y_{n2}}{\partial x}\right)_{x=x_d},$$

where $\left(\frac{\partial y_{n2}}{\partial x}\right)_{x=x_d}$ is the angle between the tangent to the bent axis of the fuselage at the location of the power plant, and the axis of the fuselage for the case when the rocket represents an ideally rigid body.

The interaction of the elastic lateral vibrations of the fuselage with the oncoming air stream is sometimes referred to as the aeroelastic oscillations. The frequency of these oscillations usually approaches the natural frequency of the fuselage vibrations. The oscillations cause undesirable lateral inertial loads on the fuselage, especially if they reach high amplitudes. The problem of stabilizing the lateral vibrations consists of damping the randomly arising oscillations or at least of not allowing them to reach amplitudes larger than the strength of the fuselage permits.

In addition to the elastic lateral vibrations, there may arise a quasi-static deflection of the fuselage due to a slow rotation of the rocket during the flight along the programmed trajectory. If the computer is not able to take the quasi-static deflection fof the fuselage into account, then the control system cannot eliminate the error in the direction of the thrust vector, and this leads to navigational errors.

Below we shall consider in detail the following two questions:

1) The effect of the elastic lateral vibrations of the fuselage on the stability of a closed system consisting of the fuselage and the control system, and

2) The effect of the elastic wiring and the elastic suspension of the power plant from the fuselage on the mechanical properties of the servodrive and the stability of the rocket.

Just as in the case when the rocket represents an ideally rigid body or when it has a rigid fuselage with a liquid filler we shall only consider small perturbations of the parameters of motion. This allows us, as far as the perturbations are concerned, to obtain a linear system of differential equations with coefficients being functions of the parameters of undisturbed motion.

Small deflections of the thrust vector, due to the lateral vibrations of the fuselage, do not, up to infinitesimals of the second order, change the acceleration of the rocket in the longitudinal direction. Both in magnitude and direction, this acceleration remains the same as the acceleration in undisturbed motion. For this reason with small perturbations the lateral motion can be considered independently of the longitudinal motions.

For a small time interval the trajectory of a guided ballistic missile can be considered a plane curve differing little from a straight line. Therefore, an undisturbed motion of a rocket in a small time interval will be considered to follow a straight line. Inasmuch

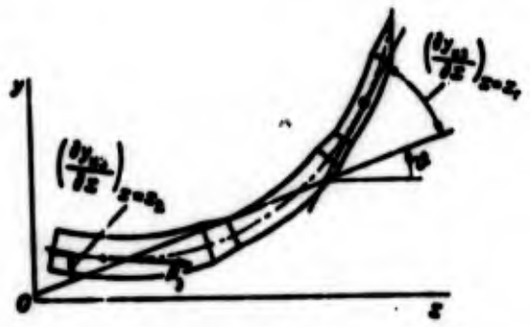

Figure 5.1

as we shall only be interested in the disturbed motion of a rocket, in studying it we shall adopt a stationary rectangular coordinate system whose longitudinal Ox axis coincides with the direction of the longitudinal axis of a rocket in undisturbed motion. The lateral axis Oy lies in the pitching plane, and the Oz axis is directed to make the Oxyz system right-handed. Thus, we shall only consider the lateral motion in the stationary rectangular system, having in mind that the sum of the Ox components of all external forces acting on the rocket is always balanced by the forces of inertia.

In the study of the elastic lateral vibrations the fuselage of the rocket is modeled by a straight inhomogeneous rod having two planes of symmetry. This model considerably simplifies theoretical work, but is only applicable to long fuselages. In the case when the fuselage is short, the principal role may be played by local vibrations of various structural elements such as vibrations of the engine on the elastic suspension, vibrations of various units including both the sensors and the elastic structural elements to which they are attached.

As far as the possible oscillations of the free surface of liquids in tanks are concerned, in many cases it is possible to take advantage of the fact that the natural frequency of the liquid is much smaller than the frequency of the elastic vibrations of the fuselage. Because of that circumstance, the liquid oscillations are usually disregarded in the analysis of the elastic vibrations of the fuselage.

If the natural frequencies of the liquid and the fuselage are close, then the coupling between the oscillations of the liquid and the elastic vibrations of the fuselage is of basic importance. This coupling can be approximately accounted for if, in determining the natural vibrational modes of the fuselage, the liquid oscillations are modeled by the oscillations of the spring-mass systems as it was done, for example, in Section 5 of Chapter IV.

In the study of the dynamic properties of the rocket the modes and the frequencies of its natural oscillations will be assumed known, since they can be determined using methods described in the previous chapter.

2. The Equations of the Perturbed Motion of the Rocket with the Account taken of the Lateral Vibrations of the Fuselage.

In the previous chapter the problem of the lateral oscillations of elastic inhomogeneous rods was discussed both with and without taking account of the axial slave force. The axial force is produced by the engine. If the engine and its suspension are considered ideally rigid in the lateral direction, then the longitudinal axis of the engine, coincident with the direction of the thrust vector, will be deflected in elastic lateral vibrations of the fuselage by an angle equal to the slope angle of the tangent to the bent axis of the fuselage at the location where the power plant frame is attached to the fuselage (see Figure 5.1). This assumption is valid in practical calculations, if the frequency of the lateral vibrations of the engine on its suspension is much higher than the frequency of the lateral vibrations of the fuselage. We shall consider that this is indeed the case, and the fuselage in the powered stage of the trajectory is subject to an axial slave force applied at x_d.

In the previous chapter a study of the forced lateral vibrations of an elastic inhomogeneous rod subject to an axial slave force encompassed several aspects. With the aid of the method of initial parameters, the forced lateral vibrations were determined without decomposition into a series in eigenfunctions. The forced lateral vibrations of the rod subject to an axial slave force were represented as a series in the eigenfunctions of the rod not subject to an axial slave force. Using the Bubnov-Galerkin method, the partial differential equations were replaced by a system of ordinary differential equations of forced vibrations in terms of generalized coordinates. Finally, it was shown that if the parameter $\beta = PR/EJ$ is small, then to a first approximation it can be assumed that the slave force decreases the natural frequency and does not change the oscillatory modes. Based on this premise, the forced vibrations may be represented as a series in the natural oscillatory modes for a rod not subject to an axial force, the natural frequency of the rod can be calculated from (4.93). The rotations of the thrust vector due to the elastic lateral vibrations can be included in both the force and the moment equations.

Let us set up the differential equations of the disturbed motion of a rocket in the plane of yaw. By symmetry, the differential equations in the pitching plane will be the same as the equations in the yawing plane. To set up these equations we shall make use of the system (4.97), obtained using the Bubnov-Galerkin method for an inhomogeneous rod subject to an axial slave force.

A displacement of any point on the elastic axis of the rocket fuselage in the stationary coordinate system Oxz (Figure 5.2) in the direction of the Oz axis will be written as

$$z(x, t) = z_M(t) + \psi(t)(x - a) + \sum_{n=1}^{\infty} f_n(x) q_n(t), \qquad (5.1)$$

where $z_M(t)$ is the displacement of the center of mass of the rocket; $\psi(t)$ the rotation angle of the rocket as a rigid body; $f_n(x)$ the natural vibrational modes of the fuselage not subject to an axial force; $q_n(t)$ is a generalized coordinate corresponding to $f_n(x)$;

a is the abscissa of the center of mass of the rocket.

The quantities $q_n(t)$, $\psi(t)$ will be assumed small. There will be no restrictions imposed on the displacements $z_M(t)$. We shall, however, assume that $\dot{z}_M(t) < v$, where v is the velocity of the center of mass of the rocket.

In unperturbed motion the direction of the longitudinal axis of the fuselage and the direction of the velocity vector v coincide with the direction of the coordinate axis Ox, so that $z(x, t) = 0$.

The motion in the yawing plane is subject to the effective thrust force P_{ef}, the control force of the vanes, Z_p, and the disturbed aerodynamic forces. The thrust P_{ef} (slave force) was taken into consideration when deriving Equations (4.97). Therefore, the generalized forces, appearing on the right in Equations (4.97), should only include the control force Z_p and the distributed aerodynamic forces.

The aerodynamic forces will be determined using the principle of stationarity [5]. According to this hypothesis, in each elementary segment of the fuselage of length dx a change in the lift force is proportional to a variation of the local angle of attack (sideslip).

As a result of the lateral motion the velocity vector v of any point on the elastic axis of the rod is deflected by a small angle.

$$\frac{1}{v}\frac{\partial z(x, t)}{\partial t},$$

and therefore, the variation of the local sideslip angle will be

$$\Delta\beta(x, t) = \frac{\partial z(x, t)}{\partial x} - \frac{1}{v}\frac{\partial z(x, t)}{\partial t}. \qquad (5.2)$$

In a fuselage segment of length dx the vector of the aerodynamic forces will be represented as consisting of two components — the elementary drage force dX and the elementary lateral dZ. The force

dZ is perpendicular to the velocity vector in the perturbed motion, v, and the direction of the force dX is opposite to the direction of vector v. We shall assume that the lateral force is proportional to the small sideslip angle, and the force of drag does not depend on the sideslip angle. The external forces acting on the rocket are shown in Figure 5.3

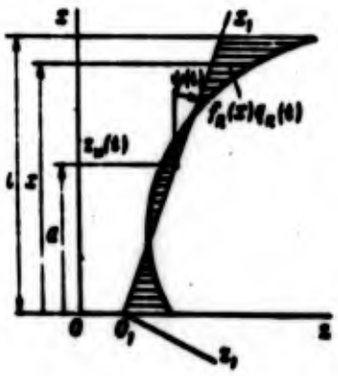

Figure 5.2

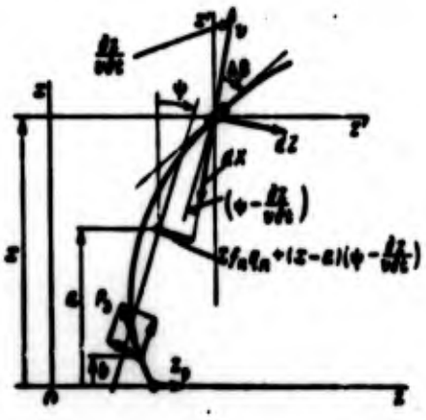

Figure 5.3

We shall denote the aerodynamic coefficients for a unit fuselage length by $c_z^1(x)$. for the lateral force and by $c_x(x)$ for drag force, where

$$\int_0^l c_z^1(x)\,dx = c_z^1, \quad \int_0^l [c_z^1(x)+c_x(x)](x-a)\,dx = -(c_z^1+c_x)(x_F-x_M),$$
$$\int_0^l c_x(x)\,dx = c_x, \quad \int_0^l [c_z^1(x)+c_x(x)](x-a)^2\,dx = I^2 c_m^1. \tag{5.3}$$

where x_F, x_M is the distance from the upper tip of the fuselage to the center of pressure and the center of mass, respectively (see Figure 1.5); c_m^1 is the coefficient of aerodynamic damping.

The elementary aerodynamic forces for a fuselage segment of length dx are equal to

$$dZ = \frac{\partial Z}{\partial x}\,dx = qSc_z^1(x)\Delta\beta\,dx, \quad dX = \frac{\partial X}{\partial x}\,dx = qSc_x(x)\,dx,$$
$$q = \frac{\rho v^2}{2}. \tag{5.4}$$

The components of the generalized forces corresponding to the generalized coordinates z_M, ψ, q_n, can be obtained using the sketch in Figure 5.3. They will be

$$Q'_z = \int_0^l \left(\frac{\partial Z}{\partial x} - \frac{\partial X}{\partial x} \frac{\partial z(x,t)}{v \partial t} \right) dx,$$

$$Q'_\psi = \int_0^l \left\{ \frac{\partial Z}{\partial x}(x-a) + \frac{\partial X}{\partial x} \left[\sum_{n=1}^{\infty} f_n q_n + (x-a)\left(\psi - \frac{\partial z(x,t)}{v \partial t} \right) \right] \right\} dx,$$

$$Q'_{q_n} = \int_0^l f_n \left[\frac{\partial Z}{\partial x} - \frac{\partial X}{\partial x} \frac{\partial z(x,t)}{v \partial t} \right] dx.$$

We shall substitute here the values of $\partial Z/\partial x$ and $\partial X/\partial x$ from (5.4). Keeping in mind (5.1) - (5.3) and integrating, we get

$$\begin{aligned}
Q'_z &= \frac{\rho v^2}{2} S \left[c_z^\beta \psi - (c_z^\beta + c_{z^\alpha}) \frac{\dot{z}_M}{v} - \frac{1}{v}(c_z^\beta + c_z)(x_p - x_M)\dot{\psi} + \right. \\
&\quad \left. + \sum_{n=1}^{\infty} q_n \int_0^l c_z^\beta(x) f'_n dx - \frac{1}{v} \sum_{n=1}^{\infty} \dot{q}_n \int_0^l c_z^\beta(x) f_n dx \right]. \\
Q'_\psi &= \frac{\rho v^2}{2} S \left\{ -(c_z^\beta + c_z)(x_p - x_M)\left(\psi - \frac{\dot{z}_M}{v} \right) + c_m^\beta l^2 \frac{\dot{\psi}}{v} + \right. \\
&\quad + \sum_{n=1}^{\infty} q_n \int_0^l [c_z^\beta(x) f'_n(x-a) + c_z(x) f_n] dx - \\
&\quad \left. - \frac{1}{v} \sum_{n=1}^{\infty} \dot{q}_n \int_0^l \left(c_z^\beta(x) + c_z(x) \right) f_n(x-a) dx \right\}, \\
Q'_{q_n} &= \frac{\rho v^2}{2} S \left[\psi \int_0^l c_z^\beta(x) f_n dx - \frac{\dot{\psi}}{v} \int_0^l \left(c_z^\beta(x) + c_z(x) \right) f_n(x-a) dx + \right. \\
&\quad + \sum_{m=1}^{\infty} q_m \int_0^l c_z^\beta(x) f'_m f_n dx - \frac{1}{v} \sum_{m=1}^{\infty} \dot{q}_m \int_0^l \left(c_z^\beta(x) + c_z(x) \right) f_m f_n dx - \\
&\quad \left. - \frac{\dot{z}_M}{v} \int_0^l \left(c_z^\beta(x) + c_z(x) \right) f_n dx \right].
\end{aligned} \tag{5.5}$$

In view of the fact that a displacement of any fuselage point (5.1) can be considered to consist of the displacement of tne fuselage as a rigid body and the displacements due to elastic vibrations, then in accordance with this also the aerodynamic forces given can

be decomposed into two groups: 1) the forces and moments proportional to the yaw angle ψ and the velocities $\dot{\psi}$ and $\dot{z}_M$ which are the same in the case of a rigid fuselage; 2) the forces and moments proprotional to the generalized coordinates q_n and velocities $\dot{q}_n$, that are due to the elastic lateral vibrations of the fuselage.

The terms making up the generalized force Q'_{q_n}, represent work done by the distributed aerodynamic forces along the possible displacements $f_n(x)$.

The components of the generalized forces due to the control force Z_p will be

$$\begin{aligned} Q'_z &= Z_p, \\ Q'_\psi &= -Z_p(x_p - x_M), \\ Q'_{q_n} &= Z_p f_n(x_p). \end{aligned} \tag{5.6}$$

Here $f_n(x_p)$ is the natural vibrational mode of the fuselage at the point of application of the lateral control force of the vanes, Z_p. The quantity $(x_p - x_M)$ represents the difference in distances measured from the upper tip of the fuselage to the point of application of the lateral control force, and the center of mass of the rocket.

According to (5.1) the values of $f_n(x)$ are measured from the straight line whose equation consists of the first two terms of (5.1), i.e., from the line O_1x_1 which will be taken to be the axis of abscissas of the $O_1x_1z_1$ frame attached to the rigid fuselage (see Figure 5.2).

It will be noted that the derivative $f'_n(x)$ is calculated in the body coordinate system $O_1x_1z_1$ whose O_1x_1 axis is directed from the tail part to the upper tip of the rocket. The derivitive $\partial z/\partial x$ is taken in the absolute coordinate system Oxz, and the direction of its Ox axis is the same as the direction of the unperturbed motion (see Figure 5.2). These two derivatives are related by the following equation:

$$\frac{\partial z(x, t)}{\partial x} = \varphi(t) + \sum_{n=1}^{\infty} f_n'(x) q_n.$$

If the derivatives $f_n'(x)$ are calculated in the coordinate system, whose 0_1x_1 axis points from the upper tip of the fuselage toward the tail part of the rocket, then in substituting these derivatives into (5.5), as well as into all the subsequent formulas of the present chapter, the signs of the derivatives $f_n'(x), f_n'(x_g), f_n'(x_p), f_n'(x_d)$ will have to be changed.

The generalized force Q_ψ will also include the moment of the Coriolis forces of inertia due to the fuel and gases. The effect of the elastic lateral vibrations on the magnitude of the Coriolis forces of inertia relative to the center of masses of the rocket will be proportional to the angular velocity of $\dot{\psi}$ and can be calculated from (1.4). This moment will be combined with the aerodynamic damping moment so that the total damping moment will be expressed by (1.21)

$$M_z = -\frac{1}{v_a}\left[\frac{\rho v_a^2}{2} S l c_m^{\omega_z} + 2\sum_{(l)} m_{cl} \int_{x_{cl}}^{l_k} (x - x_m)\, dx\right].$$

Now we shall make use of Equations (4.97). These expressions for generalized forces will be substituted into the right-hand sides of these equations. We obtain

$$m\ddot{z}_m + P_0\dot{\psi} + P_0\sum_{n=1}^{n^0} f_n'(x_i) q_n = Q_z' + Q_z',$$

$$I_z\ddot{\psi} + P_0\sum_{n=1}^{n^0} A_n q_n = Q_\psi' + Q_\psi' + M_z,$$

$$m_n\ddot{q}_n + h_n\dot{q}_n + k_n q_n + P_0\sum_{\substack{m=1 \\ m \neq n}}^{n^0} B_{nm} q_m = Q_{q_n}' + Q_{q_n}'.$$
$$(n = 1, 2, \ldots n^0)$$

Here x_d is the distance from the upper tip of the rocket to the cross section at which the engine thrust force is applied.

We shall combine in these equations the coefficients multiplying the same generalized coordinates, and set $\dot{z}_m = v_z$, $Z_p = R_{zp}'\delta$. In view of (4.98), (4.99), (5.5) and (5.6) we shall obtain the equations of

the perturbed motions of the rocket that take into account the elastic lateral vibrations of the fuselage:

$$\begin{aligned}
&\dot{v}_z + c_{v_z v_z} v_z + c_{v_z \psi} \psi + c_{v_z \dot{\psi}} \dot{\psi} + \sum_{n=1}^{\bar{n}} c_{v_z q_n} q_n + \sum_{n=1}^{\bar{n}} c_{v_z \dot{q}_n} \dot{q}_n + c_{v_z \delta} \delta = 0,\\
&\ddot{\psi} + c_{\psi\dot{\psi}} \dot{\psi} + c_{\psi\psi} \psi + c_{\psi v_z} v_z + \sum_{n=1}^{\bar{n}} c_{\psi q_n} q_n + \sum_{n=1}^{\bar{n}} c_{\psi \dot{q}_n} \dot{q}_n + c_{\psi\delta} \delta = 0,\\
&\ddot{q}_n + c_{q_n \dot{q}_n} \dot{q}_n + c_{q_n q_n} q_n + \sum_{\substack{m=1\\ m \neq n}}^{\bar{n}} c_{q_n q_m} q_m +\\
&+ \sum_{\substack{m=1\\ m \neq n}}^{\bar{n}} c_{q_n \dot{q}_m} \dot{q}_m + c_{q_n v_z} v_z + c_{q_n \psi} \psi + c_{q_n \dot{\psi}} \dot{\psi} + c_{q_n \delta} \delta = 0.
\end{aligned} \tag{5.7}$$

The following notation was used for the coefficients in the first equation

$$\begin{aligned}
c_{v_z v_z} &= \frac{1}{m v_a} \frac{\rho v_a^2}{2} S (c_z^1 + c_x),\\
c_{v_z \psi} &= -\frac{1}{m} \left(P_0 + \frac{\rho v_a^2}{2} S c_z^1 \right),\\
c_{v_z \dot{\psi}} &= \frac{1}{m v_a} \frac{\rho v_a^2}{2} S (c_z^1 + c_x)(x_p - x_m),\\
c_{v_z q_n} &= -\frac{1}{m} \left[\frac{\rho v_a^2}{2} S \int_0^l c_z^1(x) f_n' \, dx + P_0 f_n'(x_1) \right],\\
c_{v_z \dot{q}_n} &= -\frac{1}{m v_a} \frac{\rho v_a^2}{2} S \int_0^l c_z^1(x) f_n \, dx,\\
c_{v_z \delta} &= -\frac{1}{m} R_{zp}^1;
\end{aligned} \tag{5.8}$$

in the second equation

$$\begin{aligned}
c_{\psi\dot{\psi}} &= -\frac{1}{J v_a} \left(\frac{\rho v_a^2}{2} S l^2 c_m^1 + 2 \sum_{(l)} m_{cl} \int_{x_{0l}}^{l_n} (x - x_m) \, dx \right),\\
c_{\psi\psi} &= \frac{1}{J} \frac{\rho v_a^2}{2} S (c_z^1 + c_x)(x_p - x_m),\\
c_{\psi v_z} &= -\frac{1}{J v_a} \frac{\rho v_a^2}{2} S (c_z^1 + c_x)(x_p - x_m),
\end{aligned} \tag{5.9}$$

Equation (5.9) continued

$$c_{\psi q_n} = \frac{1}{I}\left\{-\frac{\rho v_n^2}{2} S \int_0^l [c_z^2(x) f_n'(x-a) + c_x(x) f_n]\, dx + \right.$$
$$\left. + P_0 [f_n(x_1) + f_n'(x_1)(x_1 - x_m)]\right\},$$
$$c_{\psi \dot{q}_n} = \frac{1}{I v_n} \frac{\rho v_n^2}{2} S \int_0^l (c_z^2(x) + c_x(x)) f_n(x-a)\, dx, \qquad (5.9)$$
$$c_{\psi\psi} = \frac{1}{I} R_{zp}^2 (x_p - x_m);$$

in the third equation

$$c_{q_n \dot{q}_n} = 2\varepsilon_n + \frac{1}{m_n v_n} \frac{\rho v_n^2}{2} S \int_0^l (c_z^2(x) + c_x(x)) f_n^2\, dx,$$
$$c_{q_n q_n} = (\omega_n^0)^2 - \frac{1}{m_n}\left[\frac{\rho v_n^2}{2} S \int_0^l c_z^2(x) f_n' f_n\, dx + \right.$$
$$\left. + \frac{P_0}{m} \int_0^l f_n' \int_0^x m(x)\, dx^2 - P_0 f_n'(x_1) f_n(x_1)\right],$$
$$c_{q_n q_m} = -\frac{1}{m_n}\left[\frac{\rho v_n^2}{2} S \int_0^l c_z^2(x) f_m' f_n\, dx - P_0 f_m'(x_1) f_n(x_1) + \right.$$
$$\left. + P_0 \int_0^l f_n'(x) f_m'(x) \int_0^x m(x)\, dx^2\right],$$
$$c_{q_n \dot{q}_m} = \frac{1}{m_n v_n} \frac{\rho v_n^2}{2} S \int_0^l (c_z^2(x) + c_x(x)) f_m f_n\, dx,$$
$$c_{q_n \psi} = -\frac{1}{m_n} \frac{\rho v_n^2}{2} S \int_0^l c_z^2(x) f_n\, dx,$$
$$c_{q_n v_z} = \frac{1}{m_n v_n} \frac{\rho v_n^2}{2} S \int_0^l (c_z^2(x) + c_x(x)) f_n\, dx,$$
$$c_{q_n \dot{\psi}} = \frac{1}{m_n v_n} \frac{\rho v_n^2}{2} S \int_0^l c_z^2(x) f_n(x-a)\, dx,$$
$$c_{q_n z} = -\frac{1}{m_n} R_{zp}^2 f_n(x_p); \quad m_n = \int_0^l m(x) f_n^2\, dx.$$

Here ω_n^0 is the natural frequency of the fuselage not subject to an axial slave force. When the rotation of the fuselage is effected not by the lateral force $R_{zp}^{\delta}\delta$ but by the control moment $M_{zp}^{\delta}\delta$ produced by a purposeful misalignment of the engine thrust forces, then

$$c_{y_s\delta}=0,$$

$$c_{\psi\delta}=-\frac{1}{l}M_{zp}^{\delta},$$

$$c_{q_n\delta}=-\frac{1}{m_n}M_{zp}^{\delta}f_n'(x_p),$$

where $f_n'(x_p)$ is the slope angle of the tangent to the natural oscillatory mode at $x = x_p$.

The equations of the perturbed motion that include the effect of the elastic vibrations fof the fuselage can also be obtained using a different method. Since the magnitude of the parameter $\beta=P_{ef}l^2/EJ$ for rockets is usually small in our deduction, we can use Equations (4.48) which were obtained without considering the slave force. One must add the generalized forces Q''' due to the slave force P_{ef} into the right-hand sides of these equations in addition to the generalized forces Q' and Q''. These forces are

$$Q_z^{\cdot}=P_{ef}\psi+P_{ef}\sum_{n=1}^{n^0}f_n'(x_1)q_n,$$

$$Q_\psi^{\cdot}=-P_{ef}\left[\sum_{n=1}^{n^0}f_n(x_1)q_n+\sum_{n=1}^{n^0}f_n'(x_n)(x_n-x_m)\right],$$

$$Q_{q_n}^{\cdot}=P_{ef}\left[\sum_{\substack{m=1\\m\neq n}}^{n^0}f_m'(x_1)f_n(x_1)-\sum_{\substack{m=1\\m\neq n}}^{n^0}\int_0^l f_n'(x)f_m'(x)\int_0^x m(x)\,dx^2\right].$$

The effect of an axial slave force on the natural frequency of the fuselage can be calculated from (4.93). Substituting in Equations (4.48) the expression for the generalized forces, we obtain

$$m\dot{v}_z=Q_z'+Q_z^{\cdot}+Q_z'',$$

$$I\ddot{\psi}=Q_\psi'+Q_\psi^{\cdot}+Q_\psi'',$$

$$m_n(\ddot{q}_n+2\varepsilon_n\dot{q}_n+\omega_n^2q_n)=Q_{q_n}'+Q_{q_n}^{\cdot}+Q_{q_n}''.$$

Combining coefficients multiplying the same generalized coordinates, we shall obtain a system of equations identical with (5.7). Only for one coefficient $c_{qn}q_n$ a different formula will be valid, namely,

$$c_{q_n q_n} = \omega_n^2 - \frac{1}{m_n} \frac{\rho v_\infty^2}{2} S \int_0^l c_z^3(x) f_n' f_n dx,$$

where ω_n can be calculated from (4.93).

In what follows when speaking of Equations (5.7), we shall no longer point out from which system they were obtained—from (4.48) or from (4.97).

In contrast to the equation for an ideally rigid rocket (1.40) the first two equations in (5.7), in addition to the aerodynamic forces and moments due to the motion of a rigid fuselage, also include the forces and moments due to the elastic lateral vibrations of the fuselage. In addition, these equations also include the forces and moments that arise as a result of the rotation of the thrust vector P_{ef}. Each oscillatory mode of the fuselage gives rise to a lateral component of force P_{ef} and the moment of this force relative to the center of mass of the rocket.

The aerodynamic forces have an effect on the values of the natural frequencies of the fuselage (see the coefficient $c_{q_n q_n}$) and usually result in a damping of the elastic vibrations (see the coefficient $c_{q_n \dot{q}_n}$). These forces also create some additional couplings between the motion of the rocket as a rigid body and the elastic vibrations of the fuselage. However, these couplings are not essential, for example, if $c_z^3(x) = c_1 m(x)$, $c_z(x) = c_2 m(x)$. Then as can be seen from (5.10) the coefficients $c_{q_n \vartheta}$, $c_{q_n \dot{\vartheta}}$, $c_{q_n \nu_z}$ will vanish, and the elastic vibrations will not be a function of the motion of the rocket as a rigid body.

In a preliminary analysis of the equations of perturbed motion it is usually assumed that: 1) the aerodynamic forces do not depend on the elastic lateral vibrations of the fuselage, 2) the aerodynamic forces, as caused by the motion of a rigid fuselage, do not give rise to elastic lateral vibrations, 3) the rotation of the thrust vector as a result of the elastic vibrations of the fuselage does not influence the motion of the rocket as a rigid body. When

these assumptions are made all the coupling coefficients between the coordinates v_z and ψ, on one hand, and $q_n (n = 1, 2, \ldots)$, on the other hand, and also between the coordinates q_n and $q_m (n \neq m)$ becomes zeros, and Equations (5.7) break up into two groups of independent equations: the equations of the perturbed motions of the rocket as a rigid body

$$\dot{v}_z + c_{v_z v_z} v_z + c_{v_z \psi} \psi + c_{v_z \dot{\psi}} \dot{\psi} + c_{v_z \delta} \delta = 0,$$
$$\ddot{\psi} + c_{\dot{\psi}\dot{\psi}} \dot{\psi} + c_{\psi\psi} \psi + c_{\psi v_z} v_z + c_{\psi\delta} \delta = 0; \tag{5.11}$$

and the equations in generalized coordinates, expressing the elastic lateral vibrations of the fuselage

$$\ddot{q}_n + c_{q_n \dot{q}_n} \dot{q}_n + c_{q_n q_n} q_n + c_{q_n \delta} \delta = 0 \quad (n = 1, 2, \ldots). \tag{5.12}$$

Equations (5.11) differ from the earlier obtained equations for an ideally rigid rocket (1.40) only in that in the first equation in (5.11) there is a term $c_{v_z \dot{\psi}} \dot{\psi}$, which accounts for the aerodynamic force component due to the rotation of the fuselage with an angular velocity $\dot{\psi}$. This force is, generally speaking, small, and therefore, is neglected in deducing Equations (1.40).

3. A Structural Block Diagram of the Closed System

The angle of rotation of the fuselage at the location of the sensor of the control system (gyroscope) can be determined from

$$\left.\frac{\partial z(x, t)}{\partial x}\right|_{x = x_g} = \psi + \sum_{n=1}^{\infty} f_n'(x_g) q_n, \tag{5.13}$$

where $f_n'(x_g)$ is the derivative taken in the body coordinate system $0_1 x_1 z_1$ of function $f_n(x)$ at the location of the gyroscope $x = x_g$.

This angle differs from the angle of rotation of the rigid fuselage, and, which is very important, depends on the location of the gyroscope along the fuselage of the rocket.

The structural block diagram of the closed system corresponding to the equations of the first approximation (5.11), (5.12), and to (5.13), is shown in Figure 5.4. The controlled object (the rocket) is shown in the diagram by several parallel blocks. The essential block here is the one that characterizes the dynamics of the rocket as a rigid body, its output coordinates being the angle ψ. The blocks characterizing the elastic vibrations of the fuselage are secondary. There may be several blocks of this type, their number depending on the properties of the control system. The output coordinate of each secondary block is taken to be the angle of rotation, arising as a result of the elastic oscillations of that cross section of the fuselage in which a sensing element of the control system is located.

Let us denote the complex transfer number of the rocket as a rigid body

$$K_0(i\omega)=\frac{\psi(i\omega)}{\delta(i\omega)}=A_0(\omega)e^{i\varphi_0(\omega)}. \tag{5.14}$$

and the complex transfer number of the block representing the n^{th} mode of elastic oscillations by

$$K_n(i\omega)=\frac{f_n(x_r)\,q_n(i\omega)}{\delta(i\omega)}=A_n(\omega)e^{i\varphi_n(\omega)}. \tag{5.15}$$

As in Chapter I and III the complex transfer number of the control system will be represented by

$$K_{AC}(i\omega)=A_{AC}(\omega)e^{i\varphi_{AC}(\omega)}. \tag{5.16}$$

The mismatch signal entering the control system is proportional to the angle

$$\psi(i\omega)+\sum_{n=1}^{n_0} f_n'(x_s)\,q_n(i\omega)=\left[K_0(i\omega)+\sum_{n=1}^{n_0} K_n(i\omega)\right]\delta=$$
$$=\left[A_0(\omega)\,e^{i\varphi_0(\omega)}+\sum_{n=1}^{n_0} A_n(\omega)\,e^{i\varphi_n(\omega)}\right]\delta,$$

where n_0 is the mode number of the elastic vibrations of the fuselage whose signals pass through the control system. In the complex plane $Z=U(\omega)+iV(\omega)$ the mismatch signal can be represented as a vector sum.

If the system is open at the exit from the control system, then the complex transfer number of the open loop will be

$$K(i\omega)=\frac{\delta_{\text{вых}}(i\omega)}{\delta_{\text{вх}}(i\omega)}=\left[K_0(i\omega)+\sum_{n=1}^{n_0} K_n(i\omega)\right]K_{\text{АС}}(i\omega)= \tag{5.17}$$
$$=\left[A_0(\omega)\,e^{i\varphi_0(\omega)}+\sum_{n=1}^{n_0} A_n(\omega)\,e^{i\varphi_n(\omega)}\right]A_{\text{АС}}(\omega)\,e^{i\varphi_{\text{АС}}(\omega)}=A(\omega)\,e^{i\varphi(\omega)}.$$

The denominator of the transfer function for an elastic rocket has as many positive real parts as there are in the denominator of the transfer function for an ideally rigid rocket. In other words, the fact that the elastic properties of the fuselage were taken into consideration does not change the number of the possitive roots (this is valid if $\beta = P_{ef}l^2/EJ \ll \beta_{cr}$ which practically speaking is always true).

In order to see this, we shall represent the transfer functions of the controlled object as

$$K_0(p)=\frac{R_0(p)}{Q_0(p)},\quad K_n(p)=\frac{R_n(p)}{Q_n(p)}.$$

Then the denominator of the transfer function will be expressed as a product of polynomials

$$Q(p)=Q_0(p)\prod_{n=1}^{n_0} Q_n(p).$$

From Equations (5.12) we find

$$Q_n(p)=p^2+c_{q_n\dot{q}_n}p+c_{q_nq_n}=0,\quad c_{q_n\dot{q}_n}>0\quad (n=1,2,\ldots).$$

The roots of all polynomials $Q_n(p)$ are complex conjugate with negative real parts. Consequently, the polynomial Q(p) has the same number of possitive roots as $Q_0(p)$ which is the denominator of the transfer function for a rocket as a rigid body.

Disregarding the simplifications that made it possible to make the transition from Equations (5.7) to the simpler equations (5.11) and (5.12), the structural block diagram shown in Figure 5.4 is nevertheless relatively complex for a preliminary analysis. A further simplification of the diagram can be made on the basis of an analysis of the complex transfer number $K(i\omega)$ (5.17).

Consider vectors $K_0(i\omega)$ and $K_n(i\omega)$. The hodograph of the vector $K_0(i\omega)$, constructed from Equations (5.11) for $0 \leqslant \omega < \infty$, is shown in Figure (5.5). Curve 1 corresponds to a statically stable rocket; Curve 2 corresponds to a statically unstable one. With an increase in frequency, the modulus of the complex number $A_0(\omega)$ rapidly decreases (for a statically stable rocket beginning with $\omega > \sqrt{c_{\varphi}}$).

The complex transfer number $K_n(i\omega)$ will be obtained from Equation (5.12)

$$K_n(i\omega) = \frac{f_n'(x_r)\varphi_n(i\omega)}{\delta(i\omega)} = \frac{-c_{\varphi_n\delta} f_n'(x_r)}{c_{\varphi_n\varphi_n} + i\omega c_{\varphi_n\dot{\varphi}_n} - \omega^2} =$$

$$= \frac{R_{zn}' f_n(x_p) f_n'(x_r)}{m_n(c_{\varphi_n\varphi_n} + i\omega c_{\varphi_n\dot{\varphi}_n} - \omega^2)} = U_n(\omega) + iV_n(\omega) = A_n(\omega) e^{i\varphi_n(\omega)}. \qquad (5.18)$$

The argument of the complex number for $\omega = 0$ depends on the sign of the product of two numbers $f_n(x_p)f_n'(x_g)$ — the value of the natural oscillatory mode of the fuselage at the location of the control element (vanes) and the value of the slope angle of the tangent to a natural oscillatory mode of the fuselage at the location of the gyroscope. When $f_n(x_p)f_n'(x_g) > 0$, the argument of the complex number $\varphi_n(0) = 0$; when $f_n(x_p)f_n'(x_g) < 0$, the argument of the complex number $\varphi_n(0) = \pi$.

If a rotation of the rocket in the Oxz plane is effected, not by means of a lateral force, $R^{\lambda}_{np}\delta$, but through a moment $M^{\lambda}_{np}\delta$, then the argument of the complex number $\varphi_n(0)$ will be determined by the sign of the product of the two numbers, $f_n'(x_p)f_n'(x_g)$. The sign of the product of these numbers plays an important role in estimating the stability of the motion of a rocket with an elastic fuselage. The hodograph of $K_n(i\omega)$ for $0 \leqslant \omega \leqslant \infty$ is shown in Figure 5.6. The modulus of the complex number $A_n(\omega)$ is large only at frequencies close to the natural frequencies of the fuselage; it is small for all remaining frequencies. The argument of the complex number $\varphi_n(\omega)$ for the case when $f_n(x_p)f_n'(x_g)>0$ changes from zero to π; for the case when $f_n(x_p)f_n'(x_g)<0$ it changes from π to zero.

If one follows the change of the moduli for $A_0(\omega)$, $A_n(\omega)$, appearing in brackets in the expression for the complex transfer number of an open loop (5.17), then the following picture will be obtained.

At small frequencies (up to frequencies slightly exceeding $\omega = \sqrt{c_{yy}}$) the modulus of $A_0(\omega)$ is large, and the moduli $A_n(\omega)$ of all the remaining vectors are very small so that the sum of all the vectors appearing in brackets in (5.17), is practically equal to the vector $A_0(\omega)e^{i\varphi_0(\omega)}$ independently of the argument values for the remaining vectors. This equality is a consequence of the fact that at small frequencies, considerably less than ω_1 the elastic vibrations of the fuselage are insignificant, and the frequency characteristic of the rocket with account taken of the elastic vibrations of the fuselage is the same as that for a rocket assumed to be a rigid body.

With an increase in frequency the modulus of $A_0(\omega)$ decreases and becomes smaller, the smaller the frequency ω. All the moduli of $A_n(\omega)$ remain small until the frequency ω approaches ω_1, which is the frequency of the first mode of the natural elastic vibrations of the fuselage. In a small frequency interval including the frequency ω_1, the modulus of $A_1(\omega)$ will be large, and the moduli of the remaining vectors will be small. The sum of all vectors in this frequency band is practically equal to the vector $A_1(\omega)e^{i\varphi_1(\omega)}$. The amplitude-

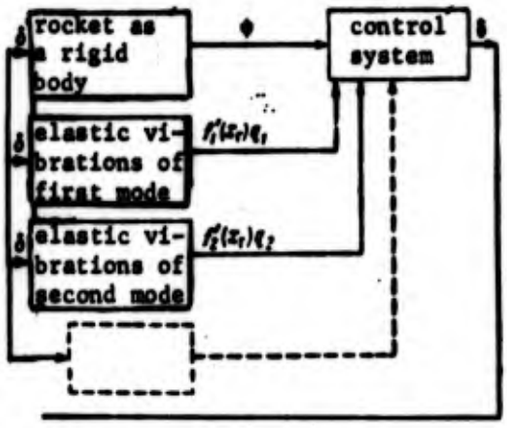

Figure 5.4

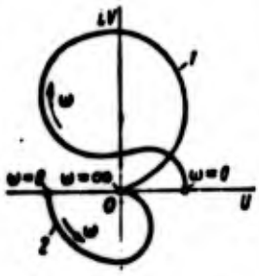

Figure 5.5

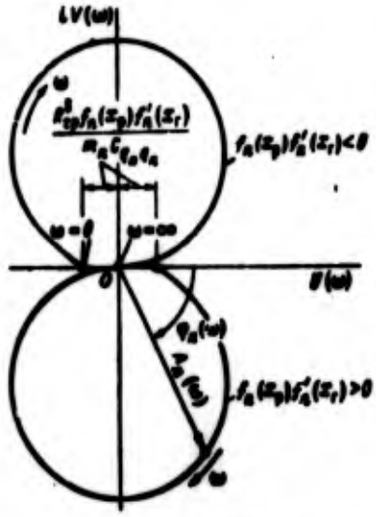

Figure 5.6

phase frequency characteristic of a rocket with an elastic fuselage is determined in this frequency band by the partial characteristic for the first elastic oscillatory mode of the fuselage.

As one moves farther along the frequency axis, in the following interval including the second natural frequency ω_2, the sum of all vectors will differ little from the vector $A_2(\omega)e^{i\varphi_2(\omega)}$ etc.

In view of the fact that the energy dissipation in elastic vibrations is small, the frequency bands in which the moduli of $A_1(\omega)$ and $A_2(\omega)$ become large, are quite narrow. Below, for brevity, instead of saying "in the frequency interval including the natural frequency ω_n^*", we shall sometimes say "for the natural frequency ω_n^*", keeping in mind of course that this is only a convention.

This discussion implies that at small frequencies the control system receives mainly the signal from the angular motions of the rigid fuselage of the rocket. At ω_1 the signal due to the first oscillatory mode is preponderant, at ω_2 the main signal comes from the second oscillatory mode, etc. This means that in the structural diagram shown in Figure 5.4, at small frequencies one can neglect

all the blocks of the controlled object with the exclusion of the block representing the first oscillatory mode etc.

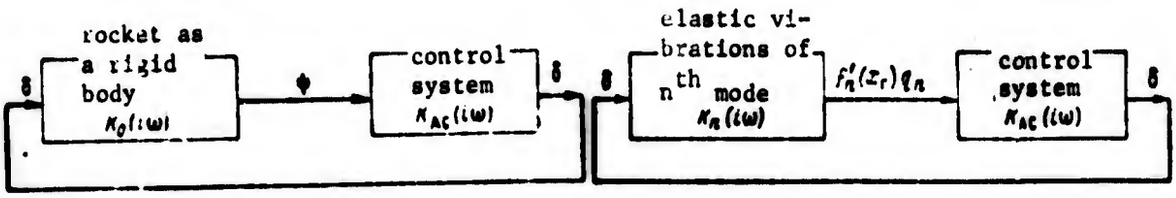

Figure 5.7

Figure 5.8

Thus, the structural block diagonal (see Figure 5.4) can be represented in the form of separate simple single-loop diagrams, namely the diagram for the rocket as a rigid body (Figure 5.7) and n_0 single-type diagrams representing the elastic vibrations of the fuselage (Figure 5.8).

It will be noted that the identification of a sum of vectors in a given frequency band with one vector can only be valid when the natural frequencies of the elastic vibrations of the fuselage are not close to one another, and the frequency of the first tone, ω_1, is considerably larger than frequencies for which the modulus of $A_0(\omega)$ has a large value. Only under these circumstances can the modulus of the sum of all vectors appearing in brackets in (5.17), in the intervals between the low-frequency band and the natural frequencies ω_1, ω_2 etc., be sufficiently small so that when multiplied by the modulus of $A_{AC}(\omega)$, it will give a product which is less than one, $A(\omega)<1$. It is only under these circumstances that the complete closed diagram (see Figure 5.4) for the stability analysis can be decomposed into simpler diagrams, shown in Figure (5.7) and (5.8). For single-stage rockets and multi-stage rockets with lateral subdivisions of each stage, these conditions are usually satisified. In the case when among the natural frequencies of the fuselage there are some which are close to one another, the role of one of the simplified diagrams will have to be played by another diagram in which the controlled object is represented by two or more parallel

blocks with close natural frequencies. Another possibility for this case is to express the elastic vibrations of the fuselage by means of a forced oscillatory mode $\phi(x, \omega)$.

In the latter case the mismatch signal $\phi'(x_r, \omega)e^{i\omega t}$, due to the lateral vibrations of the fuselage, can on the basis of (4.68) be represented as a sum of two signals. This structural block diagram is shown in Figure (5.9).

Now, we can give a simple answer to the question of how many elastic oscillatory modes of the fuselage should be considered in the stability analysis of rocket motion. All these modes have to be taken into account for which the product

$$A_n(\omega_k) A_{\lambda C}(\omega_k) \geq 1. \tag{5.19}$$

4. The Conditions for the Stability of Motion.

Here we shall limit ourselves to a simplified analysis of the stability of motion for a rocket with an elastic fuselage. In the analysis each mode of the elastic vibrations will be considered separately. Just as in all previous cases, the stability analysis will be based on linearized equations which means that the conclusions arrived at will only have a qualitative character. This type of investigation brings results that are easy to interpret, and is always advisable especially in the preliminary stage when it is necessary to determine requirements on the control system. Numerical relationships, such as the amplitude and phase margin coefficients, self-oscillation amplitudes etc., can only be obtained by analyzing more complete systems of equations for the controlled object and the controlled system. The dynamic properties of the control system should be given special attention, since with an increase in the frequency of oscillations the properties of the control system

increasingly deviate from those of its properties that are expressed by linear differential equations. To reveal the numerical relationships it is just as necessary to take into account the variability of the coefficients in the differential equations of the controlled object.

We saw in the previous section that to a first approximation a study of the stability of motion for a rocket with an elastic fuselage can be conducted using two separate closed diagrams. In one diagram the controlled object is represented as a rigid body (see Figure 5.7), in the other — the dynamic properties of the controlled object are determined by the n^{th} elastic oscillatory mode of the fuselage (see Figure 5.8).

The first closed system (for a rocket as a rigid body) is one which is most important. Only if its stability is variable can the rocket pursue a trajectory which is sufficiently close to the present trajectory. The stability analysis for this system was made in Chapter I, and we shall not dwell on it here.

Closed systems containing blocks representing the elastic vibrations of the fuselage are of secondary importance. They also should be stable, since otherwise, the elastic vibrations are able to jam the control system channels or present dangers to the fuselage.

The formula for the complex transfer number $K_n(i\omega)$ (5.18) is the same for any oscillatory mode of the fuselage. Therefore, is is enough to study the stability for an arbitrary n^{th} oscillatory mode. We shall assume that the condition (5.19) is satisfied.

As in Chapter I we shall assume that the characteristic equations of the control system do not have roots with a positive real part, i.e., that the control system is stable. An ordinary oscillatory loop with viscous friction is the controlled object, and its characteristic equation has complex conjugate roots with negative real parts.

By the frequency Nyquist criterion (see Chapter I, Section 8), the closed system (see Figure 5.8) will be stable if for $A_n(\omega)A_{AC}(\omega)>1$ the phase frequency characteristic of the open system either will actually not cross the real axis U or the number of down crossings will be equal to the number of up crossings.

Let us consider separately the phase frequency characteristic of the open loop for the system in Figure 5.8. In view of the fact that when vectors are multiplied their arguments are added (5.17), the phase frequency characteristic of an open loop will be represented by the equation

$$\varphi(\omega)=\varphi_n(\omega)+\varphi_{AC}(\omega) \quad 0<\omega<\infty. \tag{5.20}$$

The phase frequency characteristic of the control system is shown with a heavy line in Figure 5.10. To secure stability of the rocket as a rigid body at small frequencies (up to ω_0), the phase characteristic is positive. For $\omega>\omega_0$ the phase characteristic is negative. The signal produced by the control system will for $\omega>\omega_0$ have a phase lag which usually increases with increasing frequency.

The form of the phase frequency characteristic of the controlled object can be easily reproduced on the basis of Figure 5.6. Since the damping coefficient for elastic oscillations is small, almost the entire phase change takes place in a small frequency interval which includes the natural frequency of the fuselage ω_n. The phase intervals for $0<\omega<\infty$ are the following:

$$0>\varphi_n(\omega)>-\pi \text{ for } f_n(x_p)f_n'(x_r)>0,$$
$$\pi>\varphi_n(\omega)>0 \text{ for } f_n(x_p)f_n'(x_r)<0.$$

To the phase characteristic of the control system, shown in Figure 5.10, we shall add according to (5.20) the limiting values of the phase of the controlled object. When $f_n(x_p)f''(x_g)>0$, we shall add

$\varphi_n(\omega)=-\pi$, and when $f_n(x_p)/f_n'(x_g)<0$, we shall include $\varphi_n(\omega)=\pi$. The feasible phase frequency characteristic of an open loop will be found between these two limiting values.

The Nyquist criterion implies that if, with the conditions (5.19) being satisfied, the phase frequency characteristic of an open loop crosses the axes $\varphi(\omega)=0, \varphi(\omega)=-2\pi, \varphi(\omega)=-4\pi$ etc., then the closed system shown in Figure 5.8 is unstable. If, however, the characteristic does not cross these axes, then the closed system is stable. The condition (5.19) is satisified when the frequency ω is equal to the natural frequency of the fuselage ω_n. Therefore, if, for example, for $f_n(x_p)/f_n'(x_g)<0$ the natural frequency is such that $\omega_0<\omega_n<\omega_1$ or $\omega_{2*}<\omega_n<\omega_{3*}$, then the closed system is unstable. If, however, $\omega_1<\omega_n<\omega_{2*}$ or $\omega_{3*}<\omega_n<\omega_{4*}$, then the closed system is stable. Here ω_1, ω_{2*} etc. are the frequencies for which the phase lag of the control system is equal, respectively, to $\pi, 2\pi, \ldots$.

Analogous considerations are possible with respect to the phase characteristic for $f_n(x_p)/f_n'(x_g)>0$. If $\omega_0<\omega_n<\omega_1$ or $\omega_{2*}<\omega_n<\omega_{3*}$, then the closed system is stable; if $\omega_1<\omega_n<$ or $\omega_{3*}<\omega_n<\omega_{4*}$, then the closed system is unstable.

It is convenient to show the stability conditions obtained using a diagram of the stability regions in the coordinates representing the parameters of the controlled object (Figure 5.11). This type of diagram is useful because it is applicable to any oscillatory mode which satisifies the condition (5.19). In constructing the diagram it is assumed that $\omega_1>\omega_0$, since this inequality is the basis for subdividing the diagram of Figure 5.4 into two diagrams — Figures 5.7 and 5.8.

If in the analysis of the stability of motion, one takes into account the dissipation of energy due to the elastic vibrations of the fuselage, then the region of instability decreases. This is ascribed to two causes: 1) for $\varepsilon_n\neq 0$ the phase frequency characteristic of the controlled object in the resonance zone will have values that are different from the limiting ones, i.e., $0<|\varphi_n(\omega)|<\pi$;

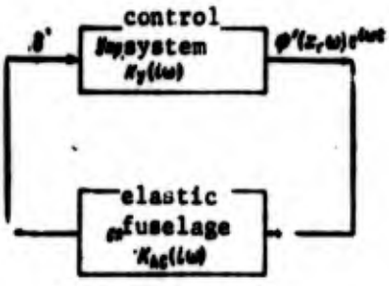

Figure 5.9

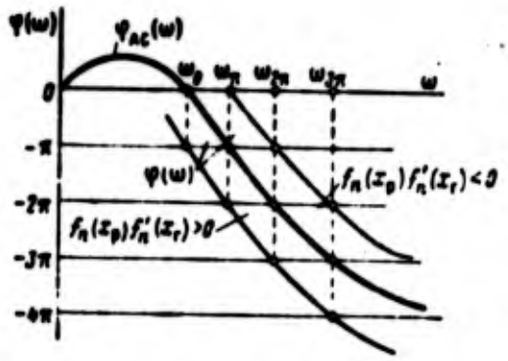

Figure 5.10

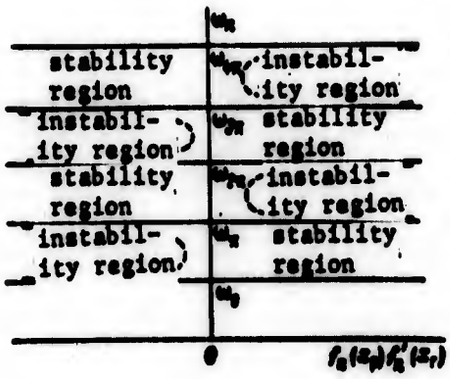

Figure 5.11

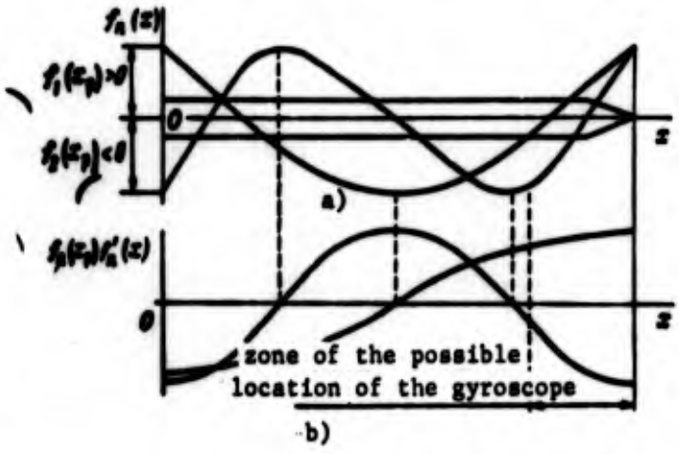

Figure 5.12

2) if the value of the product $f_n(x_p)f_n'(x_g)$ is small, the condition (5.19) may not be satisfied. The regions of instability with the energy dissipation due to elastic vibrations taken into account are in Figure 5.11 bounded by a dotted line.

Using the diagram showing the stability regions, one can solve various problems involving a stabilization of bending vibrations. More precisely, one can reveal conditions under which randomly arising bending vibrations of the fuselage will always be damped. Using the diagram, one can formulate the requirements on the phase frequency characteristic of the control system, and select the location of the gyroscope along the length of the fuselage.

Let us consider an example. It is required to select the location of the gyroscope along the rocket, and formulate the requirements on the phase characteristic of the control system under the condition that the inequality (5.19) is satisfied for the first two bending oscillatory modes. In addition, it is known that the control units are located on the front frame of the tail section and that $\omega_1<\omega_2$.

Figure 5.12a, shows plots of the first two natural oscillatory modes. The value of the first oscillatory mode at the location of the vanes is positive, $f_1(x_p)>0$; the value of the seond mode, $f_2(x_p)<0$. Figure 5.12b, shows the plots of $f_n(x_p)/f_n'(x)$ for the first and second oscillatory modes.

In connection with the gradual fuel consumption, the natural frequencies of the fuselage get larger. These frequencies are plotted as functions of flight time $\bar{t}$ in Figure 5.13. The stability regions are chosen using these frequency curves as well as the condition $\omega_1<\omega_2$ in Figure 5.11. The regions are shown in Figure 5.14.

In order for the parameters of the controlled object to lie in the stability regions, it is necessary that the following conditions be satisfied:

1) for the first oscillatory mode of the fuselage $f_n(x_p)/f_n'(x_g)>0$, for the second mode $f_n(x_p)/f_n'(x_g)<0$;

2) $\omega_0<\omega_1<\omega_2$, $\omega_2<\omega_3<\omega_{2n}$.

The second condition determines the requirements on the phase frequency characteristic of the control system; the first condition imposes restrictions on the choice of the location for the gyroscope. In the example discussed, the zone determining the possible locations of the gyroscope is located in the forward section of the fuselage (see Figure 5.12b). Keeping in mind the fact that the calculations of the oscillatory modes and especially of their derivatives are only approximate, the zone containing the possible gyroscope locations must be moved some distance away from the nodes of the function $f_n(x_p)/f_n'(x_g)$.

After the choice of the fuselage cross section for positioning the gyroscope has already been made, the numbers $f_1'(x_g)$ and $f_2'(x_g)$ are determined, and the parameters of the controlled object are plotted as functions of flight time in the diagram of the stability regions. In Figure 5.14 these time-dependent parameters are shown with two heavy lines.

However, by adjusting the phase frequency characteristics of the control system and by selecting the location of the gyroscope, it is not always possible to achieve a stabilization of the elastic fuselage vibrations. For instance, if one is required to stabilize simultaneously three or even four elastic oscillatory modes, then this problem is practically impossible to solve by selecting the gyroscope locations.

Figure 5.13

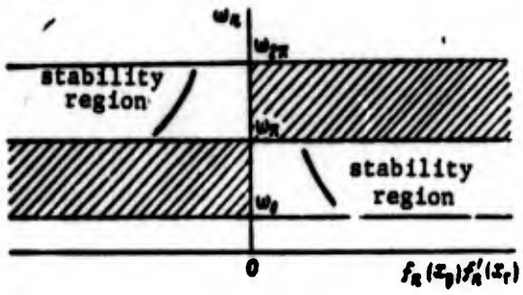

Figure 5.14

A case may occur when the frequencies of the neighboring oscillatory modes overlap, i.e., for example, the frequency of the second mode in the final phase of powered flight is greater than the frequency of the third mode at the beginning of the flight, $\omega_{2max} > \omega_{3min}$. In this case, as can be seen from the diagram of the stability regions, it is impossible to achieve stability of elastic oscillations by adjusting the phase characteristic. Stability can be achieved by building a switching capability into the control system [1, 4, 10] or by setting up two gyroscopes at different locations, where at the beginning of the flight the signals would enter the control system from one gyroscope, and in the final phase — from the other. In this scheme use can be made of the angular velocity pickups.

In this process one usually utilizes the amplitude stabilization of the elastic vibrations which is based on the fact that an open loop (see Figure 5.8) does not have roots with a positive real part. This means if conditions are created in which the inequality (5.19) will not be satisfied, then the amplitude-phase frequency characteristic of the open loop for $0 \leqslant \omega \leqslant \infty$ will never contain the point C(1,10), and the closed system will be stable.

One of the means used to lower the dynamic amplification coefficient of the control system is narrow-band filters [1,4] which in a small frequency band practically do not pass through any signals. The amplitude stabilization can also be achieved by increasing the energy dissipation of the elastic fuselage vibrations (lowering $A_n(\omega_n)$) but this method is difficult to realize.

If one utilizes the amplitude stabilization of the elastic vibrations using, for example, narrow band filters, then to be confident that the condition (5.19) is not satisfied one must know the value of the coefficient $c_{q_n \dot{q}_n}$ in Equation (5.12). Methods of determining this coefficient will be presented in the following section.

5. On Calculating the Forces of Internal Friction

Until now we have not discussed the question of the magnitude of the forces of internal friction. Moreover, if the frequency of forced oscillations significantly differs from the natural frequency of the fuselage, then it is not necessary in general to take the forces of friction in the fuselage into account. The forces of friction are essential at resonance. Without them it is impossible to determine the amplitude of the oscillations, and therefore, it is also impossible to apply the amplitude stabilization with any degree of reliability.

An extensive literature devoted to the internal friction in rods recommends various ways of taking friction into account. Formulas are suggested that express the forces of internal friction as functions of the strain, the rate of strain, the character and technique of imposing stresses on the rod, and other factors. Some of these formulas when applied to the linear problems of vibrations in homogeneous rods yield satisfactory results.

Much more complex is the problem of inhomogeneous rods, and even to a greater extent, the problem of machine-constructed structures for which there are not any exact and at the same time sufficiently simple and reliable methods of calculating the internal friction forces.

In Chapter IV we described three alternative ways of calculating the forces of friction.

The first technique is based on the Voigt hypothesis according to which the force of internal friction is proportional to the rate of strain. In the equation of the lateral vibrations (4.3) the force of internal friction in a unit length of rod can be expressed by

$$k\frac{\partial}{\partial t\,\partial x^2}\left[EJ(x)\frac{\partial y}{\partial x^2}\right].$$

The equation for the generalized coordinate is

$$\ddot{q}_n+2k_n\omega_n\dot{q}_n+\omega_n^2q_n=a_nq(t). \qquad \text{(a)}$$

where the relative damping coefficient for lateral vibrations

$$k_n=\frac{1}{2}k\omega_n$$

is proportional to the natural frequency of the fuselage vibrations.

The Voigt hypothesis is convenient in solving equations, but is inadequately confirmed in experiments.

According to the second technique the force of friction is assumed to be proportional to the rate of movement, and is called the force of viscous friction. In the equation for the lateral vibrations, (4.79) this force is represented by $h(x)\,\partial y/\partial t$. The equation for the generalized coordinate is

$$\ddot{q}_n + 2\xi_n\omega_n\dot{q}_n + \omega_n^2 q_n = a_n q(t), \qquad \text{(b)}$$

where

$$\xi_n = \frac{\varepsilon_n}{\omega_n}, \quad \varepsilon_n = \frac{1}{2m_n}\int_0^l h(x) f_n^2 dx.$$

Equation (b) has the same form as Equation (a), except that the relative damping coefficient ξ_n is inversely proportional to the natural frequency of the fuselage.

The third technique is based on the hypothesis of Ye. S. Sorokin, [17], according to which the force of friction in harmonic vibrations does not depend on the rate, but is shifted in phase relative to the elastic force by $\pi/2$. The Sorokin hypothesis is confirmed by experimental evidence.

In the equation of the lateral vibrations (4.3a) the force of friction is according to the Sorokin hypothesis expressed by terms

$$i\frac{\psi}{2\pi}\frac{\partial^2}{\partial x^2}\left[EJ(x)\frac{\partial^2 y_n}{\partial x^2}\right], \quad \psi = 2\delta = \frac{\Delta W}{W}.$$

The generalized coordinate q_n in forced harmonic vibrations can be determined from Equation (4.59).

The relative damping coefficient ξ_n and the coefficient of energy absorption in vibrations represented by ψ usually cannot be determined by means of calculations. These coefficients are integral quantities, and their values can be determined most simply directly from experiments. In particular, this is true for rocket fuselages in which the structural friction is preponderant.

There are two methods of experimentally determining the forces of friction. The first is based on studying the damping of the natural vibrations of the rocket fuselage, and the second on studying forced vibrations. The curves of natural damped vibrations or the resonance curves are determined experimentally. The coefficients of interest to us can be found from the experimental results, making certain assumptions about the character of friction.

Equations (a) and (b) area completely identical, and since the damping coefficient is determined at a natural frequency, no disagreement arises in the experimental determination of ξ_n for Equations (a) and (b).

The natural vibrations described by Equations (a) and (b) take place according to the formula

$$q_n = D_0 e^{-\varepsilon_n t} \sin(\omega_n' t + \alpha_n), \tag{5.21}$$

where D_0 and α_n represent the initial displacement and the phase of vibrations, and ω_n' is the natural frequency of the vibrations of the system with damping:

$$\omega_n' = \omega_n \sqrt{1 - \xi_n^2}.$$

Here both for the rocket fuselages and for rods, $\xi_n \ll 1$. The intensity of the damping depends on the value of the coefficient $\varepsilon_n = \xi_n \omega_n$ (Figure 5.15). From (5.21) we see that the ratio of the maximum displacements in two consecutive cycles, measured at t and t + τ, where τ is the period of the natural vibrations, is equal to a constant

$$\frac{D_1}{D_2} = \frac{D_2}{D_3} = \cdots = e^{\varepsilon_n \tau}.$$

The natural logarithm of this quantity will be denoted by δ. Then

$$\delta = \ln\left(\frac{D_1}{D_2}\right) = \varepsilon_n \tau \approx 2\pi \xi_n. \tag{5.22}$$

The quantity δ which describes the rate of damping is called a logarithmic decrement of oscillations.

From (5.22) we shall determine the relative damping coefficient

$$\chi_n = \frac{\delta}{\omega_n}.$$

If for an experimentally obtained curve the ratios of the displacements D_1/D_2, D_2/D_3 cannot be considered a constant, then the friction in the system does not correspond to the Voigt hypothesis, and is not proportional to the first degree of speed. In particular, in dry friction the difference of displacements in two consecutive cycles is equal to a constant. Methods of deciphering the experimental curves can be found in the literature devoted to the subject, for example, in [9].

To obtain the experimental curve of damped vibrations, the fuselage of the rocket is suspended in a vertical or a horizontal position. The elastic lateral vibrations of the fuselage are produced by a vibrator which is then instantaneously removed. The vibrations are recorded on a tape using an attached vibrograph (if the supports of the fuselage are fixed) or a loop oscillograph. In the latter case wire strain gauges are used, glued to the extended and compressed sides of the fuselage.

The forced harmonic vibrations are measured for various ratios of the vibrator frequency to the natural frequency of the elastic vibrations of the fuselage.

If the fuselage is acted upon by a concentrated lateral external force $P_0 e^{i\omega t}$, then the right-hand side of Equations (a) and (b) will be

$$a_n e^{i\omega t}, \quad a_n = \frac{P_0 f_n(x_p)}{m_n}.$$

where $f_n(x_p)$ is the value of the natural oscillatory mode at the point of the application of the external force.

The amplitude of the forced harmonic vibrations is equal to

$$q_n^0 = \frac{P_0 f_n(x_p)}{m_n \omega_n^2 \sqrt{(1-\gamma_n^2)^2 + 4\xi_n^2 \gamma_n^2}}, \quad \gamma_n = \frac{p}{\omega_n}.$$

At resonance for small values of ξ_n

$$(q_n^0)_{max} \approx \frac{P_0 f_n(x_p)}{m_n 2\xi_n \omega_n^2}, \quad \xi_n \approx \frac{P_0 f_n(x_p)}{2(q_n^0)_{max} \omega_n^2 m_n}. \tag{5.23}$$

When the maximum amplitude $(q_n^0)_{max}$ is experimentally determined, one can calculate the unknown coefficient ξ_n.

According to [18], the relative damping coefficient for a rocket has a value on the order of 0.02.

If we only deal with structural friction, then the amplitude of forced harmonic vibrations is on the basis of (4.59) equal to

$$q_n^0 = \frac{P_0 f_n(x_p)}{m_n \omega_n^2 \sqrt{(1-\gamma_n^2)^2 + \left(\frac{\psi}{2\pi}\right)^2}}.$$

At resonance for small values of ψ

$$(q_n^0)_{max} = \frac{P_0 f_n(x_p)}{m_n \omega_n^2 \frac{\psi}{2\pi}}, \quad \frac{\psi}{2\pi} = \frac{P_0 f_n(x_p)}{m_n \omega_n^2 (q_n^0)_{max}}. \tag{5.23a}$$

In deducing Equation (4.3a) it was assumed that the energy absorption coefficient in vibrations, ψ, does not depend on the amplitude of vibrations. The validity of this assumption can be verified experimentally. For this purpose it is necessary to set up harmonic vibrations in the fuselage that have different amplitudes, and find the relationship between the coefficient ψ and the amplitude of the vibrations.

Depending on the hypotheses used, the analysis of experimental data may yield either the relative damping coefficient ξ_n or the absorption coefficient ψ. If we make use of the Voigt hypothesis of the hypothesis of viscous friction, then from (5.23) we shall find the relative damping coefficient ξ_n. If the Sorokin hypothesis is used, then from (5.23a) the energy absorption coefficient ψ will be found.

The relationship between the force of friction in the rocket fuselage and the character of vibrations (frequency and amplitude) is in reality, apparently, more complex than the hypotheses of Voigt, Sorokin, and of viscous friction would seem to indicate. This is in particular indicated by a large scatter of the experimental data in a determination of the damping coefficients, and also by the fact that these coefficients are dependent on the frequency and the amplitude of the vibrations.

To make the analysis of the stability of lateral elastic vibrations possible to a first approximation, it is enough to know the amplitudes of the forced vibrations of the fuselage in the resonance zone. The amplitudes can be calculated using any of the hypotheses about the frictional forces as long as the coefficients ξ_n and ψ are known.

If the coefficients ξ_n and ψ can be determined experimentally using the resonance method, then from a single experiment on the basis of (5.23) and (5.23a) we obtain

$$\xi_n = \frac{\psi}{4\pi}.$$

Consequently, the amplitudes of forced elastic vibrations, calculated for $\gamma_n = 1$, will not depend on the choice of the hypothesis if one takes $\xi_n = \psi/4\pi$. In this sense for resonance vibrations it makes no difference which hypothesis about the frictional forces is selected. Of primary importance are only the values of ξ_n or ψ.

6. Methods of Stabilizing Elastic Vibrations

The term "stabilization of the elastic vibrations of a rocket" is usually understood to mean the damping of these vibrations, i.e., the imposition of such properties on the closed system, consisting of the elastic fuselage and the control system, that the randomly arising vibrations are always damped. For practical reasons, elastic autovibrations with small amplitudes may sometimes be allowed.

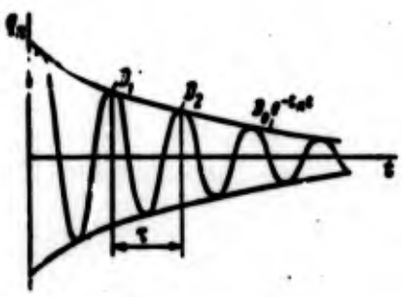

Figure 5.15

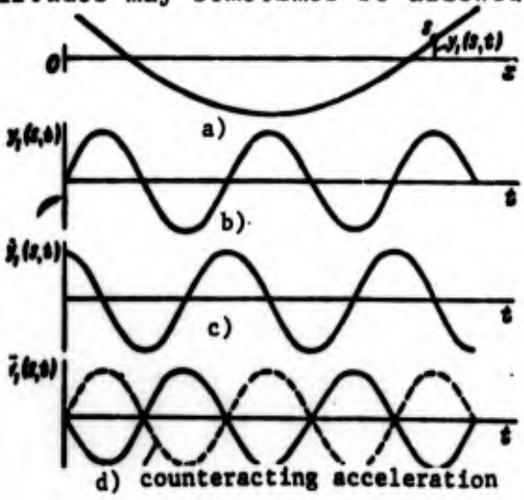

Figure 5.16

In Section 4. we discussed the problem of stabilizing the elastic vibrations using the same control system that is supposed to stabilize the angular motion of the rocket as a rigid body. Since natural elastic vibrations are always damped, the control system should under no circumstances weaken the damping process. In this connection new requirements will be imposed on the phase frequency characteristic of the control system.

However, the technique of stabilizing elastic vibrations using the angular control system is not unique. The elastic vibrations can be intensely damped using a special servosystem [21]. In this system sensors are used whose position is of critical importance, and depends on the elastic oscillatory modes of the fuselage.

Let us consider as an example the first mode of the elastic harmonic vibrations of the fuselage (Figure 5.16a). For each point, on the bent axis of the rod, one can construct a time diagram describing the lateral motion of this point. All points located above the Ox axis have a phase shift of 180° compared to points located below this axis.

Let us select an arbitrary point s on the elastic axis of the fuselage. The time-dependence of the deflection $y_1(s,t)$ at that point is shown in Figure 5.16b; Figures 5.16c and d, respectively, show the plots of velocity $\dot{y}_1(s,t)$ and acceleration $\ddot{y}_1(s,t)$. For harmonic vibrations the phase shift between the acceleration, velocity, and the displacement amounts to 90°. Such time diagrams can be obtained by placing the acceleration, velocity, and displacement pickups at a preselected point.

The most obvious way of liquidating elastic vibrations of the fuselage is to cancel them with vibrations having the same frequency and amplitude, but opposite in phase.

The effect of quenching the vibrations can be practically achieved in several ways. For example, a counteracting vibrational mode can be produced when the role of the sensing element of the control system is played by an accelerometer whose signal is input into an auxiliary servomechanism controlling the vanes of the thrust vector. If the role of the sensor is played by a velocity indicator, then to obtain an analogous result the phase shift should amount to 90° (or 270°). Let us consider the vibration quenching effect in more detail.

The equation for the generalized coordinate q_4^n characterizing the elastic vibrations of the fuselage is

$$\ddot{q}_n + 2\varkappa_n \omega_n \dot{q}_n + \omega_n^2 q_n = a_n \lambda(t).$$

Three sensors can be simultaneously used: acceleration, velocity, and displacement pickups. Their signals will be used as signals of negative feedback with definite amplification coefficients

$k_{\ddot{q}_n}$, $k_{\dot{q}_n}$, k_{q_n}. Let us substitute the expressions for these signals into the equation for q_n, to obtain a differential equation of the closed system

$$\ddot{q}_n + 2\xi_n\omega_n\dot{q}_n + \omega_n^2 q_n = -k_{\ddot{q}_n}\ddot{q}_n - k_{\dot{q}_n}\dot{q}_n - k_{q_n}q_n.$$

Collecting coefficients for the same variables, we get

$$(1+k_{\ddot{q}_n})\ddot{q}_n + (2\xi_n\omega_n + k_{\dot{q}_n})\dot{q}_n + (\omega_n^2 + k_{q_n})q_n = 0. \tag{5.24}$$

Equation (5.24) can be written as

$$\ddot{q}_n + 2\xi_n'\omega_n'\dot{q}_n + (\omega_n')^2 q_n = 0, \tag{5.25}$$

where

$$2\xi_n'\omega_n' = \frac{2\xi_n\omega_n + k_{\dot{q}_n}}{1+k_{\ddot{q}_n}}, \qquad (\omega_n')^2 = \frac{\omega_n^2 + k_{q_n}}{1+k_{\ddot{q}_n}}. \tag{5.26}$$

Equation (5.25) is the same as the equation of the natural elastic vibrations of the fuselage

$$\ddot{q}_n + 2\xi_n\omega_n\dot{q}_n + \omega_n^2 q_n = 0.$$

The coefficients of this equation, however, differ from the coefficients of Equation (5.25). The relationships among these coefficients are determined by (5.26). The natural frequency of the system ω_n' in (5.26) can be increased or decreased as compared to the natural frequency of the fuselage ω_n.

The newly-formed dynamic system has also a new relative damping coefficient ξ_n' (5.26) that can be increased to a critical or supercritical value. The possibility of increasing the damping of a system by adding negative feedback signals offers great advantages.

If in the process of the amplitude stabilization the suppression of signals is achieved by placing a sensor near the mode of oscillation or by means of filters (passive method), then in the active method sensors are placed at points where maximum signals can be obtained which then are used to suppress vibrations that gave rise to these signals in the first place. If the sensors generate signals of all modes, then the location sensors can be of great significance. This problem can be solved using Equation 5.24 and taking into account the natural oscillatory modes of the fuselage as well as the location of the control elements of the fuselage of the rocket.

The feedback signals can be generated using more than just sensors of the linear quantites $\bar{y}_n, \dot{y}_n, y_n$. With the same results, one can also use sensors of such angular quantities as

$$\frac{\partial^2 y_n}{\partial x \partial t}, \quad \frac{\partial^2 y_n}{\partial x \partial t}, \quad \frac{\partial y_n}{\partial x},$$

since

$$\delta_{nzz} = \frac{\partial^2 y_n}{\partial x \partial t} = f''_n \ddot{q}_n, \quad \delta_{nzz} = \frac{\partial^2 y_n}{\partial x \partial t} = f''_n \dot{q}_n, \quad \delta_{nzz} = \frac{\partial y_n}{\partial x} = f'_n q_n.$$

Figure 5.17 shows a structural block diagram used to stabilized elastic lateral vibrations of a large booster rocket [21] in which the angular signals are used alongside of linear signals.

The method described is based on definite phase relationships. Their realization is, however, accompanied by enormous difficulties, and therefore this method is not in wide use.

Another method of stabilizing elastic vibrations is presented in [19]. A control jet engine (of vernier type) with small thrust is mounted on the fuselage of the rocket.

A rate gyroscope, measuring the angular velocity of the rocket, is placed within the same cross section where the vernier jet engine was mounted. The movable nozzle of the vernier engine (or the thrust vector acting along the normal to the rocket axis) is controlled by a signal from a rate gyroscope which is proportional to

the angular velocity of the rocket. Thus, the stabilization loop will contain an additional feedback consisting of the vernier engine and the rate gyroscope, which is used to produce a lateral force proportional to the angular velocity of the lateral vibrations of the fuselage.

By a proper choice of the location of the rate gyroscope, one can achieve the result that the lateral force will cancel the elastic vibrations. The canceling of these vibrations will be much more effective if the following coefficient is made very large

$$\frac{R_v f_n(x_v) f_n'(x_v)}{m_n},$$

where R_v is the thrust of the vernier jet engine; $fn(x_v)$, $f_n'(x_v)$ are the oscillatory mode and the slope angle of the tangent to the oscillatory mode and the location of the vernier engine and the rate gyroscope; m_n is the effective mass of the fuselage in vibrations according to the n^{th} oscillatory mode.

It is sometimes advisable for the control systems to use both active and passive methods of suppressing elastic vibrations.

7. The Elastic Lateral Autovibrations

In Sections 4 and 6, the stability analysis for a rocket with the elastic vibrations of the fuselage taken into account was done on the basis of linear differential equations. The actual dynamic system is considerably more complex than the model used in calculations.

The main difference is that the equation of the control system is nonlinear. The angular control channel in the plane of pitch produces a command signal directing the rotation of the transvector. This signal changes with time, and therefore strictly speaking, the linearization of the control system characteristics should be done at various working points.

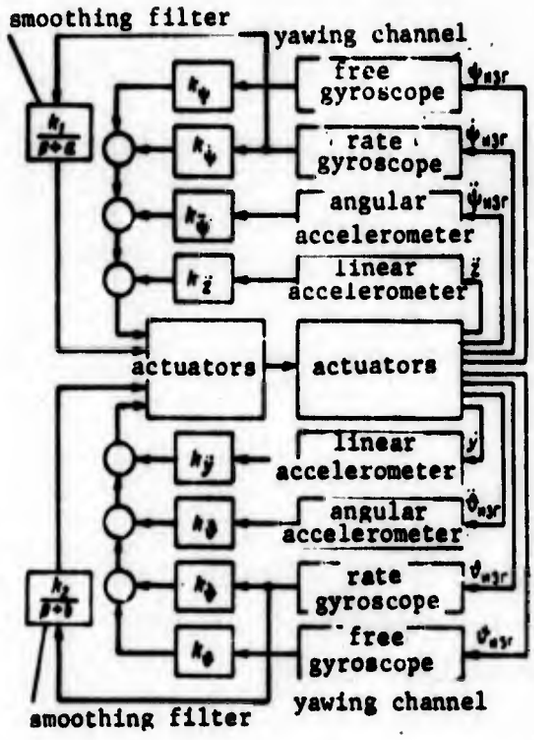

Figure 5.17

The dynamic characteristics of the control system to a considerable extent depend also on the conditions of operation such as the temperature, vibrations, voltages in the power source etc. Potentiometer sensors which produce stepwise signals and various smoothing filters make the properties of the control system more complicated, and make it more difficult to describe it with differential equations and to linearize these equations.

In addition, the properties of the controlled object and the control system change from product to product because of the structural and technological parameter variation. For this reason the frequency characteristics of the control system even for a fixed amplitude of the input signal represent not just one curve, but a whole band in which the actual characteristics may be located. The same can be said about the frequencies and modes of the natural vibrations of the fuselage, and the effectiveness of the control units.

The causes enumerated above are enough to turn a system containing a small stability margin into an unstable system under the actual conditions. Therefore, it is necessary to produce sufficiently large stability margins.

In Section 4 it was shown that it is extremely difficult to secure simultaneous stability of several oscillatory modes of the fuselage. In any case the stability margins for certain oscillatory modes may be very small; even with a small deflection of the system

parameters from their nominal values it is possible that unstable motion will be the result.

On the basis of linear equations, one can only make a conclusion about the damping or the intensifying of randomly produced vibrations with the course of time. As the amplitudes increase, the nonlinear terms, removed during linearization, because essential, and the analysis of the subsequent motion of the system can only be made retaining these nonlinear terms.

The control actuator whose velocity characteristic is shown in Figure 5.18 is one of the essential nonlinear loops in the control system. Its characteristic exhibits a typical saturation behavior. If the command current $i<i_0$, then the characteristic is linear, and the rate amplification coefficient, defined by the slope angle of the characteristic is equal to $k_\delta^{\cdot}$.

Assume that the linearized system is unstable if the amplification coefficient is $k_\delta^{\cdot}$. The hodograph of an open loop, expressed by the equation

$$K(i\omega)=K_n(i\omega)K_{AC}(i\omega)=A_n(\omega)A_{AC}(\omega)e^{i\varphi(\omega)},\ \varphi=\varphi_n(\omega)+\varphi_{AC}(\omega),$$

in the complex plane is shown in Figure 5.19 as curve 1.

As the amplitude of the vibrations increases, there will come a moment when the current $i>i_0$, and the control actuator will work under nonlinear conditions. If for $i>i_0$ the characteristic of the control actuator is linearized, then the equivalent (averaged over the period of oscillations) amplification coefficient of the actuator will be less than $k_\delta^{\cdot}$. (In Figure 5.19 the smaller amplification coefficient is associated with a hodograph represented by the dotted line 2.) The linearized system all the same still remains unstable, and its amplitude will continue to increase with time.

The larger the amplitude of vibrations, the stronger the inequality $i > i_k$ will be, and the equivalent amplification coefficient of the actuator will be that much smaller than k_i.

Suppose that the amplification coefficient of the actuator corresponding to the command current amplitude i_p is equal to $k_{\delta}^{\cdot}$, p and that the hodograph of the open loop that corresponds to that coefficient is shown in Figure 5.19 as curve 3. The hodograph passes through point C(1, i0), and this shows that the system is at a borderline of stability.

It can be seen that the vibrations with amplitude i_p are stable periodic vibrations which are referred to as autovibrations. In fact if a small increase in the amplitude of vibrations is imparted to the vibrating system, then for $i > i_p$ the equivalent amplification coefficient of the actuator will be less than k_{i_p}; in this case the hodograph of the open loop will be represented by curve 4. This hodgraph corresponds to a stable system; the vibrations will be damped until the amplitude of the command current becomes equal to i_p. The hodograph will again pass through C(1, i0); the system returns to the starting unperturbed motion.

If in a system vibrating with amplitude i_p, one decreases slightly the amplitude, then the curve 2 which is associated with unstable motion will become the hodograph. The amplitudes will increase until they again reach i_p which is associated with a hodograph shown as curve 3; the system again returns to its initial motion.

Consequently, the vibrational motion characterized in the complex plane by point C(1, i0), is stable. These are indeed auto-oscillatory conditions. The frequency of the autovibrations, practically speaking, differs little from the natural frequency of the elastic vibrations of the rocket fuselage.

The time plot of vibrations is shown in Figure 5.20.

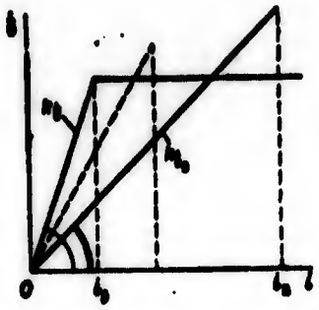

Figure 5.18

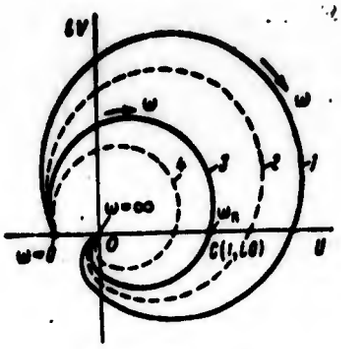

Figure 5.19

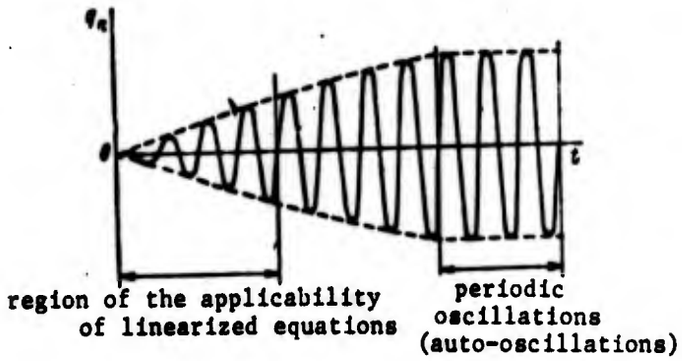

Figure 5.20

The autovibrations take place in a closed system consisting of the fuselage and the control system. The role of the energy source in this case is played by the control system. All the loops of the dynamic system execute vibrations with the same frequency ω_p but with different amplitudes. The amplitude of the command current i_p is associated with the amplitude δ_p of the vibrations of the control element.

The frequency and amplitude can only be determined by solving the nonlinear equations of the closed system. The solution can be obtained using the method of harmonic linearization [13], using digital computers or analog computers which include the actual control system. In the latter case the properties of such a control system will be most completely investigated.

If the amplitudes of autovibrations are so small that the linear Equation (5.12) can be considered valid, then the amplitude of the elastic vibrations of the fuselage can be calculated from this equation by setting in it $\delta = \delta_p \sin \omega_p t$. We shall get

$$\ddot{q}_n + c_{q_n \dot{q}_n} \dot{q}_n + c_{q_n q_n} q_n = a_n \delta_n \sin \omega_n t.$$

The amplitudes q_n^0 are determined more accurately when

$$\omega_n^2 \neq c_{q_n q_n}.$$

With elastic autovibrations the channel of the angular control system is burdened with signals which with respect to the rocket stabilizing signals, (the rocket being considered a rigid body), can be considered an interference. Since the characteristics of the control system are nonlinear, the interference may be able to increase the time constants and lower the amplification coefficient which will lead to an impairment of stability with respect to other degrees of freedom.

The elastic autovibrations give rise to lateral inertial loads on the fuselage, and therefore, are damaging. But, if the amplitudes and frequencies of the autovibrations are small, then the inertial loads will be small, and therefore, not dangerous to the fuselage. Such autovibrations can be allowed, and to allow them is wiser than to stabilize elastic vibrations using complex methods and overcome great difficulties. Such a solution, however, should be undertaken separately for each case.

8. Natural Lateral Vibrations of the Fuselage For a Rocket with a Revolving Engine.

If the guidance control is achieved by rotating the main engines, then the inertial characteristics of these engines will have an influence on the dynamic properties of the rocket [7, 10].

In order to reveal the dynamic properties of the rocket, we shall find the equations of the lateral vibrations of an elastic fuselage for a rocket with a revolving engine. We assume that the engine is mounted in the tail section of the rocket, and is a rigid body. In addition to the notation introduced in Section 7 of Chapter IV, we shall use the following notation: m_d is the mass of the revolving engine, l_d is the distance from the center of mass of the engine to its axis of rotation (the axis of rotation is located ahead of the center of mass), I_d is the moment of inertia relative to the axis to rotation, k_d is the coefficient of the angular rigidity of the engine's mounting to the fuselage with a jammed control actuator, P_c is the thrust of the control revolving engine, P is the full engine thrust, δ is the angle of rotation of the engine relative to a tangent to the bent axis of the fuselage at the point of suspension, l is the length of the axis up to axis of rotation of the engine, h_d is the coefficient of viscous friction.

The fuselage is in this case modeled by an elastic inhomogeneous rod with length l with a rigid body (engine) suspended from a spring which is hinged to the right-hand end. The diagram is shown in Figure 5.21.

The equation of the lateral vibrations of the rod subject to a slave force was obtained in Section 7 of Chapter IV. It is

$$\frac{\partial^2}{\partial x^2}\left[EJ(x)\frac{\partial^2 y}{\partial x^2}\right]+\frac{\partial}{\partial x}\left[N(x)\frac{\partial y}{\partial x}\right]+m(x)\frac{\partial^2 y}{\partial t^2}+h(x)\frac{\partial y}{\partial t}=q(x,t).$$

In the given case a rigid body is attached to the right end of the elastic rod. The forces of inertia due to the motion of the rigid body together with the rod for $\delta=0$, will be included in the equation of motion of the rod. For this purpose we shall make use of the Dirac delta function (see page 261). We obtain

$$\begin{aligned}&\frac{\partial^2}{\partial x^2}\left(EJ(x)\frac{\partial^2 y}{\partial x^2}\right)+\frac{\partial}{\partial x}\left(N(x)\frac{\partial y}{\partial x}\right)+m(x)\frac{\partial^2 y}{\partial t^2}-\\&-l_1\frac{\partial^3 y}{\partial x\,\partial t^2}\Big|_{x=l}\Delta'(x-l)+m_2\left(\frac{\partial^2 y}{\partial t^2}+l_2\frac{\partial^3 y}{\partial x\,\partial t^2}\right)\Big|_{x=l}\Delta(x-l)-\\&-m_2 l_1\frac{\partial^3 y}{\partial t^2}\Big|_{x=l}\Delta'(x-l)+h(x)\frac{\partial y}{\partial t}=q(x,t).\end{aligned}\qquad(5.27)$$

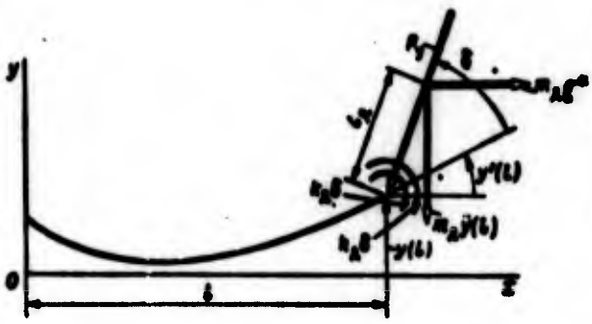

Figure 5.21

The forces due to the deflection of the rigid body by an angle δ as well as the lateral component $P_y\delta$ will be thought of as the external forces which in Equation (5.27) were denoted in general by $q(x,t)$.

Using the Dirac delta function, we have

$$q(x, t)=q'(x, t)-P_y\delta\Delta(x-l)-m_2l_1\ddot{\delta}\Delta(x-l)+ \\ +I_1\ddot{\delta}\Delta'(x-l)+m_2l_1g^*\delta\Delta'(x-l). \tag{5.28}$$

where $q'(x,t)$ is the linear aerodynamic force; g^* is the longitudinal acceleration of the rocket produced by the engine thrust outside of the field of the Earth's gravitation. The Coriolis forces will not be taken into consideration here.

We shall apply the Bubnov-Galerkin method to Equations (5.27) and (5.28). The solution will be written as a series

$$y(x, t)=y_M(t)+\vartheta(t)(x-x_M)+\sum_{n=1}^{n^*}f_n(x)q_n(t).$$

where $y_M(t)$, $\vartheta(t)$ are the generalized coordinates of the rigid rod; $q_n(t)$ is the generalized coordinate of the elastic vibrations; $f_n(x)$ is the natural oscillatory mode of a rod with free ends in the absence of the thrust; x_M is the coordinate of the center of mass of the rod without the rigid body (without the engine).

Upon making the transformations necessary to obtain a system of ordinary differential equations by means of the Bubnov-Galerkin method(see Section 8 Chapter IV), we obtain

$$m^*\ddot{y}_u + P\theta + c_{y\ddot{\theta}}\ddot{\theta} + P\sum_{n=1}^{n^0} f'_n(l)q_n + \sum_{n=1}^{n^0} c_{y\ddot{q}_n}\ddot{q}_n +$$
$$+ P_y\delta + m_\Delta l_\Delta \ddot{\delta} = \int_0^l q'(x, t)\,dx,$$
$$I^*\ddot{\theta} + A_{\theta\ddot{y}}\ddot{y}_u + P\sum_{n=1}^{n^0} A_{\theta q_n} q_n + \sum_{n=1}^{n^0} A_{\theta\ddot{q}_n}\ddot{q}_n +$$
$$+ A_{\theta\delta}\delta + A_{\theta\ddot{\delta}}\ddot{\delta} = \int_0^l q'(x, t)(x - x_u)\,dx, \qquad (5.29)$$
$$m_n^*\ddot{q}_n + h_n\dot{q}_n + k_n q_n + P\sum_{\substack{m=1\\ m\neq n}}^{n^0} B_{q_n q_m} q_m +$$
$$+ \sum_{\substack{m=1\\ m\neq n}}^{n^0} B_{q_n\ddot{q}_m}\ddot{q}_m + B_{q_n\ddot{y}}\ddot{y}_u + B_{q_n\ddot{\theta}}\ddot{\theta} + B_{q_n\delta}\delta + B_{q_n\ddot{\delta}}\ddot{\delta} = \int_0^l q'(x, t) f_n\,dx$$
$$(n = 1, 2, \ldots, n^0),$$

where m^* is the mass of the rod and the rigid body; I^* is the moment of inertia of the rod and the rigid body relative to the lateral axis through the center of mass of the rod; m_n^* is the effective mass of the rod and the rigid body;

$$m^* = m_\Delta + \int_0^l m(x)\,dx,$$
$$I^* = \int_0^l m(x)(x - x_u)^2\,dx + I_\Delta + m_\Delta(l - x_u)^2 + 2m_\Delta l_\Delta(l - x_u),$$
$$m_n^* = \int_0^l m(x) f_n^2\,dx + m_\Delta f_n^2(l) + 2m_\Delta l_\Delta f'_n(l) f_n(l) + I_\Delta f'^2_n(l).$$

The coefficients h_n and k_n are determined from (4.99), and $A_{\theta q_m} = A_m$, $B_{q_n q_m} = B_{nm}$ — from (4.98). For the remaining coefficients in Equations (5.29) the following notation is used:

$$c_{y\ddot{\theta}} = m_\Delta(l - x_u + l_\Delta),$$
$$c_{y\ddot{q}_n} = m_\Delta[f_n(l) + l_\Delta f'_n(l)],$$
$$A_{\theta\ddot{y}} = m_\Delta(l - x_u + l_\Delta),$$

$$A_{\ddot{q}_n} = I_2 f_n'(l) + m_2 [(l - x_M + l_1) f_n(l) + (l - x_M) l_2 f_n'(l)],$$

$$A_{\ddot{\delta}} = P_y (l - x_M) + m_2 g^* l_2,$$

$$A_{\ddot{\delta}} = I_2 + m_2 l_2 (l - x_M),$$

$$B_{q_n \ddot{q}_m} = m_2 [f_m(l) f_n(l) + l_2 f_m(l) f_n'(l) +$$

$$+ l_2 f_m'(l) f_n(l)] + I_2 f_m'(l) f_n'(l),$$

$$B_{q_n \ddot{y}} = m_2 [f_n(l) + l_2 f_n'(l)],$$

$$B_{q_n \ddot{\delta}} = I_2 f_n'(l) + m_2 [(l - x_M + l_1) f_n(l) + (l - x_M) l_2 f_n'(l)],$$

$$B_{q_n \delta} = P_y f_n(l) + m_2 g^* l_2 f_n'(l),$$

$$B_{q_n \dot{\delta}} = I_2 f_n'(l) + m_2 l_2 f_n(l),$$

where $f_n(l)$, $f_n'(l)$ are the natural oscillatory mode and its derivative at the point of suspension of the engine; $(l - x_M)$ is the distance between the point of suspension of the engine and the center of mass of the rod.

Let us set up the equation of the angular vibrations of the engine relative to the axis of rotation. The moment of friction arising in deflections of the engine will be taken to be proportional to the angular velocity $\dot{\delta}$. The proportionality coefficient will be denoted by h_d.

In a stationary coordinate system Oxy, the engine together with the axis of rotation executes a translational movement with acceleration g^* in the direction opposite to the direction of the coordinate axis Ox, and with acceleration $\ddot{y}(l)$ in the Oy direction. In setting up the equation of the angular oscillations of the engine, one must take into consideration the forces of inertia rising in the translational motion of the engine $m_2 g^*$ and $m_2 \ddot{y}(l)$. These forces are applied at the center of mass of the engine, and are shown in Figure 5.21. Assuming the angular oscillations to be small, we get

$$I_2 \left(\ddot{\delta} + \frac{\partial \ddot{y}}{\partial x \partial t^2} \Big|_{x=l} \right) + m_2 l_2 \frac{\partial \ddot{y}}{\partial t^2} \Big|_{x=l} +$$

$$+ m_2 g^* l_2 \left(\delta + \frac{\partial y}{\partial x} \Big|_{x=l} \right) + h_d \dot{\delta} + k_d \delta = 0 \qquad (5.30$$

or

$$I_z\ddot{\delta}+m_z l_z\ddot{y}_n+[I_z+m_z l_z(l-x_m)]\ddot{\delta}+$$
$$+\sum_{n=1}^{n^0}[I_z f_n'(l)+m_z l_z f_n(l)]\ddot{q}_n+m_z g^0 l_z\sum_{n=1}^{n^0}f_n'(l)q_n+$$
$$+m_z g^0 l_z\delta+(m_z l_z g^0+k_z)\delta+k_z\dot{\delta}=0. \qquad (5.31)$$

Assuming that the natural frequencies of the elastic fuselage are sufficiently scattered, we shall consider a system with two degrees of freedom, namely the elastic vibrations of the fuselage in its n^{th} mode, and the rotation of the engine. For simplicity we assume $h_n = h_d = 0$. On the basis of (5.29) and (5.31) we get

$$\ddot{q}_n+\omega_n^2 q_n+\frac{c_n}{m_n^0}(\ddot{\delta}+\omega_{nd}^2\delta)=0,$$
$$\ddot{\delta}+\omega_z^2\delta+\frac{c_n}{I_z}(\ddot{q}_n+\omega_{zn}^2 q_n)=0. \qquad (5.32)$$

Here ω_n is the partial frequency of the elastic vibrations of the rocket fuselage with a rigidly mounted engine, ω_d is the partial frequency of the angular oscillations of the engine with the fuselage kept stationary, m_n^0 is the reduced mass of the rocket:

$$\omega_n^2=\frac{k_n}{m_n^0},\quad \omega_z^2=\frac{k_z+m_z l_z g^0}{I_z},$$
$$c_n=I_z f_n'(l)+m_z l_z f_n(l), \qquad (5.33)$$
$$\omega_{nd}^2=\frac{P_y f_n(l)+m_z l_z g^0 f_n'(l)}{c_n},$$
$$\omega_{zn}^2=\frac{m_z l_z g^0 f_n(l)}{c_n}.$$

If the engine executes harmonic oscillations with frequency ω_{nd}, then on the basis of the first equation in (5.32) one can conclude that the oscillations of the engine will not have any effect on the n^{th} elastic oscillatory mode of the fuselage. This conclusion indicates that the lateral component of the thrust vector is balanced by the force of inertia of the engine. This property is very important in estimating the stability of the system.

In American literature $\omega_{n\delta}$ is called the engine reaction zero frequency. On the basis of (5.33) each mode of the elastic vibrations of the fuselage is associated with a frequency $\omega_{n\delta}$ which depends on the value of the mode and its derivative at the point of suspension of the engine, $f_n(l), f_n'(l)$.

From the second equation in (5.32) it follows that if the elastic vibrations of the fuselage occur with frequency ω_{in}, then they will not cause any oscillations of the engine. However, $\omega_{in} \ll \omega_{n\delta}, \omega_n, \omega_d$, and as a result this property is of no practical interest.

Setting in (5.32)

$$q_n = q_n^0 e^{i\omega t}, \quad \delta = \delta_0 e^{i\omega t},$$

we shall obtain an equation for determining the natural frequencies of the system in (5.32) as

$$(\omega_n^2 - \omega^2)(\omega_1^2 - \omega^2) - \frac{c_n^2}{m_\delta J_\Sigma}(\omega_{in}^2 - \omega^2)(\omega_{n\delta}^2 - \omega^2) = 0. \tag{5.34}$$

Let the coefficient of inertial coupling between the two partial systems be denoted by

$$b_n^2 = \frac{c_n^2}{m_\delta J_\Sigma}.$$

If the rocket is controlled by rotating the main engines (the force P_c is large), then $\omega_{n\delta} \gg \omega_{in}$. Therefore, to a first approximation in Equation (5.34) we let $\omega_{in} = 0$. We get

$$(1 - b_n^2)\omega^4 - (\omega_n^2 + \omega_1^2 - b_n^2\omega_{n\delta}^2)\omega^2 + \omega_n^2\omega_1^2 = 0.$$

From this equation one can determine two natural frequencies of the system. Multiple frequencies will determine the boundary of stability. The condition for the multiplicity of frequencies can be found from

$$\omega_n^2 + \omega_1^2 - b_n^2\omega_{n\delta}^2 - 2\omega_n\omega_1\sqrt{1 - b_n^2} = 0.$$

The last equality can be tranformed to obtain the equation for the stability boundary in the form

$$\frac{\omega_d}{\omega_n} = \sqrt{1-b_n^2} \pm b_n \sqrt{\frac{\omega_{ni}^2}{\omega_n^2} - 1}. \qquad (5.35)$$

The boundaries of the stability regions are shown in Figure 5.22. The boundaries are constructed from Equation (5.35) in the coordinates ω_d/ω_n, b_p for various values of $e_n^2 = \omega_{ni}^2/\omega_n^2$. Large engine reaction zero frequencies are associated with large values of the coefficients e_n. Each value of e_n corresponds to two boundaries of instability — the upper and lower. The region of instability is located between them. With an increase of e_n the region of instability tends to grow larger. For $e_n = 1$, the region of instability reduces to a line, and for $e_n < 1$ the system is always stable.

As the mode number goes up the natural frequency of the fuselage also rises, and thus the ratio ω_d/ω_n decreases. For low mode numbers, this ratio may be $\omega_d/\omega_n > 1$, and for high mode numbers $\omega_d/\omega_n < 1$. For $e_n > 1$ for all mode numbers of the fuselage the ratios ω_d/ω_n should be such that they lie in stability regions (see Figure 5.22).

The relations among the partial frequencies, corresponding to the stability conditions, can also be expressed in a different manner. We shall assume that the frequencies of the elastic vibrations are given. Then the stability conditions will be $\omega_{ni} < \omega_n$. If $\omega_{ni} > \omega_n$, then we should have $\omega_{ni} < \omega_d$.

Thus, a system with two degrees of freedom — one elastic oscillatory mode of the fuselage and a rotation of the engine — will be stable if the engine reaction zero frequency is less than even one of the partial frequencies ω_n or ω_d.

Let us consider some characteristic features of the dynamic properties of the system with a control actuator.

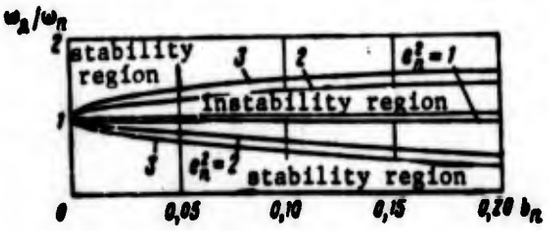

Figure 5.22

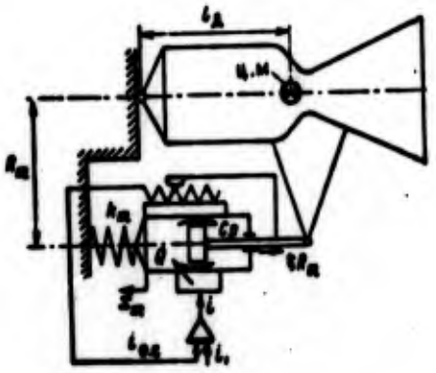

Figure 5.23

9. The Effect of the Elastic Suspension of a Rotating Engine on the Stability of Motion

Figure 5.23 shows a scheme of the servomechanism consisting of the rotating engine, the control actuator, the feedback, and the amplifier. The axis of rotation of the engine is located on the longitudinal axis of the fuselage. The engine is rotated by means of the control actuator. The potentiometer of the negative feedback is located between the housing of the hydraulic cylinder of the control actuator and the stem. The feedback current $i_{o.c.}$ from the potentiometer enters the amplifier and combines there with the current i_1 from the correcting circuit of the control system, and as a command current i enters the control elements of the control actuator.

The control actuator produces a moment to rotate the engine, equal to pFR_m, where p is the pressure drop in the cavities of the cylinder, F is the area of the pistion, R_m is the lever arm.

The equation of small angular oscillations of the engine will be obtained from (5.30) by setting $k_d\delta = -pFR_m$. We shall have

$$I_2\left(\frac{d^2\delta}{dt^2}+\frac{d^2y(l)}{dx\,dt^2}\right)+m_1\frac{d^2y(l)}{dt^2}l_1+$$
$$+m_1g^*l_1\left(\delta+\frac{\partial y(l)}{\partial x}\right)+h_2\dot{\delta}=pFR_m. \qquad (5.36)$$

Under the influence of pressure drop, the piston with the stem of the actuator is displaced by ω_n, where δ is the rotation angle of the engine, and the hydraulic cylinder moves in the opposite direction by

$$x_m=\frac{pF}{k_m}, \qquad (5.37)$$

where k_m is the effective rigidity coefficient of the elastic elements of the servo and of the mounting of the actuator. In writing (5.37) the inertial forces of the hydraulic cylinder were considered negligible.

The feedback current is proportional to the sum of the displacements of the piston and the cylinder, so that

$$i_{o.c}=k_n(\delta R_m+x_m). \qquad (5.38)$$

Here m_n* is the amplification coefficient of the feedback potentiometer.

Denoting the amplification coefficient of the amplifier with respect to the main signal by k_c, and with respect to the feedback signal by $k_{o.c.}$, and assuming the amplifier to be ideal, we obtain an equation for the command current (the input coordinate of the control element in the actuator)

$$i=k_y i_1-k_{o.c}i_{o.c}. \qquad (5.39)$$

The liquid intake Q across the cylinder is expressed by a nonlinear equation. After linearization this equation is reduced to [3, 7, 10].

$$Q=k_q i,$$
$$Q=F\dot{x}_m+FR_m\dot{\delta}+cp+\frac{V_m}{4B}\dot{p}. \qquad (5.40)$$

Here k_v is the linearized amplification coefficient of the control element, c is the linearized coefficient characterizing the flow of liquid from one cavity to the other through gaps between the piston and the cylinder, V_m is the liquid volume in the working cavity of the hydraulic cylinder, B is the volume modulus of liquid compression.

In the right-hand side of the second equation in (5.40) the first two terms express the liquid rate of flow due to the expansion of the working cavity of the hydraulic cylinder. The third and fourth term express the rate of flow due to the flow of liquid into the cavity with a smaller pressure, and due to the compressibility of the fluid.

Equations (5.36) - (5.40) express the dynamic properties of the servomechanism. Eliminating from them the variables x_m, i, $i_{o.c.}$, Q, and P, we get an equation of the servomechanism

$$a_0\dddot{\delta}+a_1\ddot{\delta}+a_2\dot{\delta}+a_3\delta=k_0k_yi_1+b_0\frac{\partial^2y(l)}{\partial t^2}+b_0'\frac{\partial^3y(l)}{\partial x\,\partial t^2}+$$
$$+b_1\frac{\partial y(l)}{\partial t}+b_1'\frac{\partial^2y(l)}{\partial x\,\partial t}+b_2'\frac{\partial y(l)}{\partial x\,\partial t}+b_3'\frac{\partial y(l)}{\partial x}. \qquad (5.41)$$

Here we used the following notation:

$$a_0=\frac{l_2V_m}{4BFR_m}+\frac{l_2F}{k_mR_m},$$
$$a_1=\frac{l_2k_c}{k_mR_m}+\frac{l_2c}{FR_m}+\frac{V_mk_3}{4BFR_m}+\frac{k_1F}{k_mR_m},$$
$$a_2=\frac{V_mm_3g'l_1}{4BFR_m}+\frac{k_1k_c}{k_mR_m}+\frac{k_2c}{FR_m}+FR_m+\frac{Fm_3g'l_1}{k_mR_m},$$
$$a_3=\frac{k_cm_3g'l_1}{k_mR_m}+\frac{cm_3g'l_1}{FR_m}+k_cR_m, \qquad (5.42)$$
$$k_c=k_0k_{o.c}k_m.$$

$$
\begin{aligned}
b_0 &= -m_x l_x \left(\frac{F}{k_m R_m} + \frac{V_m}{4BFR_m}\right), \\
b_0' &= -I_x \left(\frac{F}{k_m R_m} + \frac{V_m}{4BFR_m}\right), \\
b_1 &= -m_x l_x \left(\frac{k_c}{k_m R_m} + \frac{c}{FR_m}\right), \\
b_1' &= -I_x \left(\frac{k_c}{k_m R_m} + \frac{c}{FR_m}\right), \\
b_2' &= -m_x g^\circ l_x \left(\frac{F}{k_m R_m} + \frac{V_m}{4BFR_m}\right), \\
b_3' &= -m_x g^\circ l_x \left(\frac{k_c}{k_m R_m} + \frac{c}{FR_m}\right).
\end{aligned}
\tag{5.43}
$$

The induced motion of the servomechanism takes place both under the influence of current i_1, produced by the correcting circuit of the control system, and due to the lateral motions of the fuselage (induced through the suspension point).

If to Equation (5.41) one adds the equations of the lateral motions of the fuselage and the equations of the control system (without the servo), then one obtains the equations of the perturbed motion of the rocket as a closed dynamic system. The structural block diagram of this system is shown in Figure 5.24. The block diagram of the servo is delineated there by a dotted line.

A lateral displacement of any point on the axis of the elastic fuselage will be represented by a series (5.1) or (4.95). Then the equations of perturbed motion of the fuselage will be identical with Equations (5.29). In Equation (5.41) we must set

$$
\begin{aligned}
y(l) &= z_u(l) + \varphi(l)(l - x_u) + \sum_{n=1}^{n^\circ} f_n(l) q_n(l), \\
y'(l) &= \varphi(l) + \sum_{n=1}^{n^\circ} f_n'(l) q_n(l).
\end{aligned}
\tag{5.44}
$$

The linearized equation of the control system without the servomechanism will be

$$i_1 = K'_{AC}(p)\, y'(x_1). \tag{5.45}$$

where $K'_{AC}(p)$ is a transfer function;

$$y'(x_1) = \psi(t) + \sum_{n=1} f'_n(x_1) q_n(t).$$

Equations (5.29), (5.41), and (5.45) together with (5.44) express to a first approximation the dynamic properties of the closed system shown in Figure 5.24.

Assuming that the natural frequencies of the system are not close to one another, we obtain from Equations (5.29) and (5.41) in view of (5.44) the transfer function of the essential part of an open loop, consisting of one n^{th} mode of the elastic vibrations of the fuselage and the servomechanism:

$$K'_{p.n}(p) = \frac{f'_n(x_1) q_n(p)}{i_1(p)} = \frac{R'(p)}{Q'(p)}. \tag{5.46}$$

To simplify the analysis, we take $h_d = h_n = 0$, $c = 0$ (no passasge of liquid through the hydraulic cylinder), $B = \infty$ (the liquid is incompressible). These assumptions do not change the structure of Equation (5.41), but at the same time simplify the formulas for the coefficients in (5.42) and (5.43).

On the basis of (5.41) - (5.44) we have

$$\left[\left(p + \frac{h_1}{F}\right)p^2 + \omega_n^2\left(p + \frac{h_1}{F}\right)\right]q_n + \left[b_0\left(p + \frac{h_1}{F}\right)p^2 + b_2\left(p + \frac{h_1}{F}\right)\right]q_n = \frac{k_1 k_2 k_m R_m}{l_2 F} i_1. \tag{5.47}$$

Here

$$b_0 = \frac{1}{l_2}\left[l_2 f'_n(l) + m_2 l_2 f_n(l)\right] = \frac{c_2}{l_2}.$$

$$b_2 = \frac{m_2 \varepsilon^2 l_2 f'_n(l)}{l_2}.$$

Assuming

$$\omega_{in}^2 = \frac{b_2}{b_0} = \frac{m_n R^2 l_n f_n'(l)}{c_n}$$

and adding to (5.47) the equation for the generalized coordinate q_n — the first equation in (5.32) — we get

$$(p^2+\omega_n^2)\delta + \frac{c_n}{l_0}(p^2+\omega_{in}^2)q_n = \frac{k_y k_y k_m R_m}{l_n F\left(p+\frac{k_c}{F}\right)} i_1,$$

$$\frac{c_n}{m_n}(p^2+\omega_{in}^2)\delta + (p^2+\omega_n^2)q_n = 0.$$

Hence we find

$$q_n = \frac{\Delta_{q_n}}{\Delta},$$

$$\Delta_{q_n} = -\frac{c_n}{m_n}\frac{k_y k_y k_m R_m}{l_n F}\frac{(p^2+\omega_{in}^2)}{p+\frac{k_c}{F}} i_1,$$

$$\Delta = (p^2+\omega_n^2)(p^2+\omega_n^2) - \frac{c_n^2}{m_n l_n}(p^2+\omega_{in}^2)(p^2+\omega_{in}^2).$$

The numerator of the transfer function (5.46) is

$$R'(p) = -\frac{l_n f_n'(l) + m_n l_n f_n(l)}{m_n}\frac{k_y k_y k_m R_m}{l_n F} f_n'(x_r)(p^2+\omega_{in}^2).$$

Teh Denominator Q'(p) is transformed into the form of two factors

$$Q'(p) = \left(p+\frac{k_c}{F}\right)\left[(p^2+\omega_n^2)(p^2+\omega_n^2) - b_n^2(p^2+\omega_{in}^2)(p^2+\omega_{in}^2)\right].$$

Since $k_c/F>0$, the root of the first factor is negative. The second factor is a characteristic polynomial of the system (5.32), and its properties were examined in the previous section.

On the partial frequencies, let us now impose the requirements that the factor Q'(p) with respect to p^2 has two different real negative roots (the system has two different natural frequencies ω_1 and ω_2):

$$Q'(p) = \left(p+\frac{k_c}{F}\right)(1-b_n^2)(p^2+\omega_1^2)(p^2+\omega_2^2).$$

Setting $p = i\omega$, we obtain the complex transfer number as

$$K'_{p.o}(i\omega) = -f_n(l) f'(x_r) \frac{N_n}{\frac{k_c}{F} + i\omega} \frac{\omega_{n4}^2 - \omega^2}{(\omega_1^2 - \omega^2)(\omega_2^2 - \omega^2)}, \qquad (5.48)$$

where

$$N_n = \left(l_n \frac{f'_n(l)}{f_n(l)} + m_n l_n \right) \frac{k_\omega k_y k_m R_m}{m_n l_n F (1 - b_n^2)}.$$

For a rod with free ends the ratio $f'_n(l)/f_n(l) > 0$ for any oscillatory mode. Therefore, it is always true that the real number $N_n \geq 0$.

Depending on the sign of the product of the two numbers $f_n(l) f'_n(x_g)$ the hodograph of the complex transfer number $K'_{p.o}(i\omega)$ in the complex plane $Z = U + iV$ may start (for $\omega = 0$) either at the positive half-axis U if the product is negative or at the negative half-axis U if the product is positive. In the first case the phase angle $\varphi'_{p.o}(0) = 0$, in the second $\varphi'_{p.o}(0) = \pi$.

Since the function

$$\frac{N_n}{\frac{k_c}{F} + i\omega}$$

is the complex transfer number of the servomechanism, we shall combine it with the complex transfer number of the control system

$$K_{AC}(i\omega) = K'_{AC}(i\omega) \frac{N_n}{\frac{k_c}{F} + i\omega} = A_{AC}(\omega) e^{i\varphi_{AC}(\omega)}.$$

The remaining part of (5.48) will be considered a complex transfer number of the controlled object which has the form

$$K_{p.o}(i\gamma) = f_n(l) f'_n(x_r) K'_{p.o}(i\gamma), \qquad (5.49)$$

where

$$\gamma=\omega/\omega_1,$$

$$K^{\circ}_{p.o}(i\gamma)=-\frac{\left(\frac{\omega_{n1}}{\omega_1}\right)^2-\gamma^2}{\left[\left(\frac{\omega_2}{\omega_1}\right)^2-\gamma^2\right](1-\gamma^2)}=A^{\circ}_{p.o}(\gamma)e^{i\varphi^{\circ}_{p.o}(\gamma)},$$

and ω_1, ω_2 are the natural frequencies of the elastic fuselage with an elastically suspended rotating engine; it will be agreed that $\omega_1>\omega_2$.

In the previous section it was shown that the natural frequencies ω_1 and ω_2 of the system will be real and discrete if the following conditions are satisfied:

$$\omega_{n1}<\omega_n.$$

When $\omega_{n1}>\omega_n$, then we should have $\omega_{n1}<\omega_d$.

We shall assume that the partial frequencies ω_n and ω_d are not close to each other, and that the frequencies of the system differ very little from the partial frequencies. Without loss of generality, we take $\omega_1>\omega_2$. Then between the engine reaction zero frequency and the frequencies of the system two relations are possible:

$$\omega_{n1}<\omega_2<\omega_1 \tag{5.50}$$

$$\omega_2<\omega_{n1}<\omega_1. \tag{5.51}$$

Now let us consider the properties of the complex transfer number (5.49). Partial characteristics of $K^{\circ}_{p.o}(i\gamma)$ for (5.50) are shown in Figure 5.25, and for the relation (5.51) in Figure 5.26. In the first case the phase frequency characteristic $\varphi^{\circ}_{p.o}(\gamma)$ starts with $\varphi^{\circ}_{p.o}(0)=\pi$ at frequency ω_{n1}, increases to 2π, and at the natural frequencies ω_2 and ω_1 it suffers a jump of π in the direction of phase lag. In the second case the lag alternates with a lead, and as a result the phase frequency characteristic lies between π and zero.

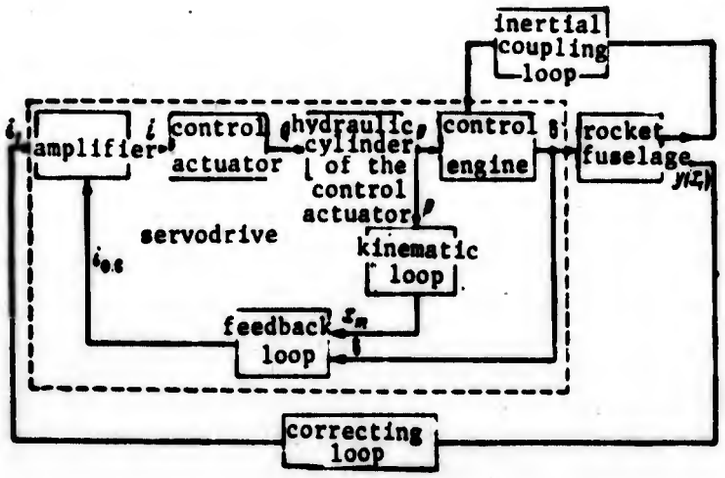

Figure 5.24

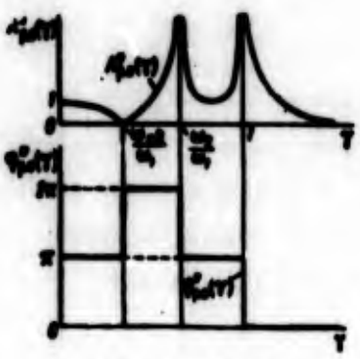

Figure 5.25

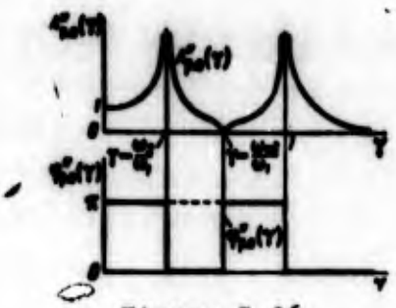

Figure 5.26

Because of friction, the flow of liquid in the hydraulic cylinder, and the compressiblity of the liquid, the frequencies of the system ω_1 and ω_2 change slightly, and, which is most important, the modulus of the complex transfer number $A_{p.o}(\gamma)$ is finite at the natural frequencies.

The hodographs of the complex transfer numbers $K_{p.o}(i\gamma)$ $0 < \gamma < \infty$ with account taken of the energy dissipation in oscillations are shown in the complex plane $Z = U + iV$ in Figure 5.27 and 5.28; Figure 5.27 corresponds to the inequality in (5.51), and Figure 5.28 to the inequality in (5.50)

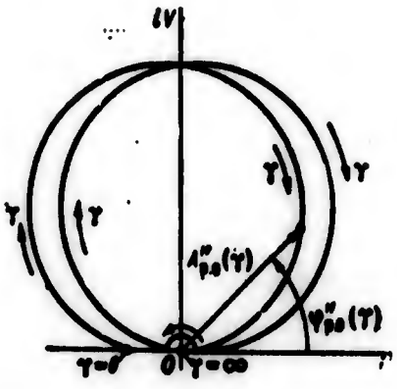

Figure 5.27

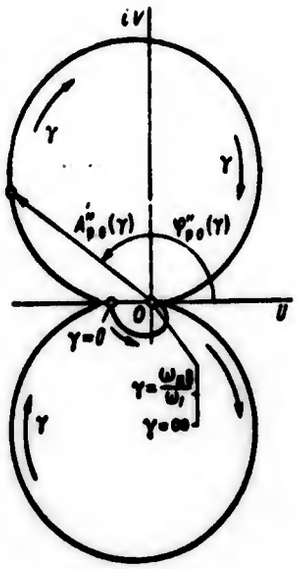

Figure 5.28

The graph of $K'_{p.0}(i\gamma)$ up to the constant multiplier in (5.49) expresses the amplitude phase frequency characteristic of the controlled object consisting of the elastic fuselage and an elastically suspended rotating engine.

The constant factor in (5.49) changes the hodograph scale (see Figure 5.27 and 5.28); if the product $f_n(l)f'_n(x_r)<0$, then signs are reversed in both the real part U and imaginary part V of the complex transfer number.

On the basis of the graph of $K'_{p.0}(i\gamma)$, one can formulate the requirements on the phase frequency characteristic of the control system $K_{AC}(i\omega)$ just as it was done in Section 4. Let us use the Nyquist frequency criterion, and for this purpose let us consider the phase frequency characteristic of the entire open loop.

$$\varphi_{p.0}(\gamma)+\varphi_{AC}(\gamma)=\varphi(\gamma).$$

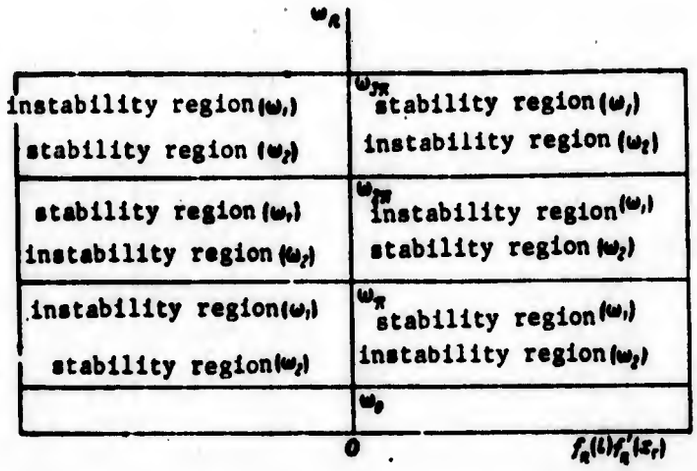

Figure 5.29

We assume that the phase frequency characteristic of the control system is as shown in Figure 1.19. The phase frequency characteristics of the controlled object for various relative values of the characteristic frequencies are shown in Figures 5.25 and 5.26.

If the inequality (5.50) is satisfied, and $f_n(l)f_n'(x_0)>0$, then the system will be stable when the relative values of the characteristic frequencies are the following:

$$\omega_0<\omega_1<\omega_{\pi}, \quad \omega_{2\pi}<\omega_3<\omega_{3\pi}, \quad \omega_{\pi}<\omega_2<\omega_{2\pi}. \tag{5.52}$$

If $f_n(l)f_n'(x_0)<0$, then the system will be stable when

$$\omega_0<\omega_2<\omega_{\pi}, \quad \omega_{\pi}<\omega_1<\omega_{2\pi}, \quad \omega_{2\pi}<\omega_3<\omega_{3\pi}. \tag{5.53}$$

The regions of stability corresponding to (5.50) and the relations (5.52) and (5.53) in the coordinates $f_n(l)f_n'(x_0)$, ω_{π} are shown in Figure 5.29. The regions of instability, corresponding to the frequencies ω_1 and ω_2 are also shown there. In order to stabilize the motion, the frequencies of the system ω_1 and ω_2 should lie between various characteristic frequencies of the control system.

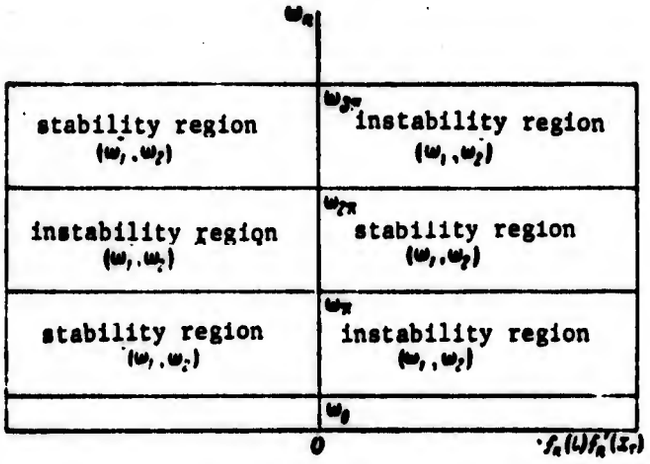

Figure 5.30

In Figure 5.30, the stability regions correspond to the inequality (5.51). In contrast with the relation (5.50) here the frequencies of the system ω_1 and ω_2 may be located between the same characteristic frequencies of the control system. For example, the system will be stable for $f_n(l)f_n'(x_0)<0$ if $\omega_x<\omega_2<\omega_{2x}$, $\omega_x<\omega_1<\omega_{1x}$.

In the above considerations we dealt everywhere with the linearized system of equations. In reality the coefficients k_v, c, h_d, depend on the amplitudes, velocities, and pressures in the cavities of the hydraulic cylinder, and therefore the properties of the real system may differ considerably from the properties of the linearized system.

REFERENCES

1. Beyli. A measurement of the Bending Modes as a Method of Coping with the Effect of Aeroelasticity on the Control Loop. Voprosy raketnoy tekhniki, 1961, No. 6.

2. Bil. Dynamic Stabilityh of an Elastic Rocket Subject to Constant and Pulsating Thrust Forces, Raketnaya tekhnika i kosmonavtika, No. 3, 1965.

3. Boyer. Hydraulic rocket Servosystems. Voprosy raketnoy tekhniki, No. 7, 1961.

4. Veymeyer, Sporing. An Application fof a Closed Self-Adjusting Loop in a Rocket Control System. Voprosy raketnoy tekhniki, No. 2, 1964.

5. Grossman, Ye. P. Kurs vibratsiy samoleta (A course in Airplane Vibrations). Oborongiz, 1940.

6. Ishlinskiy, A. Yu. Mekhanika giroskopicheskikh sistem(Mechanics of Gyroscopic Systems). Izdatel'stvo AN SSSR, 1963.

7. Koenig, Effect of the Reactive Force on the Bending Mechanical Characteristics of a Rocket. Voprosy Raketnoy tekhniki, No. 5, 1965.

8. Layanis, Fontenot. Analysis of the Vibrations of a Booster Cluster. Raketnaya tekhnika i kosmonavtika, No. 3, 1963.

9. Kunayev, I. P, Elementy rascheta tochnikh priborov, sb. statey (Elements of Precision Instrument Calculations) Collection of articles. Oborongiz. 1954

10. Lyukens, Methods of Analyzing the Control System of a Large Elastic Rocket. Voprosy raketnoy tekhniki. No. 9, 1961.

11. Naylend, A self-adjusting Control System for a Large Elastic Rocket. Voprosy raketnoy tekhniki, No. 1, 1962.

12. Panovko, Ya. G. Vnutrenneye treniye pri kolebaniyakh uprugikh sistem (Internal Friction During Vibrations of Elastic Systems) Fizmatgiz, 1960.

13. Popov, Ye. P. Dinamika sistem avtomaticheskogo regulirovaniya (Dynamics of Automatic Control Systems) Gostekhizdat, 1954.

14. Rapoport, I. M. Kolebaniya uprugikh obolochek, chastichno zapolnennykh ideal'noy zhidkost'yu (Oscillations of Elastic Shells partially Filled with an Ideal Liquid). Mashgiz, 1967.

15. Rapoport, I. M. Dinamika uprugogo tela, chastichno zapolnennogo zhidkost'yu (Dynamics of an Elastic Body Parially Filled with Liquid) Mashgiz, 1967.

16. Rott, A Simplified Analysis of the Damping Effect of Jet Streams. Raketnaya tekhnika i kosmonavtika, No. 4, 1964.

17. Sorokin, Ye. S. Metod predvaritel'nogo analiza ustoychivosti s uchetom aerouprugosti konstruktsii rakety (On the Question of Inelastic Resistance of Building Materials During Vibrations) TsNITS Stroyizdat, 1954.

18. Freyn, Vong. A Method of a Preliminary Stability Analysis taking Account of the Aeroelasticity of Rocket Designs. Voprosy Raketnoy tekhniki, No. 8, 1963.

19. Frid, Miller. An Enhancement of Automatic Pilot Stability by damping the Bending Vibrations of the Rocket Fuselage, Voprosy raketnoy tekhniki. No. 5, 1962.

20. Elli, Ledbetter. Calculations and measurement of the Natural Oscillations of Multi-Stage Booster Rockets. Raketnaya tekhnika i kosmonavtika. No. 2, 1963.

21. Andrew, Johnson. Automatic Control of Aeroelastic Oscillations, Voprosy raketnoy tekhniki. No. 7, 1964.

SYMBOL LIST

ENGLISH PAGE.	RUSSIAN CHARACTER	ENGLISH MEANING	TYPED AS
18	$S_п$	Pipe flow-passage cross sectional area	S_t
19	$l_п$	Distance from upper tip of rocket to engine nozzle	l_t
19	$M_к$	Coriolis moment	M_c
19	$M_д$	Aerodynamic force moment	M_D
19	$Y_{г.р}$	Lift force on a vane	$Y_{g.r.}$
19	$X_{г.р}$	Drag force on a vane	$X_{g.r.}$
19	$M_{г.ш}$	Hinge moment on a vane	$M_{g.sh}$
20	$q_г$	Gas impact pressure	q_g
20	$S_г$	Characteristics area of jet vane	S_g
20	$l_г$	Characteristic length of jet vane	l_g
20	$\delta_г$	Rotation angle of jet vane	δ_g
20	$c^{\delta}_{yг}$	Coefficient	c^{δ}_{yg}
20	$c_{xг}$	Coefficient	c_{xg}
20	$c^{\delta}_{mг}$	Coefficient	C^{δ}_{mg}
20	$Y_{в.р}$	Force on air vane	$Y_{v.r.}$
26	$\bar{a}_{пер}$	Centrifugal acceleration	$\bar{a}_{per}$
26	$\bar{a}_к$	Coriolis acceleration	$\bar{a}_c$
26	$\dot{\varphi}_{пр}$	Present angular velocity	$\dot{\varphi}_{pr}$
27	$\delta_{пр}$	Preset angle of rotation	δ_{pr}
27	$\alpha_{пр}$	Preset angle of attack	α_{pr}
27	$P_э$	Effective engine thrust	P_{ef}

ENGLISH PAGE	RUSSIAN CHARACTER	ENGLISH MEANING	TYPED AS
50	ГП	gyroscopic pickup	GP
51	у	amplification	a
51	у.о.с	feedback signal ampl	a.f.s.
51	о.с	feedback	f
54	$M_{упр}$	control moment	M_c
54	$M_{пр}$	preset control moment	M_{pr}
54	$M_{воз}$	moment to parry wind disturbances	M_{per}
54	$M_{стб}$	stabilizing moment	M_{st}
60	$a_п$	amplitude of periodic oscillations	a_p
75	$Z_в$	wind force	Z_w
75	$M_{ув}$	wind moment	M_{yw}
75	$Z_р$	control force	Z_c
177	$P_э$	effective engine thrust	P_{ef}
180	$M_д$	moment of damping forces	M_d
191	$\alpha_н$	angle of attack	α_n
206	$\varphi_{зап}$	phase lag	ϕ_{lag}
226	$\omega_п$	frequency of a partial sys.	ω_p
226	$a_п$		a_p
255	$\gamma_Б$	specific density	γ_B
278	$\beta_{кр}$	critical value of β	β_{cr}
294	г	gyroscope	x_g
294	$x_д$	coordinate along the fuselage length	x_d

ENGLISH PAGE	RUSSIAN CHARACTER	ENGLISH MEANING	TYPED AS
332	изг	bending	b
333	$R_в$	thrust of a vernier engine	R_v
336	$i_п$	amplitude of periodic oscillations	i_p
339	$m_д$	mass of the rotating engine	m_d
344	R_y	thrust of the control revolving engine	P_c
347	у	amplifier	c
	сек	second	sec
	кГ		kgf

UNCLASSIFIED

Security Classification

DOCUMENT CONTROL DATA - R & D

(Security classification of title, body of abstract and indexing annotation must be entered when the overall report is classified)

1. ORIGINATING ACTIVITY *(Corporate author)*
Foreign Technology Division
Air Force Systems Command
U. S. Air Force

2a. REPORT SECURITY CLASSIFICATION
UNCLASSIFIED

2b. GROUP

3. REPORT TITLE

LIQUID PROPELLANT ROCKET AS A CONTROLLED OBJECT

4. DESCRIPTIVE NOTES *(Type of report and inclusive dates)*
Translation

5. AUTHOR(S) *(First name, middle initial, last name)*

Kolesnikov, K. S.

6. REPORT DATE	7a. TOTAL NO. OF PAGES	7b. NO. OF REFS
1969	362	108

8a. CONTRACT OR GRANT NO.	9a. ORIGINATOR'S REPORT NUMBER(S)
F33657-70-D-0607	
b. PROJECT NO. 6040104	FTD-HC-23-461-69
c.	9b. OTHER REPORT NO(S) *(Any other numbers that may be assigned this report)*
d. DIA Task No. T65-04-18A	

10. DISTRIBUTION STATEMENT
Distribution of this document is unlimited. It may be released to the Clearinghouse, Department of Commerce, for sale to the general public.

11. SUPPLEMENTARY NOTES	12. SPONSORING MILITARY ACTIVITY
	Foreign Technology Division Wright-Patterson AFB, Ohio

13. ABSTRACT

The book discusses the differential equations of the perturbed motion of a rocket for three different dynamic models: an ideally rigid body; an elastic inhomogeneous rod; a rigid body with cavities partially filled with liquid. In the study of the dynamic characteristics of the rocket, the oscillations of liquid in tanks were replaced by the oscillations of mathematical pendulums, since the differential equations for the two phenomena are completely analogous. Results are given of an experimental investigation of the fuel oscillating in tanks. A presentation is made of the methods of determining the modes and frequencies of the natural vibrations of the fuselage with and without taking the slave force into consideration. On the basis of an analysis of the dynamic rocket properties, a determination is made of the amplitude-phase frequency characteristics of the rocket, and of those features of the characteristics that are due to the fuel oscillating in tanks and the elastic vibrations of the fuselage. A stability analysis of rocket motion leads to a formulation of additional requirements on the frequency characteristics of the control system and on the location of the gyroscope along the fuselage. Attention is given to certain methods of stabilizing the oscillating motion of fuel in tanks as well as the elastic vibrations of the fuselage.

DD FORM 1 NOV 68 1473

UNCLASSIFIED

Security Classification

14 KEY WORDS	LINK A		LINK B		LINK C	
	ROLE	WT	ROLE	WT	ROLE	WT
Liquid Propellant Rocket Laplace Equation						